

The PHO2 family
of ubiquitin conjugating enzymes
in *Arabidopsis thaliana*
and its contribution to
plant programmed cell death

Inaugural-Dissertation
zur Erlangung des Doktorgrades
der Mathematisch-Naturwissenschaftlichen Fakultät
der Universität zu Köln



vorgelegt von
Karolin Eifler
aus Meisenheim
Köln, 2010

Berichterstatter:

Prof. Dr. George Coupland

Prof. Dr. Jürgen Dohmen

Prüfungsvorsitzende:

Prof. Dr. Ute Höcker

Tag der Disputation:

7. Juni 2010

Die vorliegende Arbeit wurde am Max-Planck-Institut für Pflanzenzüchtungsforschung in Köln in der Abteilung Entwicklungsbiologie der Pflanzen (Direktor: Prof. Dr. George Coupland) und in den Max F. Perutz Laboratories in Wien in der Arbeitsgruppe von Prof. Dr. Andreas Bachmair angefertigt.



„Es ist nicht die Gewohnheit des Wahren, ohne Verhüllung zu kommen und
sich von jedem erkennen zu lassen.“
Erich Kästner

Contents

Abstract	xvii
Zusammenfassung	xix
1 Introduction	1
1.1 Programmed cell death	1
1.1.1 Programmed cell death in plants	2
1.2 Posttranslational modification with ubiquitin	4
1.2.1 Ubiquitin: structure and function	4
1.2.2 The ubiquitin conjugation cascade	6
1.2.3 The 26S Proteasome	9
1.2.4 The orchestra for ubiquitylation in <i>Arabidopsis thaliana</i>	10
Ubiquitin genes	10
Ubiquitin activating enzymes	11
Ubiquitin conjugating enzymes	11
Ubiquitin ligases	12
Deubiquitylating enzymes	12
1.3 Ubiquitylation in programmed cell death	13
1.4 The PFU proteins in <i>Arabidopsis thaliana</i> and their mammalian homologues	15
1.4.1 PHO2 and its role in phosphate signaling	15
1.4.2 The closest mammalian homologue of PHO2 is E2-230K	17
1.4.3 The distant homologue BRUCE/Apollon functions in mammalian apoptosis and cytokinesis	19
1.5 Aim of this work	20
2 Results	23
2.1 Gene and protein structure of the <i>PFU</i> family	23
2.1.1 The PFU family is divided into two subgroups	23
2.1.2 Cloning of the <i>PFU2</i> open reading frame	27
2.1.3 Determination of the length of the <i>PFU2</i> leader	28
2.1.4 Analysis on the alternative gene model of <i>PFU3</i>	29
2.2 Analysis on <i>pfu</i> mutants reveals new function for PFU proteins	31
2.2.1 Identification of homozygous T-DNA insertion lines	31

2.2.2	Analysis of transcript levels in mutant plants	33
2.2.3	Production of multiple knockout plants	35
2.2.4	Different mutant phenotypes	35
	Only <i>pho2</i> mutants accumulate P _i in shoots	35
	ubK48R induced cell death is impaired in <i>pfu</i> mutants	36
	Higher resistance of <i>pfu</i> mutants to ozone treatment	39
	PFU2 responses to nitric oxide	39
	The stress response to a pathogen is decelerated in <i>pfu1-1 pho2-10</i> mutants	42
2.3	Subcellular localization of the PFU proteins	43
2.3.1	Cloning of EGFP/mRFP fusion constructs	43
2.3.2	Transient expression of the fusion constructs in <i>Nicotiana benthamiana</i> PFU1 is present in nucleus and cytoplasm	44
	PFU3 is highly expressed in the nucleus	45
	PFU2 and PHO2 are restricted to the cytoplasm	46
	Coexpression of PFU fusion proteins in <i>Nicotiana benthamiana</i> . . .	48
2.3.3	Expression of EGFP/mRFP fusion proteins in transgenic <i>Arabidopsis</i> <i>thaliana</i> lines	49
	PFU1-EGFP localization in stably transformed <i>Arabidopsis</i> plants .	51
	High expression of PFU3 in the nuclei of <i>Arabidopsis</i> root cells . . .	51
	PHO2 shows diffuse localization in the cytoplasm	52
	Coexpression of PFU1-EGFP and PHO2-mRFP in <i>Arabidopsis thaliana</i>	53
2.4	Interaction studies in <i>Saccharomyces cerevisiae</i>	54
2.4.1	Autoactivation of PFU proteins	54
2.4.2	TUP1 fusion proteins in a yeast two hybrid assay	57
2.4.3	Interaction studies with C-terminus of PFU proteins in yeast . . .	61
2.5	Biochemical analysis with recombinantly expressed PFU proteins	62
2.5.1	Cloning of overexpression constructs	63
	Multiple constructs to overexpress the C-terminus	63
	Constructs to obtain only the UBC domain for ubiquitylation assays	66
	Recombinant proteins bearing both UBC and C-terminal domain .	66
2.5.2	Analysis of the solubility of the different recombinant PFU proteins Different attempts to increase the solubility of the C-terminal domain of PFU1	68
	Purification of recombinant proteins bearing the UBC domain . . .	73
2.5.3	Interaction studies via Co-Immunoprecipitation	75
2.5.4	<i>In vitro</i> ubiquitylation assays	76
3	Discussion	79
3.1	A class of extraordinary E2s in <i>Arabidopsis thaliana</i>	79
3.1.1	Specific features of PHO2 and the PFU proteins identified in a bioinformatic approach	79
3.1.2	PFU2: a target for microRNAs ?	81

3.1.3	Alternative structure of <i>PFU3</i> is not supported	82
3.2	The PFU proteins bear an important function in plant programmed cell death	83
3.2.1	T-DNA insertions lines of <i>PHO2</i> and the <i>PFU</i> genes with altered transcript levels	83
3.2.2	Only <i>pho2</i> mutants show P_i accumulation in the shoot	84
3.2.3	Mutation of <i>PHO2</i> and the PFU proteins suppresses the ubK48R phenotype	85
3.2.4	<i>PHO2</i> and <i>PFU1</i> sense oxidative stress caused by ozone treatment .	87
3.2.5	<i>PFU2</i> needed for response to nitric oxide	88
3.2.6	<i>PHO2</i> and <i>PFU1</i> work together in the response to biotic stress . .	90
3.3	The two subfamilies show different subcellular localization patterns	91
3.3.1	<i>PFU1</i> and <i>PFU3</i> are imported into the nucleus	92
3.3.2	<i>PHO2</i> and <i>PFU2</i> are restricted to the cytoplasm	93
3.3.3	<i>PHO2</i> responds to <i>PFU1</i> overexpression	95
3.4	Molecular analysis of <i>PFU1</i> and <i>PHO2</i> via expression in yeast	97
3.4.1	Auto-activity of <i>PHO2</i> and <i>PFU1</i> : a new assay to test functionality?	98
3.4.2	Putative interaction of <i>PHO2</i> and <i>PFU1</i> might be highly regulated	99
3.4.3	C-terminal domain not sufficient for interaction	101
3.5	Biochemical analysis of recombinant PFU proteins	103
3.5.1	A long road to success: how to obtain soluble PFU protein fragments	103
3.5.2	Co-IP and functionality assays still in the fledgling stages	106
3.6	A first model summarizing the results of this thesis	108
4	Material and Methods	111
4.1	Material	111
4.1.1	Bacterial strains	111
4.1.2	Yeast strain	111
4.1.3	Plant material	111
4.1.4	Vectors	112
4.1.5	Plasmids used in this thesis	113
4.1.6	Chemicals	113
4.1.7	Enzymes	113
4.1.8	Size standards	113
4.1.9	Oligonucleotides	114
4.1.10	Antibodies	114
4.1.11	Bioinformatic Tools and Databases	114
4.2	Methods	115
4.2.1	Work with <i>Escherichia coli</i>	115
	Cultivation and storage of <i>Escherichia coli</i>	115
	Preparation of competent <i>E. coli</i> cells	115
	Transformation of <i>E. coli</i>	116
	Plasmid preparation from <i>E. coli</i>	116
4.2.2	Work with <i>Agrobacterium tumefaciens</i>	116

	Cultivation and storage of <i>Agrobacterium tumefaciens</i>	116
	Preparation of competent <i>A. tumefaciens</i> cells	116
	Transformation of <i>A. tumefaciens</i>	116
	Plasmid preparation from <i>A. tumefaciens</i>	117
4.2.3	Work with <i>Saccharomyces cerevisiae</i>	117
	Cultivation and storage of yeast cells	117
	Yeast transformation	117
	Yeast trickle tests	118
	Protein extracts of yeast cells for Western blotting	118
4.2.4	Work with <i>Arabidopsis thaliana</i>	118
	Cultivation of <i>Arabidopsis thaliana</i>	118
	Sterilization of <i>Arabidopsis</i> seeds	119
	Floral dip transformation of <i>Arabidopsis thaliana</i>	119
	Plant crosses	119
	Preparation of <i>Arabidopsis</i> samples for microscopic analysis	120
	Microscopic analysis	120
	Determination of the P _i content in <i>Arabidopsis</i> leaves	120
	Induction of the <i>ubK48R</i> transgene	120
	Ozone treatment of <i>Arabidopsis</i> plants	120
	Nitric oxide treatment of <i>Arabidopsis</i> plants	121
	Pathogen treatment of <i>Arabidopsis plants</i>	121
4.2.5	Work with <i>Nicotiana benthamiana</i>	121
	Transient expression of proteins in <i>Nicotiana benthamiana</i>	121
4.2.6	Handling nucleic acids	122
	Quick DNA extraction from <i>Arabidopsis thaliana</i>	122
	High-throughput DNA isolation with the BioSprint 96	122
	RNA extraction from <i>Arabidopsis thaliana</i>	122
	PCR	123
	RT-PCR	124
	Colony-PCR	124
	Agarose gels	124
	DNA purification from agarose gels	125
	Precipitation of nucleic acids	125
	Generation of blunt ends	125
	DNA digestion with restriction enzymes	126
	Ligation	126
	Site directed mutagenesis	127
	Sequencing	127
4.2.7	Handling proteins	127
	SDS-PAGE	127
	Coomassie staining	128
	Western blot	128
	Overexpression of recombinant proteins in <i>E. coli</i>	129

Purification of recombinant proteins from <i>E. coli</i> via His-tag under native conditions	129
Purification of recombinant proteins from <i>E. coli</i> via His-tag under denaturing conditions	130
Purification of recombinant proteins from <i>E. coli</i> via Strep-tag . . .	130
Dialysis	130
Co-Immunoprecipitation	130
<i>In vitro</i> thioester reaction	131
<i>In vitro</i> ubiquitylation assay	132
Appendices	133
A Plasmids used or constructed in this thesis	135
B Oligonucleotides	141
C Abbreviations	145
References	149
Acknowledgements	167
Erklärung	169
Curriculum Vitae	171

List of Figures

1.1	Events of programmed cell death occurring through the life cycle of a plant	3
1.2	Structure of Ubiquitin	5
1.3	The ubiquitin conjugation cascade	8
1.4	The 26S proteasome	9
1.5	Model of the phosphate signaling cascade involving PHO2 and miRNA399	16
1.6	Model of the ubiquitylation mechanism proposed for E2-230K/UBE2O . .	18
2.1	Alignment of the PHO2 and the three PFU protein sequences	24
2.2	Alignment showing part of the C-terminus of PFU2 and PHO2 together with a selection of the eukaryotic homologues	25
2.3	Schematic overview on the protein structure of the PFU family	26
2.4	Cloning strategy for PFU2 into the sequencing vector pBluescript II SK+ .	27
2.5	Schematic overview on the mRNA structure of <i>PFU2</i> and the oligo positions used for determination of the length of the <i>PFU2</i> leader	28
2.6	RT-PCR results to determine the length of the <i>PFU2</i> leader sequence . . .	29
2.7	Analysis of the <i>PFU3</i> gene structure	30
2.8	Gene structure of the <i>PFU</i> genes and position of T-DNA insertions	31
2.9	Genotyping of the T-DNA insertion lines	32
2.10	RT-PCR determining the <i>PFU</i> transcript levels in wild type and mutant plants	34
2.11	Phosphate measurements in wild type and mutant plants	36
2.12	Altered response to ubK48R induced cell death in <i>pfu</i> mutant plants . . .	37
2.13	RT-PCR to analyze the <i>ubK48R</i> transcript levels in wild type and mutant plants	38
2.14	Ozone treatment of wild type and mutant plants	39
2.15	Treatment of wild type and mutant plants with 0.2 mM sodium nitroprusside	41
2.16	Treatment of wild type and mutant plants with 0.1 mM sodium nitroprusside	41
2.17	PFU1-EGFP expression in epidermal cells of <i>Nicotiana benthamiana</i>	45
2.18	Epidermal cells of <i>Nicotiana benthamiana</i> expressing PFU3 fusion proteins	46
2.19	Subcellular localization of PFU2 in <i>Nicotiana benthamiana</i> cells	47
2.20	Microscopic images of <i>Nicotiana benthamiana</i> cells expressing PHO2-mRFP	48
2.21	Coinfiltration of PFU1-EGFP and PHO2-mRFP into <i>Nicotiana benthamiana</i> leaves	49

2.22	<i>Arabidopsis</i> root cell expressing the pER8-PFU1-EGFP construct	51
2.23	PFU3 is only located in the nucleus of stably transformed <i>Arabidopsis</i> plants	52
2.24	Localization of PHO2-mRFP in stably transformed <i>Arabidopsis thaliana</i> plants	53
2.25	Transcript levels of <i>PFU1-EGFP</i> and <i>PHO2-mRFP</i> in F3 plants bearing both transgenes under the β -estradiol inducible promoter.	54
2.26	A standard yeast two hybrid assay	55
2.27	Test for autoactivation of the <i>HIS3</i> gene by the DBD-PFU1 and DBD-PHO2 constructs	56
2.28	Yeast two hybrid assay with the TUP1 repressor domain	57
2.29	First test for interaction of PFU1 and PHO2 with the TUP1 repressor domain	59
2.30	Second test for interaction of PFU1 and PHO2 with the TUP1 domain . .	59
2.31	Protein expression levels of the DBD- and TUP1 fusion proteins in yeast determined via western blot	60
2.32	Standard yeast two hybrid assay with the C-termini of PFU1 and PHO2 .	62
2.33	Schematic overview of the overexpression constructs of the C-terminal domain of PFU1 in pET42c bearing only a single His-tag	64
2.34	Overexpression constructs cloned to analyze the solubility of the PFU1 C-terminus fused to a various number of protein tags	65
2.35	Overexpression constructs of the C-terminal domain of PHO2	65
2.36	Scheme summarizing the constructs produced to overexpress the UBC domain of PFU1 and PHO2	66
2.37	Different overexpression constructs bearing the UBC- and C-terminal domains of PFU1 and PHO2	67
2.38	Coomassie stained gel visualizing the protein overexpression of different constructs in Rosetta <i>E. coli</i> cells	69
2.39	Different purification steps of the C-terminus of PFU1 documented on a western blot	70
2.40	Comparison between the amount of soluble protein under denaturing conditions and under native conditions on a western blot	70
2.41	Different attempts to increase the solubility of the C-terminal domain of PFU1	71
2.42	Attempt to renature the C-terminal domain of PFU1 via dialysis	72
2.43	Western blot displaying the elution steps after purification of PHO2UBC, PFU1UBC and PHO2UBCCT	73
2.44	Coomassie stained polyacrylamide gel documenting the different purification steps of the longer UBCCT fragments fused to a GST-tag	74
2.45	Co-immunoprecipitation experiments with PFU1 and PHO2	76
2.46	Thioester formation assays with E2-25K, PHO2UBC and PFU1UBC . . .	77
3.1	Comparison of the PHO2-mRFP localization and the YFP-AtRab5 distribution	94
3.2	A first model of a putative molecular mechanism of the PFU proteins summarizing the results and hypotheses obtained in this thesis	109

List of Tables

2.1	Oligos used to identify homozygous T-DNA insertion lines	33
2.3	Homozygous <i>pfu</i> double, triple and quadruple mutant combinations	35
2.5	<i>pfu2-1</i> mutant plants are more resistant to NO treatment	41
2.7	Ion leakage measurements	43
2.9	EGFP/mRFP fusion protein expression in the F2 generation of <i>Arabidopsis thaliana</i> lines stably transformed with pER8 fusion constructs and analyzed under the confocal microscope	50
2.11	Oligos used for site directed mutagenesis.	57
4.1	Standard PCR programs to amplify short (up to approx. 1500 bp) and longer DNA fragments	123
4.2	A standard protocol for cDNA synthesis with the SuperScript TM II RT	124
4.3	A standard protocol for the blunting reaction	126
4.4	A typical reaction mix for digesting DNA	126
4.5	Reaction mix for a standard ligation	127
4.6	Ingredients for a 12 % polyacrylamide gel	128
4.7	Thioester reaction mix	132

Abstract

Programmed cell death (PCD) is essential for various developmental processes and stress responses in the life cycle of a plant. The ubiquitin-proteasome system has been shown to regulate multiple mechanisms with a suspected role in the initiation and execution of plant programmed cell death. However, only little is known about the exact function of enzymes involved in ubiquitylation during cell death responses. This thesis gives first insights into the molecular and physiological characteristics of the PHO2 family of ubiquitin conjugating enzymes in *Arabidopsis thaliana* and demonstrates the important role of these proteins during the programmed cell death response to abiotic and biotic stresses.

The protein family consists of four members that are unusually large for ubiquitin conjugating enzymes and possess in addition to the characteristic UBC domain a long N-terminal extension and a C-terminal domain highly conserved throughout the plant kingdom. Two subgroups can be distinguished according to the homology in the N-terminal part: the two larger proteins PHO2 and PFU2 (**PHO2-family ubiquitin conjugating enzyme 2**) on the one hand and the two smaller ones PFU1 and PFU3 on the other.

PHO2 and PFU2 were identified to be absent from the nucleus and restricted to the cytoplasm. PFU1 and PFU3 were shown to be present inside the nucleus. Only PFU1 could also be detected in the cytoplasm.

Whereas PFU1 and PFU3 seem to be rather plant specific, homologues of PHO2 and PFU2 can be found throughout the whole eukaryotic kingdom, but are missing from the model organisms *Saccharomyces cerevisiae* and *Schizosaccharomyces pombe*. The closest mammalian homologue is E2-230K, which is shown to display both E2 and E3 function, but its exact function in the cell is still unknown. The more distantly related homologue BRUCE has been described to be an inhibitor of apoptosis.

Complete knockout mutants could be identified for PHO2, PFU1 and PFU3, whereas the *PFU2* transcript is only downregulated in the T-DNA insertion line analyzed in this thesis. Mutation of either PHO2, PFU1 or PFU2 leads to suppression of cell death caused by expressing a mutated form of ubiquitin in plants. Apart from this, *pfu1* and *pho2* mutants show less cell death symptoms than wild type plants under ozone treatment. In contrast, the *pfu2* mutant line is less sensitive to nitric oxide treatment than wild type plants. In addition, the hypersensitive response to a bacterial pathogen is delayed in the *pfu1 pho2* double mutant, suggesting that both proteins are functionally interdigitated.

These findings show that the PHO2 family of ubiquitin conjugating enzymes is needed to initiate programmed cell death in response to various stresses presumably by sensing

reactive oxygen species or reactive nitrogen species, which highly accumulate in the cell during PCD.

Further experiments with recombinant PFU1 and PHO2 protein fragments revealed that especially the C-terminal domain of the proteins is highly insoluble. Various modifications of the constructs were needed to finally obtain a soluble PHO2 fragment containing the UBC and the C-terminal domain, which can be used in future biochemical assays to test the functionality of the ubiquitin conjugating enzymes and to solve the three-dimensional structure of the highly conserved C-terminal domain.

Zusammenfassung

Programmierter Zelltod (PCD) ist an zahlreichen Entwicklungsvorgängen und Stressreaktionen beteiligt und daher essentiell für den Lebenszyklus einer Pflanze. Das Ubiquitin-Proteasom-System reguliert dabei eine Vielzahl zellulärer Vorgänge, die vermutlich eine Rolle in der Einleitung und Ausführung des PCD spielen. Es ist bisher allerdings nur sehr wenig über diese Ubiquitylierungsprozesse und die daran beteiligten Enzyme bekannt.

Die vorliegende Arbeit bietet erste Einblicke in die biochemischen und physiologischen Eigenschaften der PHO2-Familie von ubiquitin-konjugierenden Enzymen in *Arabidopsis thaliana*. Dabei wird gezeigt, dass diese Enzyme bei der Reaktion auf abiotischen und biotischen Stress und dem daraus resultierenden PCD eine wichtige Rolle spielen.

Die Proteinfamilie besteht aus vier Mitgliedern, die für ubiquitin-konjugierende Enzyme ungewöhnlich groß sind. Sie besitzen zusätzlich zur charakteristischen UBC-Domäne einen langen N-terminalen Bereich sowie eine weitere C-terminale Domäne, die im gesamten Pflanzenreich hochkonserviert ist. Anhand von Homologien im N-terminalen Bereich lässt sich die Familie in zwei Untergruppen einteilen: die beiden größeren Proteine PHO2 und PFU2 (PHO2-family ubiquitin conjugating enzyme 2) auf der einen und die beiden etwas kleineren Proteine PFU1 und PFU3 auf der anderen Seite.

Während PHO2 und PFU2 ausschließlich im Cytoplasma lokalisiert sind, konnte eine Lokalisation für PFU3 nur im Nukleus gezeigt werden. Einzig PFU1 war in beiden Kompartimenten zu finden.

Im Gegensatz zu PFU1 und PFU3, die eher pflanzenspezifisch sind, gibt es PHO2/PFU2-Homologe in einer Vielzahl weiterer eukaryotischer Organismen. Sie fehlen jedoch in den beiden Modellorganismen *Saccharomyces cerevisiae* und *Schizosaccharomyces pombe*. In Säugetieren weist E2-230K die größte Homologie zu PHO2 und PFU2 auf und besitzt *in vitro* sowohl E2- als auch E3-Funktion. Eine bestimmte Funktion in der Zelle konnte jedoch für dieses Protein noch nicht nachgewiesen werden. Stattdessen ist bekannt, dass BRUCE, dessen Proteinsequenz etwas weniger homolog ist, den programmierten Zelltod in Säugetierzellen inhibiert.

Für PFU1, PFU3 und PHO2 konnten im Rahmen dieser Arbeit Mutanten charakterisiert werden, bei denen das jeweilige Protein komplett ausgeschaltet ist. Im Falle der *pfu2*-Mutante dagegen wurde gezeigt, dass das Transkript lediglich herunterreguliert ist.

Die Eigenschaften dieser Mutanten wurden unter verschiedenen Wachstumsbedingungen näher untersucht. Dabei konnte gezeigt werden, dass Zelltod, der durch Expression einer mutierten Form von Ubiquitin in der Pflanze ausgelöst wird, in *pho2*-, *pfu1*- und *pfu2*-Mutanten

stark beeinträchtigt ist. Außerdem weisen ozonbehandelte *pfu1*- und *pho2*-Mutanten im Vergleich zu Wildtyppflanzen weniger Zelltodsymptome auf. Die *pfu2*-Mutante dagegen ist resistenter gegenüber Stickstoffmonoxidbehandlungen als der Wildtyp. Darüber hinaus konnte für die *pfu1 pho2*-Doppelmutante eine verspätete Reaktion in Folge bakteriellen Pathogenbefalls beobachtet werden, was auf eine funktionelle Interaktion von PFU1 und PHO2 hindeutet.

Diese Ergebnisse zeigen, dass die PHO2-Familie von ubiquitin-konjugierenden Enzymen benötigt wird, um PCD in der Pflanze als Antwort auf unterschiedliche Stresssituationen einzuleiten. Die Proteine scheinen dabei auf bestimmte oxidative oder Stickstoffmonoxid-Signale zu reagieren, die sich während des PCD stark anreichern.

Weitere Untersuchungen an rekombinanten PFU1- und PHO2-Proteinfragmenten ergaben, dass insbesondere die C-terminale Domäne dieser Proteine sehr unlöslich ist. Einige Modifikationen der Überexpressionkonstrukte waren nötig, um schließlich ein stark lösliches PHO2-Fragment zu erhalten. Dieses Fragment kann in künftigen Untersuchungen dazu verwendet werden, die Funktionalität der Proteinfamilie näher zu untersuchen und die dreidimensionale Struktur der hochkonservierten C-terminalen Domäne aufzuklären.

Chapter 1

Introduction

For centuries it was believed that aging, senescence and death are inevitable bad destinies without any benefit for the organism or the whole community, and that these processes mainly occur after the organism has passed the reproductive state (Weissmann 1891). However, death is far from being restricted to old cells or tissues. We now know that death even occurs in embryonic cells, e.g. during the development of the xylem in plants (Greenberg 1996) or the differentiation of bones in animals (Olsen et al. 2000). Controlled cell death is also highly important in the adaptation against diseases and parasites (Lam et al. 2001). The benefits of cell death for the organism become even more clear when analyzing cells with genetic defects that disregulate the cell death response. These cells very often undergo uncontrolled proliferation or premature cell death, which can lead to cancer, autoimmune diseases or neurodegeneration (Fesik 2005). Due to all of these important functions and the fact that the cell death programs are genetically determined, cell death is now recognized to be an essential process for life. Therefore, it became of special interest for the biological and medical community, to understand how organisms control and execute this programmed cell death.

1.1 Programmed cell death

At least two different cell death processes can be distinguished. On the one hand, cell death occurs in response to exogenous factors such as trauma, diseases or toxins. This accidental cell death is known as 'necrosis' and is characterized by swelling and rupture of the cell and release of the cytoplasmic content (Krysko et al. 2008). On the other hand, a genetically determined cell suicide program exhibiting a multitude of important functions in animals and plants shows completely different characteristic features. The cell shrinks by blebbing of the plasma membrane and shows nuclear fragmentation, chromatin condensation and inactivation of the DNA-repair enzyme PARP (poly-ADP-ribose-polymerase) (Ameisen 2002). This and the activity of endonucleases lead to the formation of DNA fragments that can be visualized as a ladder-like pattern on an agarose gel. Apart from this, programmed cell death in contrast to necrosis requires ATP (Nicotera et al. 1999), and the phosphatidyl

serine is relocated to the outer side of the plasma membrane (Schlegel and Williamson 2001). These characteristics of a cell undergoing programmed cell death can be found in both plant and animal cells.

It is hypothesized that programmed cell death (PCD) was invented during evolution as a response to viral infections, where it provides a mechanism to limit viral replication and propagation to the surrounding cells (Ameisen 2002). Host-parasite interaction might therefore have provoked the development of the diverse molecular machinery of PCD in both plants and animals. Even in unicellular bacteria and yeast examples for controlled cell suicide can be found. However, most of the studies on the molecular mechanism underlying programmed cell death were so far carried out in the mammalian system.

The well described programmed cell death in animals is a sequence of events, summarized under the term 'apoptosis', and can be triggered by external factors as well as internal programming. The key regulators are specific cysteine proteases, called caspases, that cleave substrates at aspartic acid residues. Known substrates are other caspases, DNA repair enzymes, lamins in the nuclear envelope, cytoskeletal proteins and many other cellular proteins that usually prevent the cell from apoptosis (Riedl and Shi 2004). Caspases are localized in the cytosol as inactive proenzymes. Cell death signals lead to cleavage of these precursors, oligomerization and activation, which is usually prevented by inhibitor of apoptosis proteins (IAPs, Bader and Steller (2009)) or members of the BCL-2 family (Youle and Strasser 2008). For example, some members of the BCL-2 protein family also prevent disruption of the mitochondrial membrane, as release of cytochrome c from the mitochondria also triggers the caspase cascade. However, the BCL-2 family also contains proapoptotic members such as Bax and Bak that induce the release of apoptotic proteins from mitochondria. This clearly demonstrates the high complexity of the molecular mechanism underlying programmed cell death, still giving only a glance on what is known in animals so far.

1.1.1 Programmed cell death in plants

In contrast to animals, the molecular events occurring during the programmed cell death in plants are largely unknown. Although examples for homologues of mammalian apoptotic proteins exist in plants, such as Bax inhibitor-1 (Sanchez et al. 2000), PIRIN, known to stabilize complexes of apoptotic proteins (Orzáez et al. 2001), and Apoptosis inducing factor AIF (Lorenzo et al. 1999), only very few were identified so far. Genomic sequencing of many plant species revealed that the classic vertebrate caspases are apparently missing. The plant genome encodes distant homologues of caspases, called metacaspases, that regulate PCD but do not exhibit a caspase-specific proteolytic function (Watanabe and Lam 2005). Still, PCD can be prevented by caspase inhibitors (Lam and Del Pozo 2000), suggesting that cell death mechanisms similar to the animal apoptosis exist in plants. Only recently a caspase-like protein, called phytaspase has been identified in tobacco, which is an aspartate-specific protease that is synthesized as a proenzyme and essential during PCD responses to abiotic and biotic stresses (Chichkova et al. 2010).

Plant cells undergoing programmed cell death show the same DNA laddering, induction

of proteases, membrane blebbing and relocation of phosphatidyl serine to the outer face of the plasma membrane as observed in mammalian cells. Expression of mammalian antiapoptotic proteins in tobacco increased resistance to pathogens that would usually lead to a hypersensitive response, a special form of plant programmed cell death (Dickman et al. 2001). However, the observations made so far do not definitely prove that both plants and animals share common cell death mechanisms.

At least two different types of programmed cell death can be distinguished in plants. On the one hand, the hypersensitive response to pathogens is a very rapid and transient process, which destroys the infected tissue and protects the rest of the plant from pathogen spread. This fast cell suicide program exhibits several characteristic features, such as ion fluxes, changes in protein phosphorylation and release of reactive oxygen species (Mur et al. 2008).

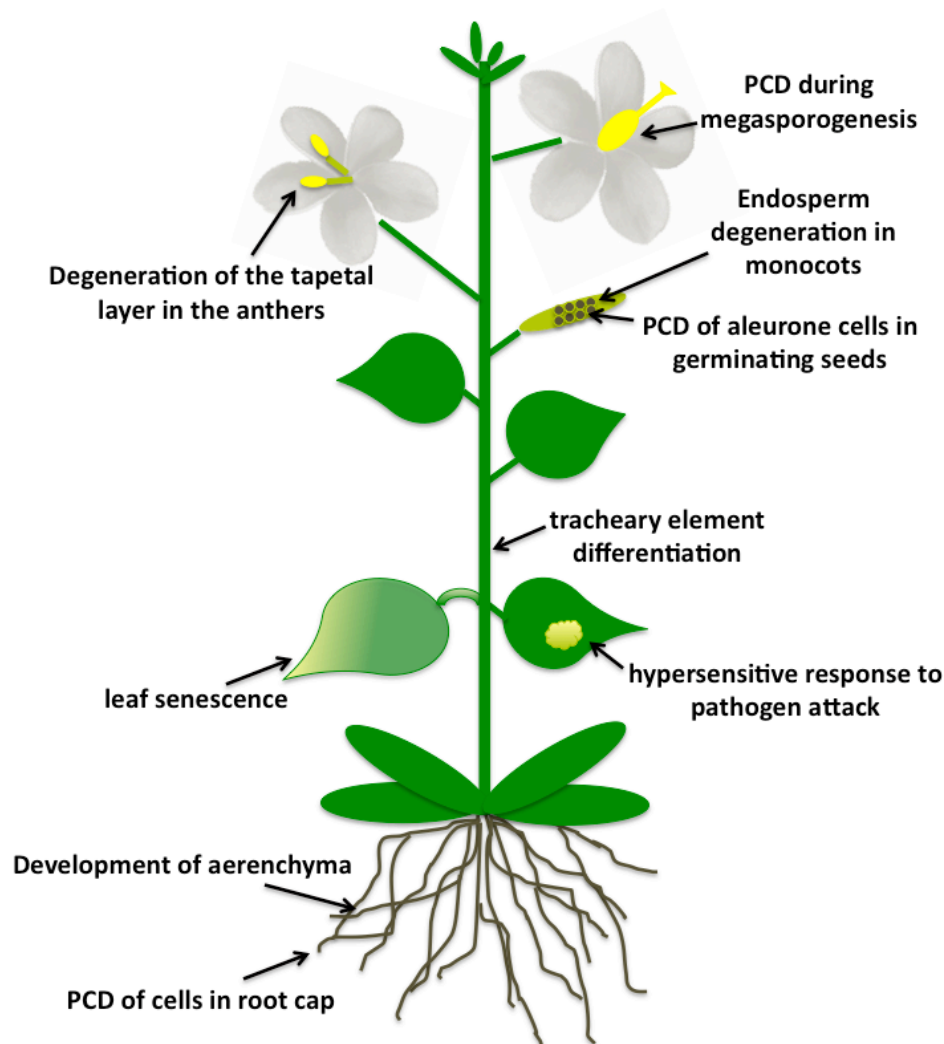


Figure 1.1: Events of programmed cell death occurring through the life cycle of a plant

On the other hand, there are slower forms of programmed cell death occurring during the development of the plant. The most obvious of these slower cell death processes is the senescence of leaves, flower parts and, in the case of annual species, the whole plant. Thus, resources can be recycled by redistribution to younger leaves and reproductive organs. Yet, PCD plays important roles throughout the plant life cycle. The aleurone cells die in the process of germination (Fath et al. 2002). The development of the xylem involves secondary wall thickening and death of the protoplast (Turner et al. 2007). PCD also occurs in the abscission of siliques or during the development of the megaspore. Other examples for programmed cell death events during plant development are summarized in Figure 1.1. As described for the hypersensitive response, programmed cell death during plant development is also induced by reactive oxygen species (Gechev et al. 2006). Apart from this, it is highly regulated on the transcriptional level and by other intercellular signals, such as changes in the plant hormone composition or posttranslational modifications of proteins, e.g. via phosphorylation or ubiquitylation.

1.2 Posttranslational modification with ubiquitin

The dynamics and diversity of the proteome are highly extended by the huge variety of posttranslational modifications occurring in a cell. In addition to the attachment of phosphate, methyl or acetyl groups, the eukaryotic cell has established a mechanism to covalently attach small proteins to certain substrates. At the beginning of the 1980s the first such small protein modifier was described by Aaron Ciechanover, Avram Hershko and Irwin Rose and was named ubiquitin (Ciechanover et al. 1980; Hershko et al. 1981). Due to its vital role in the physiology of cells and organisms, its discovery was of such a great importance for the scientific world that the investigators were rewarded with the Nobel Prize for Chemistry in 2004.

1.2.1 Ubiquitin: structure and function

Ubiquitin consists of 76 amino acids and is the most structurally conserved of all known eukaryotic proteins. In all higher plants, the amino acid sequence of ubiquitin is identical and differs only by one residue from the protein of *Chlamydomonas*, by two residues from the sequence of *Saccharomyces cerevisiae* and by three from animal ubiquitin (Callis et al. 1995).

The three-dimensional structure of ubiquitin is formed by a five-strand β sheet surrounding a diagonally orientated α helix (Fig. 1.2). This so-called ubiquitin superfold is also found in other related protein modifiers such as SUMO or NEDD8/Rub1, although these proteins show only low overall sequence similarity compared to ubiquitin. Even prokaryotes possess proteins bearing a ubiquitin fold, which are therefore the potential ancestors of ubiquitin. Still, they do not share the same function in acting as a signal by covalent attachment to a certain substrate. Instead, two of such ubiquitin fold proteins in bacteria, Moad (Lake

et al. 2001) and ThiS (Wang et al. 2001), catalyze the insertion of sulfur into the cofactors molybdopterin and thiamin, respectively.

Apart from its typical fold, ubiquitin possesses a flexible C-terminus, which is terminated by a Gly-Gly motif. The last glycine residue (G76) forms an isopeptide bond with the ϵ -amino group of an internal lysine residue of a substrate.

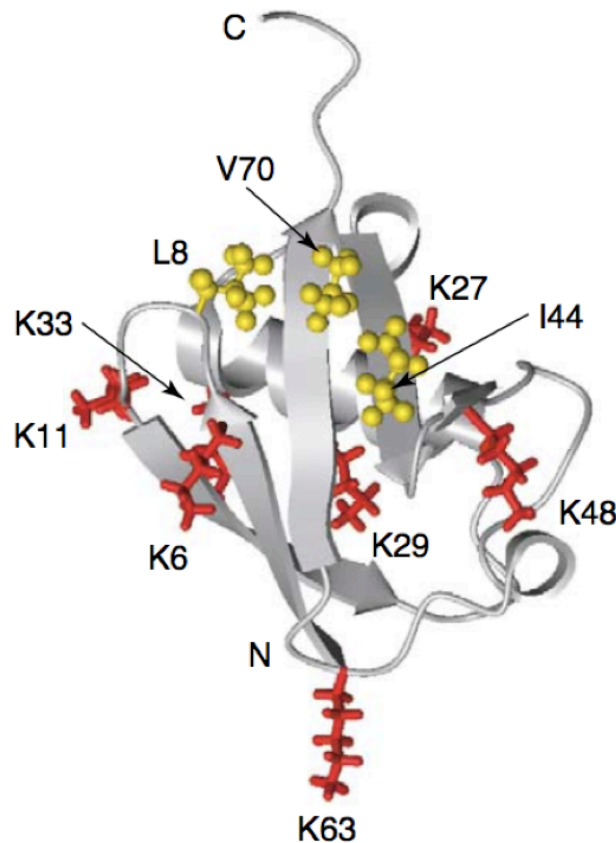


Figure 1.2: Structure of Ubiquitin. The ubiquitin fold is formed by a five-stranded β sheet and an α helix lying inbetween (grey). The seven lysine residues are shown in red and the hydrophobic residues on the surface important for the interaction with multiple Ub-binding domains (Mueller et al. 2004) are shown in yellow. Image taken from Pickart and Fushman (2004).

Ubiquitin itself possesses seven lysine residues (K6, K11, K27, K29, K33, K48 and K63, Fig. 1.2), which can be covalently bound by a second ubiquitin molecule. Thus, a huge variety of theoretical configurations of polyubiquitin chains can be formed, e.g. 7 forms of diubiquitin and 70 forms of triubiquitin (Xu et al. 2009). This holds an extensive number of possible signals that can be distinguished within the cell. Quantitative proteomics in *Saccharomyces cerevisiae* have revealed that all lysine residues are used for chain formation *in vivo* (Xu et al. 2009). In *Arabidopsis thaliana* recent mass spectrometric analysis of ubiquitylated proteins have identified substrates modified with ubiquitin chains using six of the seven lysine residues for chain formation (Saracco et al. 2009). Only K27 linkages

could not be detected, which might be because the ϵ amino group of K27 is most difficult to access by ubiquitin ligases.

Ubiquitylated substrates are sorted into different cellular pathways and the length and linkage of the ubiquitin chain determines the fate of the substrate. The most abundant ubiquitin signal within all eukaryotic cells is a K48-linked polyubiquitin chain, which is well described to target the substrate for protein degradation via the 26 S proteasome (Chau et al. 1989). Still, there are exceptions where K48 chains do not lead to degradation but regulate the activity of the substrate, e.g. of the transcription factor Met4 in *S. cerevisiae*, which activates genes in the methionine biosynthesis pathway (Kuras et al. 2002).

In contrast, K63 ubiquitin chains have many non-proteolytic functions in several distinct pathways, such as DNA damage tolerance (Spence et al. 1995), hormone signaling (Yin et al. 2007), ribosomal protein synthesis (Spence et al. 2000) and endocytosis (Mukhopadhyay and Riezman 2007), but clear evidence for them being involved in proteasomal degradation *in vivo* is still missing (Xu et al. 2009).

Other more unconventional polyubiquitin chains linked through K6, K11, K29 and K33 were shown to be involved in proteasomal protein degradation in *S. cerevisiae* (Xu et al. 2009). Apart from that, K29 polyubiquitin chains attached to the Notch signaling modulator DTX lead to degradation of the substrate via the lysosome (Chastagner et al. 2006). Together with K33-linked chains K29 chains were also described to regulate the activity of two AMPK-related kinases (Al-Hakim et al. 2008).

K6 polyubiquitin chains can be assembled by the BRCA1/BARD1 complex and are recognized by the proteasome. Still, in contrast to substrates marked by K48 chains, K6-polyubiquitylated BRCA1 is rather stabilized than degraded (Wu-Baer et al. 2003). The anaphase promoting complex (APC) is a RING E3 ligase that triggers, apart from several nonproteolytic functions, protein degradation to promote cell cycle progression. It has been shown that the APC induces protein degradation preferentially by assembling K11-linked chains rather than K48-linked chains. K11-linked chains lead to efficient proteasomal degradation both *in vivo* and *in vitro* (Jin et al. 2008). *In vitro* studies also revealed that even more complex ubiquitin polymers using different linkages can be attached to certain substrates (Kirkpatrick et al. 2006). A mass spectrometric analysis in *Arabidopsis* raises the possibility that these ubiquitin polymers also occur *in planta* (Saracco et al. 2009).

Apart from this huge variety of protein modifications via polyubiquitin chains, several proteins are modified by just a single ubiquitin molecule. This monoubiquitylation is involved in several cellular processes, such as histone modification, endocytosis and the release of retroviruses from the plasma membrane (Hicke 2001).

To ensure the production and the metabolism of this huge variety of ubiquitin-protein conjugates an enormous machinery of enzymes is acting within the cell.

1.2.2 The ubiquitin conjugation cascade

Ubiquitin is attached to substrates via an enzymatic cascade involving three different classes of enzymes (Fig. 1.3.)

First, the C-terminus of ubiquitin has to be activated to be able to attack an amino group

of a substrate. This step is mediated by the ubiquitin activating enzyme or E1 and requires ATP. Initially a ubiquitin-adenylate intermediate is formed, which reacts with a cysteine residue of the E1 enzyme to form an E1-ubiquitin thioester. It could be shown for the mammalian enzyme, UBA1, that the E1 becomes asymmetrically loaded with two ubiquitin molecules at two different active sites. While one molecule is covalently bound to the active cysteine residue, a second ubiquitin is adenylated at a different catalytic site (Haas et al. 1982).

In a second step, ubiquitin is transferred from the E1 to an active cysteine residue within a highly conserved domain (UBC domain) of the ubiquitin conjugating enzyme or E2 by transthioylation. An HPN tripeptide (histidine-proline-asparagine) at the N-terminal side of the active cysteine and a tryptophan residue on the C-terminal side, which has been shown to make contact to the third member of the ubiquitylation cascade, the E3 ligases, are general signatures of this UBC domain (Michelle et al. 2009). The double loading of the E1 seems to be important for the transfer of ubiquitin to the UBC domain of the E2, as this step can be accelerated by adding adenylated ubiquitin (Pickart et al. 1994). Apart from that, doubly loaded E1 enzyme shows a much higher affinity to the E2 in nanomolar ranges compared to unloaded enzyme, which can be very easily separated from the E2 by gel filtration (Schulman and Harper 2009). The docking site for the E1 enzyme on the E2 overlaps with the docking site of the E3 enzyme or ubiquitin ligase. Therefore the E2 has to shuttle between both partners during one reaction cycle (Eletr et al. 2005). Apart from influencing the specificity of the target, the E2 can also determine the type of ubiquitylation. For example, UBC13 type E2 enzymes are specifically attaching K63 polyubiquitin chains to the targets with the help of an Ub-E2 variant (UEV) called MMS2 (Hofmann and Pickart 1999). These UEVs contain the conserved UBC domain but lack the active site cysteine. The third group of enzymes in the ubiquitin conjugation cascade, the E3 ligases, directly interacts with both the E2 and the substrate and thereby confirms together with the E2 the specificity of the substrate. According to the different transfer mechanisms we can distinguish between two different classes of E3 ligases (Fig. 1.3). The HECT (**h**omologous to **E6-associated protein C-terminus**) ligases have a direct role in catalysis by first transferring ubiquitin from the E2 to an internal cysteine residue within the conserved HECT domain and then further attaching it to a lysine residue of the substrate.

In contrast, the RING (**r**eally **i**nteresting **n**ew **g**ene) and RING-like or U-box E3s, the latter possessing a modified RING domain not binding Zn^{2+} , facilitate ubiquitylation of the substrate by bringing the E2 and the substrate into closer contact. Then ubiquitin is transferred directly from the E2 to the substrate. RING ligases can either act as monomers, such as Mdm2, a negative repressor of the tumor suppressor p53 (Thut et al. 1997), or they are part of large multi-protein complexes, such as the anaphase-promoting complex (Eloy et al. 2006).

Although the three common members of the ubiquitylation cascade have been identified, the fundamental mechanism of the assembly of ubiquitin chains is still unknown. Ubiquitin molecules can either be attached to the growing chain on a substrate one at a time, or polyubiquitin chains are first assembled on the E2 (or the E3 in the case of HECT ligases) and are then repositioned onto the substrate (Hochstrasser 2006).

There are also exceptions to this standard ubiquitylation cascade. *In vitro* it could be shown that substrates can be monoubiquitylated without the help of an E3 (Hoeller et al. 2007). This process only requires a substrate possessing a ubiquitin-binding domain. This domain can then bind to a ubiquitin molecule that is attached to the catalytic cysteine residue of the E2, and ubiquitin is directly transferred to a lysine residue of the substrate. Finally, the presence of a multitude of deubiquitylating enzymes (DUBs) that are able to cleave ubiquitin moieties from the substrate proves once more that ubiquitylation is a highly fine-tuned reversible posttranslational modification that is comparable to other regulatory processes, such as phosphorylation.

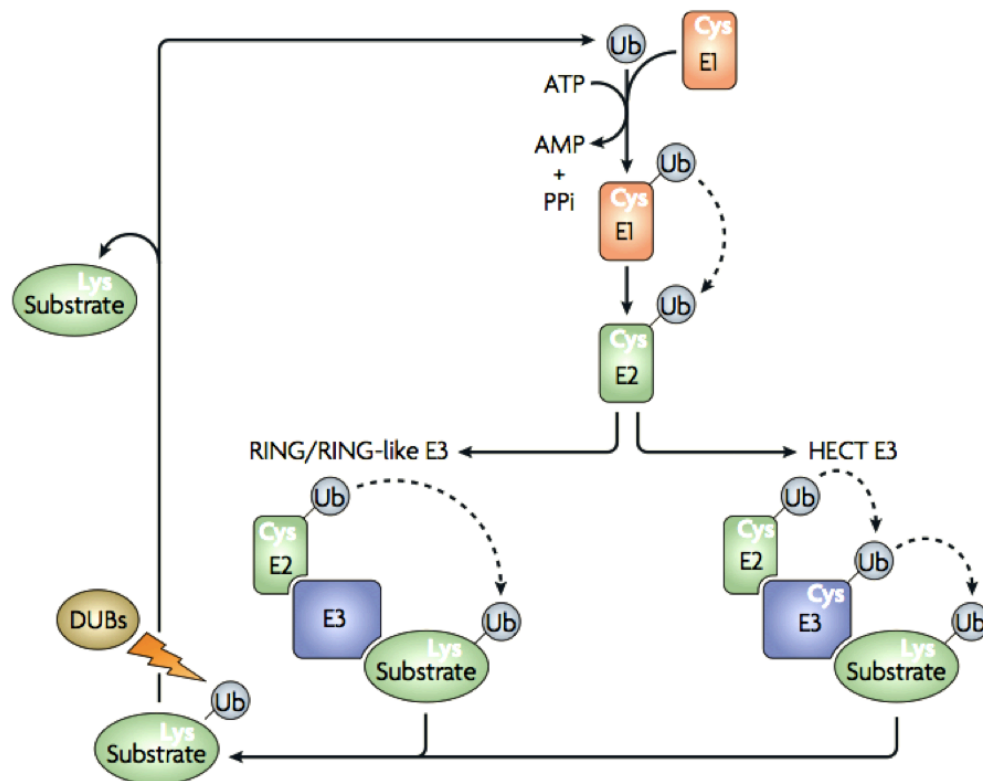


Figure 1.3: The ubiquitin conjugation cascade. Ubiquitin (grey) is activated by the use of ATP and forms a thioester with an internal cysteine residue of the ubiquitin activating enzyme (E1, in red). From there, it is further transferred to the catalytic site of the ubiquitin conjugating enzyme (E2, in green). The third step is catalyzed by the ubiquitin ligases (E3, in blue), which directly bind to the substrate. We distinguish between two different classes of E3 enzymes. In the case of the HECT ligases, ubiquitin is first transferred from the E2 to a cysteine residue within the HECT domain of the ligase and from there it is attached to a lysine residue of the substrate. In contrast to this, the RING/RING-like E3s form a scaffold to bring the E2 and the substrate into close proximity. Then ubiquitin is directly transferred from the E2 to the substrate. Ubiquitylation is a reversible process, as deubiquitylating enzymes (DUBs, in brown) are able to cleave ubiquitin from other proteins. Image taken from Ravid and Hochstrasser (2008).

1.2.3 The 26S Proteasome

Regulatory, misfolded or damaged proteins can be marked by a ubiquitin chain longer than four ubiquitin moieties and in most of the cases linked via lysine 48, which targets them for degradation via the 26S proteasome. This large ATP-dependent protease can be found in the nucleus and cytosol of both plant and animal cells (Vierstra 1996).

Although multiple isoforms of the proteasome have been identified in plants (Yang et al. 2004), the standard design of this particle consists of at least 33 subunits that are forming a cylindrical multicomplex of approximately 2.5 MDa (Schrader et al. 2009). In the absence of ATP, this complex dissociates into two subcomplexes, the 20S core particle and the 19S regulatory particle (Fig. 1.4, panel A).

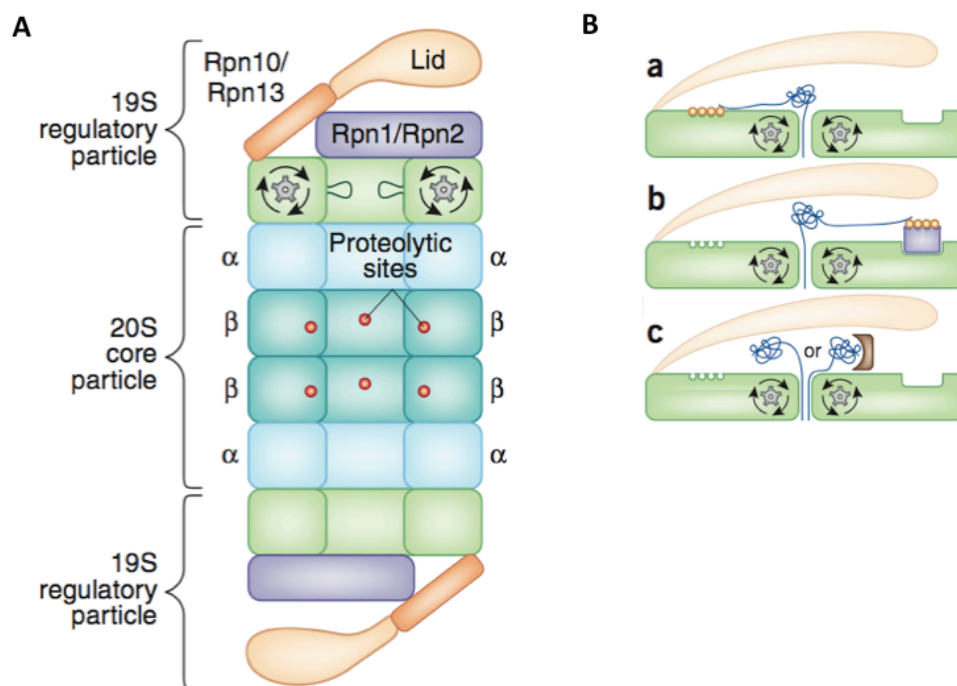


Figure 1.4: A: Structure of the 26S proteasome. B: Different mechanisms of the proteasome to recognize substrates. a – The ubiquitin chain linked to the substrate binds to the subunits Rpn10 and Rpn13 of the 19S regulatory particle. b – Special adaptor proteins bind to both the ubiquitin chain of the substrate and the 19S regulatory particle. c – Substrates lacking a ubiquitin chain directly bind to the regulatory particle either without (left side) or with (right side) the help of adaptor proteins. Image taken from Schrader et al. (2009)

Four heptameric rings are forming the 20S core particle (blue). The outer two rings are assembled by seven α subunits (light blue) and the two central rings by seven related β subunits (dark blue). The α ring forms a small channel of about 13 Å, so that only previously unfolded proteins are able to enter the core particle (Groll et al. 2000). The inner β rings contain different proteolytic functions (red dots), such as peptidylglutamylpeptide-

hydrolyzing, trypsin-like and chymotrypsin-like activities, so that they are able to break all kinds of peptide bonds (Voges et al. 1999).

The 19S regulatory particle consists of 19 subunits and can be subdivided into the lid (orange) and the base (green and purple), the latter containing a ring of six AAA-ATPases (grey wheels). It associates to one or both ends of the core particle and regulates substrate recognition, unfolding and translocation of the protein to the proteolytic chamber (Finley 2009).

Substrates of the proteasome can be recognized via different mechanisms (Fig. 1.4, panel B). On the one hand a protein can directly bind to certain subunits of the 19S regulatory particle, such as Rpn10 (Deveraux et al. 1994) and Rpn13 (Husnjak et al. 2008), via the attached ubiquitin chain (a). Apart from that, special adaptor proteins that bind both the ubiquitin chain and the proteasome can direct the substrate to the proteasome (b). Finally, some proteins are targeted to the proteasome without being bound to a ubiquitin chain (c). This has been documented for the mammalian ornithine decarboxylase (Murakami et al. 1992). The variety of different recognition mechanisms provided by the 26S proteasome demonstrates once again the complexity and specialization of the ubiquitin-proteasome system.

1.2.4 The orchestra for ubiquitylation in *Arabidopsis thaliana*

In *Arabidopsis thaliana* more than 1700 genes corresponding to nearly 6 % of the proteome were identified to be involved in the production and metabolism of the ubiquitylation machinery (Vierstra 2009). This exceeds the portion of phosphorylation in both extent and consequences and underlines the importance of this modification in plants.

Ubiquitin genes

Like in all other eukaryotes ubiquitin is synthesized from fusion-protein precursors and is therefore unique among plant proteins. The transcripts contain either ubiquitin polymers, in which each gene is expressed head-to-tail to the next ubiquitin gene, or ubiquitin is fused to the 5' end of a different coding region. *Arabidopsis* expresses polyubiquitin genes of 3, 4, 5 and 6 single ubiquitin coding regions (Callis et al. 1995). In the fusion proteins ubiquitin is attached to one of the two different ribosomal subunits or to the small ubiquitin-like modifier RUB1 (related to **u**biquitin).

To provide the cell with the necessary pool of ubiquitin molecules, several polyubiquitin genes and all ubiquitin fusion genes are expressed at the same time and deubiquitylating enzymes cleave the single ubiquitin moieties from the precursor proteins. Despite the huge variety of ubiquitin precursor proteins, each coding region results in the same protein sequence of 76 amino acids.

Ubiquitin activating enzymes

As E1 enzymes in general have little impact on substrate specificity, *Arabidopsis* contains only two E1 proteins, UBA1 and UBA2. Expression studies showed that these enzymes are co-expressed in all tissues and cells observed and the encoded proteins seem to bear similar enzymatic properties (Hatfield et al. 1997). This suggests that the two homologues have redundant functions in *Arabidopsis* in contrast to the mammalian E1 enzymes, which recognize and load different E2 enzymes (Jin et al. 2007). However, a deletion in the *Arabidopsis* UBA1 gene leads to suppression of the constitutive resistance phenotype observed for the *suppressor of npr1-1 constitutive 1* (*snc1*) mutant. In contrast, a mutation of UBA2 does not suppress *snc1* (Goritschnig et al. 2007). The deletion mutant of UBA1 is also more sensitive to a virulent pathogen and is impaired in the hypersensitive response to avirulent bacteria. This suggests that at least in the disease resistance these two proteins possess different functions.

Ubiquitin conjugating enzymes

In contrast to the small family of E1 enzymes in *Arabidopsis*, the number of ubiquitin conjugating enzymes is predicted to be with 37 family members much higher (Kraft et al. 2005), demonstrating the impact of this component of the ubiquitylation cascade on target specificity and ubiquitylation type. A recent phylogenetic approach comparing the protein family of ubiquitin conjugating enzymes in seven different model organisms throughout the whole eukaryotic kingdom (*Homo sapiens*, *Mus musculus*, *Drosophila melanogaster*, *Caenorhabditis elegans*, *Schizosaccharomyces pombe*, *Saccharomyces cerevisiae* and *Arabidopsis thaliana*) has revealed that the *Arabidopsis* genome is the richest of all in E2 genes, again stressing the importance of the ubiquitylation pathway in plants (Michelle et al. 2009). The whole family of ubiquitin conjugating enzymes in *Arabidopsis* can be divided into 12 subfamilies, 3 of them possessing no closer homologue in *Saccharomyces cerevisiae* (Bachmair et al. 2001). All of these proteins contain the highly conserved 150 amino acid catalytic core domain, the UBC domain (Inter-Pro IPR000608), bearing the active site cysteine for ubiquitin binding. Whereas most of the family members in *Arabidopsis* consist of only this core domain, some contain either a C-terminal extension, which might be important for localization, or an N-terminal extension. Only one group of E2 enzymes exhibits both an unusually large N-terminal extension and an additional C-terminal domain. These extraordinary proteins are the main subject of this thesis and are further described in chapters 1.4, 2 and 3.

Until now, 16 of the E2 enzymes of *Arabidopsis* have been characterized biochemically to be functional ubiquitin conjugating enzymes either through their ability to form a ubiquitin thioester or to catalyze E1-dependent ubiquitylation (Kraft et al. 2005). Still, only little is known about the actual function and specificity of the E2s *in planta*, mainly because mutants of the respective proteins have only been poorly analyzed so far. Apart from that, expression studies on the mRNA levels of the E2s (Kraft et al. 2005) and the microarray data available at Genevestigator (Zimmermann et al. 2004) show a broad expression of the

genes with no specific regulation or expression in any tissue or developmental stage, again giving no indication for a particular function.

Ubiquitin ligases

In contrast to the ubiquitin conjugating enzymes, much more is known about the specific function of ubiquitin ligases *in planta*, which are clearly the key factors to define substrate specificity. With around 1300 genes encoding for ubiquitin ligase components, they exhibit the highest portion of the genome compared to E1 and E2 enzymes (Smalle and Vierstra 2004). Also in *Arabidopsis* we can distinguish between two groups of E3 ligases. On the one hand, only seven genes encode proteins bearing a HECT domain for E2 binding (Bachmair et al. 2001), whereas on the other hand more than 60 U-box-type and more than 475 RING E3 ligases are predicted (Stone and Callis 2007), showing the major role of this type of ligase in plant ubiquitylation.

Arabidopsis possesses both monomeric E3 ligases, such as PRT6 (Garzón et al. 2007) involved in the N-end rule pathway, and multisubunit ligase complexes, such as the Anaphase Promoting Complex (Capron et al. 2003) or the Cullin RING ligases (Schwechheimer and Villalobos 2004), whose domains to bind the substrate and the E2 lie on separate proteins. The Cullin RING ligases consist of a Cullin protein, which forms a scaffold to bind a RING protein at its C-terminus for E2 interaction and a substrate recognition module at its N-terminus. In the case of Cullin 1 based E3 ligases, this substrate recognition part consists of the **A**rabidopsis **S**uppressor of **K**inetochores **P**rotein 1 (ASK1) and a specific F-box protein, which directly interacts with the substrate. The gene family encoding F-box proteins is with more than 700 members the largest gene family in *Arabidopsis*. In contrast, humans only possess 68 and mice only 74 genes encoding F-box proteins. This demonstrates that the ubiquitin proteasome system is highly expanded and diverse especially in plants, which makes a functional analysis based on known mammalian proteins difficult. Most proteins involved in ubiquitylation in plants seem to exhibit a plant-specific function, because obvious counterparts are missing in other eukaryotes (Vierstra 2009).

Deubiquitylating enzymes

Deubiquitylating enzymes (DUBs) are essential to recycle ubiquitin moieties during the degradation of polyubiquitylated proteins. Apart from this, they also exhibit regulatory functions as they can reverse a ubiquitin signal during specific processes. This was for example described for the DUBs UBP3 and UBP4 that are critical during the pollen development in *Arabidopsis* (Doelling et al. 2007). *Arabidopsis thaliana* contains at least 30 genes encoding putative DUBs (Smalle and Vierstra 2004). These can be subdivided into three different groups. The group of ubiquitin carboxyl-terminal hydrolases contains only two members in *Arabidopsis*, whereas the second group is represented by only one protein called RPN11, which is found in the lid of the 26S proteasome. The third and largest group of DUBs consists of 27 ubiquitin-specific thiol proteases that are called UBPs. This variety of deubiquitylating enzymes in *Arabidopsis* that make ubiquitylation a reversible

process, further expands the possibilities of the ubiquitylation machinery in controlling and conducting a multitude of plant processes.

1.3 Ubiquitylation in programmed cell death

As described in chapter 1.1, programmed cell death is an active process that can be triggered by external and internal factors and is highly regulated on the transcriptional and posttranslational level. The enormous influence of the posttranslational modification via ubiquitin on the regulation of programmed cell death has been repeatedly reported in both mammals and plants. Still, the first connection between apoptosis and the ubiquitylation machinery was made when detecting an increased expression of ubiquitin and the proteasome in muscle cells of the Hawkmoth *Manduca sexta* undergoing programmed cell death (Schwartz et al. 1990).

As to date much more is known about the process of apoptosis in mammals, many more examples for the involvement of ubiquitin in PCD have been described in mice and human cells. Especially the degradation of important regulators through the ubiquitin-proteasome system seems to be a common mechanism to induce or inhibit programmed cell death. Maybe the most famous of such regulators degraded by the ubiquitin-proteasome system is the tumor suppressor p53. It is a transcription factor inducing the expression of a variety of proapoptotic genes. The RING ubiquitin ligase Mdm2 is responsible for the degradation of p53 and is therefore an important negative regulator of apoptosis (Fang et al. 2000).

Apart from this, several other pro- and antiapoptotic proteins, such as the inhibitor of apoptosis proteins (IAPs), have been described to be regulated via the ubiquitin-proteasome system (Jesenberger and Jentsch 2002). Apart from their baculovirus inhibitor of apoptosis repeat (BIR) motif many of these proteins also exhibit a RING domain (Srinivasula and Ashwell 2008). One protein of the IAP family, BRUCE/Apollon, has even been described to possess both E2 and E3 function itself and will be the main topic in Chapter 1.4.3.

Also in plants, several examples are known to date that directly connect the ubiquitylation process with programmed cell death. Inhibition of the ubiquitin-proteasome machinery, either via expression of a mutated form of ubiquitin (Becker et al. 1993; Schlögelhofer et al. 2006) or via downregulation of subunits of the proteasome (Kim et al. 2003), has been shown to induce programmed cell death in *Arabidopsis thaliana* and *Nicotiana benthamiana*, respectively. Both slow cell death processes in plants, such as leaf senescence, and fast cell death responses, such as the hypersensitive response to pathogens, involve members of the ubiquitin machinery.

Mutation of the F-box protein ORE9 for example leads to a delayed age-dependent, dark-induced or phytohormone-induced senescence, showing that this protein is a positive regulator of the senescence process (Woo et al. 2001). A second protein described to be a positive regulator of the slow programmed cell death during senescence is the arginyl-tRNA:protein arginyl transferase encoded by the gene *AtATE1*. This protein is a component of the N-end rule pathway and transfers arginine to the N-terminus of certain substrates, which leads to degradation via the proteasome. Plants with a mutation in this protein also

show a delayed age-dependent and dark-induced leaf senescence and are therefore called *delayed leaf senescence1* (*dls1*) mutants (Yoshida et al. 2002). A third example of a protein regulating senescence via the ubiquitin-proteasome system is the Senescence-associated E3 ubiquitin ligase 1 (SAUL 1). However, in contrast to *ore9* and *dls1* mutant plants, *saul 1* mutants show a premature cell death under low light conditions, indicating that this protein is a negative regulator of plant senescence (Raab et al. 2009).

The hypersensitive response to pathogen attack is a fast cell death program, which is also known to be impaired in plants with a defective ubiquitin-proteasome pathway. Tobacco plants expressing a ubiquitin variant with a lysine to arginine exchange at position 48 have been described to be less sensitive to treatment with tobacco mosaic virus (Becker et al. 1993). Apart from that, the ubiquitylation machinery is also used during the hypersensitive response of monocots. Protein polyubiquitylation has been shown to be upregulated in the defense response of barley to a mildew fungus (Dong et al. 2006). This might be explained by the fact that regulated proteolysis of both endogenous and pathogen-produced proteins can contribute to the defense response.

In addition, to date several single components of the ubiquitin machinery have been described to be directly involved in the regulation of the hypersensitive response to pathogens. The E3 ubiquitin ligase Plant U-box 17 (PUB17) from *Arabidopsis* and its homologues in tobacco and tomato are required for the induction of programmed cell death during the hypersensitive response (Yang et al. 2006). A second example for a protein of the ubiquitin-proteasome system regulating PCD in the hypersensitive response is the U-box protein Spotted Leaf 11 (SPL11) in rice. It also exhibits E3 ligase activity but is in contrast to PUB17 a negative regulator of the programmed cell death response to pathogens. The *spl11* mutant shows spontaneous cell death events and enhanced resistance to rice fungal and bacterial pathogens (Zeng et al. 2004).

On the other hand, bacterial proteins are shown to interact with the ubiquitin system of the plant and by this to inhibit the hypersensitive response. The protein AvrPtoB of *Pseudomonas syringae* for example is introduced into plant cells and possesses E3 ligase activity. It is therefore able to ubiquitylate substrates directly involved in the regulation of PCD. Mutations in this protein lead to a decreased virulence of the bacterial pathogen (Janjusevic et al. 2006). Several additional examples are known to date and show that the ubiquitin-proteasome pathway seems to be a favorable target for pathogen effectors, which manipulate the host protein degradation machinery as a virulence strategy (Zeng et al. 2006).

The competition between plants and pathogens might therefore be a major driving force for the development of the manifold and highly expanded ubiquitylation system in plants.

1.4 The PFU proteins in *Arabidopsis thaliana* and their mammalian homologues

Due to the multitude of proteins involved in the ubiquitylation processes in plants, the function of the majority of the components has not been identified so far. Especially the function of the ubiquitin conjugating enzymes in plants has only been poorly analyzed. A family of four unusually large ubiquitin conjugating enzymes in *Arabidopsis thaliana* has been specified to possess, apart from the typical UBC domain, an unusually large N-terminal extension and also an additional C-terminal domain and therefore represents an exception in the family of UBC proteins (Bachmair et al. 2001). Only one member of this family has been described so far to be involved in phosphate signaling and is named PHO2 (Bari et al. 2006). As the other three family members possess a structure related to PHO2 (*At2g33770*, UBC24), these proteins were designated PFU1 (*At3g15355*, UBC25), PFU2 (*At2g16920*, UBC23) and PFU3 (*At1g53020*, UBC26) for PHO2 family ubiquitin conjugating enzyme. To date nothing is known about the actual function of the PFU proteins in plants, and a first attempt to prove the function of PHO2 and PFU1 as ubiquitin conjugating enzymes via *in vitro* thioester formation experiments has failed because both proteins turned out to be insoluble when recombinantly expressed in *E. coli* (Kraft et al. 2005). However, homologues of PHO2 and its closest relative PFU2 could be found in higher eukaryotes and have already been described in the literature. The following chapters therefore summarize what is known about PHO2 in phosphate signaling and the function of its mammalian homologues.

1.4.1 PHO2 and its role in phosphate signaling

The locus of *PHO2* was first described when analyzing the inorganic phosphate (P_i) content of *Arabidopsis* mutants obtained via ethyl methylsulfonate (EMS) mutagenesis (Delhaize and Randall 1995). Under high transpiration rates, the leaves of the *pho2* mutants become necrotic, which is a sign for P_i toxicity. The *pho2* mutant accumulates 2- to 5-fold more P_i in shoots than wild type plants whereas the content in roots remains the same. This phenotype could also be observed for plants that constitutively express miRNA399 (Fujii et al. 2005). The P_i content of the shoots is more than two times higher than in wild type plants, and under a high transpiration rate the margins of the leaves become necrotic. In contrast to wild type plants, the mRNA of *PHO2* is not detectable at all in these miRNA399 overexpressing lines, suggesting that miRNA399 directly regulates the *PHO2* transcript. In wild type plants miRNA399 is induced by low P_i , whereas the *PHO2* mRNA is suppressed. Five target sites for miRNA399 were identified in the 5' UTR of *PHO2* and are necessary for the suppression of PHO2 under low P_i (Fujii et al. 2005). These observations suggest that miRNA399 expression enhances the P_i uptake from the roots into the shoots by suppressing PHO2, which seems to be a negative regulator of this process. The negative effect of PHO2 on P_i uptake is further supported by the fact that phosphate starvation-induced genes, such as P_i transporter genes, are already upregulated

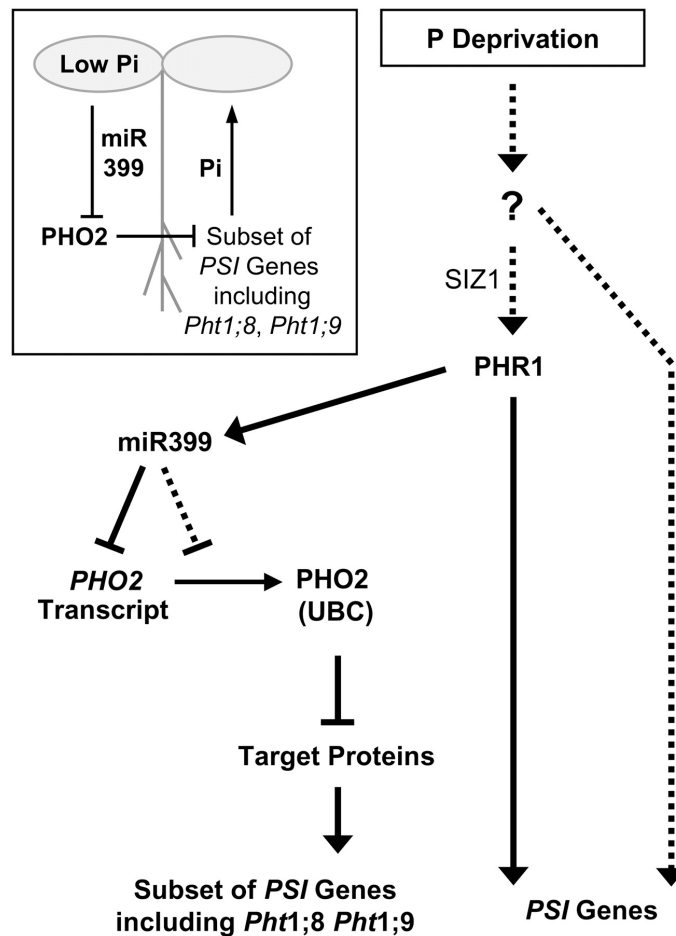


Figure 1.5: Model of the phosphate signaling cascade involving PHO2 and miRNA399. Under P_i deprivation PHR1, which is regulated by SIZ1, induces miRNA399 expression and a number of other phosphate starvation-induced (PSI) genes that are independent of PHO2. The upregulated miRNA399 leads to decreased levels of *PHO2* transcript, which then no longer suppresses the expression of PSI genes, such as the phosphate transporters *Pht1;8* and *Pht1;9*. The inset demonstrates the translocation of miRNA399 from the shoot to the root under low P_i content in the shoot. Picture taken from Bari et al. (2006).

in *pho2* mutants when the plants are grown under high phosphate conditions.

Upregulation of phosphate starvation-induced genes could also be observed for plants mutated in the MYB factor Phosphate starvation response 1 (PHR1), which can be SUMOylated by the SUMO E3 ligase SIZ1 (Miura et al. 2005). Apart from this, the high expression of miRNA399 is impaired in the *phr1* mutant. This suggests that PHR1 operates upstream of PHO2 and miRNA399 in P_i signaling. Figure 1.5 gives an overview on the P_i signaling pathway in *Arabidopsis* involving PHO2 and miRNA399. If the P_i content in the shoots is low, miRNA399 is overexpressed and leads to downregulation of the *PHO2* transcript in roots. By this, starvation-induced genes such as phosphate transporters are no

longer downregulated and P_i is taken up by the plant. This model requires the translocation of miRNA399 from the shoot to the root, and indeed grafting experiments revealed that wild type root stocks grafted with shoots overexpressing miRNA399 contain mature miRNA399. This clearly indicates the movement of miRNA399 from shoots to roots via the phloem (Lin et al. 2008).

Additional fine-tuning of the phosphate signaling pathway involving PHO2 is performed by a class of small noncoding RNAs with sequence similarity to miRNA399, e.g. *IPS1*. In contrast to miRNA399, overexpression of this small RNA leads to increased accumulation of the *PHO2* mRNA (Franco-Zorrilla et al. 2007). *IPS1* contains a mismatched loop at the expected cleavage site and therefore does not enhance cleavage of the *PHO2* mRNA but sequesters with miRNA399. This mechanism is termed as 'target mimicry' and nicely demonstrates the complex regulation of the signaling pathways in plants.

Apart from the P_i overaccumulation phenotype, the *pho2* mutant plants have been described to possess a higher sensitivity to cytokinin treatment than wild type plants (Lan et al. 2006). Cytokinins have been demonstrated to be involved in P_i sensing (Franco-Zorrilla et al. 2005), but the underlying mechanism is still unclear.

The content of arsenate in *pho2* mutant plants was also analyzed, because arsenate has been shown to be taken up by P_i transporters and nothing is yet known about its translocation from the root to the shoot. However, the shoots of the *pho2* mutant plants contained similar or only slightly higher arsenate concentrations when compared to wild type levels (Quaghebeur and Rengel 2004).

In summary, PHO2 could be clearly described to be involved in phosphate signaling and its regulation via miRNA399 could be nicely demonstrated. Still, no direct substrates of PHO2 could be identified so far and its function on the molecular level remains unanswered.

1.4.2 The closest mammalian homologue of PHO2 is E2-230K

Different phylogenetic reports on the ubiquitin conjugating enzymes in *Arabidopsis thaliana* and their homologues in other eukaryotic organisms demonstrate that the unusually large PFU proteins with an N-terminal and C-terminal extension seem to lack homologues in the yeast species *Saccharomyces cerevisiae* and *Schizosaccharomyces pombe* (Bachmair et al. 2001; Kraft et al. 2005; Michelle et al. 2009). However, homologues could be identified in higher eukaryotes. In the phylogenetic approach performed by Michelle et al. (2009) homologues of the PFU family in *Arabidopsis* could be identified in both *Caenorhabditis elegans* and *Drosophila melanogaster* (Michelle et al. 2009). The mouse genome was described to possess three genes belonging to this subfamily, whereas four homologues were identified in humans.

The closest mammalian homologue of the PFU proteins is E2-230K, also called UBE2O. It is highly expressed only in the reticulocyte stage of the erythroid differentiation (Wefes et al. 1995) and is known to ubiquitylate, apart from nonphysiological substrates, such as denatured histones or lysozyme (Klemperer et al. 1989), also endogenous proteins of erythroid cells without the help of an additional E3 ligase (Berleth and Pickart 1996).

In contrast to other ubiquitin conjugating enzymes, E2-230K/UBE2O is inactivated by

the addition of inorganic arsenite, which is known to react with vicinal sulfhydryl sites within proteins (Stevenson et al. 1978). Even after addition of competitive compounds, such as dithiotreitol (DTT), this inactivation is irreversible (Klemperer et al. 1989). In contrast, inhibition by aromatic phenylarsenoxides can be reversed by DTT, which might occur due to the different polarity of the reagents (Berleth and Pickart 1996). Interestingly, the ubiquitylation of substrates is completely abolished by addition of phenylarsenoxides, but the E2-230K/UBE2O–ubiquitin adduct formation is only partly inhibited. This can be explained by the presence of at least three cysteine residues in the active site of the protein, two of which are able to form a thioester with ubiquitin. Figure 1.6 shows a model of the ubiquitylation mechanism proposed for E2-230K/UBE2O.

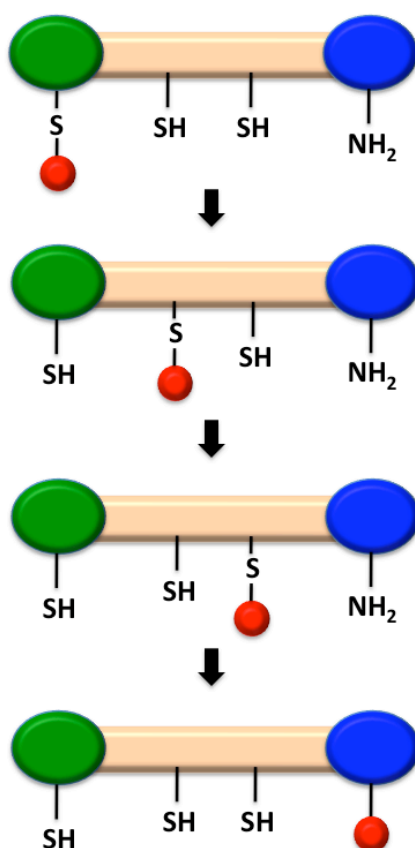


Figure 1.6: Model of the ubiquitylation mechanism proposed for E2-230K/UBE2O. Ubiquitin (red) is transferred from the E1 (green) to the first internal cysteine residue of E2-230K/UBE2O (apricot). Then it is passed to the second cysteine residue of E2-230K/UBE2O. From there ubiquitin is loaded onto a lysine residue of the substrate (blue). Picture taken from Berleth and Pickart (1996) and modified.

Ubiquitin is transferred from the E1 to the first cysteine residue of E2-230K/UBE2O. Then it is passed from the first to the second internal cysteine residue and finally transferred from

this second cysteine residue to a lysine residue of the substrate. The partial inhibition of forming a E2-230K/UBE2O–ubiquitin conjugate under treatment with phenylarsenoxides can then be explained by binding of this reagent to the second cysteine residue and a third cysteine residue nearby, which is not directly involved in thioester formation with ubiquitin. So ubiquitin can bind to the first cysteine residue but cannot be further transferred to the second cysteine of the E2.

In summary, these data clearly suggest that E2-230K/UBE2O functions as a hybrid protein bearing both E2 and E3 function, but still nothing is known about putative substrates or the actual function of E2-230K/UBE2O in the erythroid differentiation.

1.4.3 The distant homologue BRUCE/Apollon functions in mammalian apoptosis and cytokinesis

In contrast to E2-230K/UBE2O, much more is known about the function of the distantly related mammalian homologue of the PFU proteins called BRUCE (**B**IR repeat containing **u**biquitin-conjugating **e**nzyme) (Hauser et al. 1998) or Apollon (Hao et al. 2004). This giant protein (528 kDa) bears, apart from the UBC domain at the C-terminus, a single **b**aculovirus **i**nhibitor of **a**poptosis **r**epeat (**BIR**) motif at its N-terminus. Therefore it belongs to a class of proteins that are indispensable for their antiapoptotic activity and are called **i**nhibitor of **a**poptosis **p**roteins (**IAPs**) (Srinivasula and Ashwell 2008). BRUCE/Apollon is associated to membranes but not imbedded into the lipid bilayer and is localized in the Trans Golgi Network (TGN), the vesicular system (Hauser et al. 1998) and at the midbody ring during cytokinesis (Pohl and Jentsch 2008).

In humans the protein is highly expressed in several cancer cell lines and treatment of these cells with antisense oligonucleotides against BRUCE/Apollon increased the sensitivity to apoptosis inducing reagents (Chen et al. 1999). This suggests that BRUCE/Apollon is, like other proteins with BIR domains, an inhibitor of apoptosis.

Analyses on the homologues in *Drosophila melanogaster* and mice underline these findings. Flies expressing deletion mutants of BRUCE/Apollon show an enhanced apoptosis response induced by the cell death activators Reaper and Grim (Vernooy et al. 2002).

In mice the protein has been described to polyubiquitylate and therefore facilitate degradation of the proapoptotic proteins Smac and caspase-9, which both contain an IAP-binding motif (Hao et al. 2004). This motif is also found in the proapoptotic protein HtrA2, which cleaves BRUCE/Apollon with its serine protease activity (Sekine et al. 2005), and induces cell death in BRUCE/Apollon deficient cells. Apart from that, the abundance of BRUCE/Apollon during apoptosis is also regulated by degradation via the ubiquitin-proteasome system and via cleavage by multiple caspases (Qiu and Goldberg 2005).

As observed for E2-230K/UBE2O, BRUCE/Apollon has also been shown to ubiquitylate its substrates in an E3-independent manner, showing that it also functions as an E2/E3 hybrid protein (Bartke et al. 2004).

Apart from degrading the active form of Smac, BRUCE/Apollon is also able to degrade the Smac precursor protein. In addition, it can bind to the procaspase-9 and keeps it from

being cleaved into the active form, which induces apoptosis by cleaving other downstream caspases such as caspase-3 (Qiu and Goldberg 2005). This function of inhibiting also the proapoptotic precursor proteins is unique in the IAP family and might explain why BRUCE/Apollon is the only essential IAP in mammals. BRUCE/Apollon deficient mice show perinatal lethality and growth retardation, which is accompanied by an impaired placenta development (Lotz et al. 2004). Still, these problems cannot be directly traced back to an altered apoptotic response as the number of apoptotic cells is equal in WT and BRUCE/Apollon-deficient mice. In contrast, the number of proliferating cells is significantly reduced in the mutant. This can be explained by the recent observation that BRUCE/Apollon does not only exhibit an important function as an antiapoptotic protein, but is also a key player during the abscission stage in cytokinesis (Pohl and Jentsch 2008). In the final stage of this process BRUCE/Apollon moves from the vesicular system to the midbody ring, which is the target site for membrane vesicles and membrane fusion. A depletion of BRUCE/Apollon leads to incomplete separation of the two daughter cells and finally to cytokinesis-associated cell death, demonstrating the importance of this E2 not only in the regulation of apoptosis but also during cell proliferation.

1.5 Aim of this work

The fact that *Arabidopsis thaliana* contains 37 putative ubiquitin E2s suggests that each of these proteins might exhibit specific roles during the life cycle of the plant, as demonstrated for the UBC protein BRUCE/Apollon in mammals. Still, only very little is known about the actual functions of these proteins in the plant cell.

In comparison to the other members of the UBC protein family, whose size usually range between 14-30 kDA, PHO2 and the PFU proteins represent exceptions, as these proteins contain long N- and C-terminal extensions and are therefore with 60-120 kDA much larger. Despite their uniqueness in plants, to date only PHO2 has been described to be involved in the phosphate signaling pathway (Bari et al. 2006), where its exact function on the molecular level is still not identified. Furthermore, nothing is known at all about the role of the three PFU proteins in plants.

Hence, the main aim of this work was to identify plant processes that require the functionality of PHO2 and the PFU proteins, with a special focus on plant programmed cell death, and to describe the behavior of these proteins on the molecular level.

Therefore, first the structure of the genes and proteins should be dissected, and a phylogenetic analysis including other eukaryotic homologues was initiated to reveal conserved domains and motifs that indicate putative functions or mechanisms.

To identify processes that involve PHO2 and the PFU proteins, it was planned to analyze knockout mutants and compare them to wild type under different growth conditions. Especially the role of these proteins in plant programmed cell death was of main interest, as the distant homologue BRUCE/Apollon is described to be involved in this process in mammals (Bartke et al. 2004; Qiu and Goldberg 2005). To achieve this, the effect of the

ubK48R transgene, leading to PCD in wild type (Schlögelhofer et al. 2006), should be analyzed in the mutant background. Apart from this, the effect on the mutants under other PCD inducing conditions such as ozone and NO treatment or pathogen attack should be described.

The behavior of PHO2 and the PFU proteins on the molecular level was planned to be analyzed via three different approaches.

First, the subcellular localization of the proteins should be identified via expression of fusion proteins with fluorescent markers both transiently in *Nicotiana benthamiana* and in stably transformed *Arabidopsis thaliana* plants.

In a second approach, putative interactors of PHO2 and the PFU proteins should be identified in a yeast two hybrid screen. As the analysis of the knockout mutants and the subcellular localization experiments already provided indications for a putative interaction of PHO2 and PFU1, the relationship between these two proteins was in special focus. Apart from that, the functionality of these proteins was intended to be analyzed by mutating the conserved cysteine residue in the UBC and C-terminal domain of both PHO2 and PFU1, and by expressing these proteins in yeast.

Last but not least, recombinant PHO2 and PFU1 protein fragments should be produced via overexpression in *E. coli* to analyze the E2 function of these proteins in *in vitro* thioester formation assays. Apart from this, these recombinant proteins were also planned to be used in co-immunoprecipitation experiments to further analyze the interaction between PHO2 and PFU1 and to solve the three-dimensional structure of the C-terminal domain, which was of special interest during this work due to its high conservation throughout the plant kingdom.

In summary, this PhD thesis should represent a first approach to describe the specific role of PHO2 and the PFU proteins in plant programmed cell death and should give first insights into the molecular function of these extraordinary ubiquitin conjugating enzymes in *Arabidopsis thaliana*.

Chapter 2

Results

Apart from its function in the phosphate starvation response (Bari et al. 2006), nothing is known about the actual role and the molecular mechanism that PHO2 exhibits in *Arabidopsis thaliana*. The remaining members of the PHO2 family of ubiquitin conjugation enzymes, PFU1-3, have not been described at all so far. Hence, the present thesis deals with a variety of approaches to describe the properties and functions of these proteins in plants. Knockout lines of the *PFU* genes served to identify new pathways the proteins are participating in, and fusions to fluorescent marker proteins revealed the subcellular localization *in planta*. In addition, the biochemical characteristics of the PFU proteins were analyzed in yeast two hybrid assays and with the help of recombinantly expressed proteins in *Escherichia coli*. Overall, this work represents a first summary giving new insights into the biochemical and physiological function of the PFU protein family in *Arabidopsis thaliana*.

2.1 Gene and protein structure of the *PFU* family

Before examining the properties of the PFU proteins in plants, both protein and gene structure were analyzed, which is necessary for cloning the correct open reading frames that are also expressed *in planta*. Apart from this, knowing gene and protein structures helps to understand the relationships between the different family members and gives insights into the transcriptional regulation of the genes.

2.1.1 The PFU family is divided into two subgroups

An alignment of the predicted protein sequences of PFU1 (accession number: NP_188154), PFU3 (AAO64853), PFU2 (NP_179284) and PHO2 (NP_850218) performed with the MUSCLEvs4.0 protein multiple sequence alignment software (Edgar 2004) revealed several characteristic features of the PFU protein family (Fig. 2.1). PFU2 (1102 aa) and PHO2 (907 aa) both possess a much longer N-terminus than the other two family members PFU1 (609 aa) and PFU3 (543 aa). They also show higher sequence similarity in this domain

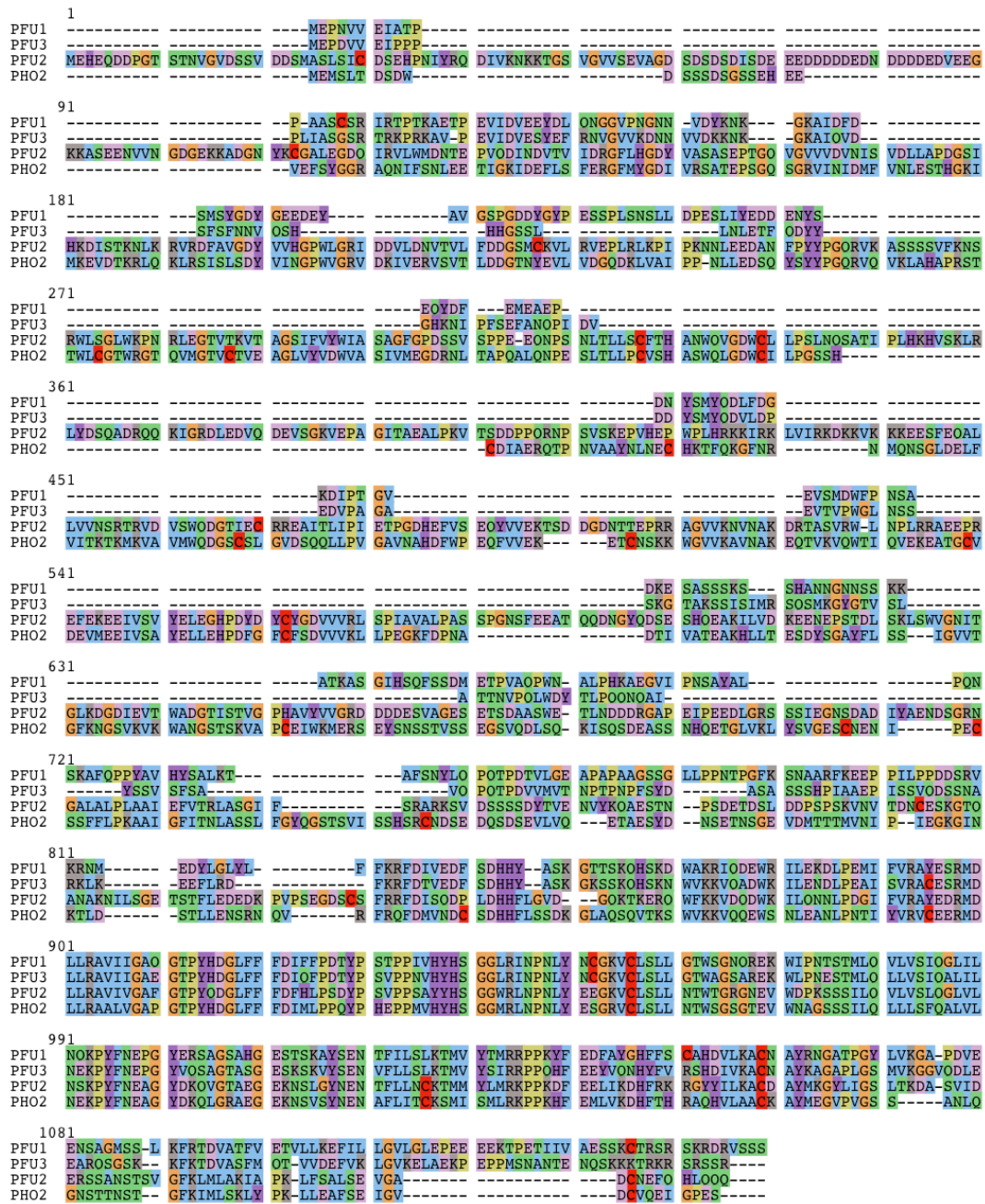


Figure 2.1: Alignment of the PHO2 and the three PFU protein sequences performed with the MUSCLEv4.0 software (Edgar 2004). Seaview version 4.1 was used as a graphical sequence alignment editor (Gouy et al. 2010). The colour code of the amino acids is as follows: KR - grey (positively charged), AFILMVW - blue (hydrophobic side chains), NQST - green (polar uncharged side chains), HY - purple, C - red, DE - rose (negatively charged), P - yellow, G - orange.

when compared to PFU1 and PFU3, so that the PFU protein family can be divided into two subgroups: the two larger members PFU2 and PHO2 on the one hand and PFU1 and PFU3 on the other. Apart from this, the alignment revealed that all four proteins share a high sequence similarity in the C-terminal part. Previous sequence analysis performed by Bachmair et al. (2001) showed that this part contains the UBC domain with the conserved cysteine residue responsible for the thioester reaction with ubiquitin. The positions of the UBC domains are as follows: aa 336-485 in PFU1, aa 275-424 in PFU3, aa 854-1003 in PFU2 and aa 666-815 in PHO2. A search in the PROSITE database (Hulo et al. 2007) identified no additional known protein domains, families or functional sites.

Phylogenetic analyses performed with the help of Dr. M. Novatchkova at the IMP in Vienna indicate that, whereas PFU1 and PFU3 seem to be plant specific, PFU2 and PHO2 clearly cluster together with the mammalian E2-E3 hybrid protein E2-230K, also called UBE2O, and more distantly with BRUCE, an inhibitor of apoptosis in mammals (Pohl and Jentsch 2008). Homologues were found throughout the whole eukaryotic kingdom including mammals (*Homo sapiens* and *Mus musculus*), birds (*Gallus gallus*), fish (*Gasterosteus aculeatus*), insects (*Drosophila melanogaster* and *Apis mellifera*) and fungi (*Laccaria bicolor* and *Ustilago maydis*) (Fig. 2.2). However, homologues in both yeast species *Saccharomyces cerevisiae* and *Schizosaccharomyces pombe* are missing.

All four PFU proteins possess a C-terminal extension behind the UBC domain that is highly conserved throughout the family. An alignment performed with the PFU proteins

		↓		↓				
Art	PHO2	KNSVSYNENAF	LITCKSMISMLR	KPKHFEMLVKDH	FTHRAQ--HVL	AACKAYME·		
Viv	PHO2	KNSISYNENAF	IGTCRSILYLLR	NPPKHF	EAVEEHFNQCSQ--HFL	LACKAYME·		
Art	PFU2	KNSLGYNENTF	LLNCKTMMYLMR	KPKDFEELIKDH	FRKRGY--YILKAC	DAYMK·		
Viv	PFU2	KNSLSYNENTF	LLNCKTMMYLMR	KPKDFEELVKDH	FKRQGY--YILKAC	DAYMK·		
Hos	UBE2O	ENSR	CYNEMALIRVVQ	SMTQLVRRP	PEVFEQEI	RQHFSTGGW--RLVNRI	ESWLE·	
Mum	Ube2o	ENSR	CYNEMALIRVVQ	SMTQLVRRP	PEVFEQEI	RQHFVGGW--RLVNRI	ESWLE·	
Gag	UBE2O	ENSR	CYNEMTLIRVVQ	SMMQLLRP	VEVFEHEI	REHFR	CNGW--RLVSR	IESWLE·
Gaa		ENSR	CYNEMALIKMVQ	SMTLLQNP	VVEVFKQEI	QEHF	FASSGW--RLVHRL	DAWLE·
Drm	CG10254	ENSR	VYNEMAI	IKIAQSTVKQL	TNPPLIFRNELI	EHFK	EFGT--ELYARM	RAWSE·
Apm	UBE2O	ENSR	MYNEMVVLKLVQ	AQTKLLQH	PPPVKDIIIEHF	KRHAK--KLLQ	RLELWME·	
Lab		VNSR	LYSEKAYVLSR	GFVRRAL	EIPLGGLEEE	INWLYY	NKGRLEK	VLRDARRLIE·
Usm		LASR	MYNEKAYILSR	GFVKKVLES	RPAGFEDEVEL	FYLRSG	KLRNV	VESAERLLQ·

Figure 2.2: Alignment showing part of the C-terminus of PFU2 and PHO2 together with the eukaryotic homologues, performed by Dr. M. Novatchkova, IMP Vienna. The position of the cysteine residue highly conserved in plants is marked by a red arrow, whereas a cysteine residue conserved in mammals is lying closer to the UBC domain and labelled by a blue arrow. Art – *Arabidopsis thaliana*, Viv – *Vitis vinifera*, Hos – *Homo sapiens*, Mum – *Mus musculus*, Gag – *Gallus gallus*, Gaa – *Gasterosteus aculeatus*, Drm – *Drosophila melanogaster*, Apm – *Apis mellifera*, Lab – *Laccaria bicolor*, Usm – *Ustilago maydis*

and their eukaryotic homologues revealed that a cysteine residue in the C-terminal domain is at this position highly conserved only in plants. It could be found for the homologues in rice, corn, *Medicago truncatula*, wine and poplar and is even present in the mosses *Selaginella moellendorffii* and *Physcomitrella patens* and in algae such as *Micromonas*

pusilla. A cysteine residue conserved in the mammalian homologues, in birds and in fish is lying closer to the UBC domain and could possibly exhibit the E3 function described for E2-230K/UBE2O (Berleth and Pickart 1996).

In addition to the phylogenetic approach, the bioinformatic tool PredictNLS online (<http://cubic.bioc.columbia.edu/cgi/var/nair/resonline.pl>) was applied to identify putative nuclear localization signals in the PFU protein sequences. For PFU1 a nuclear localization signal was predicted to be located at the C-terminus of the protein (aa 597-602). PFU3 contains several positively charged arginine and lysine residues at the C-terminus (aa 536-540) as well, which were not identified by the bioinformatic tool but still might function as an NLS. A second signal was predicted to lie close to the N-terminus of PFU3 at position aa 20-54. So both members of the plant specific subgroup were predicted to be imported into the nucleus. In contrast, no NLS sequence was found for PHO2, and the only putative signal identified for PFU2 is located in the middle of the protein sequence (aa 427-440), suggesting that the possibility of a nuclear localization is very low for these proteins.

In contrast, a second bioinformatic tool predicting the subcellular localization of a protein based on its amino acid sequence, WoLF PSORT (<http://wolfpsort.org/>), gives localization in the nucleus as a result for all four members of the family, with PFU2 showing the highest (14.0) and PHO2 the lowest probability (10.0).

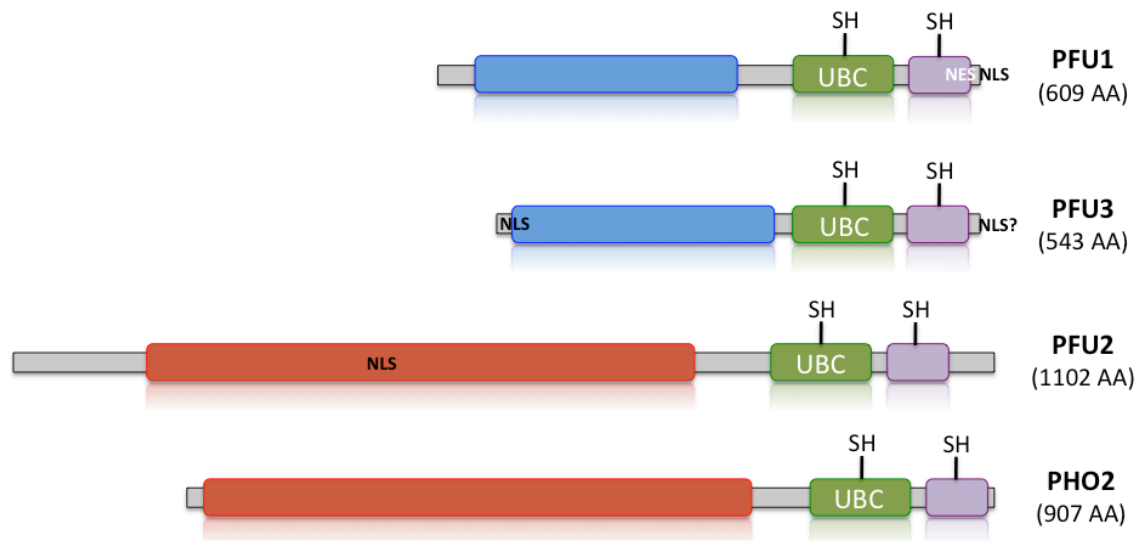


Figure 2.3: Schematic overview on the protein structure of the PFU family. According to the similarities in the N-terminus the protein family can be divided into two subgroups: PFU1 and PFU3 (blue N-terminal domain) on the one hand and the two larger members PFU2 and PHO2 (red N-terminal domain) on the other. All four proteins contain a ubiquitin conjugating domain (green) with a conserved cysteine residue (-SH) and show homology in their C-terminus (purple) exhibiting an additional conserved cysteine residue. The domains predicted to bear nuclear localization signals are marked by the abbreviation NLS in black, whereas the nuclear export signal predicted for PFU1 is labelled by the abbreviation NES in white.

A search for nuclear export signals in PFU1 and PFU3 performed with the NetNES 1.1 Server (la Cour et al. 2004) gave a positive result only for PFU1, where the putative signal is lying shortly in front of the NLS sequence between aa 569-574.

All characteristic features of the PFU protein family taken from these bioinformatic analysis are summarized in Fig. 2.3.

2.1.2 Cloning of the *PFU2* open reading frame

To properly analyze a protein family, the first condition to be fulfilled is obtaining the correct open reading frames for all genes of interest. Whereas the cDNAs of *PFU1*, *PFU3* and *PHO2* could be easily ordered, a *PFU2* cDNA was not available at the RIKEN repository (<http://rarge.gsc.riken.jp/cdna/cdna.pl>) and the full length ORF consisting of 3309 bp could also not be obtained via a single PCR step. Therefore primers were designed to amplify the cDNA in three parts, which should be ligated together afterwards making use of internal restriction sites within the gene.

The first part ranged from the start codon to a *SpeI* restriction site at 1198 bp, the second part from the *SpeI* site to a *PshAI* site at position 2323 bp and the third part from the *PshAI* restriction site to the end.

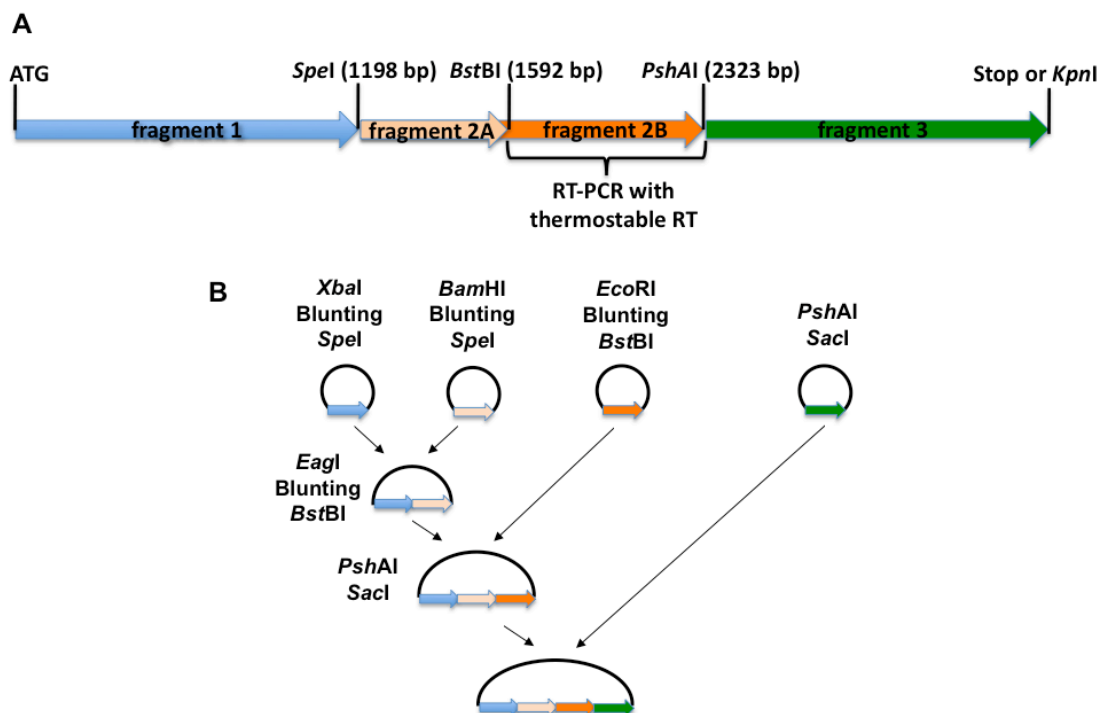


Figure 2.4: Cloning strategy for PFU2 into the sequencing vector pBluescript II SK+ (pSK): The ORF of *PFU2* was divided into 4 fragments, which were amplified separately and ligated together using restriction sites occurring inside the gene.

Only the first (oligos 746A-LET2startdn and 747A-LET2Speup) and the third part (oligos 750A-LET2Pshdn and 751A-LET2endup) could be easily amplified from wild type RNA, whereas the middle part of the gene had to be divided again using the *Bst*BI restriction site at 1592 bp (Fig. 2.4, panel A). The fragment *Spe*I-*Bst*BI (oligos 805A-LET2Spedn2 and 807A-LET2Bstup) was, similar to the front and the last part of the gene, obtained from RNA using the Superscript II Reverse Transcriptase (Invitrogen). In contrast, the fragment *Bst*BI-*Psh*AI (oligos 806A-LET2Bstdn and 808A-LET2Pshup2) could only be obtained from RNA with the help of the thermostable Transcriptor First Strand Reverse Transcriptase (Roche). Each of the fragments was cloned into the pBluescript II SK+ vector (Stratagene) at the *Sma*I restriction site and finally ligated together using the cloning strategy described in Fig. 2.4, panel B.

2.1.3 Determination of the length of the *PFU2* leader

The closest homologue of *PFU2*, *PHO2*, possesses an unusually long 5' leader sequence and its transcript is regulated by miRNA399. As *PFU2* shares high structural similarity with *PHO2* including the positions of the introns within the coding region, it became of interest, whether this gene also contains a long 5' leader sequence and might be regulated by miRNAs on the transcriptional level. Therefore, apart from cloning the open reading frame of the *PFU2* gene, the length of the leader at the 5' end was determined analyzing cDNA products obtained from Columbia wild type RNA. Seven different downstream oligos were designed to check for the starting point of the leader. Figure 2.5 summarizes the structure

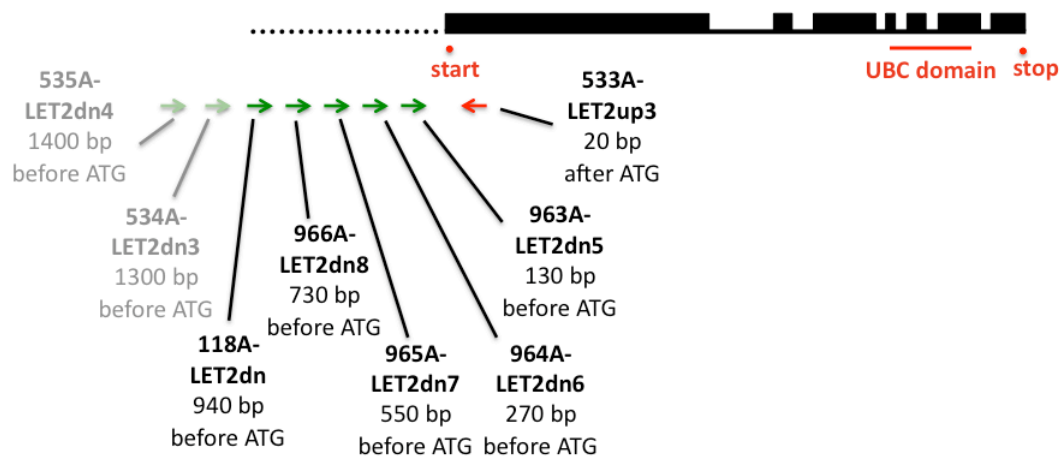


Figure 2.5: Schematic overview on the mRNA structure of *PFU2* and the oligo positions used for determination of the length of the *PFU2* leader. Exons are indicated as thick black bars with the introns as thin lines inbetween. The positions of the downstream and upstream oligos used for the RT-PCR are marked by green and red arrows, respectively. Downstream oligos not giving RT-PCR products anymore are shown in light color. The leader is represented by a dotted line and starts at least 940 bp before the ATG.

of *PFU2* and the position of the oligos chosen for this analysis. The upstream oligo at position 20 behind the ATG was used for cDNA synthesis. For each oligo combination, relatively weak PCR products were obtained. To assure that these bands indeed contain fragments of the *PFU2* leader each product was excised from a gel, purified and cloned into the pCR2.1 TOPO vector (Invitrogen) to sequence it. An RT-PCR product corresponding to the predicted 5' sequence of *PFU2* could be detected for all downstream oligos up to oligo 118A-LET2dn at position 940 bp before the ATG. Still, none of the PCR products received from the oligos further upstream showed any similarity to the *PFU2* sequence. Fig. 2.6 compares the RT-PCR results using the downstream reading oligo 534A-LET2dn3, binding 1300 bp before the ATG and giving no PCR products corresponding to the 5' sequence of *PFU2*, to the results obtained with the 118A-LET2dn oligo, showing a thick band at the expected size of 960 bp. These observations give evidence that the mRNA leader of *PFU2* starts at least 940 bp upstream of the start codon.

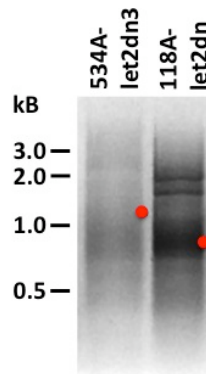


Figure 2.6: RT-PCR results with RNA from Columbia wild type plants using the downstream reading oligos 534A-LET2dn3 and 118A-LET2dn, respectively, together with the upstream reading oligo 533A-LET2up3. The expected sizes of the PCR products are labelled by red dots.

2.1.4 Analysis on the alternative gene model of *PFU3*

For *PFU3*, two different gene models were predicted. The RIKEN cDNA encodes a protein of 543 amino acids with one UBC domain from aa 275-424 (<http://www.brc.riken.go.jp/lab/epd/catalog/cdnaclone.html>). In contrast, an alternative structure is proposed by the SALK database (<http://signal.salk.edu/>), where the protein possesses 1163 amino acids and contains, in addition to the first UBC domain, two more UBC domains at position aa 605-758 and at position aa 921-1044 (Fig. 2.7, panel A).

To find out whether the longer gene is transcribed, RT-PCR experiments were performed with Columbia wild type RNA (Fig. 2.7, panel B). As a positive control, a gene fragment within the gene proposed by the RIKEN database was chosen (primer pair 1: 976A-LET3dn9 + 975A-LET3up9). Both the PCR product from genomic DNA and the product received

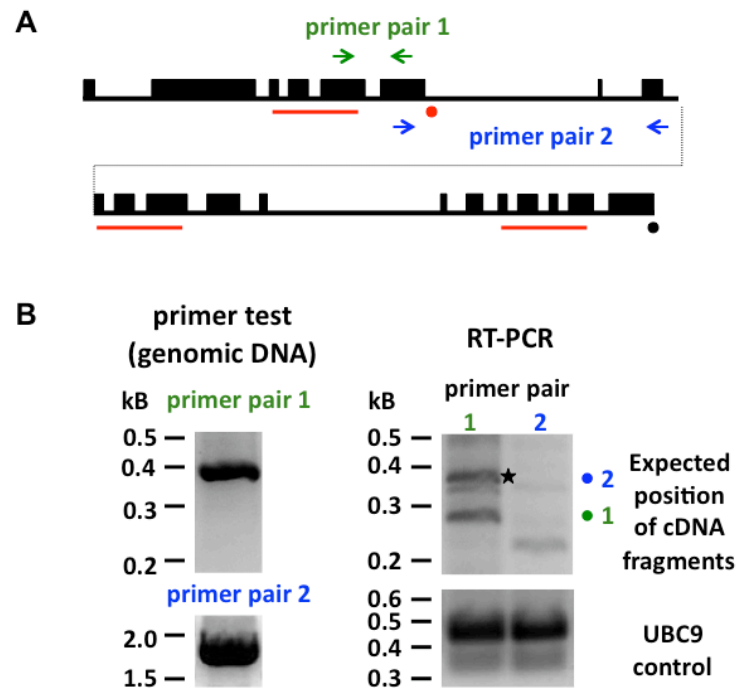


Figure 2.7: A: The scheme describes the structure of the *PFU3* gene predicted by the SALK database. The positions of the oligos used for the analysis are indicated by arrows. Exons are shown as thick bars, introns as thin lines. Red lines underneath the gene display the positions of the three UBC domains predicted by SALK. The red dot indicates the STOP codon suggested by RIKEN, whereas the black dot stands for the STOP codon found in the SALK database. B: PCR products could be detected for both primer pairs with genomic DNA (left panels). The RT-PCR results are shown on the right panels. A DNA fragment of the expected size is detectable for primer pair 1 (green) but not for primer pair 2 (blue). The expected heights of the bands for primer pairs 1 and 2 are indicated by a green and a blue dot, respectively. For primer pair 1 a PCR product from genomic DNA is also visible after the RT-PCR (asterisk). As an internal control the *UBC9* transcript levels are shown on the lower panel.

from cDNA could be clearly detected at the expected sizes of 387 bp and 277 bp, respectively. In contrast, a PCR product from cDNA could not be obtained with oligos amplifying a region just after the STOP codon predicted by RIKEN (primer pair 2: 967A-LET3dn5 + 968A-LET3up5). No band is visible at the expected size of 344 bp. Still, a PCR with genomic DNA resulted in a product of the predicted size of 1842 bp, showing functionality of the oligos. Another internal control for the RT-PCR reactions was performed by co-amplification of the *UBC9* cDNA. *UBC9* is one of the ubiquitin conjugating enzymes highly expressed in *Arabidopsis thaliana*. The upstream oligo for amplification of *UBC9* was mixed with the upstream oligo used for cDNA synthesis of each *PFU3* fragment. In both cases, the amount of *UBC9* PCR product was equal, showing that the cDNA synthesis for both *PFU3* fragments was properly performed. These results support the *PFU3* gene

structure predicted by the RIKEN database whereas the longer gene model found in the SALK database could not be verified.

2.2 Analysis on *pfu* mutants reveals new function for PFU proteins

The exact function of the PFU protein family in *Arabidopsis thaliana* is still unknown. Therefore T-DNA insertion lines were analyzed to identify knockout lines of the *PFU* genes. These were then compared to wild type plants under different growth conditions.

2.2.1 Identification of homozygous T-DNA insertion lines

T-DNA insertion lines were either ordered from the SALK Institute Genomic Analysis Laboratory (SIGnAL) or from the Syngenta Arabidopsis Insertion Library (SAIL) and homozygous T-DNA insertion lines were identified with the help of Kerstin Luxa in our lab.

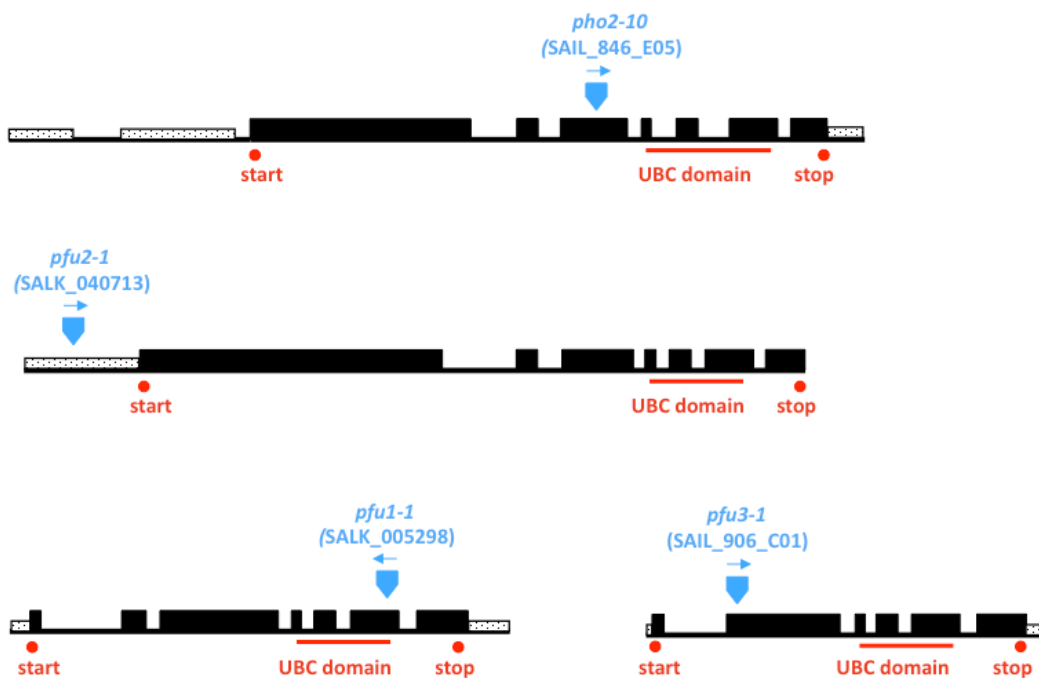


Figure 2.8: Gene structure of the *PFU* genes and position of T-DNA insertions (blue). Exons are shown as thick bars, introns as thin lines. The dotted bars represent the non-translated parts of the *PFU* genes.

Figure 2.8 summarizes the structure of each gene and the position of the T-DNA insertion within the gene. For *PFU1* (SALK_005298), *PFU3* (SAIL_906_C01) and *PHO2*

(SAIL_846_E05) the insertions lie within an exon of the coding region. Only for *PFU2* (SALK_040713) the T-DNA insertion was not localized in the coding sequence but in the previously identified 5' leader region of the gene.

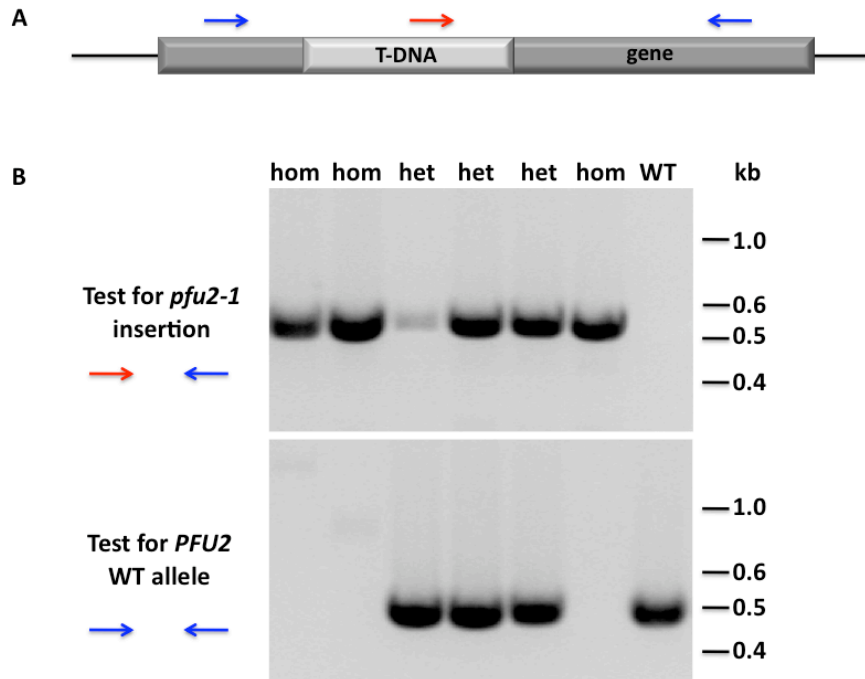


Figure 2.9: A: Oligo positions used to determine the genotype of the T-DNA insertion lines. Blue arrows indicate gene specific oligos, the red arrow marks the position of the insertion specific oligo. B: Results of a genotyping PCR for the *pfu2-1* insertion line. The presence of the T-DNA insertion was tested in the upper lane with the insertion specific oligo (red arrow) and the gene specific upstream oligo (blue arrow). The lower lane shows the test for the wild type allele with the gene specific oligos (blue arrows). WT = wild type plants, het = heterozygous for the T-DNA insertion, hom = homozygous for the T-DNA insertion

The genotype of the plants was determined via PCR. Two oligos that bind within the gene and one binding in the T-DNA insertion have been designed for each of the *PFU* genes (Fig. 2.9, panel A). A PCR product occurring with the combination of the insertion specific oligo and a gene specific oligo shows that a T-DNA insertion is present in at least one of the two alleles resulting in either homo- or heterozygous plants. If in addition no PCR product is detectable with the gene specific oligos, these plants are homozygous for the T-DNA insertion. Wild type plants not containing any T-DNA insertion are lacking a PCR product with the insertion specific oligo and only show a band when testing with the gene specific oligos. Homozygous T-DNA insertion lines could be identified for all four *PFU*

genes and were named as follows: *pfu1-1*, *pfu2-1*, *pfu3-1* and *pho2-10*. A typical example for a genotyping PCR is shown for plants of the *pfu2-1* insertion line in Figure 2.9, panel B.

Table 2.1: Oligos used to identify homozygous T-DNA insertion lines

Insertion line	Test for insertion	Test for WT allele
<i>pfu1-1</i>	SALK LBa1 + 117A-LET1dn	141A-LET1up + 117A-LET1dn
<i>pfu2-1</i>	SALK LBa1 + 198A-LET2up1	533A-LET2up3 + 534A-LET2dn3
<i>pfu3-1</i>	Garlic LB1 + 429A-LET3up4	235A-LET3startdn + 429A-LET3up4
<i>pho2-10</i>	Garlic LB1 + 120A-LET4up	120A-LET4up + 161A-LET4dn

2.2.2 Analysis of transcript levels in mutant plants

Before analyzing mutant and wild type plants under different growth conditions, the transcript levels of the *PFU* genes were compared via RT-PCR. Therefore RNA was extracted from two week-old Columbia and *pfu* mutant seedlings. This RNA was used to synthesize cDNA with the upstream reading oligo also taken for the subsequent PCR. As an internal standard, the upstream reading oligo for amplification of *UBC9* was included in each cDNA synthesis to afterwards check for equal amounts of the *UBC9* transcript via PCR.

The RT-PCR results are summarized in Figure 2.10. The transcript level of *PFU1* was tested with oligos 117A-LET1dn and 789A-LET1UBCup, covering a large part (1450 bp) of the open reading frame of *PFU1*, which consists of 1830 bp. A *PFU1* transcript could only be detected for wild type but not for the *pfu1-1* mutant plants (Figure 2.10, panel A). The *UBC9* fragment with a size of 435 bp, amplified with the oligos AtUBC9Ndedn and AtUBC9Notup, showed the same level in both mutant and wild type samples. This indicates that the *PFU1* gene is completely knocked out in the *pfu1-1* mutant plants.

The results obtained for the *pfu3-1* plants were quite similar. The cDNA of *PFU3* was amplified with the oligos 235A-LET3startdn and 975A-LET3up9. The expected size of the PCR fragment was approximately 1460 bp, which is well visible for the wild type sample (Fig. 2.10, panel B). In the mutant lane, no transcript is detectable although similar amounts of the *UBC9* transcript show the functionality of the RT-PCR. In conclusion, the *pfu3-1* mutant plants also show a complete knockout of the respective gene.

In contrast, the analysis of the *PFU2* transcript levels showed a different result. As the complete open reading frame of *PFU2* could not be amplified during cloning of the gene, the transcript levels of wild type and mutant plants were compared making use of two different primer pairs. The first pair 746A-LET2startdn and 747A-LET2Speup amplified the front part of the gene, from the start codon to the *SpeI* restriction site at position

1198 bp. The second fragment was amplified with the oligo pair 750A-LET2Pshdn and 999A-LET2endups and runs at 1015 bp on the gel. In both cases, the amount of PCR product generated from the mutant cDNA was much less than from WT cDNA (Fig. 2.10, panel C). However, the transcript is still detectable in the mutant plants, showing that in the case of the *pfu2-1* mutant line, the transcript is only knocked down and not fully absent. The *UBC9* control of the *pfu2-1* plants gives a band a little more intense than seen for the wild type plants, showing that in both cases the cDNA synthesis was properly performed. Finally, the transcript levels of *PHO2* in *pho2-10* mutant plants and wild type plants were compared using the oligos 527A-LET4Ndn and 525A-LET4Cup. This leads to amplification of the whole *PHO2* open reading frame and resulted in a DNA fragment of approximately 2730 bp. Again wild type plants showed expression of the gene, whereas in the mutant plants the *PHO2* transcript was completely absent (Fig. 2.10, panel D). The *UBC9* control showed gene expression in both cases. These results proved that also in the T-DNA insertion line of *PHO2* the gene is completely knocked out.

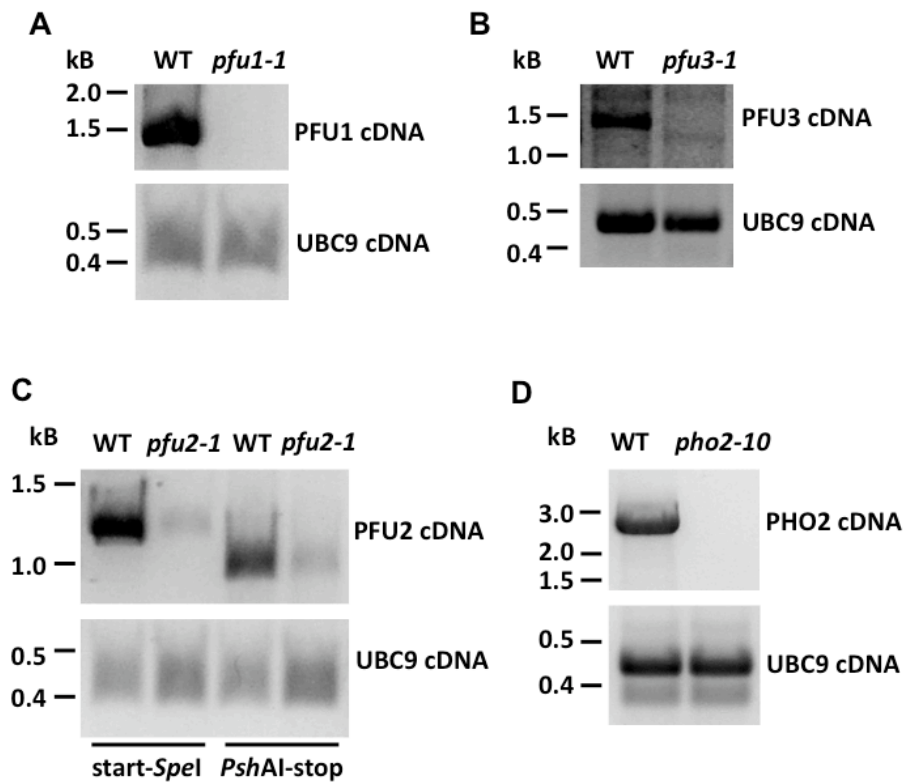


Figure 2.10: RT-PCR results comparing transcript levels of *PFU1* (A), *PFU3* (B), *PFU2* (C) and *PHO2* (D) in both wild type (WT) and mutant plants. The *PFU* specific cDNA results are shown in the upper panels, whereas the *UBC9* control for each comparison is illustrated in the respective lower panel.

2.2.3 Production of multiple knockout plants

Although RT-PCR results showed that the transcript levels are severely reduced in the mutant plants, a mutant phenotype can, due to gene redundancy, very often only be detected if two or more genes of a gene family are knocked out. To circumvent this problem, the single mutants were crossed by Dr. Andreas Bachmair to produce double, triple and quadruple *pfu* mutants. The subsequent genotyping revealed homozygous plants for all mutant combinations summarized in Table 2.3.

Table 2.3: Homozygous *pfu* double, triple and quadruple mutant combinations

double mutants	triple mutants	quadruple mutant
<i>pfu1-1 pfu2-1</i>	<i>pfu1-1 pfu2-1 pfu3-1</i>	<i>pfu1-1 pfu2-1 pfu3-1 pho2-10</i>
<i>pfu1-1 pfu3-1</i>	<i>pfu1-1 pfu2-1 pho2-10</i>	
<i>pfu1-1 pho2-10</i>		
<i>pfu2-1 pho2-10</i>		

2.2.4 Different mutant phenotypes

Only little is known about the actual function of the PFU proteins *in planta*. To find out more about the pathways these proteins are involved in, mutant plant growth was tested under several growth conditions and compared to wild type to identify possible differences. In the following chapters, only experiments revealing obvious phenotypes are described, although several additional growth conditions were tested such as different cadmium, arsenate, potassium and calcium concentrations.

Only *pho2* mutants accumulate P_i in shoots

One member of the PFU protein family, PHO2, has already been described to be involved in signal transduction during the phosphate starvation response in *Arabidopsis* (Bari et al. 2006). Knockout mutants of *PHO2* show an excessive overaccumulation of P_i in shoots due to an increase of phosphate uptake and subsequent translocation from the roots to the shoots. To check whether the related PFU proteins are also involved in the regulation of phosphate metabolism, seeds of the four different *pfu* single mutants and the double mutants *pfu1-1 pho2-10*, *pfu2-1 pho2-10* and *pfu1-1 pfu3-1* were sent to Dr. W. R. Scheible at the IPK Gatersleben and the P_i content of these plants was measured using a colorimetric micromethod (Itaya and Ui 1966).

The T-DNA insertion line of *PHO2* obtained from SAIL showed the expected overaccumulation of P_i in shoots with approximately 1.4 mg/g fresh weight (Fig. 2.11). In contrast, the other *pfu* single mutants *pfu1-1*, *pfu2-1* (Fig. 2.11) and *pfu3-1* did not show any P_i

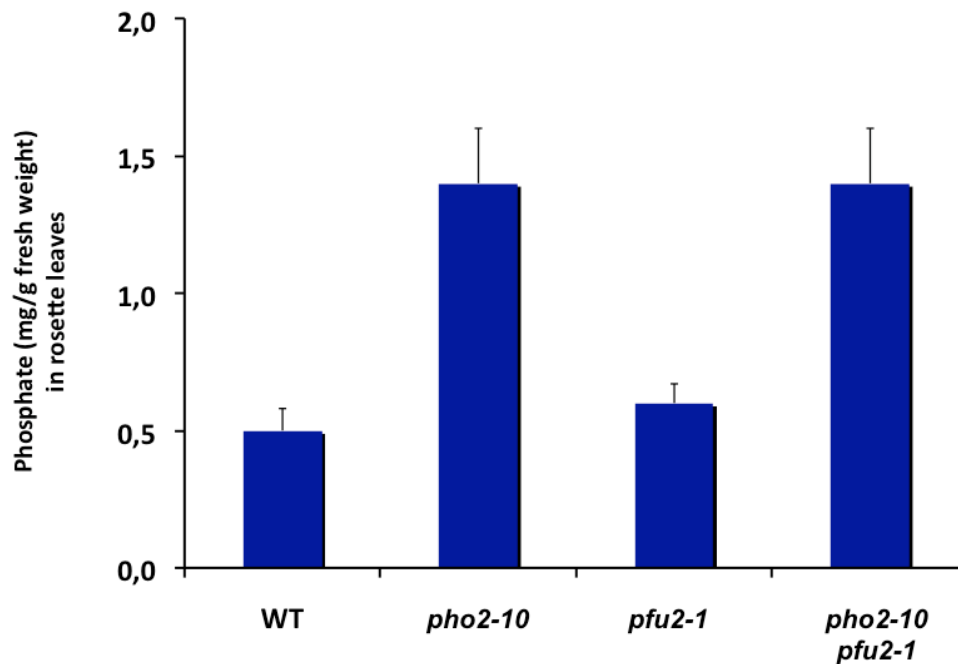


Figure 2.11: Phosphate content in rosette leaves of *pho2-10*, *pfu2-1* and *pfu2-1 pho2-10* mutant plants in comparison to wild type (WT) plants.

overaccumulation. The P_i values corresponded to the amount of approximately 0.5 mg/g fresh weight detected for wild type plants, indicating that either a single mutation of one of the related *PFU* genes is not sufficient to change the P_i content of the plants, or that these proteins are not at all involved in phosphate signaling.

Furthermore, the double mutants *pfu1-1 pho2-10* and *pfu2-1 pho2-10* (Fig. 2.11) did not show any alteration in the P_i content in comparison to the *pho2-10* single mutant. Results for the *pfu1-1 pfu3-1* double knockout are still missing.

ubK48R induced cell death is impaired in *pfu* mutants

As the phosphate measurements did not reveal any function of PFU1, PFU2 or PFU3 in phosphate signaling, other pathways had to be examined to identify possible roles of the PFU proteins in plants. The function of the closest PFU relative in mammals, E2-230K/UBE2O, is still unknown, but the more distantly related homologue BRUCE has been shown to be involved in programmed cell death as an inhibitor of apoptosis (Bartke et al. 2004).

To address the question whether the PFU proteins are involved in programmed cell death regulation in plants, the *pfu* mutants were crossed to a plant line expressing a form of ubiquitin where lysine 48 is mutated to arginine. Plants expressing this mutated ubiquitin under a dexamethasone inducible promoter are impaired in proteolysis and therefore undergo

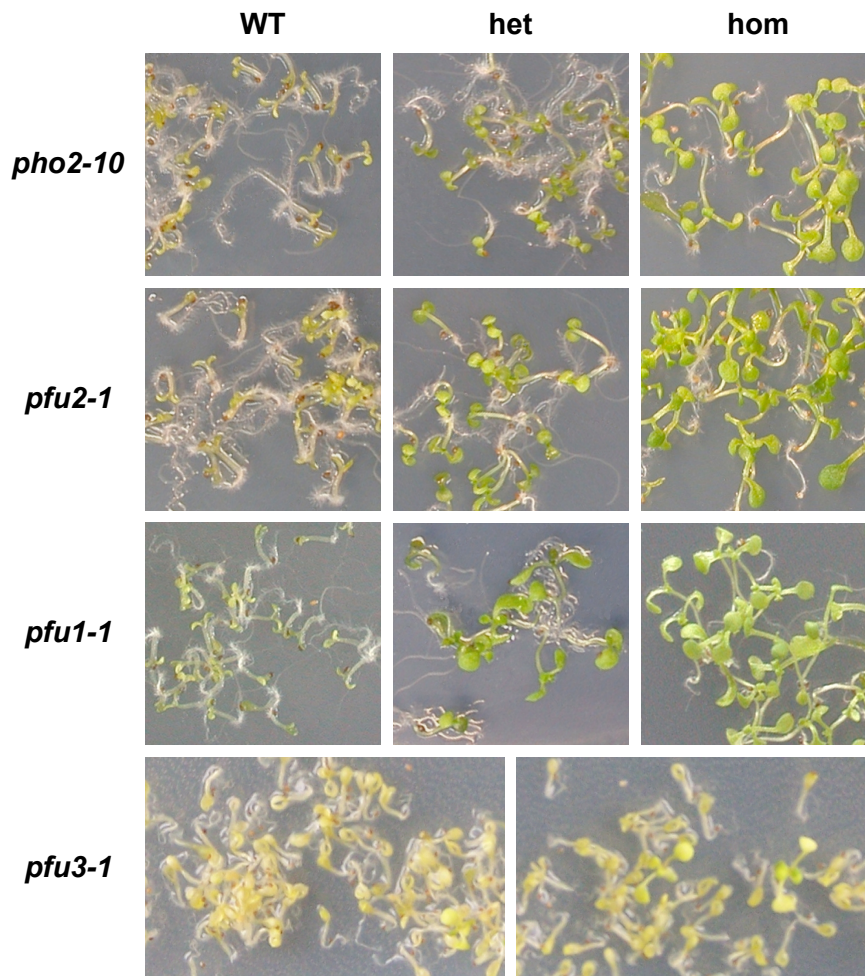


Figure 2.12: Altered response to *ubK48R* induced cell death in *pfu* mutant plants: Seeds of plant lines all exhibiting the *ubK48R* transgene were grown on MS plates containing hygromycin for selection and dexamethasone for transgene induction. Plant growth was monitored 5 days after germination. The first column shows the positive control for each assay, meaning the cell death occurring after *ubK48R* induction in wild type (WT) background. The second column summarizes the results in plants identified to be heterozygous (het) for the respective mutation. The effect on programmed cell death caused by homozygous mutation (hom) in the respective *PFU* gene is shown in the third column. For the *pfu3-1* mutation, results with heterozygous plants were not collected.

programmed cell death during a very early developmental stage (Schlögelhofer et al. 2006). If this *ubK48R* transgene is now expressed in a homozygous *pho2-10* mutant background, plants lack early cell death induction observed for wild type plants and show non-restricted normal growth (Fig. 2.12). The same suppression of plant death could be observed for homozygous *pfu1-1* und *pfu2-1* mutants (assays performed by Dr. M. Garzon), indicating

a major role of the PFU proteins in the induction of programmed cell death. Even plants containing a T-DNA insertion in just one of the *PFU1* alleles (heterozygous plants) were able to suppress the *ubK48R* induced cell death nearly to the same extent as could be seen for the homozygous mutant background (Fig. 2.12). This was not the case for heterozygous *pho2-10* mutants, which show the same growth perturbation as wild type plants. Heterozygous *pfu2-1* mutants seem to represent an intermediate between *pfu1-1* and *pho2-10* mutation, as these plants show a reduced but still detectable growth when expressing *ubK48R*. The only mutation not suppressing programmed cell death in the *ubK48R* assay at all was *pfu3-1*, even though plants were homozygous for the T-DNA insertion (Fig. 2.12).

To verify that the decrease of cell death induction observed for the *pfu* mutants is not due to a loss of *ubK48R* transgene expression, RT-PCR analyses were performed with *pfu1-1* mutant plants expressing *ubK48R*, as these showed the most severe phenotype. The mRNA of the *ubK48R* transgene was amplified by the use of the downstream oligo 144A-pTAdn, binding at the 5' end, and the upstream oligo 200A-DHFRup, binding at the DHFR fragment close to the 3' end of the transgene. The expected PCR product possessing a size of approximately 2 kb could be detected for both wild type and *pfu1-1* background (Fig. 2.13). The expression of *UBC9* was again used as an internal standard and showed that the amount of RNA in both samples was equal. Besides, the PCR fragment obtained was definitely deriving from the *ubK48R* mRNA and not from the genomic DNA, as the negative control lacking the reverse transcriptase did not give any band at the expected height. These results demonstrate that the phenotype in programmed cell death observed with the *ubK48R* transgene assay can be definitely traced back to the mutation in *pfu1-1* and is not explained by a lower transgene expression. Hence, PFU1, PFU2 and PHO2 seem to play a major role in the initiation of programmed cell death in plants.

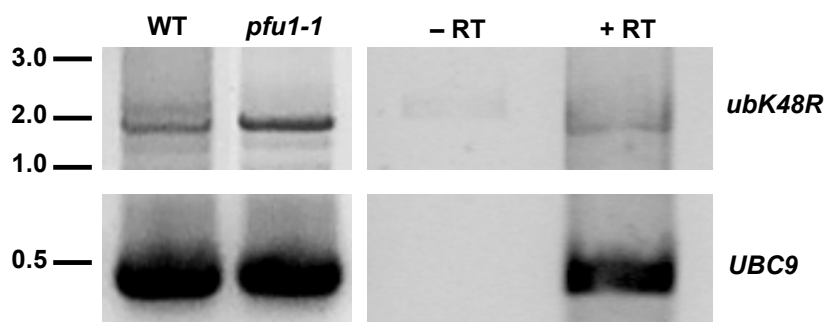


Figure 2.13: RT-PCR results to verify that the *ubK48R* transgene is expressed equally in both wild type and *pfu1-1* mutant background. Amplification of the *ubK48R* open reading frame from genomic DNA is excluded by comparing samples without (-RT) and with (+RT) reverse transcriptase. *UBC9* expression levels to ensure proper cDNA synthesis are shown in the lower panels.

Higher resistance of *pfu* mutants to ozone treatment

It is well known that reactive oxygen species, such as ozone or hydrogen peroxide, are key players in the regulation of many plant processes including the initiation of programmed cell death during stress responses or leaf senescence. In the previous chapter the PFU proteins were identified to also play a major role in the initiation of programmed cell death in plants. Due to this connection it now became of interest whether the PFU proteins are somehow affected by the treatment with reactive oxygen species.

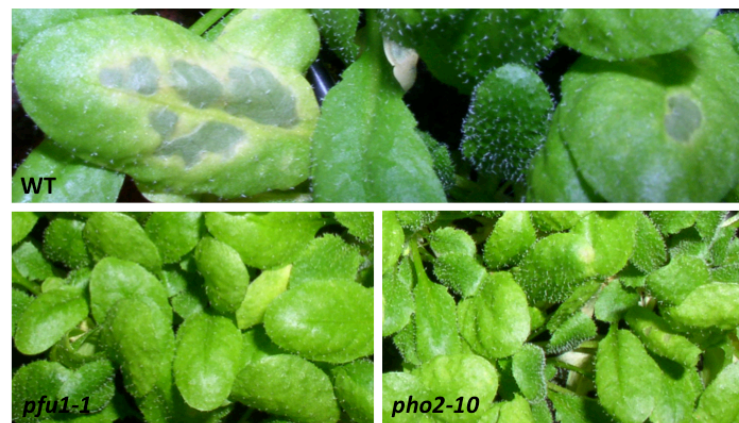


Figure 2.14: Leaf phenotype of four week-old wild type (WT), *pfu1-1* and *pho2-10* plants that were exposed to 350 ppb of ozone for two days.

In collaboration with Dr. Dieter Ernst at the Helmholtz Centre Munich, plants of the *pfu* single mutant lines were analyzed under ozone treatment. Four week-old mutant and wild type plants were exposed to 350 ppb of ozone for two days. Afterwards the leaf phenotype was monitored. Ozone treatment of wild type *Arabidopsis* plants induces stress responsive genes resembling an accelerated foliar senescence (Miller et al. 1999). Hence, after 2 days of exposure, wild type leaves showed yellowing and, unlike the senescence process, even severe lesions (Fig. 2.14).

This intense stress response could also be detected for *pfu2-1* single mutants. In contrast, the response of *pfu1-1* and *pho2-10* mutant plants to ozone was much weaker and was restricted to only minor leaf yellowing. After two days, no severe leaf lesions were visible at all. These results indicate that a single mutation in either PFU1 or PHO2 is sufficient to interrupt the stress signaling pathway induced by ozone and suggest that these proteins are important for sensing oxidative signals leading to programmed cell death.

PFU2 responses to nitric oxide

Nitric oxide was first identified to be a unique diffusible second messenger in animals (Lowenstein and Snyder 1992) but is now also well known to regulate an enormous amount of plant processes, such as plant development (Leshem 1996) and stress responses (Grün

et al. 2006). It functions in the signaling pathways in response to various abiotic stresses such as drought, UV and ozone but is also involved in the hypersensitive response to pathogens (Delledonne et al. 2001). In conclusion, apart from other functions, nitric oxide is a key regulator in the programmed cell death signaling. As an NO donor, the salt sodium nitroprusside is therefore capable to provoke programmed cell death in plants.

Making use of this reagent, the question can be solved whether the PFU proteins are, apart from their function in oxidative stress caused by ozone, also able to sense signals caused by nitric oxide treatment.

However, before testing the *pfu* mutants in such an assay, the concentration of sodium nitroprusside had to be set to a value where Columbia wild type plants only show a slow cell death reaction lasting several days. Therefore, Columbia seeds were grown for one week in three continuously shaking flasks containing liquid Gamborg's B5 medium. Then a different concentration of sodium nitroprusside (sodium nitroferricyanide(III) dihydrate) was added to each flask every second day. Wild type plants exposed to 0.5 mM sodium nitroprusside were dead two days after the first treatment. In contrast to this, plants treated with 0.2 mM sodium nitroprusside were dying only very slowly, showing no green leaves anymore when the treatment was stopped three weeks after the first addition of NO. At this timepoint, plants exposed to 0.1 mM sodium nitroprusside were still partly green.

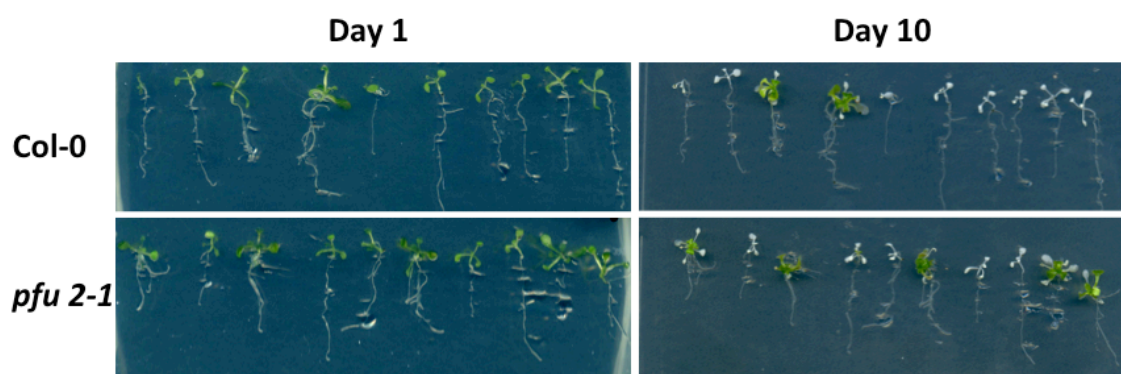
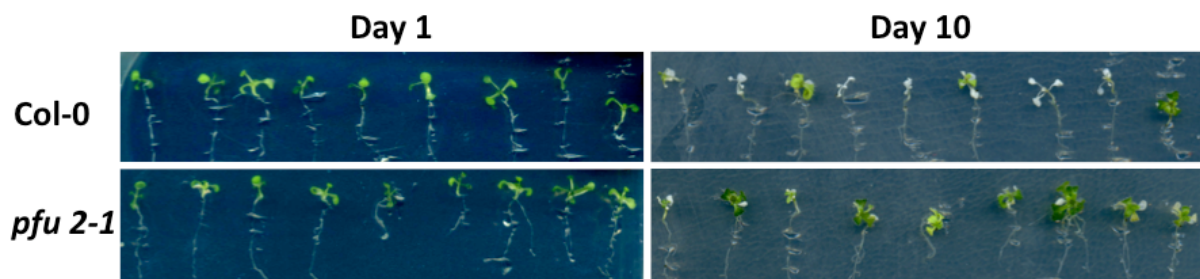
Due to this observation, the subsequent comparison of wild type plants and *pfu* mutants was performed with 0.2 mM sodium nitroprusside added every second day to the flask. Again plants were first grown for one week before the treatment was started. None of the mutant lines showed any obvious phenotype concerning leaf senescence. As observed for the wild type plants all mutants died very slowly showing no green parts anymore three weeks after the first NO addition. Only *pfu2-1* plants showed a slight increase in lateral root formation, which was hard to monitor in the liquid medium and could not be reproduced in a second similar trial.

The difficulty to identify possible *pfu* phenotypes with this experimental setup can be explained by the extreme volatility of NO, which can easily leak out of the flasks. Therefore a new setup was chosen, which also offered the possibility to better quantify plant death. Columbia wild type plants and *pfu2-1* mutants were grown for ten days on normal MS plates and were then transferred to plates containing 0.2 mM sodium nitroprusside. The phenotype of the plants was monitored each day after the transfer and the amount of dead seedlings per plant line, showing no green parts at all anymore, was counted.

The experiment was repeated twice with a total of 90 plants per line. In neither of these cases the *pfu2-1* mutant line showed an increase in lateral root formation, but the number of surviving plants differed greatly from the number observed for wild type. Table 2.5 summarizes the percentage of plants surviving after four days of exposure obtained from both experiments. The mean value was calculated from the percentages received for each of the independent experiments and the standard deviation is shown behind. Whereas only around 11 % of the wild type plants survived, approximately 27 % of the *pfu2-1* mutants were able to withstand the treatment showing a nearly three times higher survival rate. During both experiments, the number of surviving plants did not change anymore after five days on the NO plates. The surviving plants stayed green, but did not grow any further.

Table 2.5: *pfu2-1* mutant plants are more resistant to NO treatment

Genotype	surviving plants after 4 days of exposure to 0.2 mM sodium nitroprusside
WT	11 % +/- 4
<i>pfu2-1</i>	27 % +/-1

**Figure 2.15:** NO treatment (0.2 mM) of wild type (WT) and *pfu2-1* mutants. Plants were first grown for ten days on plates without supplement before transferring them to MS plates containing 0.2 mM sodium nitroprusside. Pictures were taken on the day of the transfer (day 1) and again after ten days (day 10).**Figure 2.16:** NO treatment (0.1 mM) of wild type (WT) and *pfu2-1* mutants. Plants were first grown for ten days on plates without supplement before transferring them to MS plates containing 0.1 mM of sodium nitroprusside. Pictures were taken on the day of the transfer (day 1) and again after ten days (day 10).

Still, when transferred back to normal MS plates lacking sodium nitroprusside, growth was restored showing that the plants were still viable.

To visually demonstrate the higher resistance of the *pfu2-1* mutants to NO, one of the plates with plants before and after ten days of exposure to 0.2 mM sodium nitroprusside is shown in Fig. 2.15. Out of the ten plants per line only two wild type plants on this plate survived the treatment, compared to five plants in the case of the *pfu2-1* mutant line.

Apart from these experiments, wild type and mutant plants were also analyzed once on a plate containing 0.1 mM sodium nitroprusside (Fig. 2.16). Although the percentage of surviving plants for both wild type (40 %) and *pfu2-1* mutants (100 %) is much higher, the ratio between the two lines is the same as observed in the experiments with 0.2 mM sodium nitroprusside. The *pfu2-1* mutant plants are nearly three times more resistant to NO treatment than wild type plants, demonstrating once more that the PFU2 protein seems to be necessary to properly execute NO induced programmed cell death in plants.

The stress response to a pathogen is decelerated in *pfu1-1 pho2-10* mutants

The *pfu* phenotypes identified in the previous chapters showed that the PFU proteins exert an important role in programmed cell death responses to abiotic stress. However, also biotic stress caused by plant pathogens induces a very fast cell death program called hypersensitive response (Mur et al. 2008). Since the PFU proteins are affected by oxidative signals, and reactive oxygen species are known to transmit stress signals during a hypersensitive response, the question arose whether the PFU proteins are also participating in programmed cell death induced by pathogen attacks.

In collaboration with Dr. N. Schlaich at the RWTH Aachen, the resistance of the *pfu* mutants to a bacterial pathogen was analyzed and compared to wild type *Arabidopsis* plants. Therefore five week-old plants were infiltrated with *Pseudomonas syringae* pv tomato (*Pst*) DC3000 at a high concentration of 5×10^7 cfu/ml. The bacterial strain used was avirulent as it contained the type III effector gene *AvrRpt2* (Whalen et al. 1991), but still caused non lethal programmed cell death reactions of the plants. Leaf samples were collected from each plant line directly after infiltration and at several additional timepoints up to 21 hours after infiltration. To determine the amount of programmed cell death the samples were washed in ddH₂O, which was then used to measure conductivity levels. Cell death results in ion leakage from the tissue. These ions were solubilized in water and changed the conductivity of the solution. Thus, higher conductivity levels corresponded to a stronger programmed cell death response of the plants.

In total, the experiment was repeated four times for the single mutant lines *pfu1-1* and *pho2-10* and for the *pfu1-1 pho2-10* double mutant. To more easily compare the values, wild type conductivity was equated with 100 %. The mean percentage out of the four experiments was calculated for each line at 7 hours and 21 hours after the infection and is summarized together with the standard deviation in Table 2.7.

These values revealed that the single mutants *pfu1-1* and *pho2-10* exhibited the same response to the infiltration with the pathogen as detected for wild type plants. Only the value of 120 % for *pfu1-1* after seven hours exceeded wild type levels, but the standard

Table 2.7: Ion leakage measurements

Genotype	Ion leakage 7 h after infiltration in % of WT	Ion leakage 21 h after infiltration in % of WT
<i>pfu1-1</i>	120 +/- 10 %	106 +/- 5 %
<i>pho2-10</i>	97 +/- 3 %	99 +/- 5 %
<i>pfu1-1 pho2-10</i>	84 +/- 5 %	90 +/- 7 %

deviation was in this case very high. Interestingly, the *pfu1-1 pho2-10* double mutant showed with 84 % less programmed cell death than wild type after seven hours. However, the cell death response seemed to be only delayed as the conductivity values nearly gained wild type levels again after 21 hours. This observation indicates that the PFU proteins are apart from abiotic stress also involved in biotic stress responses. Still, the initiation of programmed cell death after bacterial pathogen attack is only delayed if both PFU1 and PHO2 are mutated, suggesting that both proteins might act in the same signaling pathway.

2.3 Subcellular localization of the PFU proteins

The physiological analyses on the *pfu* knockout plants revealed possible functions of the PFU proteins in plants. Still, the question about their actual function on the molecular level remains unanswered. Before performing biochemical assays to solve this problem, the subcellular localization of the proteins was analyzed, which very often gives additional indications on the pathways the proteins of interest are involved in.

2.3.1 Cloning of EGFP/mRFP fusion constructs

Different fluorescent proteins were fused to the carboxyl terminus of the PFU proteins. The constructs for PFU1, PFU3 and PHO2 were obtained from Dr. A. Bachmair. PFU1 was fused to the enhanced form of the green fluorescent protein (EGFP). In contrast, the construct received for PHO2 was a fusion protein with the monomeric form of the red fluorescent protein (mRFP; Jach et al. (2006)). For PFU3 both the EGFP and the mRFP fusion was obtained.

So far, no fusion constructs were available for PFU2. Thus, after cloning the open reading frame of *PFU2* into the pBluescript II SK+ vector as described in chapter 2.1.2, the gene was extended with EGFP and mRFP. Therefore the STOP codon was changed for a *KpnI* restriction site, making use of the oligo 837A-LET2Kpnup. To enhance the transcription

of the transgene *in planta*, the omega leader, a 5'-leader sequence of the tobacco mosaic virus (Gallie et al. 1987), was added by ligating the oligos 876A-OmXNdetop and 877A-OmXNdebot in between restriction sites *Xho*I and *Nde*I of the pBluescript II SK+ construct. Afterwards, this modified form of *PFU2* was cloned into the two different plant expression vectors p3, possessing a constitutive 35S promoter, and pER8, bearing a β -estradiol inducible promoter. The *PFU2* construct in pBluescript II SK+ was first cloned into p3 already containing EGFP, making use of the restriction sites *Xho*I and *Kpn*I. To clone the mRFP fusion, the EGFP between restriction sites *Kpn*I and *Xba*I was changed for mRFP, obtained from the pER8-PHO2-mRFP construct. Then the PFU2-EGFP and PFU2-mRFP fragments were cut out of p3 using *Xho*I and *Xba*I and ligated between the *Xho*I and *Spe*I sites of the pER8 vector.

Finally, the following six fusion constructs were available in both p3 and pER8 vector for the subsequent subcellular localization assays: PFU1-EGFP, PFU2-EGFP, PFU3-EGFP, PFU2-mRFP, PFU3-mRFP and PHO2-mRFP. These constructs were transformed into *Agrobacterium tumefaciens* to express them in plants.

2.3.2 Transient expression of the fusion constructs in *Nicotiana benthamiana*

A fast method to analyze the localization of the fusion proteins is transient expression in the heterologous plant system *Nicotiana benthamiana*. *Agrobacteria* bearing the p3 constructs with the constitutive 35S promoter were infiltrated into the leaves of four week-old plants, and the infected tissue could be analyzed under the confocal microscope already three days afterwards.

PFU1 is present in nucleus and cytoplasm

Due to the 35S promoter in the p3 vector, PFU1-EGFP was highly expressed throughout the infiltrated tissue. Within the cell, the PFU1 fusion protein was located in both cytoplasm and in the nucleus. As the vacuole of a typical plant cell occupies most of the cell interior, the cytoplasm bearing the fluorescent fusion protein was pressed to the plasma membrane and was therefore only visible as a thin belt. Still, cytoplasmic strands that pass through the cell were detectable (Fig. 2.17, panel A).

A higher magnification revealed that parts of the PFU1 protein were packed in small vesicles or aggregates occurring all over the cytoplasm (Fig. 2.17, panel B). The PFU1 fusion protein in the nucleus was evenly distributed. However, it was obviously excluded from the nucleolus (Fig. 2.17, panel C).

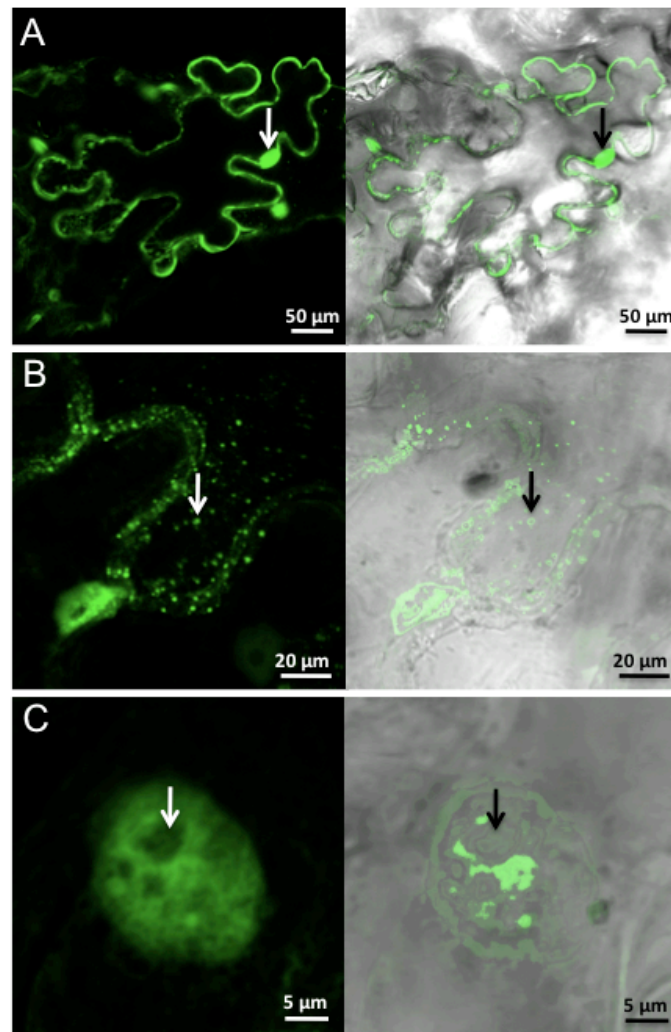


Figure 2.17: PFU1-EGFP expression in epidermal cells of *Nicotiana benthamiana*. A: Overview over the whole cell with PFU1 expression in both cytoplasm and nucleus (arrow). B: Magnification of the cytoplasm and the nucleus uncovers the formation of small vesicles or aggregates (arrow) containing the fusion protein. C: Close-up of the nucleus reveals exclusion of PFU1 from the nucleolus (arrow).

PFU3 is highly expressed in the nucleus

For the closest relative of PFU1, PFU3, EGFP and mRFP fusions were available and used for infiltration of *Nicotiana benthamiana* leaves. Both combinations showed the same subcellular localization of the protein. PFU3 could only be detected in the nucleus and was completely absent in the cytoplasm (Fig. 2.18). Again the EGFP fusion was easy to detect, whereas with the RFP filter the autofluorescence of the chloroplasts became visible (Fig. 2.18, panel C), which made visualization of the PFU3-mRFP fusion protein more difficult.

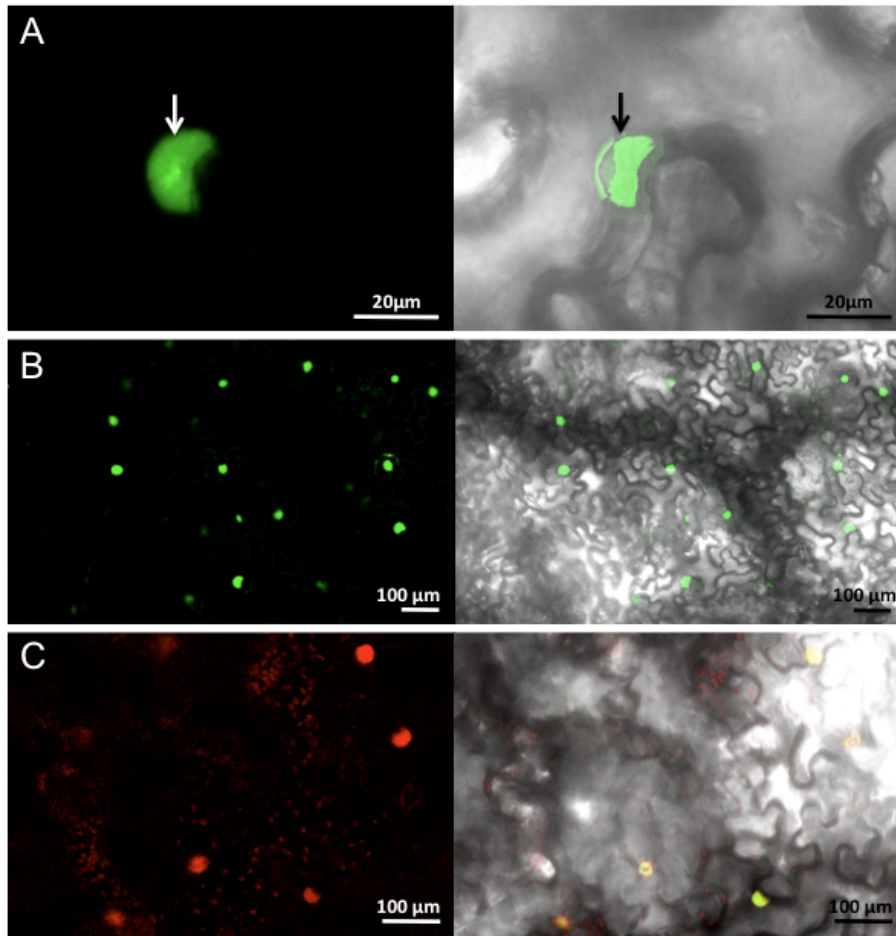


Figure 2.18: Epidermal cells of *Nicotiana benthamiana* expressing PFU3 fusion proteins. A: PFU3-EGFP expression is only visible in the nucleus (arrow). B: Overview on several epidermal cells pointing out the restriction of PFU3 to the nucleus. C: PFU3-mRFP is also located in the nucleus. Smaller red spots indicate the autofluorescence of the chloroplasts.

PFU2 and PHO2 are restricted to the cytoplasm

The fusion proteins of the two larger members of the protein family, PFU2 and PHO2, both show the same localization when transiently expressed in *Nicotiana benthamiana* leaves. Both are only visible in the cytoplasm and are in contrast to the other members of the PFU family completely excluded from the nucleus (Fig. 2.19 and Fig. 2.20).

The EGFP and mRFP constructs of PFU2 show similar results. Fluorescence is only visible in the cytoplasm surrounding the nucleus (Fig. 2.19, panel B and D). The EGFP signal was much more intense and, in contrast to the mRFP construct, the protein was also visible in big vesicle-like structures located close to the plasma membrane (Fig. 2.19, panel A). In addition to this, cytoplasmic strands were detectable for both EGFP and mRFP fusions.

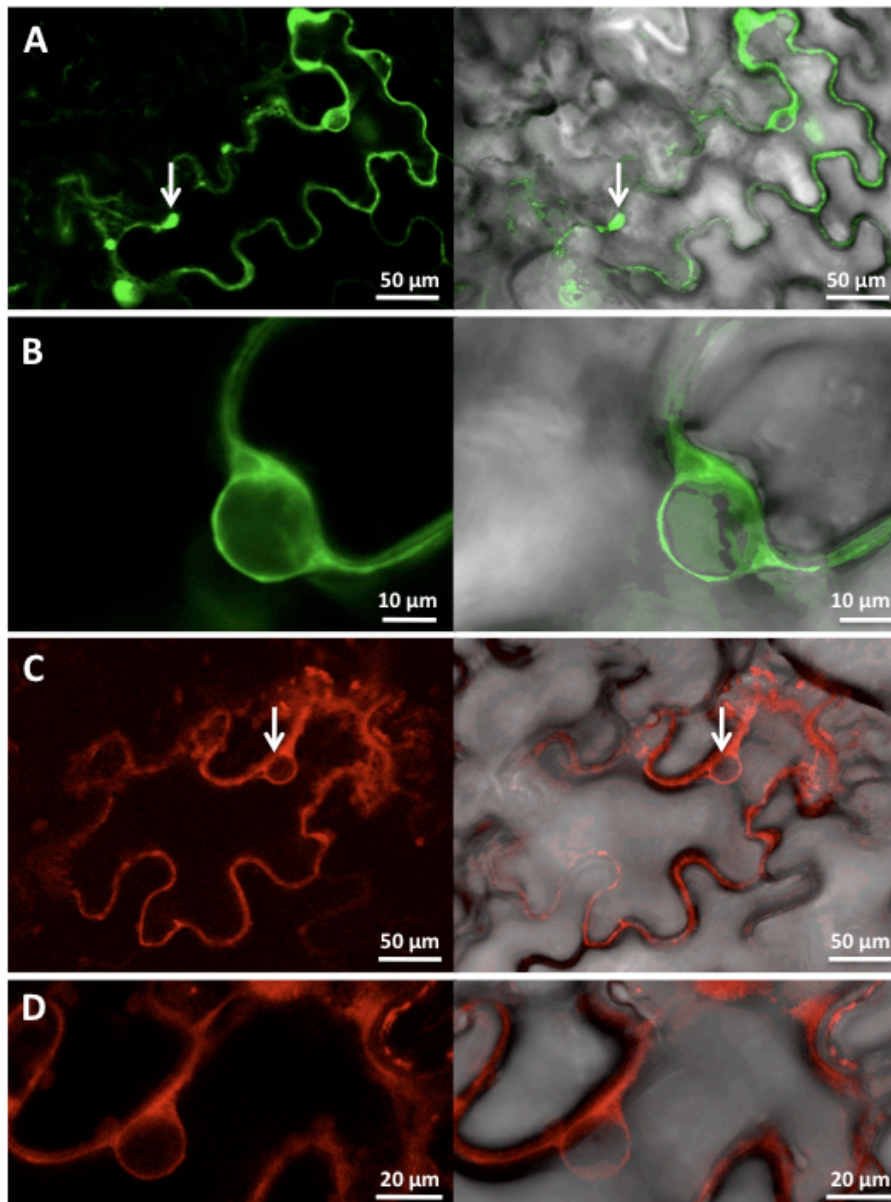


Figure 2.19: Subcellular localization of PFU2 in *Nicotiana benthamiana* cells. A: Epidermal cell expressing the PFU2-EGFP construct only in the cytoplasm. Apart from that, the protein is visible in vesicle-like structures (arrow). B: Higher magnification of the nucleus surrounded by the fluorescing cytoplasm. C: PFU2-mRFP is also expressed only in the cytoplasm of the cell. The non-fluorescing nucleus is marked by an arrow. D: Higher magnification of the region around the nucleus.

The PHO2-mRFP fusion protein was also fluorescing only in the cytoplasm enclosing the nucleus. Fig. 2.20 demonstrates the diffuse expression of the protein throughout this

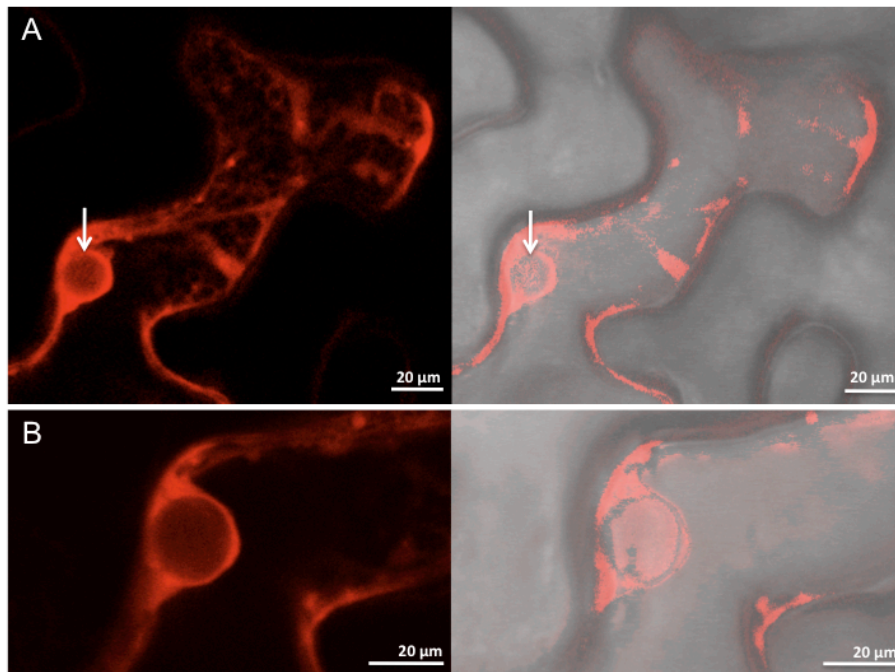


Figure 2.20: Microscopic images of *Nicotiana benthamiana* cells expressing PHO2-mRFP.

A: Construct is only expressed in the cytoplasm excluding the nucleus (arrow). Multiple cytoplasmic strands passing through the cell are visible. B: Close-up of the region around the nucleus showing diffuse distribution of the PHO2 protein in the cytoplasm.

compartment also giving examples of cytoplasmic strand formation. Vesicle-like structures as detected for the PFU2-EGFP construct were not visible.

Coexpression of PFU fusion proteins in *Nicotiana benthamiana*

While comparing wild type plants with the *pfu* mutants under biotic stress induced by a bacterial pathogen, a delayed programmed cell death response could be detected for the *pfu1-1 pho2-10* double mutant. This observation rose the question whether the two proteins PFU1 and PHO2 act in the same pathway and maybe colocalize or even interact with each other. Therefore the two fusion proteins PFU1-EGFP and PHO2-mRFP were coinfiltrated into *Nicotiana benthamiana* leaves. This experiment was repeated four times with inconsistent results. Interestingly, during the first two experiments PHO2-mRFP colocalized with PFU1-EGFP in the nucleus (Fig. 2.21), although the single infiltration of PHO2-mRFP into the leaves still showed the same restriction of the protein to the cytoplasm. In contrast, a coinfiltration of PFU3-EGFP and PHO2-mRFP did not result in any relocation of PHO2 to the nucleus. Unfortunately these observations could not be reproduced in a third and fourth experiment. Here, the PHO2-mRFP protein stayed in the cytoplasm when coexpressed with PFU1-EGFP. However, these experiments indicate that a coexpression of PHO2 and PFU1 might lead to a relocation of PHO2 to the nucleus.

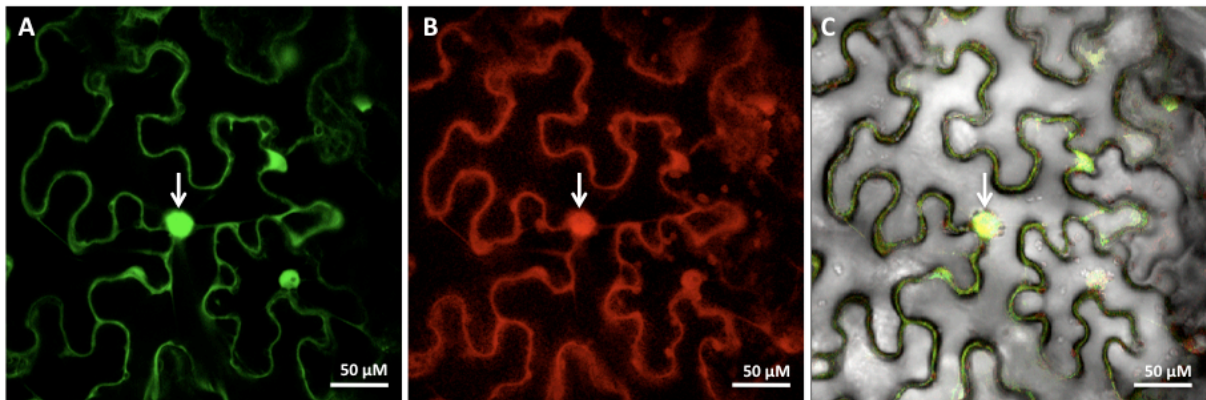


Figure 2.21: Coinfiltration of PFU1-EGFP and PHO2-mRFP into *Nicotiana benthamiana* leaves resulted in relocation of PHO2-mRFP usually restricted to the cytoplasm. PFU1-EGFP and PHO2-mRFP are in this case both localized in the nucleus (arrow). A: Microscopic image of an epidermal cell with the GFP filter visualizing the PFU1-EGFP protein. B: The same epidermal cell under the RFP filter displaying the localization of the PHO2-mRFP protein. C: Overlay of both pictures with the cell under transmitted light.

2.3.3 Expression of EGFP/mRFP fusion proteins in transgenic *Arabidopsis thaliana* lines

Although the transient expression of the single proteins in *Nicotiana benthamiana* gave clear and consistent results, it is still a heterologous system and might therefore give a different outcome than the actual subcellular localization of the PFU proteins *in vivo*. To circumvent this problem, the localization was analyzed additionally in transgenic *Arabidopsis thaliana* plants. *Agrobacterium* bearing the pER8 constructs were used to transform Columbia wild type plants via the floral dip method. The progeny of these plants was sown on hygromycin plates to select for transformants, which were then transferred onto soil and the existence of the transgene was verified via PCR. Seeds of the F2 generation were grown on hygromycin plates for ten days before they were transferred to plates containing 5 μ M β -estradiol for transgene induction. To detect the EGFP constructs, plants had to be induced for three days on these plates, whereas expression of the mRFP constructs was only visible after four to five days of induction. Table 2.9 summarizes the intensity of the protein expression for the different plant lines determined via microscopic analysis.

For all proteins except for PFU2 stably transformed plant lines expressing the fluorescent fusion protein could be verified. Still, the expression levels differed between the different plant lines and some of the transgenic lines verified via PCR did not show any expression at all. Very strong expression could be detected for both PFU3 constructs. The EGFP construct showed the highest fluorescence intensity and was expressed in nearly all root cells analyzed. PFU1-EGFP was easy to detect as well and was expressed in a high number of root cells. In contrast to this, the PHO2-mRFP expression was very hard to recognize, as only a few root cells were expressing the protein.

Table 2.9: EGFP/mRFP fusion protein expression in the F2 generation of *Arabidopsis thaliana* lines stably transformed with pER8 fusion constructs and analyzed under the confocal microscope. (–) no expression, (+) expression, (++) high expression, (+++) extremely high expression, (n.a.) line not available

plant line	PFU1-EGFP	PFU3-EGFP	PFU3-mRFP	PHO2-mRFP
1	–	++	++	+
2	++	+	+	–
3	+	++	–	–
4	–	++	+	++
5	+	+	++	–
6	+	–	–	–
7	++	++	–	–
8	++	+	++	–
9	–	+++	–	–
10	–	++	++	–
11	–	++	++	–
12	n.a.	–	++	+
13	n.a.	++	+++	–
14	n.a.	–	+	–
15	n.a.	++	+	–
16	n.a.	++	++	+
17	n.a.	++	–	++
18	n.a.	–	++	+
19	n.a.	n.a.	+++	+
20	n.a.	n.a.	n.a.	++

For the closest homologue of PHO2, PFU2, transformants could only be obtained with the EGFP construct. Plants of the F1 generation were able to grow on hygromycin plates and the subsequent PCR verified that they contained the correct transgene. However, the F2 generation was not resistant to hygromycin anymore, although the transgene could still be amplified from genomic DNA. Microscopic analysis was also negative for all 17 plant lines examined. The transformation of wild type plants with the PFU2-EGFP construct was repeated a second time, but again the results were exactly the same. The F2 generation lost its ability to grow on hygromycin and the roots did not show any fluorescence at all.

PFU1-EGFP localization in stably transformed *Arabidopsis* plants

As observed for the p3 construct in *Nicotiana benthamiana*, PFU1-EGFP is located in both the cytoplasm and the nucleus (Fig. 2.22). In the root cells of *Arabidopsis* the cytoplasm is pressed to the cell wall, but a diffuse expression of the fluorescent protein is also visible around the nucleus, proving that the signal is located in the cytoplasm and is not detected due to autofluorescence of the cell wall. However, vesicle-like structures in the cytoplasm, as observed during the transient expression, were in this case completely absent.

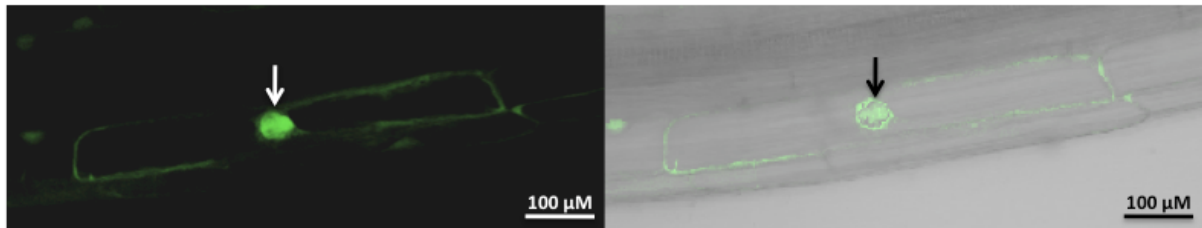


Figure 2.22: *Arabidopsis* root cell expressing the pER8-PFU1-EGFP construct. Plants of the F2 generation were grown for ten days on hygromycin plates and then induced for three days on plates containing 5 μM β -estradiol before analyzing them under the confocal microscope. The fusion protein is located in the cytoplasm and in the nucleus (arrow).

High expression of PFU3 in the nuclei of *Arabidopsis* root cells

In accordance with the results of the transient expression of PFU3 in *Nicotiana benthamiana*, both PFU3-EGFP and PFU3-mRFP were located only in the nuclei of the *Arabidopsis* root cells. Figure 2.23 (panel A) shows a root tip expressing PFU3-EGFP in nearly all of the cells analyzed. The only part of the root not expressing the transgene is the zone above the apical meristem. A close-up of the cells (Fig. 2.23, panel B) further illustrates the restriction of PFU3 to the nucleus. The faint signal around the cell was due to the autofluorescence of the cell walls. This signal was absent when analyzing the PFU3-mRFP protein with the RFP filter. Again the protein was only fluorescing in the nucleus (Fig. 2.23, panel C).

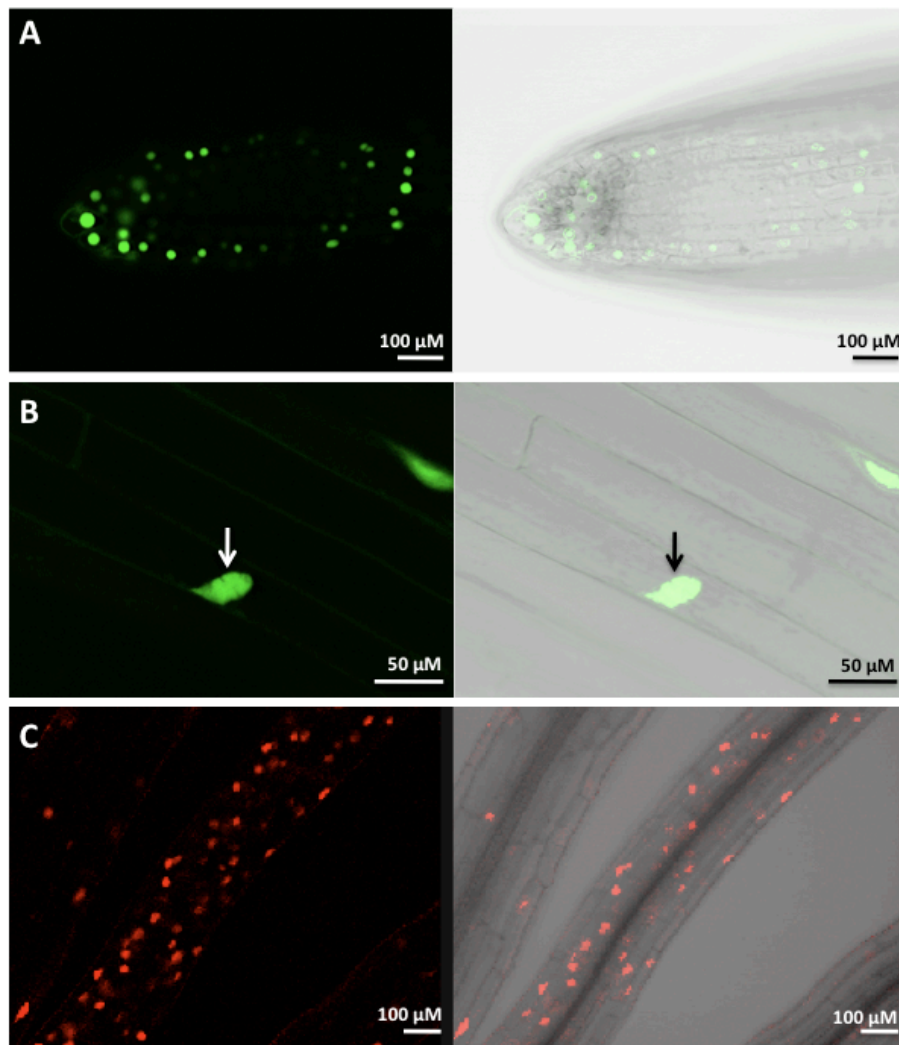


Figure 2.23: PFU3 is only located in the nucleus of stably transformed *Arabidopsis* plants. A: Root tip expressing PFU3-EGFP in nearly all cells except for the area above the apical meristem. B: Higher magnification of a root cell bearing PFU3-EGFP only in the nucleus (arrow). C: Roots expressing PFU3-mRFP, which is marking the nuclei of the cells.

PHO2 shows diffuse localization in the cytoplasm

The PHO2-mRFP signal was very hard to detect. Only a few root cells were expressing the fusion protein and the signal was very faint. Still it was obvious that, as observed for the transient expression, the PHO2-mRFP fusion protein showed a diffuse distribution throughout the cytoplasm with cytoplasmic strands spanning through the cell (Fig. 2.24, panel A). When analyzing the nuclei of the cells, it became clear that also in stably transformed *Arabidopsis* plants, PHO2 is completely absent in this organelle, but is expressed in the surrounding cytoplasmic area (Fig. 2.24, panel B).

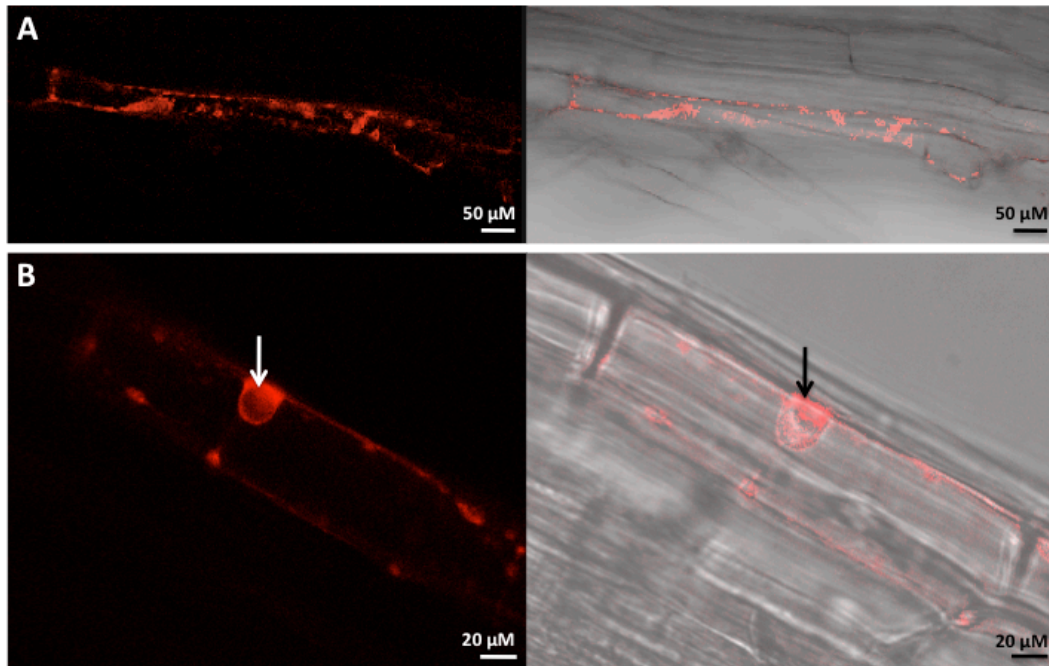


Figure 2.24: Localization of PHO2-mRFP in stably transformed *Arabidopsis thaliana* plants. A: Diffuse expression of PHO2-mRFP in the cytoplasm of a root cell. B: PHO2-mRFP is completely absent from the nucleus (arrow), but is located in the surrounding cytoplasm.

Coexpression of PFU1-EGFP and PHO2-mRFP in *Arabidopsis thaliana*

As transient expression in *Nicotiana benthamiana* gave inconsistent results regarding the colocalization of PFU1 and PHO2 in the cell, *Arabidopsis thaliana* plants bearing the inducible PFU1-EGFP construct were crossed with plants possessing the pER8-PHO2-mRFP transgene. The progeny of these plants was tested via PCR to contain both transgenes. Seeds of the F2 generation were sown on hygromycin plates containing either no supplement, 1mM Azacytidine or 4 μ M Trichostatin. These reagents were added to suppress possible gene silencing via methylation. After one week on these plates, the seedlings were transferred to plates containing β -estradiol for induction of the transgenes. Colocalization of PFU1-EGFP and PHO2-mRFP was analyzed under the microscope after four days of induction. All of the plants expressed the PFU1-EGFP fusion protein in both cytoplasm and nucleus. Still, the PHO2-mRFP protein could not be detected in any of the cells including plants grown on Azacytidine or Trichostatin. The F3 generation was also positively tested for the existence of both transgenes in the genomic DNA. However, only the PFU1-EGFP fusion protein was visible under the microscope. To analyze whether the *PHO2-mRFP* transcript is downregulated, RNA of plants of the F3 generation was purified and cDNA was synthesized with the upstream reading oligos 471A-GFPup1 and 524A-RFPNseq. For the subsequent PCR, the oligos 117A-LET1dn and 471A-GFPup1 were used for the *PFU1-EGFP* mRNA resulting in a PCR product of 2060 bp. The *PHO2-mRFP*

transcript was amplified with oligos 526A-LET4Cdn and 524A-RFPNseq giving a product of 630 bp. The mRNA for both transgenes *PFU1-EGFP* and *PHO2-mRFP* could be detected in induced plants (Fig. 2.25), so that gene silencing of *PHO2-mRFP* on the transcriptional level could be excluded. These results indicate that *PHO2-mRFP* is posttranscriptionally downregulated if *PFU1-EGFP* is overexpressed in the plants. Hence, by this means a possible colocalization of *PHO2* with *PFU1* could not be investigated.

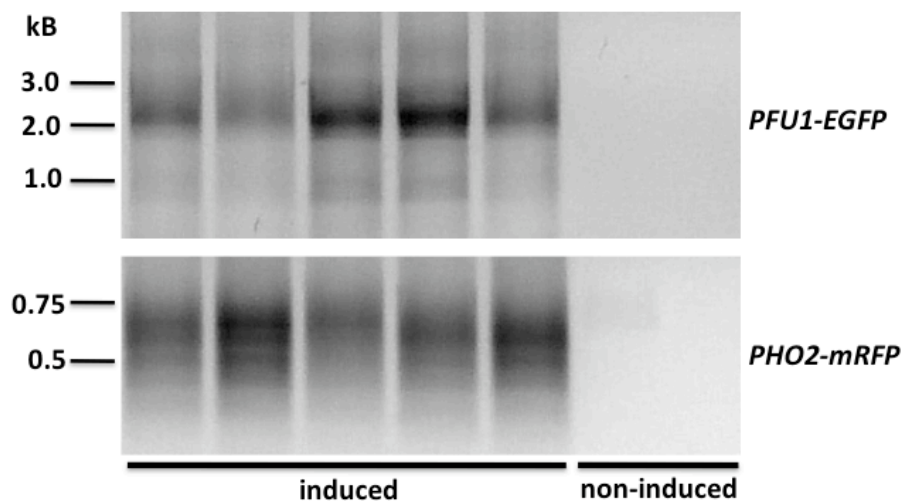


Figure 2.25: Transcript levels of *PFU1-EGFP* and *PHO2-mRFP* in F3 plants bearing both transgenes under the β -estradiol inducible promoter.

2.4 Interaction studies in *Saccharomyces cerevisiae*

Several results of the mutant screening and the subcellular localization analysis gave indication for a possible interaction between *PFU1* and *PHO2*. The double mutant *pfu1-1 pho2-10* showed a delayed programmed cell death response to biotic stress, and both transient expression of EGFP/mRFP fusion proteins in *Nicotiana benthamiana* and transgenic *Arabidopsis thaliana* plants revealed an effect on *PHO2* when coexpressed with *PFU1*. Still, interaction could not be proven by these experiments. Due to this, a yeast two hybrid assay was established to identify a putative interaction between *PFU1* and *PHO2*.

2.4.1 Autoactivation of *PFU* proteins

Both *PFU1* and *PHO2* were cloned into the yeast expression vector pGBKT7. In this vector the N-terminus of inserted proteins is fused to amino acids 1-147 of the GAL4 DNA binding domain, and the fusion proteins are expressed in yeast under the control of the constitutive *ADH1* promoter. To receive these constructs, the pER8 plasmids containing *PFU1-EGFP* and *PHO2-mRFP*, respectively, were cut with *Asp718*. Then the ends were filled up before

the linearized vector was cut again with *NdeI* in the case of *PFU1* and *NcoI* in the case of *PHO2*. The obtained open reading frames of the *PFU* genes were afterwards ligated into the yeast vector cut with *SmaI* and either *NdeI* or *NcoI*. The resulting constructs were transformed into the yeast strain PJ96-4 α . As the pGBKT7 vector contains a *TRP1* auxotrophic marker, yeast transformants could be identified on plates lacking tryptophan. The yeast strain PJ96-4 α possesses a *HIS3* gene under the inducible GAL4 promoter. Binding of the complete GAL4 activator protein leads to expression of genes controlled by this promoter. Yeast cells expressing the bait protein fused to only the GAL4 DNA binding domain (DBD) should therefore not be able to grow on SC –His plates (Fig. 2.26, panel A). In a standard yeast two hybrid screen a prey protein, which is fused to the activation domain (AD), is expressed from a second plasmid. Yeast cells only express the *HIS3* gene and are able to grow on SC –His plates, if bait and prey interact and the Gal4 DNA binding domain gets into contact with the GAL4 activation domain (Fig. 2.26, panel B). Interaction of the two proteins of interest can therefore be identified by growth of the yeast cells on plates lacking histidine.

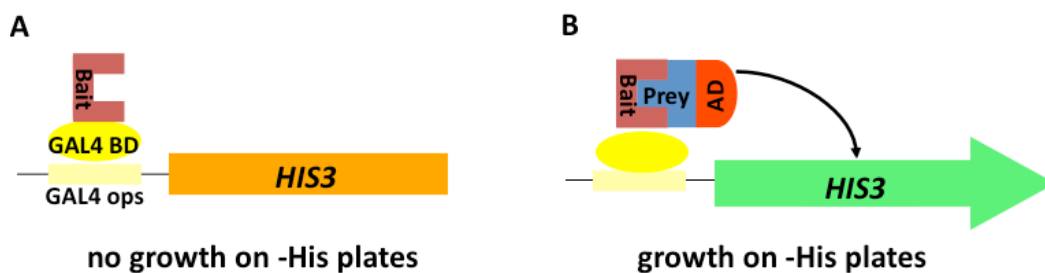


Figure 2.26: A standard yeast two hybrid assay. A: The *HIS3* gene under the control of the GAL4 promoter (GAL4ops) is not active, if only the bait protein fused to the GAL4 DNA binding domain (GAL4 BD) is present. B: Interaction of a prey protein fused to the GAL4 activation domain (AD) with the bait leads to activation of the *HIS3* gene and to growth of the yeast cells on plates lacking histidine.

Unfortunately, when testing the yeast strains expressing only the DBD-PFU1 or DBD-PHO2 fusion protein on SC –His plates, these cells were able to grow without expression of any prey protein fused to the GAL4 activation domain (Fig. 2.27). In contrast to this, the empty strain not expressing any DBD-PFU fusion protein did not show any growth on these plates. These results indicate that PFU1 and PHO2 lead, when fused to the GAL4 DNA binding domain, to transcriptional activity of the GAL4 promoter without the need of the GAL4 activation domain. A search for interactors with the whole PFU1 or PHO2 proteins was due to this fact impossible via a standard yeast two hybrid screen.

One possibility to circumvent the problem of autoactivation is to use smaller peptides of the protein of interest as a bait. However, in this case one important issue is the possible loss of interesting interactors. Therefore in a first step minor changes in the protein structure of PFU1 and PHO2 were tested to alter autoactivity. Both proteins contain a UBC domain with a highly conserved cysteine residue possibly binding ubiquitin during a conjugation

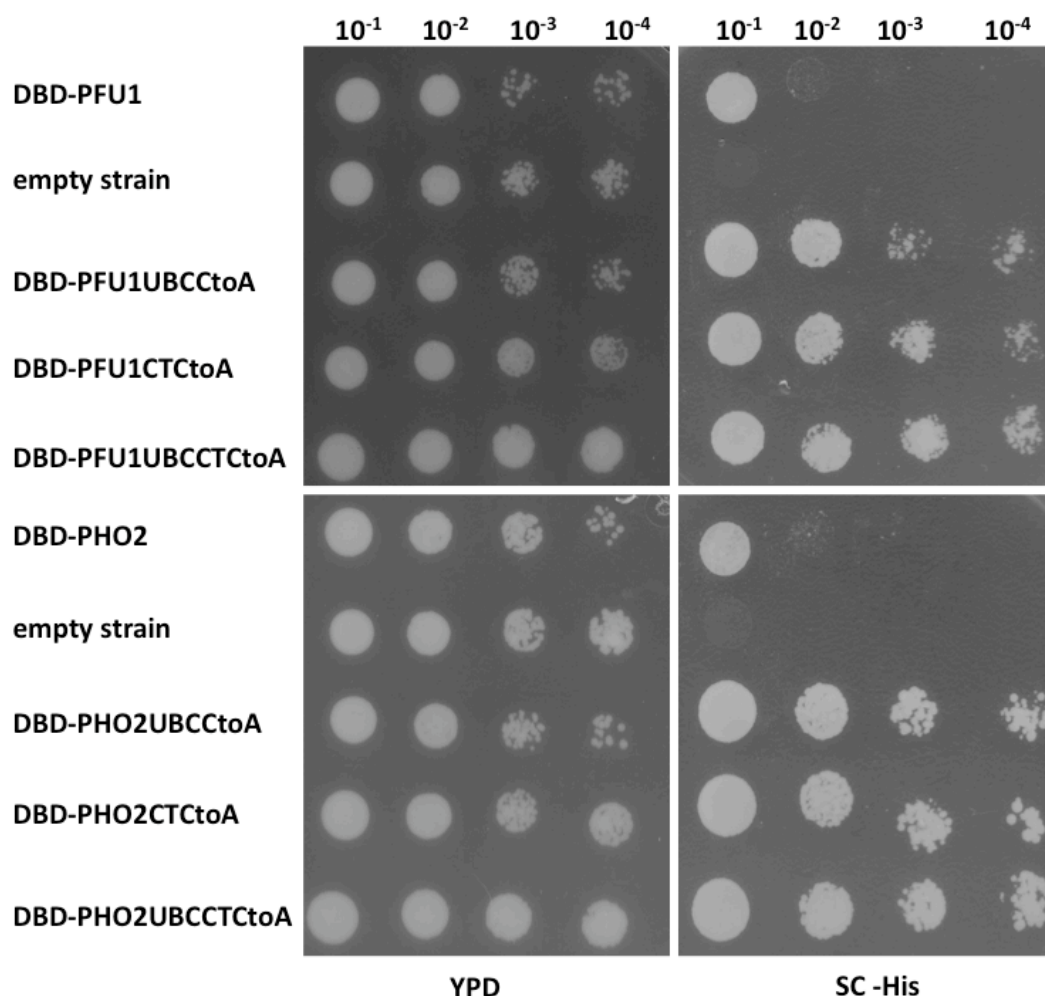


Figure 2.27: Test for autoactivation of the *HIS3* gene by the DBD-PFU1 and DBD-PHO2 constructs and by the respective CtoA mutants on SC –His medium. Growth of the different strains on normal YPD medium is shown as a control.

cascade. In addition both share homology in their C-terminus with a second very well conserved cysteine residue. These cysteine residues were exchanged by alanine via site directed mutagenesis. The oligos used for this experiment are summarized in Table 2.11. Apart from the single exchanges also constructs bearing a mutation of both cysteine residues (DBD-PFU1UBCCTCtoA and DBD-PHO2UBCCTCtoA) were tested on SC –His plates for autoactivation. All of these mutated constructs still displayed autoactivity and the yeast cells were able to grow on medium lacking histidine (Fig. 2.27). Interestingly, the mutated forms of PFU1 and PHO2 conferred an even higher ability to grow on SC –His plates than the non-mutated proteins, although growth differences on the YPD control plate were relatively minor. So the CtoA mutants of PFU1 and PHO2 were not useful to identify interactions in a standard yeast two hybrid assay as well.

Table 2.11: Oligos used for site directed mutagenesis.

construct	first oligo	second oligo
DBD-PFU1UBCCtoA	1063-LET1UBCCystop	1064-LET1UBCCysbot
DBD-PFU1CTCtoA	1065-LET1CCystop	1066-LET1CCysbot
DBD-PHO2UBCCtoA	1067-LET4UBCCystop	1068-LET4UBCCysbot
DBD-PHO2CTCtoA	1069-LET4CCystop	1070-LET4CCysbot

2.4.2 TUP1 fusion proteins in a yeast two hybrid assay

As a standard yeast two hybrid assay with the prey fused to a GAL4 activation domain was not applicable for PFU1 and PHO2, an alternative assay was established with the prey proteins fused to the yeast TUP1 repressor domain (Hirst et al. 2001). In this method, yeast cells solely expressing the autoactivating protein fused to the GAL4 DNA binding domain are transcribing the *HIS3* gene and are growing on SC –His plates (Fig. 2.28, panel A). If now the autoactivating bait interacts with a prey protein fused to the TUP1 repressor, the transcription of the *HIS3* gene is inhibited and the yeast cells are no longer able to grow on SC –His medium (Fig. 2.28, panel B). So interaction of the two proteins of interest can be identified by the failure of the yeast cells to grow on plates lacking histidine.

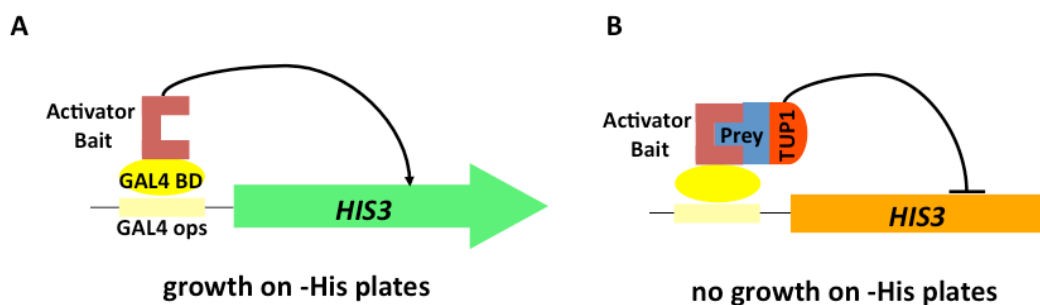


Figure 2.28: Yeast two hybrid assay with the TUP1 repressor domain. A: The bait protein fused to a GAL4 DNA binding domain is activating the *HIS3* gene without any interactor and cells are able to grow on SC –His plates. B: Interaction of the autoactivating bait protein and a prey protein fused to a TUP1 repressor leads to suppression of the *HIS3* gene expression and cells cannot grow on SC –His plates anymore.

To receive TUP1 fusion proteins of PHO2 and PFU1, the activation domain in the yeast expression vector pGAD424 was exchanged to amino acids 1-200 of the TUP1 repressor. First, a new *KpnI* restriction site facilitating the subsequent cloning was introduced in between the *ADH1* promoter and terminator by cutting the vector with *HindIII* and

ligating oligos 1061-GADH3link2bot and 1062-GADH3link2top into the linearized vector. Then the two oligos 997A-H3TUPdn and 998A-H3TUPup were designed to amplify the *TUP1* fragment from the vector pIOX049 (Hirst et al. 2001). This fragment was ligated in between the *Hind*III and *Kpn*I restriction sites of pGAD424. To introduce STOP codons in all three different reading frames an additional STOP codon was introduced behind the *TUP1* fragment by ligating oligos 1075-GADstopexttop and 1076-GADstopextbot into the vector cut with *Kpn*I and *Nde*I. This also supplied an additional *Nco*I site behind the *Nde*I site for subsequent cloning. The final construct was proven to contain the correct *TUP1* fragment via sequencing and was called pGAD-TUP1.

The *PFU1* and *PHO2* fragments were cut out from the vectors containing the EGFP or mRFP fusion constructs with *Kpn*I and either *Nde*I in the case of *PFU1* or *Nco*I in the case of *PHO2*. Then pGAD-TUP1 was cut with the same restriction enzymes and the *PFU* genes were cloned behind *TUP1*, resulting in fusion proteins where the TUP1 repressor domain is linked to the N-terminus of the PFU proteins.

The interaction between PFU1 and PHO2 was now tested with these constructs. Therefore the PJ96-4 α strain already expressing the DBD-PHO2 construct was transformed with either TUP1-PFU1 to check for heterodimerization or with TUP1-PHO2 to check for homodimers, and positive transformants were selected on plates lacking tryptophan as a marker for the pGBKT7 plasmid and leucine as a marker for the pGAD-TUP1 vector. As a negative control, the same strain was transformed with the empty pGAD-TUP1 vector. Indeed the negative control showed growth on plates lacking histidine because the *HIS3* gene expression was activated by the DBD-PHO2 protein and the single TUP1 repressor was not sufficient to suppress growth (Fig. 2.29). In contrast to this, both the strain containing the TUP1-PFU1 construct and the cells expressing TUP1-PHO2 were no longer able to grow on SC –His medium, indicating an interaction of PHO2 with either PFU1 or with a second PHO2 protein. This then lead to the suppression of the *HIS3* expression by the TUP1 repressor domain. The control plate lacking tryptophan and leucine still showed equal growth for all three different yeast strains. Two independent yeast colonies obtained for each combination during the first transformation with the TUP1 constructs showed the same results and therefore suggested that PHO2 is able to form both heterodimers with PFU1 and homodimers with itself.

However, colonies from a second transformation with the TUP1 constructs gave different results. In contrast to the first clones expressing both DBD-PHO2 and TUP1-PFU1 (DBD-PHO2 + TUP1-PFU1#1), the colony from a second transformation (DBD-PHO2 + TUP1-PFU1 #2) showed normal growth on SC –His medium (Fig. 2.30). Also the second colony containing DBD-PHO2 and TUP1-PHO2 (DBD-PHO2 + TUP1-PHO2 #2) was able to grow, suggesting that this time the PFU proteins do not interact. Still growth of all cultures on the –Leu –Trp control plate was equal showing that all contained both the DBD and TUP1 construct.

These results suggested that the proteins might not be properly expressed in some of the yeast cultures tested. Therefore western blots were performed to determine the expression level of the different fusion proteins. Crude protein extracts of the respective yeast strains were produced and the samples were run on two separate polyacrylamide gels. Then

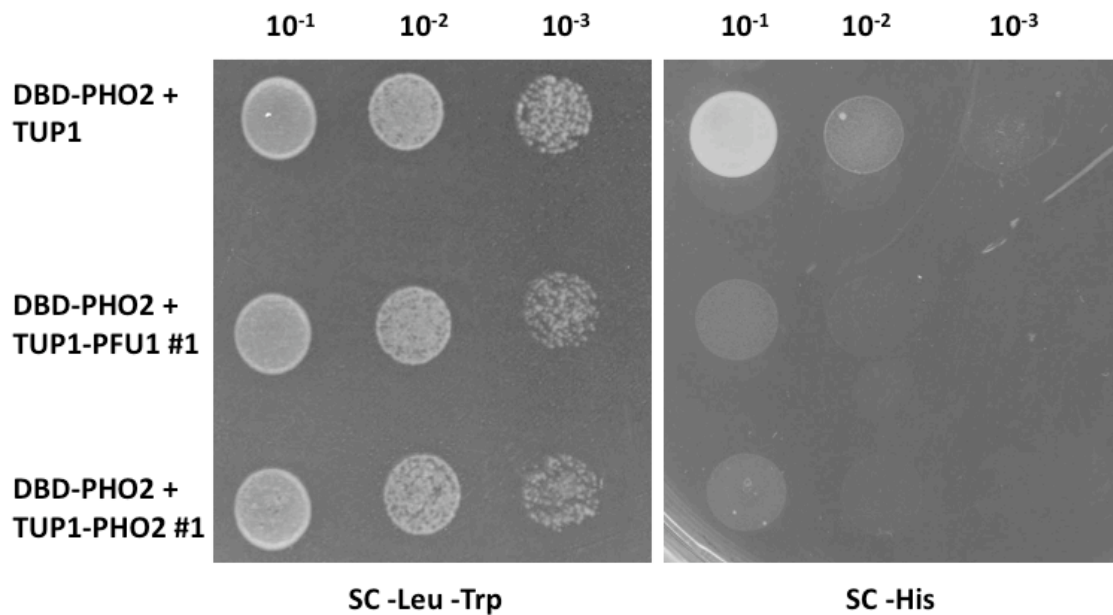


Figure 2.29: First test with PJ96-4 α cells expressing the DBD-PHO2 protein and either the single TUP1 domain or the fusion proteins TUP1-PFU1 and TUP1-PHO2. All cells show equal growth on SC -Leu -Trp. The absence of growth on SC -His for cells expressing DBD-PHO2 and TUP1-PFU1 or TUP1-PHO2 indicates hetero- and homodimerization of the proteins.

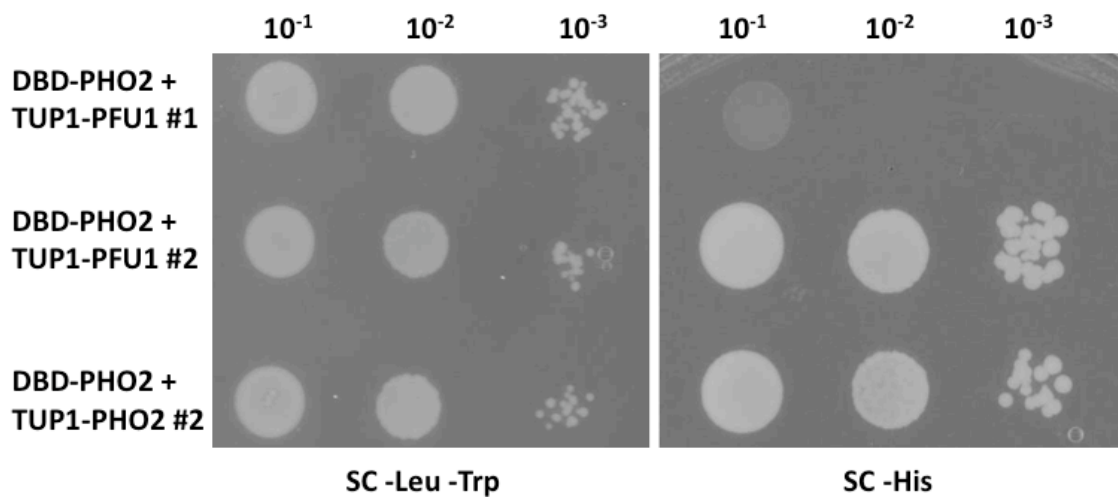


Figure 2.30: Second TUP1 test showing differences in growth on SC -His medium between colonies deriving from the first transformation (DBD-PHO2 + TUP1-PFU1#1) and clones from a second trial (DBD-PHO2 + TUP1-PFU1 #2 and DBD-PHO2 + TUP1-PHO2 #2) and conflicting with the idea of hetero- and homodimerization between the proteins.

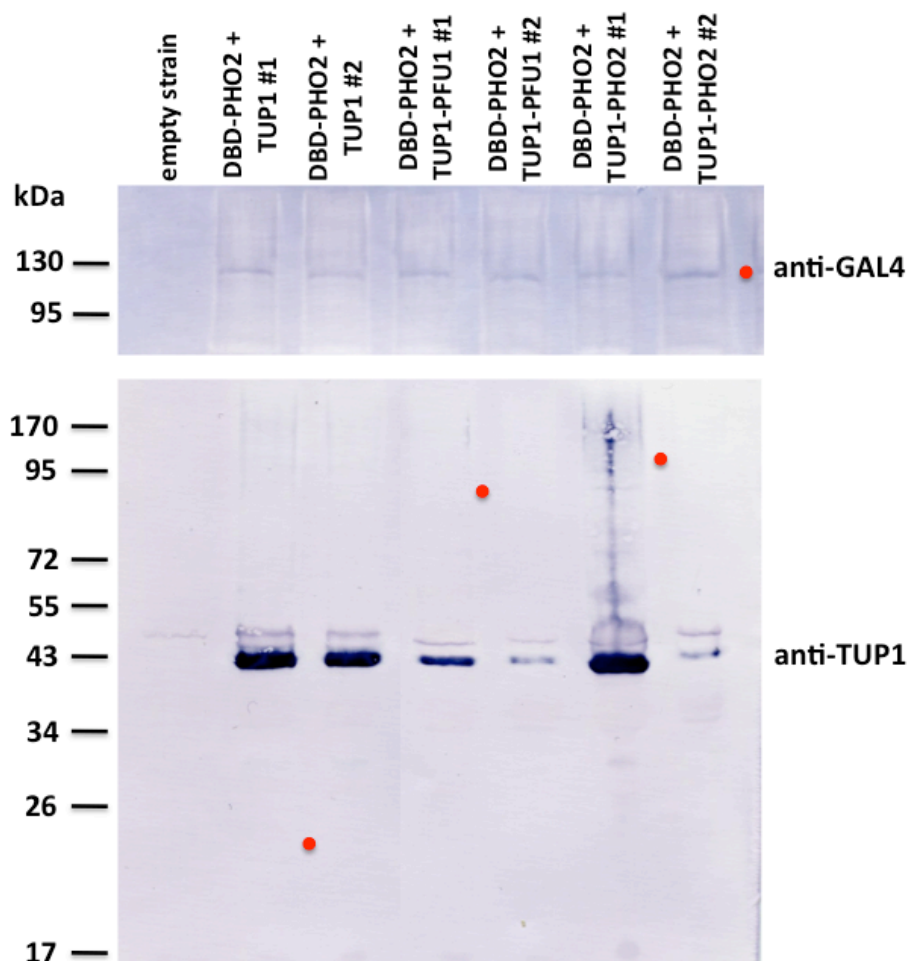


Figure 2.31: Protein expression levels of the DBD- and TUP1 fusion proteins in yeast determined via western blot. The DBD-PHO2 fusion protein was well detectable with an anti-GAL4 antibody (upper panel), whereas with anti-TUP1 antibody only the single TUP1 fragment was detectable in each lane. No signal is visible at the expected heights for the fusion proteins TUP1-PFU1 and TUP1-PHO2. Expected heights of the proteins are indicated by red dots.

proteins were blotted onto membranes. One of the membranes was incubated with an anti-GAL4(DBD) IgG2a antibody and the other one with an anti-TUP1 IgG antibody both derived from mouse and applied according to the manufacturer's manual (Santa Cruz Biotechnology, Inc.). Then the membranes were incubated with the second antibody (anti-mouse IgG alkaline phosphatase conjugate, SIGMA) and stained as described in chapter 4.2.7.

The DBD-PHO2 protein could be detected with the anti-GAL4 antibody at a height of approximately 115 kDa for all cultures except for the empty PJ96-4 α strain (Fig. 2.31). Interestingly, all yeast cultures showed the same expression of this fusion protein, so that loss of autoactivation in the clones obtained during the first transformation can be excluded.

This suggested a difference in expression of the TUP1 fusion proteins. The complete TUP1 repressor from yeast has a predicted size of 78 kDa but has been shown to run at about 99 kDa on an SDS-PAGE (Williams et al. 1991). This shift of approximately 20 kDa could also be observed when analyzing the expression of the TUP1 repressor domain used for the PFU fusion proteins on a western blot with the anti-TUP1 antibody (Fig. 2.31). Although the size of the TUP1 domain was predicted to be 22 kDa, the protein expressed from the empty pGAD-TUP1 vector could be detected at about 42 kDa. Unfortunately, also the lanes containing the two fusion proteins TUP1-PFU1 and TUP1-PHO2 only showed a band corresponding to the single TUP1 fragment. A fusion protein could neither be detected for PFU1 with a expected size of 90 kDa nor for PHO2 with an expected size of 120 kDa. Interestingly, the intensity of the TUP1 band in the lanes of the first transformation was much higher than the amount of TUP1 repressor protein in the samples of the second transformation.

2.4.3 Interaction studies with C-terminus of PFU proteins in yeast

The interaction studies in yeast with the complete PFU proteins fused to the TUP1 repressor domain did not give a definite proof for an interaction between PFU1 and PHO2. Due to this, a standard yeast two hybrid assay with prey proteins fused to the GAL4 activation domain was applied using a domain of the proteins PFU1 and PHO2 as a bait that does not exhibit autoactivation.

A structural analysis of the PFU proteins, called the protein meta-structure (Konrat 2009), was performed by Dr. R. Konrat at the Department of Structural and Computational Biology, Max F. Perutz Laboratories Vienna. This prediction of the 3D structure of the proteins revealed that the C-terminus possesses the highest ability of interacting with other proteins. Thus, the interaction of the C-termini of PFU1 and PHO2 was tested in a standard yeast two hybrid assay.

First, the C-terminus of PFU1 and PHO2 had to be cloned into the pGBKT7 vector to obtain DBD-PFU1CT and DBD-PHO2CT fusion proteins as a bait. Therefore the according gene fragments were cut out with *NdeI* and *XhoI* from the *E. coli* overexpression vector pET42c already bearing the C-termini of the *PFU* genes (described in chapter 2.5.1). Then the pGBKT7 plasmid was cut with *NdeI* and *SalI* and the fragments were ligated into the linearized vector. These constructs were transformed into the PJ96-4 α yeast strain and tested on SC –His plates for autoactivation. Compared to the DBD-PHO2 fusion protein, both the DBD-PFU1CT and DBD-PHO2CT fragment showed nearly no activation of the *HIS3* gene. Only a few cells were able to grow on medium lacking histidine and this only after four days of incubation at 30 °C (Fig. 2.32). So the interaction between the C-termini of the PFU proteins could be examined using fusion proteins with the GAL4 activation domain and then testing for a higher activation of the reporter gene.

A fusion construct with the GAL4 activation domain in the vector pGAD424 was cloned only for PFU1. Making use of the oligos 1250-LET1CEcodn and 1269-LET1Cup3 the

C-terminus of the gene was amplified from the pGBKT7 construct. These oligos introduced an *EcoRI* site at the 5' end and a *BglIII* site at the 3' end of the gene fragment to facilitate the further cloning. Then both the gene fragment and the vector were cut with these restriction enzymes and afterwards ligated together.

When coexpressed with either DBD-PFU1CT or DBD-PHO2CT, the AD-PFU1CT fusion protein did not activate the reporter gene and an increased growth on plates lacking histidine was not visible (Fig. 2.32). The four yeast strains bearing the fusion constructs of the C-termini were all unable to grow on Sc –His medium, suggesting that at least in yeast the C-termini of the PFU proteins do not directly interact.

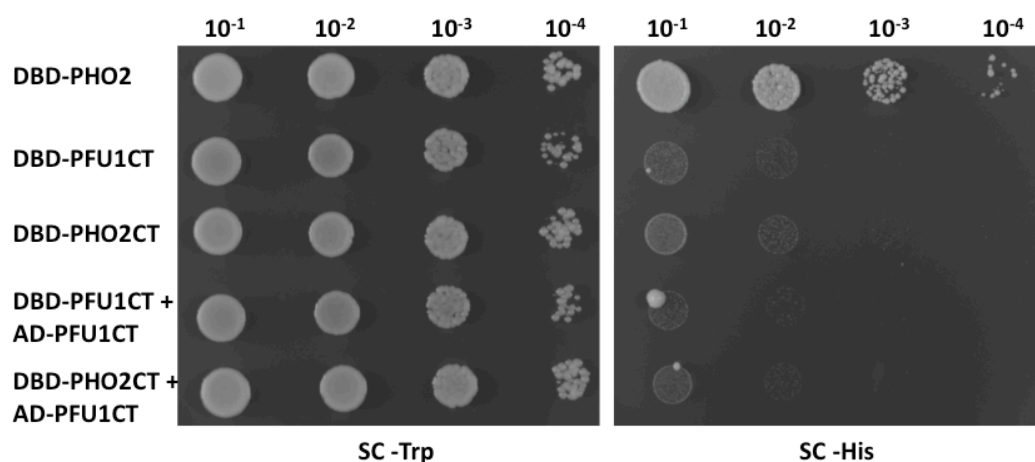


Figure 2.32: Standard yeast two hybrid assay with the C-termini of PFU1 and PHO2. All yeast strains showed equal growth on the SC –Trp control plate, but activation of the *HIS3* reporter gene was not visible for the strains bearing only the DBD-PFU1CT proteins and for the cells expressing both DBD and AD fusion proteins, showing that the C-termini of the PFU proteins do not interact in yeast.

2.5 Biochemical analysis with recombinantly expressed PFU proteins

The phenotypical analysis on the *Arabidopsis* T-DNA insertion lines revealed that the PFU proteins are involved in the initiation of programmed cell death after induction by abiotic and biotic stress and that they are responsive to oxidative signals. However, how these proteins operate on the molecular level is still unknown.

Especially the structure of the C-terminus was of great interest, as its highly conserved cysteine residue might be able to form a thioester with ubiquitin or might be involved in directly sensing oxidative signals. Therefore the C-termini of PFU1 and PHO2 were overexpressed in *E. coli* to finally solve the three-dimensional structure of this domain.

In regard of the other parts of the PFU proteins, only the function of the UBC domain could be predicted so far. Still, it has not yet been proven whether this domain is indeed able to form a thioester with ubiquitin. Recombinant PFU proteins were therefore overexpressed in *E. coli* to verify their potential function as ubiquitin conjugating enzymes in an *in vitro* ubiquitylation assay.

In a third approach recombinant PFU proteins were used to further analyze the putative interaction between PFU1 and PHO2 via co-immunoprecipitation.

2.5.1 Cloning of overexpression constructs

Due to the various applications and the diverse properties of the recombinant PFU proteins, several overexpression constructs bearing different protein fragments were cloned.

Multiple constructs to overexpress the C-terminus

As the three-dimensional structure of the conserved C-terminal domain of the PFU proteins was one of the main issues to solve with the help of recombinant proteins, the C-termini of both PFU1 and PHO2 were cloned into the pET42c vector for high-level expression under the control of the T7 promoter in *E. coli*. The gene fragments bearing the C-terminal domains starting with amino acid 487 for PFU1 and amino acid 814 for PHO2, respectively, were amplified with the following oligos that introduce restriction sites for further cloning at both ends of the PCR products: 1169-LET1Cdomdn + 1173-LET1Cup2 (*PFU1*) and 1170-LET4Cdomdn + 1174-LET4Cup2 (*PHO2*). Then both the plasmid and the gene fragments were cut with *NdeI* and *XhoI*. This step eliminates the GST-tag from the plasmid pET42c, so that after ligating the PCR fragments into the vector, a fusion protein with only a His-tag at the C-terminal end of the PFU fragments was obtained (Fig. 2.33, PFU1CT487 and Fig. 2.35, PHO2CT).

As described below (chapter 2.5.2), the C-terminus of PFU1 turned out to be highly insoluble. Hence, the solubility properties of the C-terminus of PFU1 were further analyzed by changing the starting point of the protein fragment. Therefore eight additional constructs were cloned, shortening the first construct PFU1CT487 by steps of two amino acids. To achieve this, eight additional downstream reading oligos were designed that amplified the respective gene fragments together with the upstream reading oligo 1173-LET1Cup2. Then these PCR fragments were cloned into pET42c as explained for the PFU1CT487 construct, resulting in short His-tagged proteins (Fig. 2.33).

For five of these shorter constructs (PFU1CT489, PFU1CT491, PFU1CT495, PFU1CT497 and PFU1CT501) also the mutated form with the conserved cysteine changed to alanine was amplified from the yeast vectors containing this mutation (Chapter 2.4.1) and fused to a His-tag in the pET42c vector to further analyze the solubility of the PFU1 C-terminus.

As described in Chapter 2.5.2 the changes in the C-terminal fragment of PFU1 still did not increase its solubility. Therefore the effect of different tags fused to the PFU1 C-terminus was examined. To achieve overexpression constructs for this analysis, the two fragments PFU1CT499 and PFU1CT501 were amplified with upstream reading oligos bearing either

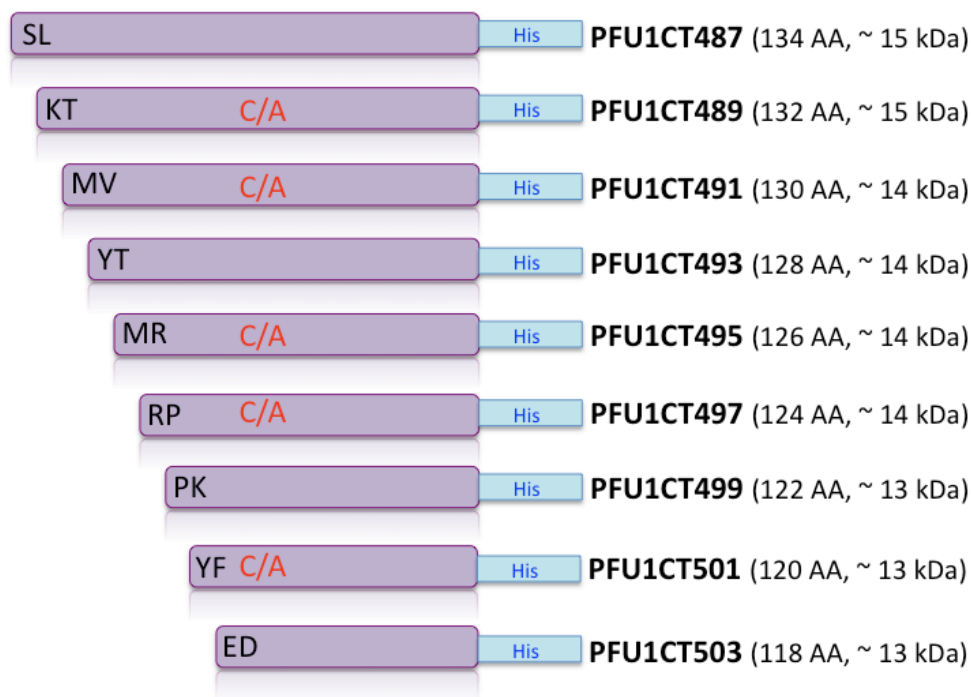


Figure 2.33: Schematic overview on the overexpression constructs of the C-terminal domain of PFU1 (purple) in pET42c bearing only a single His-tag (blue). The starting point of the protein fragment was shortened step by step by always two amino acids, and for five of these constructs also the CtoA mutated form (C/A) was analyzed.

a Flag-tag (1235-LET1CFlagup) or a Strep-tag (1234-LET1CStrepup). These oligos also contain a STOP codon just after the tag, so that the final proteins possess either Flag- or Strep-tag and did not contain any His-tag encoded by the pET42c vector anymore (Fig. 2.34). Additionally, the PFU1CT501 fragment was also tagged with both Strep- and His-tag, making use of the oligo 1238-LET1StrepHis, which lacks the STOP codon behind the Strep tag but contains an *XhoI* restriction site to be in frame with the subsequent His-tag of the pET42c vector (Fig. 2.34).

Also larger tags were tested to increase the solubility of the proteins. For this the C-termini of both PFU1 and PHO2 were cloned into the original pET42c vector still containing the GST-tag. To receive the *PFU* C-terminal fragments for this experiment the pET42c constructs described above containing PFU1CT487 and PHO2CT, respectively, were cut with *NdeI*, the ends were filled in by the Klenow reaction and the linearized vector was again cut with *PvuI*. Then the empty pET42c vector was linearized, making use of the *SpeI* restriction site, filling up the ends with Klenow and cutting again with *PvuI*. The C-terminal fragments were ligated into the vector, resulting in PFU protein fragments tagged by a GST-tag at the N-terminus and a His-tag at the C-terminus (Fig. 2.34, PFU1CT GST and Fig. 2.35, PHO2CT GST).

In a last approach to increase the solubility of the protein domains, the PFU1 and PHO2

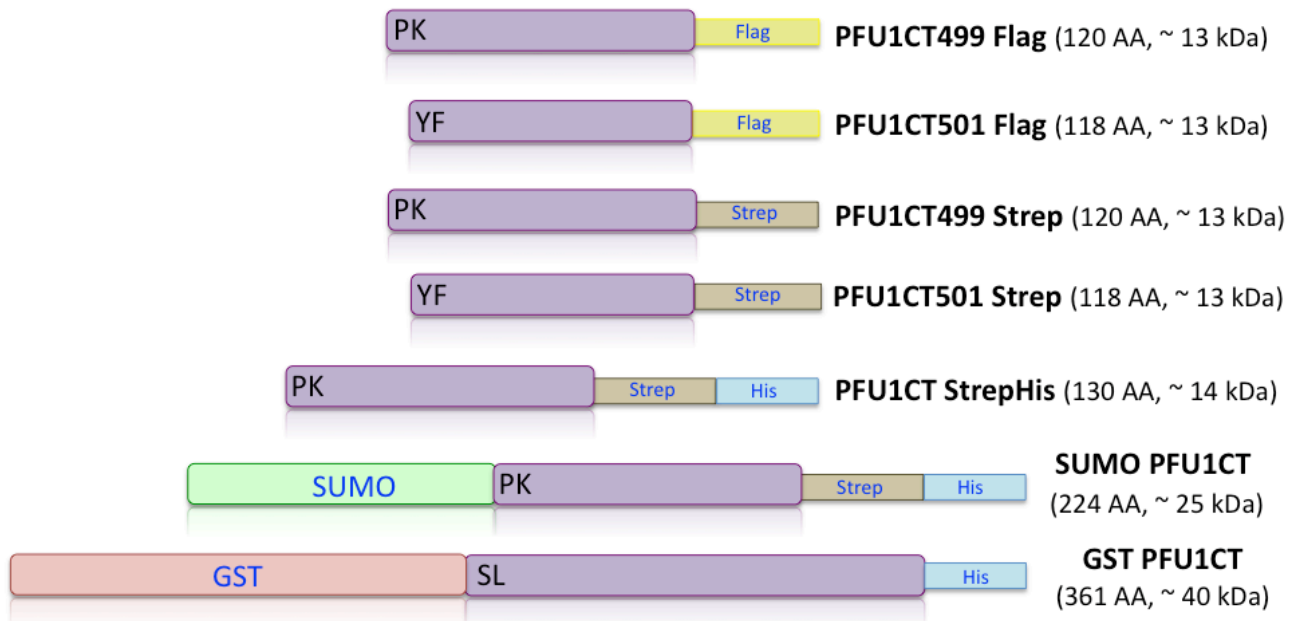


Figure 2.34: Overexpression constructs cloned to analyze the solubility of the PFU1 C-terminus fused to a various number of protein tags, such as Flag-tag (yellow), Strep-tag (brown), His-tag (blue), GST-tag (red), or to the small protein modifier SUMO (green).

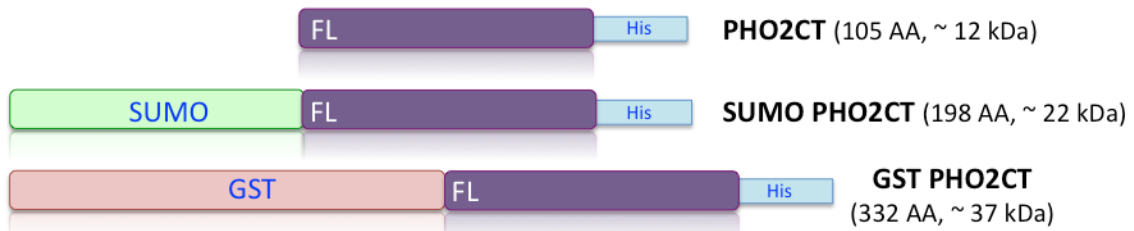


Figure 2.35: The C-terminus of PHO2 (dark purple) was either fused to only a His-tag (blue) or both His-Tag and GST-tag (red) or His-tag and SUMO (green) in the pET42c overexpression vector.

C-termini were fused to SUMO, which often helps the protein to fold properly and therefore increases solubility. The ORF of SUMO was amplified with the oligos 1242-SUMCT1fusdn and 1243-SUMCT1fusup from the vector pSUMOGG obtained from Dr. A. Bachmair. These oligos introduce restriction sites at both ends of the SUMO fragment, so that it could be easily cloned in between restriction sites *Xba*I and *Nde*I of the PFU1CTStrepHis and the PHO2CT construct, respectively. In the end the protein fragment of PFU1 contained a SUMO fragment fused to the N-terminus and both a Strep- and a His-tag at the C-terminus, whereas the PHO2 fragment possessed SUMO at the N-terminus and a His-tag at the

C-terminus (Fig. 2.34, SUMO PFU1CT and Fig. 2.35, SUMO PHO2CT).

Constructs to obtain only the UBC domain for ubiquitylation assays

The functionality of the PFU proteins to be actual ubiquitin conjugating enzymes could not be proven so far. To address this problem, the UBC domains of PFU1 (amino acids 326-490) and PHO2 (amino acids 664-823) were cloned into pET42c.

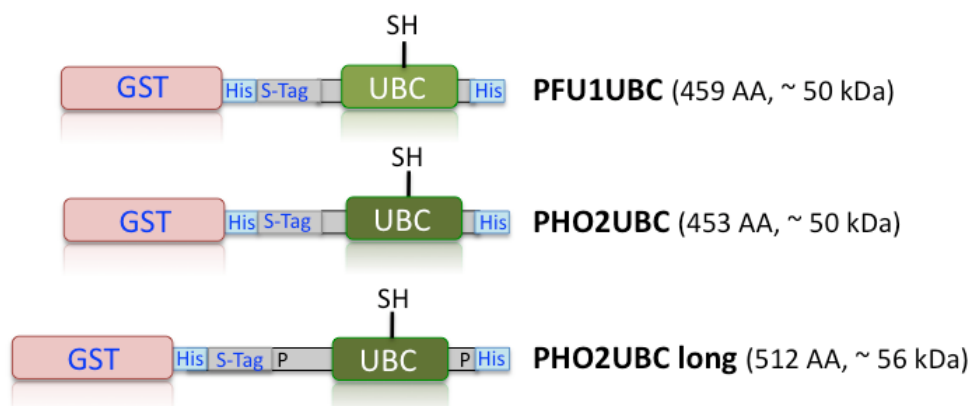


Figure 2.36: Scheme summarizing the constructs produced to overexpress the UBC domain of PFU1 (light green) and PHO2 (dark green).

Gene fragments were amplified with the oligos 788A-LET1UBCdn and 789A-LET1UBCup for *PFU1* and 752A-LET4UBCdn and 753A-LET4UBCup for *PHO2* and afterwards ligated in between restriction sites *NcoI* and *XhoI* of pET42c.

This results in proteins tagged with all tags supplied by the pET42c vector, meaning GST-tag, His-tag and S-tag at the N-terminus and an additional His-tag at the C-terminus (Fig. 2.36: PFU1UBC and PHO2UBC). As described in Chapter 2.5.2, purification of these protein fragments resulted in extracts containing many other contaminating proteins.

To improve purification, a longer fragment of PHO2 starting with the proline residue at position aa 609 and ending with another proline at position aa 828 was cloned in the same manner using the oligos 1239-LET4lgUBCdn and 1240-LET4lgUBCup (Fig. 2.36: PHO2UBClong). Due to its special properties, proline very often marks the border of a protein domain. Hence, with this cloning strategy it was hoped to improve the proper folding of the PFU protein fragments.

Recombinant proteins bearing both UBC and C-terminal domain

The closest mammalian homologue of the PFU proteins, E2-230K/UBE2O, has been shown to exhibit both E2 and E3 function (Berleth and Pickart 1996). This raised the possibility, that also the PFU proteins might be E2-E3 hybrids and can directly ubiquitylate certain substrates. To test this in *in vitro* ubiquitylation assays, larger protein fragments of PFU1

and PHO2 were recombinantly expressed in *E. coli*.

First of all the whole *PFU1* open reading frame was cloned into an *E. coli* overexpression vector. Therefore the gene fragment was cut out of a vector bearing the *PFU1-EGFP* construct with the restriction enzymes *NdeI* and *Acc65I*. Then it was cloned into the vector pETUBC27 (Budhiraja et al. 2009), which was linearized with the same enzymes. The final plasmid expressed a ca. 69 kDa protein possessing a Flag-tag and a His-tag at the C-terminus (Fig. 2.37: PFU1Flag).

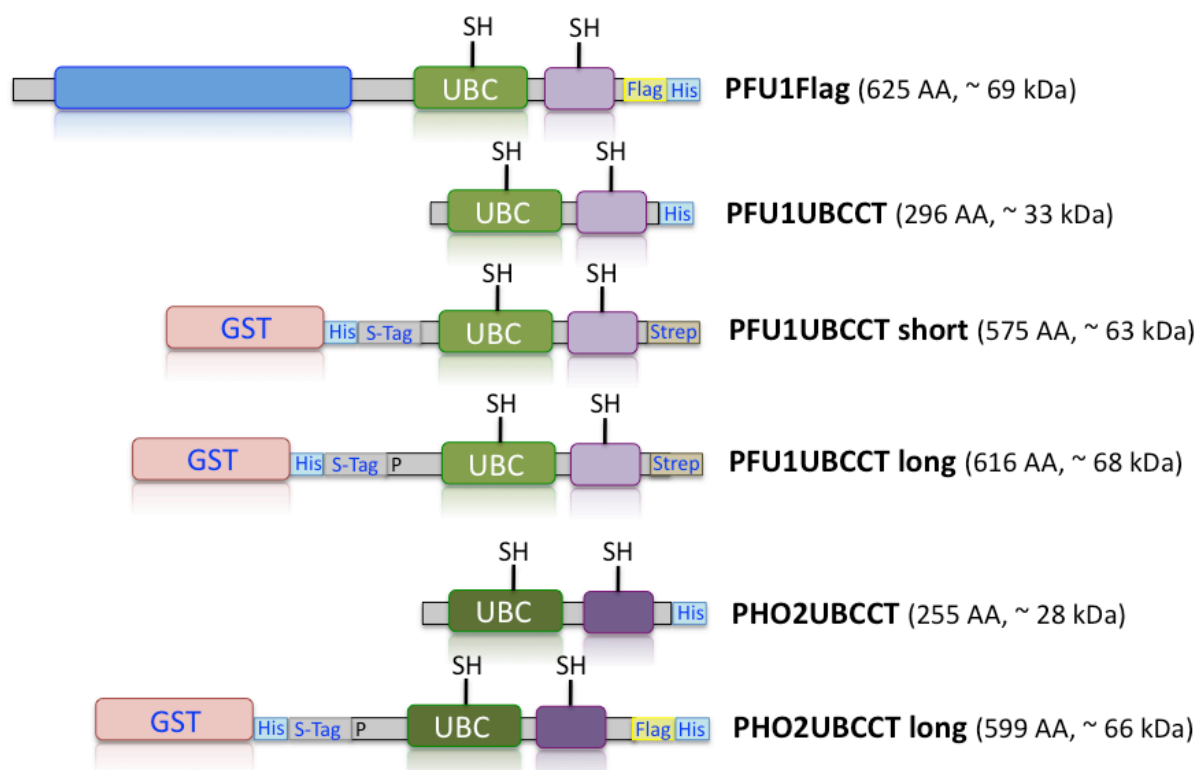


Figure 2.37: The whole PFU1 protein including the N-terminal domain (blue) and different PFU protein fragments containing the UBC (green) and C-terminal domain (purple) were cloned into an *E. coli* overexpression vector and, depending on the cloning strategy, fused to a variety of protein tags.

Unfortunately the complete PFU1 protein turned out not to be overexpressed in *E. coli* (chapter 2.5.2). Hence, apart from expressing the complete open reading frame of the genes, also shorter fragments lacking the long N-terminal extension of the proteins were cloned into an overexpression vector. For this purpose a *PFU1* gene fragment was amplified with the oligos 1171-LET1UBCdn2 and 1173-LET1Cup2 (reaching from aa 326 until the end) and a *PHO2* fragment with the oligos 1172-LET4UBCdn2 and 1174-LET4Cup2 (reaching from aa 664 until the end). These oligos added an *NdeI* restriction site to the 5' end and an *XhoI* site to the 3' end of the gene fragment to facilitate cloning into the pET42c vector cut with the same enzymes. The proteins expressed from these constructs are only tagged

with a single His-tag (Fig. 2.37: PFU1UBCCT and PHO2UBCCT).

As these proteins did not show a high solubility as well in the experiments described below (chapter 2.5.2), protein fragments exhibiting both UBC and C-terminal domain were also tagged with a GST-tag. Both a shorter *PFU1* fragment (aa 326-end) amplified with the downstream reading oligo 788A-LET1UBCdn and a longer fragment (aa 285-end) amplified with the downstream oligo 1279-LET1UBCdn3 were cloned into the pET42c vector cut with *NcoI* and *XhoI*. As in both cases the upstream reading oligo 1234-LET1CStrepup was used, the final proteins are tagged with a GST-tag, a His-tag and an S-tag at the N-terminus and with a Strep-tag at the C-terminus (Fig. 2.37: PFU1UBCCTshort and PFU1UBCCTlong). For *PHO2* only a longer fragment starting with the proline residue at position aa 609 was fused to a GST-tag. Therefore the PCR product obtained with oligos 1239-LET4lgUBCdn and 1249-LET4CFLAG was also ligated into the pET42c vector linearized with *NcoI* and *XhoI*. Due to the design of the upstream reading oligo the overexpressed protein was finally tagged with GST-tag, S-tag and His-tag at the N-terminus and with an additional Flag-tag at the C-terminus (Fig. 2.37: PHO2UBCCTlong).

2.5.2 Analysis of the solubility of the different recombinant PFU proteins

To produce high levels of overexpressed protein, the constructs described in the previous chapter were transformed into the *Escherichia coli* strain Rosetta (Novagen). These cells possess a λ prophage exhibiting the T7 RNA polymerase gene, which results in a highly efficient expression of genes under the control of the T7 promoter. Apart from this, they contain the plasmid pLysSRARE to provide tRNAs with rare codons mainly used during the translation of eukaryotic proteins. This plasmid conveys chloramphenicol resistance, so that positive transformants of the overexpression constructs were in addition to the antibiotic resistance obtained by the pET plasmid resistant to a second antibiotic.

Protein expression was induced by addition of IPTG to the cells, which binds to the lac promoter controlling the expression of the T7 RNA polymerase. A standard induction was performed with 1 mM IPTG at 30 °C. Under these conditions, most of the overexpression constructs described in the previous chapter showed a high protein accumulation after three hours of induction (Fig. 2.38). Unfortunately the complete PFU1 protein labelled with a Flag-tag was not visible on a Coomassie gel. Also overexpression in a different *E. coli* strain BL21pLysS (Stratagene) was unsuccessful. Apart from this, overexpression could also not be detected for the constructs containing the C-terminus of PHO2 (Fig. 2.38). Even under different induction conditions, such as growth at 20 °C or addition of only 250 μ M IPTG, the Rosetta cells were unable to express either PHO2CT with a single His-tag or the fusion proteins with GST-tag and SUMO.

As the C-terminus of PFU1 could, in contrast to the PHO2 C-terminus, be nicely overexpressed and PFU1 and PHO2 show high sequence similarities in this domain, the further analysis to solve the three-dimensional structure of the C-terminal domain was concentrated on the PFU1 fragment.

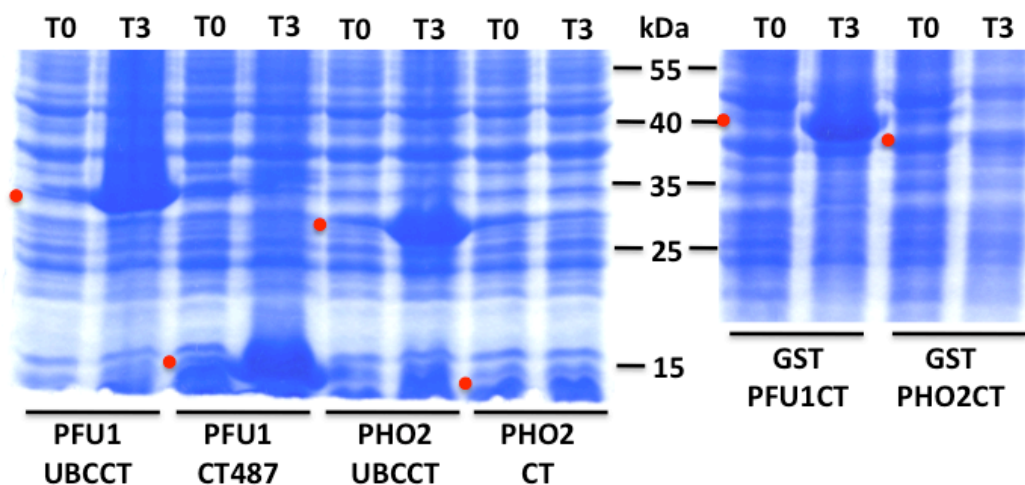


Figure 2.38: Coomassie stained gel with samples of Rosetta cells exhibiting the overexpression constructs of PFU1UBCCT, PFU1CT487, PHO2UBCCT, PHO2CT, GST PFU1CT and GST PHO2CT before (T0) and after three hours (T3) of induction with 1mM IPTG at 30 °C. The expected positions of the proteins are labelled by a red dot.

Different attempts to increase the solubility of the C-terminal domain of PFU1

Recombinant PFU proteins overexpressed in Rosetta cells and labelled with a His-tag were purified making use of Ni-NTA agarose (Qiagen). Figure 2.39 shows the first attempt to purify the PFU1CT487 protein fragment, documenting the protein on a western blot labelled with a Ni-NTA alkaline phosphatase conjugate. Although the protein was highly expressed after three hours of induction, the amount of purified protein in the elution steps was much less and hard to detect even on a western blot. Analysis of the different purification steps revealed that the amount of PFU protein in the total cell lysate was still much higher than the amount in the supernatant containing only the soluble fraction of the cell lysate after centrifugation, suggesting that most of the overexpressed PFU protein was lost because of insolubility.

This observation was supported when comparing a protein extract under denaturing conditions (8 M urea) with the soluble protein fraction under native conditions (1 M urea) (Fig. 2.40). Much more protein could be detected for both PFU1CT constructs tested when urea was added to the lysis buffer, suggesting that most of the protein is insoluble under native conditions. The amount of soluble protein was even less when inducing protein expression with 250 μ M IPTG overnight at 20 °C. However, the main explanation for this was that growth of the *E. coli* cells was decelerated at this low temperature and the total amount of overexpressed protein including the insoluble fraction was dramatically decreased.

As the C-terminal domain of PFU1 was of main interest and high amounts of soluble protein

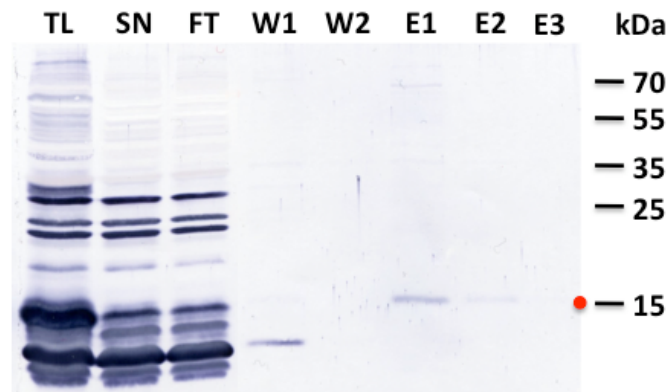


Figure 2.39: Amount of PFU1CT487 in the total lysate (TL), in the supernatant (SN) containing only the soluble fraction, in the flowthrough (FT) after addition to the column, in the flowthrough after washing step 1 (W1), in the flowthrough after washing step 2 (W2) and in the different elution steps (E1-E3) on a western blot detected with a Ni-NTA alkaline phosphatase conjugate. The expected heights of the protein is labelled by a red dot.

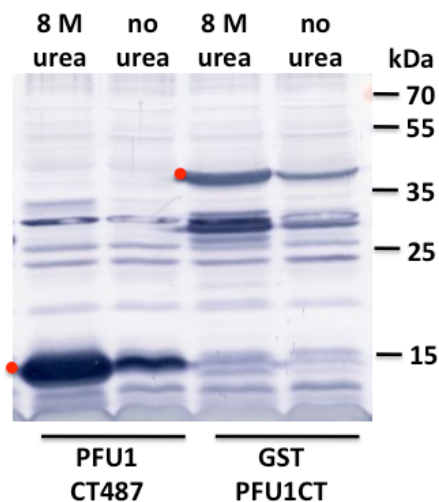


Figure 2.40: Comparison between the amount of soluble protein under denaturing conditions with 8M urea and under native conditions without urea on a western blot detected with a Ni-NTA alkaline phosphatase conjugate. The expected heights of the proteins are labelled by a red dot.

were needed to analyze the three-dimensional structure either via NMR or crystallization, the solubility properties of this protein fragment were further examined. Therefore the influence of the starting point of the domain on the solubility was tested. The eight constructs described in Fig. 2.33 were overexpressed and the amount of soluble protein after lysis was compared on a western blot (Fig. 2.41, panel A).

As the constructs were always shortened by two amino acids, a decrease in the height of the

band was visible. However, the amount of soluble protein detected after lysis did apparently not change, suggesting that different amino acid residues at the N-terminal end of the domain are not altering the solubility of the PFU1 protein fragment.

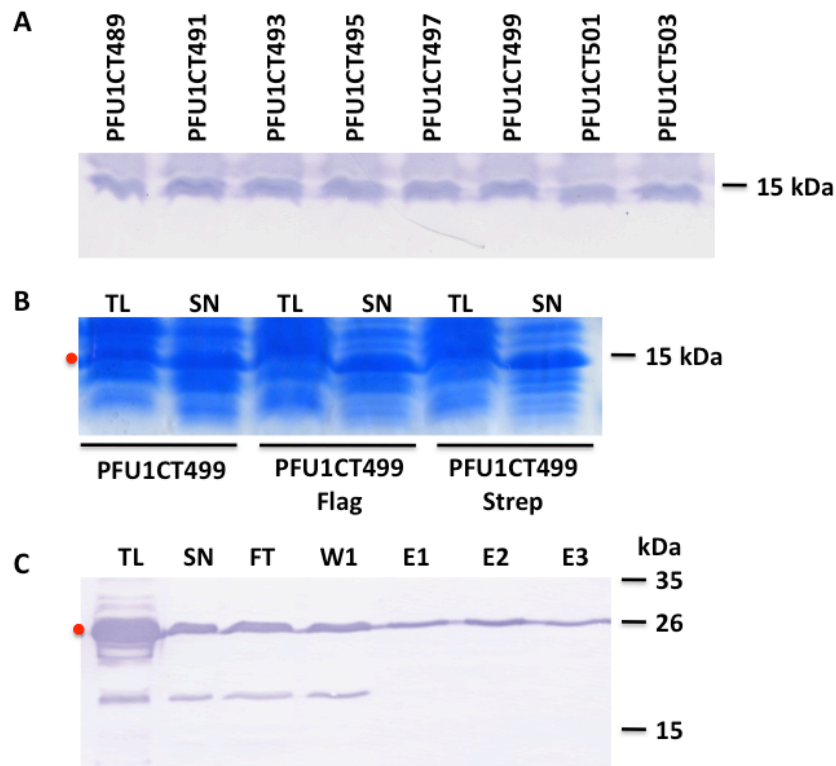


Figure 2.41: Different attempts to increase the solubility of the C-terminal domain of PFU1. The expected heights of the proteins are labelled by a red dot. A: Influence of the N-terminal amino acid residue on the solubility of the protein. The soluble fractions of the cells expressing the constructs of PFU1CT bearing different starting points were compared on a western blot detected with a Ni-NTA alkaline phosphatase conjugate. B: Coomassie stained gel comparing the total lysate (TL) and the supernatant (SN) containing the soluble protein fraction of cells expressing the three constructs PFU1CT499, PFU1CT499 Flag and PFU1CT499 Strep, respectively. C: The different purification steps of the SUMO PFU1CT fusion protein analyzed on a western blot incubated with a Ni-NTA alkaline phosphatase conjugate. TL - total cell lysate, SN - supernatant containing the soluble proteins, FT - flowthrough after application to the column, W1 - flowthrough after washing step 1, E1-E3 - elution steps 1-3

In a second series of experiments, the influence of different protein tags on the solubility of the C-terminal domain of PFU1 was analyzed. Therefore first the smaller protein fusions with either Flag- or Strep-tag were compared to the His-tagged protein already analyzed in the previous experiment. As a starting point the proline residue at position aa 499 was chosen, because this amino acid is known to disrupt regular secondary structures and due to this very often marks the border of a structural domain. The comparison of both the

complete protein content in the total lysate (TL) and the amount of the soluble protein fraction in the supernatant (SN) on a Coomassie stained gel (Fig. 2.41, panel B) revealed that neither the Flag- nor the Strep-tag altered the solubility of the C-terminal domain. The protein band representing the soluble fraction of the PFU1 C-terminus at ca. 13 kDa showed similar intensities in all three cases.

Apart from that, the C-terminus of PFU1 was fused to larger proteins such as a GST-tag or SUMO and overexpressed in Rosetta cells. As an example, Figure 2.41 (panel C) demonstrates the different experimental steps received during the purification of SUMO PFU1CT. Although the observed size was with ca. 28 kDa a little higher than expected, the protein of interest could be detected on a western blot. In comparison, the final protein amount of SUMO PFU1CT obtained in the different elution steps (E1-E3) slightly exceeded the amount of protein achieved for the His-tagged C-terminal domain (Fig. 2.39). However, a big amount of protein is also detectable in the flowthrough fraction and after the first washing step.

The increase of recombinant protein obtained in the elution steps and compared to the His-tagged PFU1 C-terminus was also observed for the GST fusion of the protein, indicating that the larger protein tags marginally facilitate the proper folding during overexpression and therefore lead to a minor increase in solubility of the PFU protein. Unfortunately, addition of these huge peptides impedes the structural analysis of the protein domain of interest via NMR, so that these recombinant proteins were only applied to further examine the interaction between PFU1 and PHO2 in co-immunoprecipitation experiments.

A final attempt was made to receive a higher amount of soluble PFU1CT labelled with a small protein tag. For this purpose the His-tagged protein fragment PFU1CT499 was first purified under denaturing conditions with 8 M urea. Then the urea was slowly removed overnight via dialysis against a buffer containing only 1 M urea. The comparison between the amount of soluble protein before and after dialysis is shown in Figure 2.42. A white

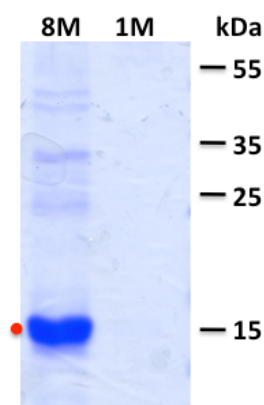


Figure 2.42: Amount of soluble PFU1CT487 protein after purification under denaturing conditions in a buffer containing 8 M urea and after dialysis in a solution with only 1 M urea. Samples were visualized on a Coomassie stained polyacrylamide gel.

cloud of precipitated protein was already visible when withdrawing the sample from the dialysis tube. As suspected from this, soluble PFU1 protein was indeed not detectable at all in the 1 M urea sample on the Coomassie stained gel, pointing out that it was impossible to renature the protein by this method.

Thus, although analyzing multiple different constructs under different overexpression and purification conditions, the high amounts of soluble protein needed for a structural analysis of the C-terminus of PFU1 either via NMR or via crystallization could not be obtained so far.

Purification of recombinant proteins bearing the UBC domain

Apart from the attempts to solubilize only the C-terminal domain of PFU1 for a structural analysis, protein fragments containing either the single UBC domain or both UBC and C-terminal domain were also purified to test them in *in vitro* ubiquitylation assays. In addition, the recombinant proteins bearing both domains were also needed to perform co-immunoprecipitation experiments with PFU1 and PHO2.

The UBC domains for both PFU1 and PHO2 fused to a GST-tag (Fig. 2.43) could be purified to a higher extent, than the C-terminal domain of PFU1 only extended by a His-tag (Fig. 2.39). PFU1UBC and PHO2UBC were both well detectable in the different elution steps on a western blot. However, a high number of additional lower molecular weight bands were visible, suggesting that the protein might have been degraded by proteases during purification. Similar results were observed for the larger UBC fragment of PHO2 (PHO2UBC long, data not shown).

In contrast to this, a first attempt to purify the UBC domain together with the C-terminus of PFU1 and PHO2, respectively, turned out to be as ineffective as observed for the purification of PFU1CT487 (Fig. 2.39). The elution steps for the PHO2UBCCT construct are shown in Figure 2.43 as an example, demonstrating that only very little protein was detectable on the western blot.

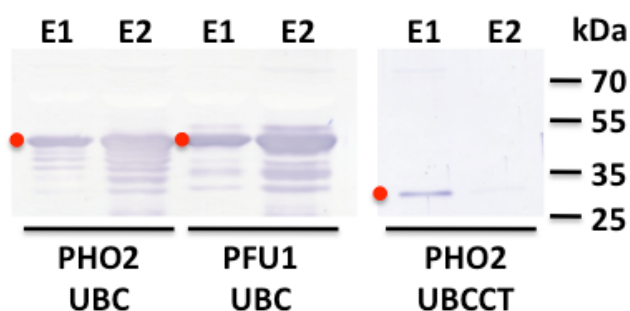


Figure 2.43: Western blot displaying the elution steps after purification of PHO2UBC, PFU1UBC and PHO2UBCCT, respectively. The His-tagged proteins were detected with a Ni-NTA alkaline phosphatase conjugate, and the expected sizes of the proteins of interest are marked by a red dot. E1, E2 - elution steps 1 and 2

While working on the C-terminus of PFU1 and the constructs containing only the UBC domain it was observed that the fusion to a GST-tag obviously increases solubility of the PFU protein fragments and leads to a more efficient purification. Therefore, constructs containing both UBC domain and C-terminus fused to a GST-tag, a His-tag and either Strep-tag in the case of PFU1 or Flag-tag in the case of PHO2 were overexpressed in *E. coli*. Apart from the additional tags, these constructs also possessed proline residues at both ends of the PFU protein fragment. Due to its specific properties proline acts as a structural disruptor in the middle of regular secondary structures and therefore often lies at the border of protein domains. Hence, this cloning strategy was chosen to improve the proper folding of the protein. The recombinant proteins were purified via the His-tag and the different purification steps were analyzed on a Coomassie stained gel. The protein PHO2UBCCT long showed an extremely high overexpression, so that both the lane with sample of the total lysate of the cells and the lane containing the sample of the supernatant were overloaded and a clear protein band at the expected height of ca. 66 kDa was hard to define (Fig. 2.44). Huge amounts of the protein were also detectable in the elution steps showing in this case a distinct band at the expected height. These results suggest that the modifications applied to the former PHO2UBCCT construct facilitate the purification of the protein and lead to a much higher solubility.

The UBCCT fragment of PFU1 showed a much higher overexpression rate and a higher solubility when fused to a GST- and Strep-tag as well (Fig. 2.44). The protein of interest

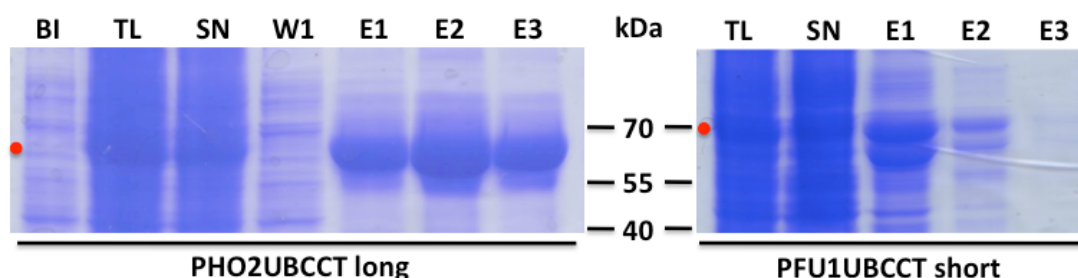


Figure 2.44: Coomassie stained polyacrylamide gel documenting the different purification steps of the longer UBCCT fragments fused to a GST-tag. The red dot indicates the expected position of the protein band. BI - before induction, TL - total cell lysate, SN - supernatant containing only the soluble proteins, W1 - flowthrough after washing step 1, E1-E3 - elution step 1-3

was clearly visible at a height of ca. 68 kDa. However, the final elution steps contained many more contaminating proteins than observed while purifying the PHO2 protein. As an example, Figure 2.44 demonstrates only the results obtained for the PFU1UBCCT short construct, but still both the shorter and the longer fragment of PFU1UBCCT were purified to equal amounts. This indicates that, at least in the case of PFU1, choosing proline residues as fragment borders did not significantly alter the solubility of the protein. Although the protein fragments described above differed in their solubility properties and purity, many were tested in subsequent Co-IP experiments and ubiquitylation assays.

2.5.3 Interaction studies via Co-Immunoprecipitation

Several observations described above have indicated a possible interaction of PFU1 and PHO2. However, the results obtained from both coexpression in plants and yeast two hybrid assays were partly contradictory. For this reason, different recombinantly expressed protein fragments of PFU1 and PHO2 were tested for interaction *in vitro*.

According to the meta-structure analysis performed by Dr. R. Konrat, the C-terminus of both proteins possesses the highest potential to be involved in interactions. Due to this, the C-terminus of PFU1 was incubated with a fragment bearing the UBC and C-terminal domain of PHO2 in a first experiment. The longer PHO2 fragment only possessed a His-Tag (PHO2UBCCT), whereas the C-terminus of PFU1 was fused to only a Strep-tag (PFU1CT499 Strep). Both proteins were purified via the respective tag and incubated together for 30 minutes at room temperature. Then Ni-NTA agarose was added for one hour to bind only the PHO2 fragment and, possibly, the interacting PFU1CT-Strep protein with it. As a negative control, the PFU1CT499-Strep fragment was incubated with the Ni-NTA agarose in the absence of the His-tagged PHO2 protein. Then the agarose beads were centrifuged and the supernatant was removed. After washing the resin three times in the tube, the beads were finally incubated in denaturing Lämmli buffer for five minutes at 99 °C and the supernatant was loaded on an SDS-PAGE. The amount of PFU1CT499-Strep was detected by blotting the proteins onto a membrane and detecting with a Strep-tactin alkaline phosphatase conjugate.

Both the negative control and the sample containing the two protein fragments showed a band at a height of 13 kDa expected for PFU1CT499-Strep, indicating that either the C-terminus was non-specifically bound to the agarose, or that the beads were not properly washed in the tubes (Fig. 2.45, panel A).

Hence, instead of the Ni-NTA agarose beads magnetizable Dynabeads Talon (Invitrogen) were applied in a second trial, because these beads are known to show much less unspecific binding and can be due to their magnetic properties washed cleaner without losing any sample. Still, when comparing the negative control and the sample containing the PHO2UBCCT fragment on a western blot, both samples showed an equal amount of remaining PFU1CT-Strep protein (Fig. 2.45, panel B), suggesting that the C-terminus of PFU1 seems to be a very sticky protein, binding also unspecifically to the Dynabeads.

In a last attempt, the highly soluble fragment of PHO2, PHO2UBCCT long, was tested to bind to the PFU1CT StrepHis protein. Both proteins were purified via the His-tag and then incubated together for 30 minutes at room temperature. To capture only the PFU1CT fragment and the putatively binding PHO2 domains, the proteins were incubated with Strep-Tactin Sepharose (IBA) for one hour and the beads were washed five times in the tube. Then the samples were incubated in Lämmli buffer and loaded onto a polyacrylamide gel. The amount of PHO2UBCCT long fragment remaining after the washing steps could already be visualized on a Coomassie stained gel (Fig. 2.45, panel C). Also in this experiment, the negative control contained the protein, which should not be able to bind to the sepharose beads. In both samples, the PHO2 protein fragment with an expected size of 66 kDa was visible. Interestingly, in all three Co-IP attempts performed, the amount of protein detected

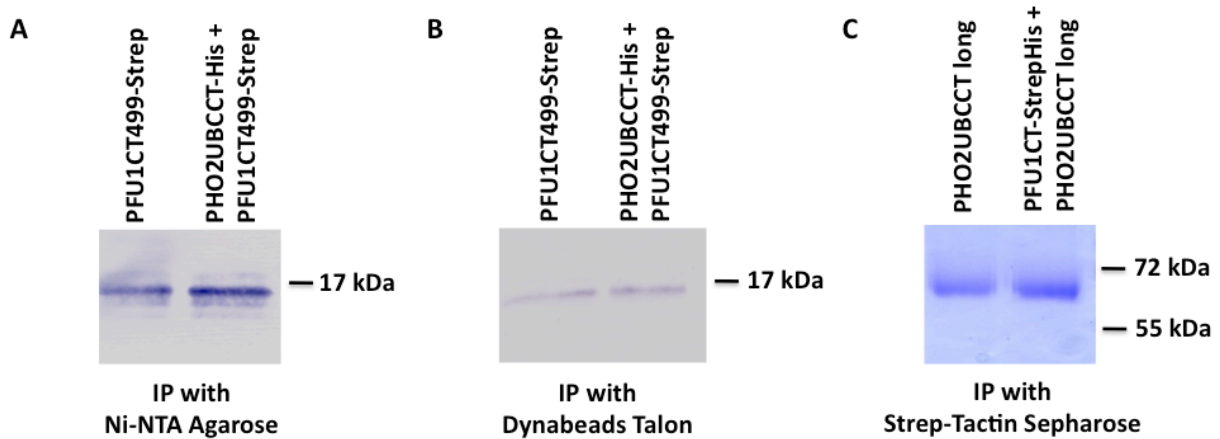


Figure 2.45: Co-immunoprecipitation experiments with PFU1 and PHO2. A: Western blot detected with a Strep-Tactin alkaline phosphatase conjugate, showing the amount of PFU1CT499 Strep after incubation with Ni-NTA agarose beads in the absence and presence of PHO2UBCCT. B: Western blot detected with a Strep-Tactin alkaline phosphatase conjugate, showing the amount of PFU1CT499 Strep after incubation with Dynabeads Talon in the absence and presence of PHO2UBCCT. C: Coomassie stained gel visualizing the amount of remaining PHO2UBCCT long protein after incubation with Strep-Tactin Sepharose in the absence and presence of PFU1CT StrepHis.

in the sample containing both PFU proteins always slightly exceeded the amount of protein remaining in the negative control. Still, the different PFU proteins showed highly unspecific binding to the beads and the putative interaction between PFU1 and PHO2 could therefore so far not be definitely proven via the *in vitro* immunoprecipitation experiments.

2.5.4 *In vitro* ubiquitylation assays

The recombinant proteins bearing only the UBC domain were analyzed in *in vitro* thioester formation assays to prove the function of the PFU proteins as ubiquitin conjugating enzymes. In a first preliminary experiment, relatively crude extracts of both proteins were mixed together with the human ubiquitin activating enzyme UBA1, ATP and ubiquitin, and the samples were detected on a western blot incubated with an anti-ubiquitin antibody obtained from rabbit to visualize the thioester formation. In addition, negative controls were performed for both proteins by leaving ATP out of the reaction mix. As a positive control, the activity of the human ubiquitin conjugating enzyme E2-25K, kindly supplied by K. Maderböck and Dr. A. Pichler at the MFPL (Vienna), was also tested in this assay. Figure 2.46 demonstrates the results for E2-25K and both PHO2UBC and PFU1UBC and directly compares the negative control lacking the ATP with two individual samples containing all compounds needed for thioester formation. A thioester with ubiquitin could be detected for E2-25K at a height of ca. 33 kDa, as expected when adding the 8 kDa of ubiquitin to the 25 kDa protein. This thioester was not formed if ATP was absent in the

reaction mix. So the results obtained for E2-25K demonstrated the functionality of the assay.

However, when comparing the negative control without ATP with the samples containing ATP, no differences in the band pattern were visible for either PHO2UBC or PFU1UBC. A band indicating a thioester was expected at a height of approximately 58 kDa for both proteins, which was not visible on the western blot (Fig. 2.46). Instead, several unexpected bands could be observed, which possibly derived from contaminating proteins in the relatively crude protein extracts shown in Figure 2.43. Thus, this first preliminary experiment revealed that at least under these conditions the UBC fragments of PFU1 and PHO2 are not capable to form a thioester with ubiquitin.

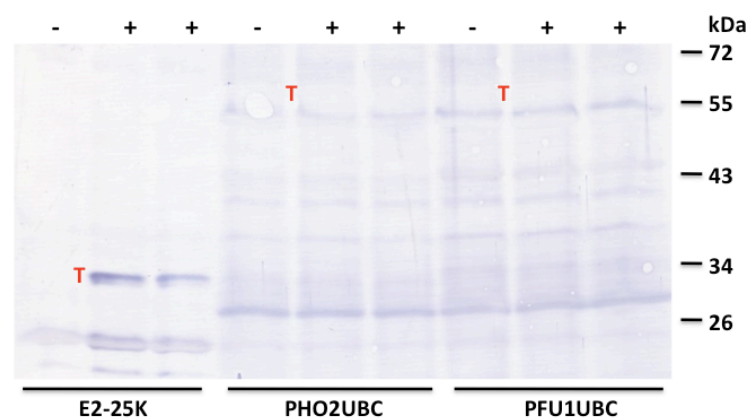


Figure 2.46: Thioester formation assays performed with E2-25K, PHO2UBC and PFU1UBC including a negative control without ATP (–) and two individual samples containing ATP (+). Proteins were blotted onto a membrane and thioester formation with ubiquitin was detected with an anti-ubiquitin antibody from rabbit as a first antibody and an anti-rabbit antibody fused to an alkaline phosphatase as a second antibody. The expected height of the thioester is marked by a red "T".

In a different attempt to prove the functionality of the PFU proteins as ubiquitin conjugating enzymes, the highly soluble fragment PHO2UBCCT was tested in an *in vitro* ubiquitylation assay. In contrast to the thioester formation described above, the covalent attachment of ubiquitin to certain substrates was analyzed, so that not only the E2 function, but also the function as a ubiquitin ligase would be shown by this experiment. This functionality as an E2-E3 hybrid protein could already be identified for the closest mammalian homologue E2-230K/UBE2O (Berleth and Pickart 1996).

As so far no putative substrates of PHO2 have been identified, it was tested whether the PHO2UBCCT long protein fragment was able to covalently attach ubiquitin to itself. This autoubiquitylation was analyzed by incubating the crude extract of PHO2UBCCT long shown in Figure 2.44 together with human ubiquitin activating enzyme, mammalian ubiquitin and either without ATP as a negative control or with ATP for three hours at room temperature. Then the reaction was stopped by incubation in Lämmli buffer for five

minutes at 99 °C and run on an SDS-PAGE. Except for ubiquitin itself, no obvious higher molecular weight bands could be detected when blotting the samples onto a membrane and detecting with an anti-ubiquitin antibody (data not shown). So at least under these conditions the PHO2UBCCT long protein fragment was unable to attach ubiquitin to itself and the functionality of PHO2 to be an E2-E3 hybrid protein could not yet be proven with this first experiment.

Chapter 3

Discussion

3.1 A class of extraordinary E2s in *Arabidopsis thaliana*

Although the family of ubiquitin conjugating enzymes in *Arabidopsis thaliana* is with 37 members highly expanded, only very little is known about their actual role during the life cycle of the plant. This work gives a first insight into the function and the molecular properties of a unique group of ubiquitin conjugating enzymes, PHO2 and PFU1-3, and demonstrates the importance of these extraordinary proteins in the regulation of programmed cell death necessary for several developmental processes and stress responses of the plant.

3.1.1 Specific features of PHO2 and the PFU proteins identified in a bioinformatic approach

First, the design of both gene and protein structure of the PFU proteins was analyzed and compared to other eukaryotic homologues in a *in silico* approach performed with the help of Dr. M. Novatchkova. As intended, this provided first information and ideas on putative localization, molecular mechanisms and potential functions of the PFU proteins in plants. The phylogenetic analysis confirmed the observation already made in former reports (Bachmair et al. 2001; Kraft et al. 2005; Michelle et al. 2009) that homologues of the PFU proteins are absent from the two yeast species *Saccharomyces cerevisiae* and *Schizosaccharomyces pombe*. This makes a functional analysis of the PFU proteins in plants even more interesting, as experiments on homologues in the single-celled eukaryotic model organisms, which usually facilitate the identification of function and molecular behavior of mammalian and plant proteins, are not possible in the case of this unique class of ubiquitin conjugating enzymes. On the other hand, homologues of the PFU proteins can be found throughout the whole eukaryotic kingdom, including fungi, insects, fish, birds and mammals (Fig. 2.2). This indicates that this special class of ubiquitin conjugating enzymes already occurred very early during the eukaryotic evolution and that PHO2 and the PFU proteins might not only bear plant-specific functions.

The protein E2-230K/UBE2O (Berleth and Pickart 1996) was, as described in previous phylogenetic analyses, again confirmed to be the closest mammalian homologue of PHO2 and the PFU proteins in plants. This protein has been shown to bear both E2 and E3 function, which could therefore also be the case for PHO2 and PFU1-3. E2-230K/UBE2O is specifically overexpressed only during the reticulocyte stage of the erythroid differentiation, which makes purification of the protein from mouse tissue and the identification of mutant phenotypes in knockout mice more difficult. Moreover, identification of its exact role during erythroid differentiation is missing, and plants do not have erythrocytes, so that no putative role for the PFU proteins could be predicted. Thus, work on the widely expressed homologues PHO2 and PFU1-3 in plants, where production of knockout mutants and analyses under different growth conditions is easier, might even facilitate the identification of a putative function of the mammalian protein.

The inhibitor of apoptosis BRUCE/Apollon (Bartke et al. 2004; Pohl and Jentsch 2008) in mammals was observed to be more distantly related to PHO2 and PFU1-3. Whereas E2-230K shows homology to PHO2 along its entire open reading frame, BRUCE only shares the UBC domain with these proteins. However, much more is known about the role of BRUCE in the regulation of apoptosis in the mammalian cell, which gave a first indication that PHO2 and PFU1-3 might also function as regulators in programmed cell death in plants.

In regard of the mammalian homologues (E2-230K: 230 kDa, BRUCE: 528 kDa), PHO2 and the PFU proteins are shorter, but still, in comparison to the rest of the ubiquitin conjugating enzymes in plants, these proteins are unusually large. Especially PHO2 and PFU2 exhibit a long N-terminal domain, which shows the highest homology to E2-230K/UBE2O. In contrast, PFU1 and PFU3 are shorter and seem to be plant specific, as their N-terminal domain shows less homology to the mammalian homologue. Thus, according to their N-terminal domain, the PFU family can be divided into two subgroups, on the one hand the highly homologous longer members of the family PHO2 and PFU2, and on the other hand the more plant specific, less homologous shorter members PFU1 and PFU3 (Fig 2.3). So far, no motifs or domains of known function could be identified for the N-terminal extension of all four plant proteins and E2-230K/UBE2O. They all lack the BIR domain shown for BRUCE to be required for the antiapoptotic function. However, a search with the bioinformatic tool HHrep (Söding et al. 2006) identified beta-rich repeats in the N-terminal domain of the PFU2 protein sequence, showing a subsignificant similarity to Tudor-like domains (Dr. M. Novatchkova, personal communication) known from the Tumour suppressor p53-binding protein-1 (53BP1). This domain is necessary for the recruitment of proteins to DNA double-strand breaks by mediating the interaction with the methylated Lys 79 of histone 3 (Huyen et al. 2004). Other prediction tools such as HHrepID (<http://toolkit.tuebingen.mpg.de/hhrepid>), though, did not show these similarities and the hits obtained with HHrep were subsignificant. Therefore, the relation to Tudor domains can only help to establish hypotheses on the function of the N-terminal domain of PFU2. Apart from the N-terminal extension, all four proteins are highly similar in their UBC domain and in a C-terminal extension. The UBC domain bears the active site cysteine residue, which is highly conserved in all eukaryotic homologues and is necessary for the thioester

formation of the E2 with ubiquitin. Apart from the UBC domain also the C-terminal extension is found in the E2-230K/UBE2O protein of all other eukaryotic organisms analyzed (Fig. 2.2). Interestingly, a cysteine residue in the C-terminal domain is highly conserved only throughout the plant kingdom. It is found in the genome of all PHO2 homologues analyzed in green algae, mosses, monocotyledons and dicotyledons. This cysteine residue could therefore bear a plant specific function such as sensing oxidative signals within the cell. It could also possess a HECT-like function as it was predicted for the two mammalian homologues E2-230K/UBE2O and BRUCE/Apollon. However, a cysteine residue at this position is not found in the mammalian protein sequence. A closer view at the C-terminal domain of E2-230K/UBE2O revealed a cysteine residue further upstream closer to the UBC domain, which is conserved in fish, birds and mammals but not found in fungi and insects. This cysteine residue could have a role in the E3 function observed for E2-230K/UBE2O. Still, these are only hypotheses and have to be proven via functional analyses such as ubiquitylation assays with plant and mammalian proteins mutated in the respective cysteine residue.

Apart from the information taken from the phylogenetic analysis, the appliance of additional bioinformatic tools provided new insight into the properties of PHO2 and the PFU proteins. Analysis on the subcellular localization of the proteins via two different prediction tools gave contradictory results. Whereas according to the WoLF PSORT program all proteins have a potential to be located in the nucleus, a nuclear localization signal could only be detected for PFU1, PFU2 and PFU3 with PredictNLS online. The NLS sequences proposed for PFU1 and PFU3 are located at the C- and N-terminus of the protein, respectively. In addition, a second motif not identified by the Predict NLS online tool but highly related to the NLS found for PFU1 is present at the C-terminus of PFU3. Taken together, these results demonstrate that for both proteins the probability of being localized in the nucleus is relatively high. In contrast, the signal predicted for PFU2 is lying in the middle of the protein, which makes a detection by the nuclear import system quite unlikely. Interestingly, with the WoLF PSORT program, this protein has the highest probability of being imported into the nucleus compared to the other PFU proteins. This shows that information obtained by bioinformatic tools can only help in giving indications for a subcellular localization of the protein of interest. Still, the exact properties of the proteins can only be determined by performing localization experiments, for example via expression of fusion proteins with fluorescent markers in the plant cell.

3.1.2 PFU2: a target for microRNAs ?

In contrast to the other members of the PHO2 like ubiquitin conjugating enzyme family, a full length cDNA of *PFU2* was not available at the RIKEN repository. As the complete open reading frame of *PFU2* consists of 3309 bp, it was divided into four different fragments that were separately amplified and ligated together with the help of restriction sites within the gene. One of these fragments could not be amplified with the SuperScript II Reverse Transcriptase (Invitrogen), but with the Transcriptor RT (Roche) (Fig. 2.4). The main explanation for this might be that the *PFU2* mRNA transcript possesses a distinct

secondary structure at this position, which is only denatured under higher temperatures such as 55° C used with the thermostable Transcriptor RT.

PFU2 shares high homology with PHO2 along the complete protein sequence. Apart from this, also the gene structure of both proteins is highly similar. Both possess a large first exon and six smaller additional exons, which are divided by six short introns (Fig. 2.8).

Therefore it became of interest whether the transcript levels of *PFU2* are, as described for *PHO2* (Fujii et al. 2005), also regulated via microRNAs. The 5' leader sequence of *PFU2* was analyzed, because five binding sites for miRNA399 were identified in the 5' UTR sequence of *PHO2* (Fujii et al. 2005). First, the length of the 5' leader of the *PFU2* transcript was determined. The RT-PCR experiments performed in this thesis with wild type RNA clearly demonstrated that the non-translated leader sequence of *PFU2* is unusually long. *PHO2* possesses a large leader of 1000 nucleotides and contains an intron in the leader sequence. This intron is missing in the *PFU2* leader sequence, indicating a different regulation of this gene. In the RT-PCR experiments described here, a downstream reading oligo at position 940 bp before the ATG gave a clear PCR product corresponding to the 5' sequence of *PFU2*. When using oligos further upstream of 940 bp before the ATG, only relatively weak and smeary bands were obtained, showing no sequence similarities to the 5' UTR of *PFU2* (Fig. 2.6). This either occurred due to the fact that the sequence further upstream is not transcribed in the plant, or the PCR was not effective enough to amplify these sequences. Therefore it cannot be ruled out that the length of the *PFU2* leader sequence even exceeds 940 nt.

A search for miRNAs binding to the 5' leader sequence of *PFU2* revealed that no target site for miRNA399 is present (Dr. M. Novatchkova, personal communication). Instead, miRNA414 has been shown to be the best candidate being able to bind the *PFU2* leader. However, this miRNA is predicted to target 954 different loci and it is not clear, whether it is expressed and is indeed a functional miRNA (Alves-Júnior et al. 2009). Therefore its impact on the regulation of *PFU2* is not clear.

Apart from miRNA target sites, at least eight different ATGs are found in the *PFU2* leader sequence. This results in the expression of several different open reading frames and is very often an indication of low steady-state levels of the transcript and reduced protein translation (Saul et al. 2009). So PFU2 might be a lowly expressed protein that is down-regulated by decreasing both mRNA stability and translation efficiency.

3.1.3 Alternative structure of *PFU3* is not supported

For the *PFU3* open reading frame, two different structures were predicted. Before working on the molecular properties of this protein, it was therefore determined in this thesis, which mRNA is actually transcribed *in planta*. The RIKEN database predicted an open reading frame encoding a shorter protein possessing only 543 amino acid residues and one single UBC domain, which is followed by one or two pseudogenes. In contrast, the SALK database suggested a much longer protein of 1163 amino acids containing three UBC domains.

The RT-PCR experiments performed in this work did not support the longer protein

structure suggested by SALK. Only a fragment in front of the Stop codon predicted by RIKEN could be amplified from two week-old wild type *Arabidopsis* seedlings. A PCR fragment behind this Stop codon located in the open reading frame proposed by the SALK database could not be obtained (Fig. 2.7). Still, the presence of the longer *PFU3* transcript cannot be completely ruled out. Several examples for alternative splicing of a transcript and expression of different versions of a protein in different tissues exist in plants (Addepalli et al. 2004). Alternative splicing is also known to occur in response to biotic or abiotic stresses (Matsukura et al. 2010).

Anyhow, to date, no ubiquitin conjugating enzyme possessing more than one UBC domain is known. Apart from that, the structure predicted by RIKEN would result in a protein that is highly homologous to PFU1, whereas the protein predicted by SALK would show a completely different structure. All of these observations and the RT-PCR results obtained in this work suggest that the presence of the longer PFU3 protein possessing three UBC domains is highly unlikely. This question could be definitely clarified by analyzing the ability of the two different transcripts in complementing a *pfu3* mutant phenotype, which could unfortunately not be identified yet.

3.2 The PFU proteins bear an important function in plant programmed cell death

Only for one member of the PHO2 family of ubiquitin conjugating enzymes, PHO2, a specific function in plants could be identified so far. It is shown to be a negative regulator of many genes induced during the P_i starvation response (Bari et al. 2006). The role of PFU1-3 during the life cycle of *Arabidopsis thaliana*, however, could not be identified yet. Therefore one task of this thesis was to identify and characterize knockout mutants for PHO2 and the PFU proteins and compare them to wild type under different growth conditions.

3.2.1 T-DNA insertion lines of *PHO2* and the *PFU* genes with altered transcript levels

T-DNA insertion lines were available for all four family members, and homozygous plants could be obtained for each of them, showing that none of these mutations results in embryo-lethality and the genes are not essential for early plant development. Before analyzing the T-DNA insertion lines under different growth conditions it had to be verified whether these mutations lead to an alteration in the *PFU* transcript levels.

For *PHO2*, *PFU1* and *PFU3* the insertion was located within an exon of the coding sequence (Fig. 2.8). This already suggested that these genes might not be properly transcribed anymore in the T-DNA insertion lines and that the protein levels might be severely reduced. Indeed, the comparison between the transcript levels of the *pho2-10*, *pfu1-1* and *pfu3-1*

insertion lines and wild type performed in this work clearly demonstrated that all three plant lines represent complete knockout mutants of the respective gene (Fig. 2.10).

In contrast, the insertion of *PFU2* was lying within the presumed mRNA leader sequence of the gene. This suggested several options. It either might lead to upregulation of the transcript levels (Halliday et al. 1999), repression of the respective gene (Nicol et al. 1998) or it could simply have no effect at all on the transcription. The results obtained for the transcript levels in the *pfu2-1* mutants clearly demonstrated that, in the case of *PFU2*, a T-DNA insertion in the leader region leads to downregulation of the mRNA levels. However, low transcript levels were still detectable showing that the *PFU2* gene was not completely knocked out (Fig. 2.10). It can also not be ruled out that the transcript levels of *PFU2* are indeed overall decreased but in specific tissues or cell types not analyzed in the present RT-PCR experiments not at all altered or even increased.

The single mutants grown under normal growth conditions did not show any obvious phenotype suggesting that the PFU proteins function in distinct, specialized pathways. However, very often single gene knockouts or silencing approaches in *Arabidopsis* do not lead to an altered morphology due to structural or functional redundancy of genes (Bouché and Bouchez 2001). Therefore, double and triple mutants of the PHO2 family ubiquitin conjugation enzymes were obtained in this thesis via crossing of the respective single mutants. Even homozygous plants of the quadruple mutant could be identified. This indicated that inhibition of the complete protein family does not lead to embryo-lethality and that the function of the PHO2 family of ubiquitin conjugating enzymes is not essential for early plant development. However, the transcript of *PFU2* was not completely absent in these mutants, so that low levels of this protein could have replaced the function of the related family members. Single, double and triple mutants did not show any obvious phenotype when grown on soil under normal growth conditions, showing that if the mutations in the *PFU* genes lead to an altered function in the plant, this phenotype is not so easy to detect. The quadruple mutant seems to be smaller in size than wild type plants, but this has to be further investigated and is just a very preliminary result. Still, this indicates that inhibition of the whole PHO2 family might perturb specific developmental processes of the plant already under normal growth conditions.

3.2.2 Only *pho2* mutants show P_i accumulation in the shoot

As no obvious phenotype was detectable neither for the single *pfu* mutants nor for the double and triple mutants under normal growth conditions, specific properties of these plants were analyzed in more detail. For one member of the protein family, PHO2, a function as a negative regulator in the phosphate starvation response was already reported before (Delhaize and Randall 1995; Bari et al. 2006). Therefore it was obvious to first analyze the impact of the other PFU proteins on the phosphate content of the plant.

The results described in this thesis indicate that a function in phosphate signaling seems to be specific for PHO2, as the single mutants of the other *PFU* genes did not show a P_i accumulation in the shoot (Fig. 2.11) demonstrated before for the *pho2* mutant (Delhaize

and Randall 1995). Still, this observation is only based on the analysis of the single mutants and it can not be definitely ruled out that also the other members of the PHO2 protein family have an impact on the phosphate starvation response. A mutation in only one of these genes might just not have been sufficient to lead to overaccumulation of phosphate due to redundancy of the genes. Therefore also the phosphate content of the double mutant *pho2-10 pfu2-1*, which is impaired in the two longer members of the PHO2 family, was tested. A higher phosphate content than observed for the single *pho2* mutant could still not be detected (Fig. 2.11), indicating that PFU2 indeed has no specific impact on the phosphate uptake. The PFU2 protein is, however, not completely knocked out in the *pho2-10 pfu2-1* double mutant and the low PFU2 levels present might be sufficient to take over the function of this protein in phosphate signalling.

Apart from this, also PFU1 and PFU3 might be able to take over the other protein's function during phosphate signaling in the respective single mutants, as these proteins are structurally highly related. The phosphate content of the *pfu1-1 pfu3-1* double mutant, lacking the complete subfamily of the shorter PHO2 family members, has not been analyzed yet, so that a role of PFU1 and PFU3 in phosphate signaling can also not be ruled out yet. In contrast to the other *pfu* single mutants, plants of the T-DNA insertion line of *PHO2* identified in this work (*pho2-10*) clearly accumulate P_i in the shoot to the same extent as described for the *pho2* mutant obtained via EMS mutagenesis in Delhaize and Randall (1995). This shows that the T-DNA insertion within the third exon of the *PHO2* gene analyzed in this work has the same influence on the phosphate content of the plants as the GtoA mutation resulting in a STOP codon at position aa 671 of PHO2 described for the EMS-induced mutant (Aung et al. 2006). It would be interesting to know whether the additional phenotypes of the *pho2-10* mutant observed in this thesis are also detectable in the EMS mutant of *PHO2*. This would indicate that these *pho2-10* phenotypes definitely derive from altered PHO2 levels and are not caused by mutations in other genes, which might be present as the average number of T-DNA insertions is described to be 1.5 per transgenic line (Alonso et al. 2003). However, it is relatively unlikely that the phenotypes derive from other mutations, as all *pfu* mutant lines were outcrossed several times. Southern blot analysis to determine the number of insertions within the plant's genome or complementation assays with the complete open reading frame of the protein would definitely solve this problem.

3.2.3 Mutation of PHO2 and the PFU proteins suppresses the ubK48R phenotype

After analyzing the phosphate content of the *pfu* mutant plants, a specific function of the PHO2-like ubiquitin conjugating enzymes PFU1-3 within the plant's life cycle was still not identified. The phylogenetic analysis performed in this thesis confirmed that BRUCE, a mammalian inhibitor of apoptosis, is distantly related to the PHO2 family. This suggested that also PHO2 and the PFU proteins might be involved in programmed cell death in plants.

A specific induction system for a ubiquitin variant in *Arabidopsis* established by Schlögelhofer

et al. (2006) helped in analyzing the effect of a mutation in the *PFU* genes on the regulation and execution of plant programmed cell death. Plants expressing this ubiquitin variant with Lys 48 exchanged by arginine contain a pool of native ubiquitin and mutated ubiquitin. Introduction of the mutated ubiquitin during chain formation inhibits prolongation of the chain and therefore ubiquitin-mediated proteolysis in the entire plant. This leads to an obvious cell death phenotype that is characterized by the appearance of necrotic lesions during the early response to transgene induction and afterwards by yellowing of the leaves and finally death of the whole plant (Fig. 2.12). The early response to the perturbation of the ubiquitin-proteasome pathway through induction of the *ubK48R* transgene resembles fast cell death reactions such as the hypersensitive response, and has been described to be not just a simple necrosis event but an active programmed cell death process, which is called transgene-induced lesion mimic (Mittler and Rizhsky 2000). The slower response to transgene induction, the yellowing of the plants resembles the leaf senescence process, a second form of programmed cell death in plants (Lim et al. 2007).

This *ubK48R* transgene was expressed in the *pho2-10*, *pfu1-1* and *pfu2-1* mutant background and the programmed cell death phenotype observed for wild type plants was clearly suppressed by the mutations in these genes, indicating that PHO2, PFU1 and PFU2 are required for the initiation of both the fast cell death response after induction of the transgene and the slower senescence-like process (Fig. 2.12). Interestingly, PHO2 has already been described to be upregulated in senescent leaves (Bari et al. 2006) and under conditions that can trigger senescence, such as nitrogen deficiency or extended darkness (Bläsing et al. 2005), which underlines the important role for this protein in the senescence process.

Only homozygous but not heterozygous *pho2-10* mutant plants suppressed this phenotype (Fig. 2.12), demonstrating that this mutation seems to be completely recessive. In contrast, heterozygous plants of the *pfu1-1* mutant line did not show any cell death response after transgene induction. Thus, the *pfu1-1* mutation seems to be dominant, which could occur due to haplo-insufficiency, meaning that the amount of PFU1 protein produced from the intact *PFU1* allele is not enough to induce the plant cell death program. This was for example demonstrated for the *ztl* mutant, where heterozygous plants are not producing enough amounts of an F-box protein, which is regulating flowering and the circadian clock (Mizoguchi and Coupland 2000). If this is also the case for PFU1, the regulation of this protein within wild type cells might be very complex and plant mechanisms involving PFU1 could be highly sensitive to changes in the protein level. Apart from this, the dominant effect of the *pfu1-1* mutation could also result from expression of a dominant negative PFU1 protein fragment. This was for example shown for the two subunits of the COP9 signalosome, CSN5A and CSN5B, in *Arabidopsis*. Mutations in their JAMM domain exhibiting an isopeptidase function involved in deubiquitylation and derubylation lead to dominant negative effects on the plant development (Gusmaroli et al. 2004).

The effect of the *pfu2-1* mutation on the cell death phenotype of the *ubK48R* transgene could also be explained by haplo-insufficiency. It rather represents an intermediate between the dominant *pfu1-1* and the recessive *pho2-10* allele, as heterozygous *pfu2-1* plants do not suppress the *ubK48R* induced cell death to the same extent as homozygous plants, but still a suppression of cell death is detectable compared to wild type levels.

The alteration of the cell death response in the *pfu1-1*, *pfu2-1* and *pho2-10* mutant background could also be caused by a reduction of the *ubK48R* transcript levels in these plants. Therefore, RT-PCR experiments were performed in this thesis to directly compare the amount of the *ubK48R* mRNA in the *pfu1-1* mutant and wild type plants. The RT-PCR products shown in Fig. 2.13 clearly indicate that the mutated ubiquitin is expressed to the same extent in the mutant plant as observed for wild type. Thus, the suppression of the programmed cell death response in the *pfu1-1* mutant background is occurring due to the lack of the PFU1 protein itself. Very likely this conclusion can also be extended to the *pfu2-1* and *pho2-10* mutant plants.

In summary, the results described here give first evidence that the two larger family members PHO2 and PFU2 and the smaller protein PFU1 exhibit an important role in both fast and slower programmed cell death processes.

In contrast to the other three mutant lines, the *pfu3-1* mutants did not show any suppression of the cell death occurring in response to perturbation of the ubiquitin-proteasome system (Fig. 2.12), suggesting that this protein is not involved in regulating programmed cell death. Anyhow, the missing phenotype for the *pfu3-1* single mutant in this system could also occur due to gene redundancy with the structurally related PFU1 protein, which has been shown to have a high impact on the initiation of the cell death response. Unfortunately, analyzing the cell death response in the *pfu1-1 pfu3-1* double mutant to find out more about the role of PFU3 in this process would very unlikely give a more obvious phenotype, as the mutation of PFU1 already shows this extreme suppression of cell death. One could quantify the cell death response in the single and double mutants, for example by measuring the chlorophyll content of the plants. Breakdown of the chloroplast and with it the degradation of the chlorophyll content is one of the major characteristics of plant senescence (Lim et al. 2007) and is often used to measure the impact of a protein mutation on the regulation of this slow cell death process in plants (Raab et al. 2009). This could help to see an effect of the *pfu3-1* mutation on the cell death suppression. Apart from this, additional assays, for example analysis of the *pfu3-1* mutant in other cell death inducing systems such as exposure to biotic or abiotic stresses, might give more insight into the role of PFU3 in programmed cell death.

3.2.4 PHO2 and PFU1 sense oxidative stress caused by ozone treatment

Ozone exposure of plants has been described as a suitable tool to increase the understanding of the complex signaling pathways involved in the regulation of programmed cell death (Rao et al. 2000). Long-term ozone treatment at relatively low concentrations causes chlorosis and premature senescence. At higher doses this extremely toxic agent causes necrotic lesions similar to the hypersensitive response occurring as a result of incompatible plant-pathogen interactions (Kangasjärvi et al. 2005). Ozone mimics responses to pathogens by inducing an oxidative burst that continues after the end of ozone exposure. Thereby it leads to expression of defense-related genes, release of ethylene, biosynthesis of salicylic

acid, induction of chromatin condensation and DNA fragmentation and many additional steps, which are also characteristic for naturally occurring programmed cell death events (Rao et al. 2000).

Thus, the comparison between wild type and *pfu* mutant plant growth under ozone treatment performed in this thesis was a direct approach to further study the function of PHO2 and the PFU proteins in programmed cell death. *Arabidopsis* wild type plants showed, as expected from previous reports (Overmyer et al. 2005), severe leaf lesions and yellowing of the leaf tissue surrounding these lesion (Fig. 2.14), which resembles the reaction of the plant after pathogen treatment (Mur et al. 2008). In contrast, the two single mutants *pho2-10* and *pfu1-1* only developed small yellow spots, but no lesions or severe chlorosis were visible. This clearly indicated that PHO2 and PFU1 seem to be necessary for the proper initiation and execution of the programmed cell death occurring in response to the abiotic PCD elicitor ozone.

The *pfu2-1* mutant, however, showed the same sensitivity to ozone exposure as observed for wild type plants, indicating that PFU2 is not involved in the programmed cell death response to ozone exposure. Still, the *PFU2* transcript is not completely knocked out in these mutants and the amount of PFU2 protein still present might be enough to conduct the function of this protein in PCD induced by ozone.

The *pfu3-1* mutant line was not tested in this assay yet, so that nothing can be said about the function of PFU3 in ozone-induced programmed cell death.

The phenotypes observed for the *pho2-10* and *pfu1-1* mutants suggest several possibilities of how PHO2 and PFU1 might regulate the initiation of programmed cell death. Ozone is degraded to reactive oxygen species (ROS) in the apoplast and leads to an intense oxidative burst in the plant (Overmyer et al. 2003). These ROS interact in a complex manner and are able to modify a multitude of cellular components. Especially thiols within lipids or proteins are the most favored targets of such modifications (Winterbourn 2008). PHO2 and PFU1 might therefore sense and further transmit these oxidative signals.

Apart from this, several plant hormones have been described to be involved in the regulation of programmed cell death (Overmyer et al. 2003). ROS are known to activate the production of jasmonic acid (JA), ethylene and salicylic acid (SA). Salicylic acid has been shown to accumulate in ozone exposed plants, and pretreatment of wild type plants with this hormone even increased the cell death occurring after ozone treatment (Rao et al. 2002). Therefore, PHO2 and PFU1 might also be somehow regulated by changes in the hormonal composition of the plant in response to oxidative signals. Interestingly, *pfu2-1*, *pho2-10* and *pfu1-1* *pho2-10* mutant plants showed a reduced germination rate and decelerated growth when treated with salicylic acid (Garzón 2008). This suggests a role for PHO2 and PFU1 in sensing this hormone and even indicates that PFU2 is involved in the response to salicylic acid and therefore also in the programmed cell death characterized by increased SA levels.

3.2.5 PFU2 needed for response to nitric oxide

Apart from reactive oxygen species and salicylic acid also nitric oxide (NO) has been shown to accumulate after ozone treatment of the plant and in response to pathogens,

and the production coincides with the formation of necrotic lesions also found during the hypersensitive response (Ahlfors et al. 2009), suggesting an important function for this molecule in ozone-induced programmed cell death. As also PHO2 and PFU1 have now been shown to be involved in regulating the cell death response to ozone treatment, it was tested in this thesis whether NO has any effect on PHO2 and the PFU proteins.

NO is a small gaseous radical that, due to its lipophilic nature, is able to diffuse across membranes and is found as a signal molecule in a multitude of physiological processes both in plants and animals (Wendehenne et al. 2001). Three different sources of NO production within the plant have been suggested so far (Leitner et al. 2009). It can either occur non-enzymatically via conversion of nitrite in the apoplast or it is produced enzymatically with the help of the nitrate reductase. Apart from this also NO synthases, which have been extensively described in mammalian cells (Beck et al. 1999), are proposed to exist in plants. However, to date none of these enzymes have been identified and the complex and pleiotropic phenotypes of NO-related mutants make the characterisation of potential NO producing enzymes very difficult (Leitner et al. 2009). In addition to NO, other reactive nitrogen species (RNS) are produced within the cell. NO can for example react with the ROS superoxide to form peroxynitrite (Romero-Puertas et al. 2007). This directly connects the signaling pathway of the reactive oxygen species with NO signaling and shows that both ROS and RNS are interacting in a complicated manner to regulate cellular processes. An additional RNS is built through reaction of NO with glutathione resulting in S-nitrosylated glutathione. This reagent can release NO or transnitrosylate other cellular components. Both processes are controlled by the enzyme GSNO reductase, which is highly conserved in pro- and eukaryotes (Liu et al. 2001). Mutant plants lacking this enzyme are impaired in growth and reproduction and show hypersensitivity to both abiotic and biotic stresses, underlining the important role of NO and RNS signals in various physiological processes (Lee et al. 2008; Rusterucci et al. 2007).

In plants, NO was first identified to play a vital role in the hypersensitive response to pathogen attack (Delledonne et al. 1998). Later it could be shown that NO controls programmed cell death events by modifying many regulating proteins, e.g. the metacaspase 9 (Belenghi et al. 2007), via its covalent attachment to the thiol side chain of a cysteine residue. With this process, called S-nitrosylation, NO is able to directly influence the activity of these proteins and is therefore important in a multitude of programmed cell death processes in plants. Apart from the hypersensitive response and ozone-induced PCD, NO and RNS are for example also shown to regulate slow PCD events such as senescence (Mishina et al. 2007).

As the previous experiments demonstrated that the PHO2 proteins are, just like NO, also involved in the regulation of programmed cell death in plants, it was now hypothesized that NO might control programmed cell death events via interaction with PHO2 and the PFU proteins. To further investigate this idea, the four single *pfu* mutant lines were compared to wild type in a liquid medium containing the NO donor sodium nitroprusside.

A subtle phenotype was only observed for the *pfu2-1* mutant during the first approach where plants seemed to produce slightly more lateral roots than wild type plants. Interestingly, NO has already been described to be involved in root development (Gupta et al. 2005),

so that this phenotype suggested a role of PFU2 in transmitting NO signals in the root. However, the root phenotype could not be reproduced in a second trial. This could be explained by the volatility of NO, which can leak out from the flask and therefore makes the regulation of the NO concentration in this approach very difficult. The NO signals in the plant have been shown to be highly regulated and small changes in the concentration can easily alter the response of the plant cell. Apart from this, the amount of roots was not measured during the first approach and the roots were difficult to examine in the liquid medium so that an increase of side roots could not be definitively proven.

Therefore a different assay to analyze the root formation of the *pfu2-1* mutant under NO treatment was established. Wild type plants and *pfu2-1* mutants were grown on plates containing different amounts of sodium nitroprusside. With this method the roots of the plants could be easily examined. However, also in this assay the *pfu2-1* mutant did not show altered root formation, suggesting that PFU2 is not involved in the NO signaling needed for proper root development.

Instead, a different phenotype could be observed showing that the *pfu2-1* mutant seemed to be less sensitive to nitric oxide treatment than wild type plants. Three times more mutant than wild type plants survived the treatment with 0.2 mM sodium nitroprusside (Tab. 2.5). This could be observed in three independent approaches, underlining the different response of wild type and mutant plants to NO treatment. The results suggest that PFU2 is able to sense signals transmitted by nitric oxide. This could either be achieved indirectly by interacting with a cellular component responsive to NO, or directly for example by S-nitrosylation of an internal cysteine residue of PFU2. The highly conserved cysteine residue in the C-terminal domain of PFU2 could be such a site for S-nitrosylation. To analyze this regulation in more detail, the activity of the protein could be examined in biochemical assays such as *in vitro* thioester assays with and without nitric oxide. It would also be interesting to analyze the effect of the *pfu2-1* on other plant processes known to involve NO signaling, e.g. seed development and germination (Borisjuk and Rolletschek 2009). This could further confirm the role of PFU2 during NO signaling.

3.2.6 PHO2 and PFU1 work together in the response to biotic stress

Both nitric oxide and ozone treatment underlined the putative role of the PHO2 family of ubiquitin conjugating enzymes in programmed cell death and the interaction with the ROS and RNS signals, which are highly induced during PCD. However, the nitric oxide treatment is just a synthetic environment chosen to elucidate features of the proteins that might have been undetected under more natural conditions such as treatment of the plants with pathogens. The ideas taken from the ozone treatment can also not be directly transferred to the processes during the hypersensitive response as the ozone-induced cell death will always be associated with ozone sensitivity (Rao et al. 2000).

Therefore the effect of the PHO2 proteins on cell death in plant-pathogen interactions was

directly analyzed in collaboration with Dr. N. Schlaich (RWTH Aachen) by infecting the mutant and wild type plants with the avirulent *Pseudomonas syringae* pv tomato strain DC3000 carrying the avirulence locus *avrRpt2* (Whalen et al. 1991). This leads to resistance of Col-0 wild type plants to this pathogen, resulting in a hypersensitive response (Mur et al. 2008). Ion leakage from the plant tissue is very often used to assay the membrane damage during the hypersensitive response in a time course and is measured by determining the conductivity levels of the surrounding solution (Pike et al. 2005). Such measurements were performed in this thesis for wild type and *pfu* mutants at different time points up to 21 hours after infection with the pathogen. Summarizing the values taken from four independent experiments revealed that single mutants showed no changes in ion leakage from the plant tissue when compared to wild type levels. This indicated that the single mutations did not alter the hypersensitive response of the plant to the bacterial pathogen. In contrast, the *pho2-10 pfu1-1* double mutant showed a mild but significant decrease in ion leakage after seven hours compared to wild type and therefore a weaker response to the pathogen. However, after 21 hours the conductivity levels were nearly the same as in wild type again, indicating that the *pho2-10 pfu1-1* double mutant was only delayed in its hypersensitive response (Tab. 2.7). These findings suggest that both PFU1 and PHO2 are involved in the induction of cell death in response to pathogens and might interact in a signaling network, which is only impaired if the two proteins with redundant function are missing. It also demonstrates that, although many characteristic features of ozone-induced PCD are similar to the hypersensitive response, the regulation steps seem to be partly different, as in the case of the ozone treatment the functional redundancy of PFU1 and PHO2 was not observed.

In summary, the analysis of the *pfu* mutants performed in this thesis clearly identified a completely new function of ubiquitin conjugating enzymes PHO2, PFU1 and PFU2 in the regulation of programmed cell death responses to abiotic and biotic stress conditions, which might be controlled by the interaction with ROS and RNS signals.

3.3 The two subfamilies show different subcellular localization patterns

The expanded analysis on the mutant lines of the PHO2 family of ubiquitin conjugating enzymes performed in this thesis has raised several possibilities on how these proteins might behave on the molecular level. To further investigate the molecular properties, the subcellular localization of these proteins was examined in this work by expressing fusion proteins with fluorescent markers. The enhanced form of GFP, which bears a point mutation leading to more efficient folding (Thastrup et al. 1995), was fused to the C-terminal end of PFU1, PFU2 and PFU3. In addition, the monomeric form of RFP (Jach et al. 2006) was fused to the C-terminus of PHO2, PFU2 and PFU3. These fusion proteins were first transiently expressed via infiltration of *Nicotiana benthamiana* plants with *Agrobacteria* containing the respective constructs. High levels of the fluorescent fusion proteins in the

plant were achieved by expressing the transgenes under the control of the 35S promoter taken from the cauliflower mosaic virus (Odell et al. 1985). To avoid silencing of the transgene, which is a common phenomenon for strong promoters (Elmayan and Vaucheret 1996), an *Agrobacterium* strain expressing the p19 protein from the tomato bushy stunt virus, known to suppress posttranscriptional gene silencing (Voinnet et al. 2003) was infiltrated into the plants together with the other strains. In the end high amounts of fusion proteins were expressed in the tobacco plants, which could be analyzed under the confocal microscope. Transient expression in *Nicotiana benthamiana* is an effective and fast method to analyze the localization of proteins in the plant. However, it is only a heterologous system and the behavior of the proteins in these cells does not need to be similar to the actual subcellular localization of the PFU proteins in *Arabidopsis thaliana*. Therefore the different EGFP/mRFP fusion constructs were also stably transformed into *Arabidopsis thaliana*, where they were expressed under the control of a β -estradiol inducible promoter to circumvent gene silencing.

3.3.1 PFU1 and PFU3 are imported into the nucleus

The bioinformatic tools applied to investigate the subcellular localization of the PFU proteins, WoLF PSORT and PredictNLS, both predicted the two smaller members of the PHO2 family of ubiquitin conjugating enzymes, PFU1 and PFU3, to be localized in the nucleus (Chapter 2.1). Apart from this, a nuclear export signal could be found only for PFU1, suggesting that this protein might be localized in both nucleus and cytoplasm. Indeed, analysis of the subcellular localization of PFU1 and PFU3 in both *Nicotiana benthamiana* and *Arabidopsis thaliana* exactly confirmed these predictions. The PFU3-EGFP fusion protein was clearly only localized in the nucleus and could not be detected in any other cellular compartment (Fig. 2.18 and 2.23). The fact that also the mRFP fusion protein shows this distinct localization in both *Nicotiana* and *Arabidopsis* demonstrates that the nuclear localization is not only a property of the EGFP fusion protein but is rather specific for the PFU3 protein. The distinct localization of PFU3 would also be consistent with the finding that this protein seems to bear a specific function in the plant, as a phenotype for the *pfu3-1* mutant could so far not be detected. In contrast, PFU1, which has been shown to play a more general role in the plant response to several stresses, is not restricted to the nucleus when fused to EGFP but can also be found in the cytoplasm of *Nicotiana* and *Arabidopsis* cells (Fig. 2.17 and 2.22). The subcellular localization of both proteins would also explain why the *pfu1-1* single mutant is able to suppress the PCD in response to induction of the mutated ubiquitin, whereas the *pfu3-1* mutant does not show any phenotype. PFU1 and PFU3 might have redundant functions in the nucleus, but PFU3 is due to its restriction to the nucleus not able to replace the function of PFU1 in the cytoplasm.

Interestingly, the PFU1-EGFP protein is forming small vesicle-like structures in the cytoplasm of *Nicotiana benthamiana* cells. Therefore, PFU1 might also be located in the Trans Golgi Network and in the vesicular system, as already described for the distant mammalian homologue BRUCE/Apollon (Hauser et al. 1998). However, the localization

of fusion proteins in vesicle-like structures or aggregates is very often an artifact observed after overexpression, particularly in transient expression (Moore and Murphy 2009). So far, the fusion protein could not be observed in vesicle like structures in stably transformed *Arabidopsis* plants. The cytoplasm of the *Arabidopsis* cells was only visible as a very thin line along the cell wall and the highest microscopic magnification was still not sufficient to visualize smaller cellular compartments. To prove the location of the PFU1-EGFP protein in vesicles belonging to the Trans Golgi Network, a marker protein definitely known to be present in these compartments should be coexpressed to look for colocalization of the two proteins. Several marker proteins of the Golgi Network and the endomembrane system are summarized in Geldner et al. (2009).

It is also important to keep in mind that the EGFP/mRFP fusion proteins produced for PFU1 and PFU3 in this thesis might not represent the actual properties of the native proteins in *Arabidopsis*. Due to the expression from either the 35S promoter or the β -estradiol inducible promoter it is very likely that the normal abundance of the proteins is highly exceeded in the localization experiments described in this thesis, which could change the localization pattern in the plant cell. It is therefore recommended to also analyze the localization of the proteins driven by their native expression signals including upstream and downstream sequences and introns (Moore and Murphy 2009). Apart from this, fusion of the fluorescent marker proteins to the C-terminal end of the proteins might mask special localization signals that would lead to a different localization of PFU1 and PFU3 within the cell. It would be interesting to analyze the localization of these proteins possessing a fluorescent marker either at the N-terminus or at internal sites.

It is also known that alternative splicing leads to different localization of the protein in the cell (Millar et al. 2009), which could be the case for PFU3. However, the longer PFU3 open reading frame predicted by SALK was not tested in this thesis, so nothing about whether this protein would show a different localization in the cell is known so far.

Very importantly, the functionality of the fusion proteins has not been shown yet and needs to be examined by complementation of the mutant lines described in the previous chapter. As so far no mutant phenotype is available for the *pfu3-1* mutant, functionality can in this way only be proven for the PFU1-EGFP protein.

3.3.2 PHO2 and PFU2 are restricted to the cytoplasm

The bioinformatic tools used to predict the subcellular localization of the proteins gave contradictory results for both PHO2 and PFU2. According to the WoLF PSORT program both proteins are predicted to be imported into the nucleus, whereas the Predict NLS tool only finds an import signal for PFU2 but not for PHO2. The analysis of the EGFP/mRFP fusion proteins, however, revealed that none of the two proteins is imported into the nucleus. Both *Nicotiana benthamiana* and *Arabidopsis thaliana* cells showed the same expression of PHO2 exclusively in the cytoplasm (Fig. 2.20 and 2.24). The PHO2-mRFP protein is not at all located in the nucleus. Interestingly, the protein shows a rather diffuse distribution, which indicates that it might be associated with the endomembrane system. Especially the localization pattern of PHO2-mRFP in *Arabidopsis* root cells resembles the distribution

seen for a marker protein of the endosomal membranes. An example of a root cell expressing a YFP fusion of this marker protein AtRab5/F2a (Vernoud et al. 2003) is directly compared to the localization pattern of PHO2-mRFP in Figure 3.1. Crossing of both plant lines to further analyze colocalization is still ongoing. First attempts to coinfiltrate both PHO2-mRFP and marker protein into *Nicotiana benthamiana* leaves failed, as the PHO2 fusion protein could not be detected under the microscope. This might occur because the plant is silencing one of the transgenes due to the high overexpression of the other protein.

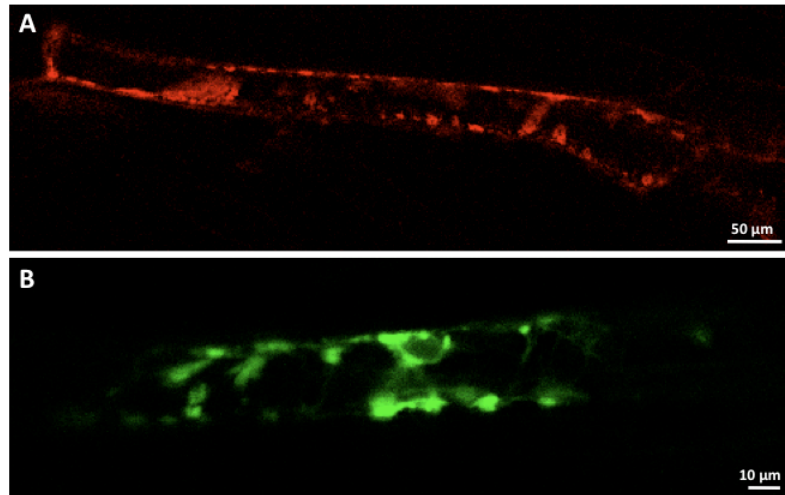


Figure 3.1: Comparison of a root cell from *Arabidopsis* plants expressing PHO2-mRFP (A) with a root cell from *Arabidopsis* plants stably transformed with pCAM-YFP-AtRab5/F2a (B, obtained from E. Nielsen, University of Michigan), which shows that both the endosomal marker protein and PHO2-mRFP exhibit the same diffuse distribution in the cell.

PFU2 could so far only be analyzed via transient expression in *Nicotiana*, as no transgenic *Arabidopsis* lines expressing either PFU2-EGFP or PFU2-mRFP in the second generation were obtained. The transformation of wild type *Arabidopsis* plants with PFU2-EGFP was repeated twice and in both cases the first generation of transformants was hygromycin-resistant whereas the second generation was not able to grow on selective plates anymore, although the presence of both hygromycin resistance and PFU2-EGFP transgene could be verified via PCR. The PFU2-EGFP fusion protein could also not be detected under the confocal microscope. This might occur because the T-DNA was inserted into a heterochromatic region that is only very lowly expressed. It is also a common observation that transgenes driven from a strong promoter are silenced by the plants. However, this usually only occurs with constitutively expressed promoters, such as the 35S promoter (Elmayan and Vaucheret 1996). Maybe, but still very unlikely, the plant is highly sensitive to expression of the PFU2 protein, so that only gametes with silenced transgene develop to seeds, even though the protein expression is under the control of an inducible promoter. Apart from this, it was already postulated in chapter 3.1.2 that PFU2 might be highly regulated at both mRNA levels and translation efficiency. It would be interesting to perform western blot analysis

with an anti-GFP antibody to analyze whether the PFU2-EGFP fusion protein is expressed at all.

However, until this problem is solved, conclusion about the subcellular localization of PFU2 can only be drawn from the heterologous system *Nicotiana benthamiana*. Both EGFP and mRFP fusion proteins showed the same expression exclusively in the cytoplasm, indicating that this is indeed the specific localization of the PFU2 protein (Fig. 2.19). Apart from this, the protein shows a relatively diffuse distribution, which indicates that it might be localized at specific structures within the cytoplasm. In the case of the PFU2-EGFP construct the protein also accumulates in vesicle-like structures, which could, as already described for PFU1, suggest that also the native PFU2 might be associated with the endomembrane system of the cell. However, vesicle-like structures could not be observed for the PFU2-mRFP protein, which is obviously expressed to a lower extent in the cell than the EGFP protein. Therefore the high accumulation in vesicle-like structures is rather occurring due to overexpression (Moore and Murphy 2009). Again this can only be verified via colocalization experiments with marker proteins.

In summary, expression of EGFP and mRFP fusion proteins both in *Nicotiana benthamiana* and in *Arabidopsis thaliana* gave consistent results for all four PFU proteins and clearly demonstrated that also on the level of subcellular localization the family can be divided into the two known subgroups. PFU1 and PFU3 on the one hand are imported into the nucleus, and PFU2 and PHO2 on the other hand are clearly completely absent from the nucleus but diffusely expressed in the cytoplasm. However, it has to be kept in mind that functionality of the fusion proteins has not been shown yet and that the results obtained in this analysis might not necessarily reflect the behavior of the PFU proteins under the control of their native promoter and without being fused to fluorescent marker proteins (Millar et al. 2009).

3.3.3 PHO2 responds to PFU1 overexpression

The pathogen treatment of the *pfu* mutant plants revealed that only the *pfu1-1 pho2-10* double mutant showed a delayed hypersensitive response (Tab. 2.7). This suggested that PFU1 and PHO2 might act in the same signaling network and it is possible that they even directly interact with each other. According to the expression of the single EGFP/mRFP fusion proteins, PFU1 and PHO2 could colocalize in the cytoplasm of the cell where both might be associated with the endomembrane system. To further analyze this putative colocalization, both strains containing PFU1-EGFP and PHO2-mRFP were coinfiltrated into *Nicotiana benthamiana* leaves.

The PFU1-EGFP protein showed the same localization in the nucleus and in the cytoplasm as described for the single infiltration experiments. Interestingly, the PHO2-mRFP fusion protein was not only present in the cytoplasm of the cells but seemed to be translocated to the nucleus (Figure 2.21). It has been described before that proteins can accumulate in one location but function in another compartment. The protein LSD1 for example is known to bind bZIP transcription factors in the cytosol, which usually act in the nucleus

to control stress responses upon oxidative stress or pathogen attack (Kaminaka et al. 2006). Also the transcription factor bZIP28 in *Arabidopsis* has been shown to be released from the ER membrane under heat stress and redistributes to the nucleus where it induces the expression of stress responsive genes (Gao et al. 2008). Therefore, it might be possible that PFU1-EGFP overexpression leads to relocation of the PHO2-mRFP fusion protein to the nucleus, where it is needed to induce the expression of genes involved in programmed cell death. This could for example be achieved via PHO2-mediated degradation of a negative regulator that inhibits the expression of these genes under normal conditions.

Unfortunately, translocation of PHO2-mRFP to the nucleus could only be observed twice. In a third and fourth coinfiltration experiment the fusion protein showed the same restriction to the cytoplasm as observed during the single infiltration. However, a confusion of the infiltrated *Agrobacteria* strains during the first experiments can be ruled out as none of the other PFU proteins, for which mRFP fusions were available (PFU2 and PFU3), showed a subcellular localization in both cytoplasm and nucleus. It was also checked several times during the first experiments with the help of λ scans under the confocal microscope that the signal observed in the nucleus with the RFP filter definitely derived from the mRFP monomer fused to PHO2 and was not observed due to an overlap of the fluorescence deriving from the PFU1-EGFP protein in these cells. One possible explanation for the differing results could be that the translocation of PHO2 to the nucleus in response to PFU1 overexpression might be highly dependent on a specific concentration of the proteins, which cannot be exactly regulated when infiltrating *Nicotiana* leaves.

The putative colocalization of PFU1 and PHO2 was also analyzed in stably transformed *Arabidopsis* plants. A plant line expressing the PFU1-EGFP transgene was crossed with plants bearing the PHO2-mRFP construct. Analysis of the F2 and F3 generation under the microscope revealed that the PFU1-EGFP protein is, as observed before, located in both nucleus and cytoplasm, whereas the PHO2-mRFP protein could not be detected at all. Interestingly, expression of the PHO2-mRFP transgene could be verified via RT-PCR (Fig. 2.25). This suggests that either the translation of the protein is highly regulated or the protein is downregulated on the posttranslational level. Whatever leads to decreased levels of PHO2-mRFP is directly connected to coexpression with PFU1-EGFP, as the PHO2-mRFP protein can be detected in plants expressing only the PHO2-mRFP transgene. It is possible that the PFU1 overexpression leads to proteasomal degradation of PHO2 and that ubiquitylation of PHO2 might be directly mediated by PFU1. Analysis of a putative interaction of PHO2 and PFU1, for example via FRET assays, might therefore be difficult with a functional PFU1 protein. It would be interesting to compare the protein levels of PHO2-mRFP in plants expressing both PFU1 and PHO2 with plants expressing only the PHO2-mRFP transgene on a western blot with an antibody specific for mRFP.

However, it cannot be excluded that PHO2 is regulated on the posttranscriptional level and that the transcript detected in the RT-PCR might be unstable. Expression of both PFU1-EGFP and PHO2-mRFP in plants that are impaired in posttranscriptional silencing, such as *rdr6* mutants lacking an RNA-dependent RNA polymerase responsible for the biogenesis of small interfering RNAs (Vaucheret 2005), might help in answering this question. Crossings of plants bearing both transgenes with an *rdr6* mutant line are ongoing.

In summary, both the observations made with stably transformed *Arabidopsis* lines bearing the PFU1-EGFP and the PHO2-mRFP transgene and the coinfiltration experiments performed in *Nicotiana benthamiana* underline the hypothesis that the PHO2 protein might somehow be regulated by PFU1. Still, whether this leads to degradation of the PHO2 protein or translocation into the nucleus cannot be answered yet. Therefore, the putative interaction of PHO2 with PFU1 was further analyzed in this thesis via yeast two hybrid experiments and co-immunoprecipitation assays with recombinant proteins.

3.4 Molecular analysis of PFU1 and PHO2 via expression in yeast

Protein-protein interactions are essential for virtually all cellular processes and are of immense importance for a proper function of the ubiquitylation machinery in the cell. Identification of interactors of the PFU proteins was intended to further analyze function and molecular mechanism of the proteins. Especially the nature of a putative interaction between PFU1 and PHO2 was of main interest during this thesis, as both mutant phenotypes and subcellular localization analysis indicated that PFU1 and PHO2 act in the same signaling pathway and PFU1 seems to have an impact on the regulation of PHO2.

Since decades the yeast two hybrid system (Fields and Song 1989) is one of the main techniques to identify interactions between eukaryotic proteins and has been improved to be better applicable also for plant proteins (Causier and Davies 2002). It is, compared to other techniques, not very labor-intensive or time-consuming, as the life cycle of yeast cells is with approximately two hours relatively short and the cells are easy to cultivate and store. Therefore the heterologous system *Saccharomyces cerevisiae* was chosen to further analyze the molecular interaction of PFU1 and PHO2.

However, while discussing the results obtained for the PFU proteins in yeast, it should always be kept in mind that, although *Arabidopsis thaliana* and *Saccharomyces cerevisiae* are both eukaryotic organisms, "plant cells are not just green yeasts" (Bassham and Raikhel 2000). Differences in membrane composition and structure and the differences in protein modification pathways in yeast might modulate the function of the PFU proteins. In particular, proteins or other molecules interacting with the PHO2 family members and contributing to their specific functions *in planta* are absent in yeast, whereas other proteins belonging to the ubiquitylation machinery of the yeast cell might interact and in doing so change the native properties of the PFU proteins. In addition, as pointed out above, interaction of the PFU proteins might also involve posttranslational modifications such as disulfide bonds, phosphorylation or glycosylation, which cannot or only inefficiently be performed in the yeast cell (Van Crielinge and Beyaert 1999).

Despite all of these disadvantages, expression of the PFU proteins in the heterologous system *Saccharomyces cerevisiae* still was a generator of several hypotheses concerning both putative interactions and functionality of the PFU proteins, and helped in designing future experiments to further investigate these ideas.

3.4.1 Auto-activity of PHO2 and PFU1: a new assay to test functionality?

The principle of the standard yeast two-hybrid assay is based on the reassembling of a functional transcription factor, which in eukaryotes usually exhibits two specific functional domains. One domain is responsible for targeting of the protein to a specific DNA sequence and the other is needed for transcriptional activation (Fields and Song 1989). The bait protein in a yeast two hybrid screen is fused to the DNA-binding domain, whereas the prey protein exhibits the activation domain. Binding of bait and prey protein then leads to reconstitution of the complete transcription factor, which activates the transcription of a reporter gene. Before testing for interaction of the two proteins it is therefore crucial to check for the ability of the bait protein fused to the DNA-binding domain to auto-activate the reporter gene. It has been described that about 10 % of randomly generated cDNAs exhibit auto-activation when fused to a DNA-binding domain (Fashena et al. 2000).

Unfortunately, also PHO2 and PFU1 were shown to auto-activate the *HIS3* reporter gene when fused to the DNA-binding domain of the GAL4 transcription factor (Traven et al. 2006). Yeasts expressing these fusion proteins were in contrast to the empty strain able to grow on plates lacking histidine (Fig. 2.27).

Truncation of specific domains that mediate auto-activation is the easiest way to circumvent this problem (Causier and Davies 2002), but often results in loss of interesting interactions in a subsequent yeast two hybrid screen. Therefore, first, only minor changes in the PFU proteins were tested to change the auto-activity.

Both PHO2 and PFU1 contain a highly conserved UBC domain typical for ubiquitin conjugating enzymes. The conserved cysteine residue of this domain is known to be essential for the thioester formation with ubiquitin, and mutation of this residue completely abolishes E2 function. This has for example been shown for the E2 UBC22 in *Arabidopsis thaliana* where exchange of the catalytic cysteine residue to alanine resulted in a complete loss of protein ubiquitylation (Kraft et al. 2005). However, impeding the catalytic function of either PHO2 or PFU1 by changing the catalytic cysteine residue of the UBC domain to alanine did not inhibit the auto-activation of the proteins at all. In contrast, both DBD-PFU1UBCCtoA and DBD-PHO2UBCCtoA constructs rather showed better growth on plates lacking histidine, although growth of non-mutated and mutated proteins was nearly similar on the control plate (Fig. 2.27). This suggests that loss of function results in an increased auto-activity of the proteins.

Interestingly, also mutation of the highly conserved cysteine residue in the C-terminal domain of both PHO2 and PFU1 resulted in the same increased auto-activity as observed for the UBCCtoA mutants. This observation raises the following hypothesis: If a CtoA mutation in the C-terminal domain has the same effect on the auto-activity as the CtoA mutation in the UBC domain, does it also influence the functionality of the protein and is therefore directly involved in ubiquitylation of the proteins?

To further analyze this idea, first the amount of PFU1 and PHO2 transcript has to be determined in yeast cells exhibiting both the mutated and the wild type protein via RT-PCR. It is possible that the wild type transcript is expressed at a lower level either due to a lower

replication rate of the plasmid or due to effects on mRNA stability. If this is not the case, it would be interesting to analyze the amount of mutant and wild type protein on a western blot with an anti-GAL4 antibody. One explanation for the decreased levels of wild type protein might be that the functional PHO2 or PFU1 protein is able to ubiquitylate itself leading to proteasomal degradation and therefore lower auto-activity of the reporter gene. Auto-ubiquitylation independent of an E3 ligase has already been shown for a number of *Arabidopsis* ubiquitin conjugating enzymes *in vitro* (Kraft et al. 2005), and also for certain animal E2 enzymes (Hoeller et al. 2007). Moreover, PFU proteins most probably combine E2 and E3 function in one protein, as observed for the closest mammalian homologue E2-230K (Berleth and Pickart 1996). This makes auto-ubiquitylation even more likely. Always assuring equal transcript levels, the test for auto-activity of the proteins could in this way even be used to further analyze the functionality of PHO2 and PFU1 under different growth conditions for example during oxidative stress or treatment of the yeast cells with nitric oxide.

3.4.2 Putative interaction of PHO2 and PFU1 might be highly regulated

The test for auto-activity of PHO2 and PFU1 revealed that both proteins are able to induce expression of the *HIS3* reporter gene already in the absence of a prey protein fused to an activation domain. The CtoA mutants also showed auto-activity, so that a standard yeast two hybrid assay to check for the interaction of PFU1 and PHO2 was not possible with the full length proteins. As truncation of the auto-activating domains of the proteins very often leads to loss of putative interaction domains, it was decided in this thesis to test the full length proteins PFU1 and PHO2 in a repressed transactivator two hybrid system (Hirst et al. 2001). In this system the prey proteins are fused to the TUP1 repressor protein, which is known to interact with histone H3 and H4 tails and suppresses transcription by reorganizing nucleosomes (Huang et al. 1997). Apart from this, TUP1 has also been described to change the activity of the RNA polymerase II and with this represses transcription (Kuchin and Carlson 1998). Therefore, fusion of the TUP1 repressor protein to the putative prey protein can be used to identify an interaction with an auto-activating protein fused to an DNA-binding domain.

In the case of this thesis, GAL4-DBD and TUP1 fusion proteins were tested with the reporter gene *HIS3*, so interaction of the bait and prey proteins would lead to repression of yeast growth on plates lacking histidine. Indeed, when comparing cells exhibiting solely the DBD-PHO2 constructs with cells containing DBD-PHO2 and either TUP1-PHO2 or TUP1-PFU1, the cells containing the TUP1 fusion proteins showed repression of the *HIS3* gene and were not able to grow on plates lacking histidine anymore (Fig. 2.29).

This clearly suggests that PHO2 is able to form homodimers with a second PHO2 protein and heterodimers with PFU1 and indicates that the regulation of PHO2 by PFU1 observed during the subcellular localization analysis might be mediated via direct interaction of the two proteins.

However, it still had to be tested whether the reduction of yeast growth is occurring due to repression of the reporter gene and not due to reduced levels of auto-activating bait protein in the cells bearing both DBD- and TUP1 fusion proteins. Therefore the amount of DBD-PHO2 protein was analyzed via western blot with an anti-GAL4 antibody (Fig 2.31). The results clearly demonstrate that the amount of DBD-PHO2 is equal in all yeast strains tested, indicating that the reduced growth of strains containing both DBD- and TUP1 fusion proteins is not occurring because of lower expression of auto-activating PHO2. Apart from this, the results of the western blot also show that at least in yeast cells coexpression with PFU1 does not result in proteasomal degradation of PHO2. It is possible that PFU1-mediated degradation of PHO2 is dependent on specific compounds that are present in *Arabidopsis* but absent in *Saccharomyces cerevisiae*, which lacks homologues of PHO2.

Unfortunately, the formation of homo- and heterodimers of PHO2 with a second PHO2 protein and PFU1, respectively, could not be verified in a second attempt with yeast cells from an independent transformation. The cells bearing both DBD-PHO2 and TUP1 fusion constructs were able to grow very nicely on plates lacking histidine showing no repression of the reporter gene at all (Fig. 2.30).

To further analyze these contradictory results, the TUP1 fusion protein levels of yeast cells obtained during the first transformation were compared to the levels in yeast cells taken from the second transformation on a western blot detected with an anti-TUP1 antibody (Fig. 2.31). Although predicted to have only a size of 22 kDa, the single TUP1 protein fragment encoded by pGAD-TUP1 could be detected well for cells exhibiting the empty vector at a height of about 42 kDa. This is consistent with the finding that the full-length TUP1 protein has been described to run at 99 kDa instead of the predicted 78 kDa (Williams et al. 1991), showing the same shift of about 20 kDa as observed for the smaller TUP1 fragment in this thesis. One explanation for this shift given by Williams et al. (1991) is a putative posttranslational modification of the protein such as addition of a carbohydrate. However, they also mention that the same shift can be observed in *E. coli* suggesting that it rather occurs due to specific properties of the primary sequence of the protein.

The yeast cells transformed with the TUP1-PHO2/PFU1 fusion constructs also only show the band corresponding to the single TUP1 protein fragment (Fig. 2.31). Neither the band of TUP1-PFU1 with a predicted size of 90 kDa (TUP1 band shift not included) nor the TUP1-PHO2 with a predicted size of 120 kDa were visible on the western blot. This suggested that the TUP1 fusion proteins are not properly expressed in the cells. However, sequence analysis clearly demonstrated that expression of the constructs should result in complete TUP1 fusion proteins in the yeast cells. A second explanation for the lack of bands corresponding to the fusion proteins would be that the TUP1 fragment is cleaved from PHO2 and PFU1 by proteases during lysis of the yeast cells. This would mean that the amount of TUP1 fragment detected on the blot directly corresponds to the amount of PHO2 or PFU1 before cell lysis.

Interestingly, the yeast cells obtained in the first transformation show a more intense TUP1 band than the cells from the second transformation, suggesting that the latter express less TUP1 fusion protein. This would explain why the interaction of PHO2 and PFU1 could not

be detected in the second test. The results obtained from co-expression of PHO2-mRFP and PFU1-EGFP in *Nicotiana benthamiana* already suggested that the impact of PFU1 on PHO2 might be dose-dependent. Therefore, also the interaction of both proteins in yeast might be highly regulated and the amount of TUP1 fusion protein in cells obtained in the second transformation might just not be enough to initiate interaction between PFU1 and PHO2.

The different expression levels of TUP1 fusion proteins in cells taken from the first and cells obtained in the second transformation might be explained by the fact that in the first transformation the DBD- and TUP1 constructs were simultaneously transformed into the empty yeast strain. In contrast, the cells of the second test were sequentially transformed first with the DBD construct and afterwards with the TUP1 plasmid. This could result in a lower number of copies of the TUP1 construct in cells obtained in the second transformation. Both the DBD and the TUP1 plasmid contain the same origin of replication and therefore need the same replication machinery. The first plasmid transformed into the cell, in this case the DBD construct, might have been replicated several times with the maximum replication rate. In contrast, the second plasmid introduced into the cell, the TUP1 construct, could not use the whole replication machinery, so that the amount of DBD plasmid copies always exceeded the amount of TUP1 plasmids. In the simultaneous transformation, however, the replication rate for both plasmids was nearly the same.

To prove this hypothesis, a second attempt to check for interaction of the proteins with cells simultaneously transformed with DBD- and TUP1 constructs should be performed. Apart from this, the transcript levels of the TUP1 fusions in yeast cells of the first and second yeast two hybrid test described in this thesis should be analyzed via RT-PCR experiments to determine whether the loss of interaction in the second test occurred due to a lower expression of the TUP1 fusion proteins. To completely circumvent the problem of less TUP1 plasmid copies in the cell, it would be possible to introduce the first construct on a centromeric vector, so that the TUP1 plasmid could use the whole replication machinery (Baruffini et al. 2009).

In summary, as observed for the co-localization analysis *in planta*, also the repressed transactivator two hybrid experiments performed in this thesis only indicate an interaction between PHO2 and PFU1 and suggest that this interaction is highly regulated. However, an interaction could not be definitely proven and further yeast two hybrid assays and *in vitro* co-immunoprecipitation experiments with PHO2 and PFU1 protein fragments are needed to finally answer this question.

3.4.3 C-terminal domain not sufficient for interaction

Instead of using the repressed transactivator two hybrid system, the auto-activating DBD fusion constructs can also be changed in such a way that the transactivation of the reporter gene is decreased and also a standard yeast two hybrid assay (Fields and Song 1989) with the prey protein fused to a GAL4 activation domain can be applied. It has been shown that, instead of using a C-terminal fusion to the DBD, an N-terminal fusion can completely change the behavior of the proteins in yeast and that these constructs even possess an

increased sensitivity for specific interaction partners (Beranger et al. 1997). Therefore, it would be interesting to also analyze PFU1 and PHO2 fused to the N-terminus of the GAL4 DNA-binding domain. This might change the auto-activity of the proteins or unmask specific regions that are necessary for the interaction with other cellular components.

Apart from this, it is also possible to delete a small region of a protein that activates transcription (Van Criekinge and Beyaert 1999). The C-terminal domain of the PFU proteins has been described to possess the highest ability for interaction with other proteins according to the meta-structure analysis (Konrat 2009) performed by Dr. R. Konrat. Testing for auto-activity demonstrated that the C-terminal fragments only show very weak activation of the *HIS3* reporter gene when fused to a DNA-binding domain (Fig. 2.32). Therefore, a standard yeast two hybrid assay was performed in this thesis analyzing the putative interaction of only the C-terminal domains of PHO2 and PFU1.

The experiments revealed that the C-terminal domains of PFU1 and PHO2 are not able to form heterodimers, as the cells bearing both the DBD-PFU1CT and the AD-PHO2CT constructs are not activating the *HIS3* reporter gene (Fig 2.32). Homodimerization of two C-terminal domains of PFU1 could also not be detected. However, these findings do not rule out that PFU1 and PHO2 are able to interact with each other. It is possible that the C-terminal domain of these proteins is just not sufficient and that also the N-terminal part might be needed to mediate interaction. Many transcription factors have been described to interact with other proteins via the same domain that is also responsible for the transcriptional activation (Hirst et al. 2001). Interaction between the transcription factor c-myc and the tumor suppressor protein Bin1 for example is mediated by the transactivation domain of c-myc (Elliott et al. 1999).

Apart from missing important interaction domains, it might also be possible that the C-terminal domain has to undergo a specific modification first before the protein fragments are able to interact. PFU1 and PHO2 have been both shown to be sensitive to oxidative stress. It is therefore possible that a specific ROS-related modification of the proteins is needed for interaction. This was for example shown for the glyceraldehyde-3-phosphate dehydrogenase, which only interacts with p54nrb (54 kDa nuclear RNA-binding protein) if it is oxidized at a specific cysteine residue (Hwang et al. 2009). The highly conserved cysteine residue in the C-terminal domain of the PFU proteins could be such a site for oxidative modification. It would therefore be interesting to analyze the interaction of PFU1 and PHO2 in yeasts grown under oxidative conditions. As this can be, to some extent, toxic for the cells, the interaction of the two proteins should also be analyzed *in vitro* by producing recombinant proteins and performing co-immunoprecipitation experiments under oxidative conditions.

Apart from further analyzing the interaction of PFU1 and PHO2 in yeast, the C-terminal fragments fused to the DNA-binding domain of GAL4 could also be used as a bait protein in screening a complete cDNA library of *Arabidopsis thaliana* in a standard yeast two hybrid assay to identify other putative interactors. Also the full length fusion proteins DBD-PFU1 and DBD-PHO2 can be used in a larger screen. However, this would be more time-consuming, as the complete cDNA library would first have to be fused to the repressor protein TUP1. It would also be interesting to test the CtoA mutants of PFU1 and PHO2 in

these screens, as substrates of the PFU proteins that are usually degraded by the proteasome might then be stabilized. Screening a complete *Arabidopsis* cDNA library would in any case be helpful to further characterize the role of PFU1 and PHO2 in *Arabidopsis thaliana*.

3.5 Biochemical analysis of recombinant PFU proteins

Analyzing the functionality of the PFU proteins *in vivo* has several advantages compared to *in vitro* experiments. The living cell is an open system always exchanging nutrients and other molecules with the environment. A variety of regulatory pathways control an enzymatic reaction *in vivo*, whereas *in vitro* assays are closed systems lacking most of these regulatory mechanisms. While performing *in vitro* experiments with the PFU proteins, it should therefore always be kept in mind that the behavior of the proteins does not need to represent the actual function *in vivo*. The tumour suppressor p14ARF for example has been shown to inhibit ubiquitylation of the E3 ligase Mdm2 *in vitro* but did not reduce the ubiquitylated form of Mdm2 *in vivo* (Xirodimas et al. 2001).

However, the functional analysis of the PFU proteins *in planta* can reach certain limitations that might be overcome with the help of *in vitro* experiments. As described above, the interaction between PFU1 and PHO2 could so far not be definitely proven via *in vivo* experiments. This might occur due to specific regulatory steps that are either absent or inhibiting this reaction under the tested growth conditions. Testing for interaction of PFU1 and PHO2 *in vitro* via co-immunoprecipitation experiments offers the possibility to easily change the conditions inside the test tube. Addition of oxidative compounds to the reaction or site-directed mutagenesis of the proteins might help to finally achieve clear results.

Apart from this, *in vitro* thioester formation and ubiquitylation assays are by now common techniques to verify the functionality of ubiquitin conjugating enzymes (Kraft et al. 2005). So far, thioester formation with ubiquitin could not be shown for the PHO2 family of ubiquitin conjugating enzymes in *Arabidopsis*.

The first step to analyze the functionality of the PFU proteins *in vitro* is the production of recombinant proteins or protein fragments. These recombinant proteins can then also be used to solve the three-dimensional structure of unknown protein domains, which might help to understand more about the specific properties of the PFU proteins. However, first a high amount of soluble protein had to be obtained for such a structural analysis.

3.5.1 A long road to success: how to obtain soluble PFU protein fragments

The C-terminal domain of the PFU proteins was of special interest in this thesis, as it is conserved in all four family members and throughout the whole plant kingdom. It has been identified by the meta-structure analysis to possess the highest probability for interaction with other protein domains and exhibits a highly conserved cysteine residue that might be functionally relevant according to the yeast experiments. Therefore analysis of the so far unknown three-dimensional structure of this domain via NMR spectrometry

or crystallization might help in identifying new properties of the PHO2-like protein family. High amounts of soluble protein are needed for such an analysis, and overexpression in *Escherichia coli* is considered to be the best way to achieve large quantities of recombinant protein (Liu et al. 2006).

However, when purifying the overexpressed C-terminal domain of PFU1 fused to a His-tag and starting with aa 487 (PFU1CT487), most of the protein fragment was lost due to insolubility (Figs. 2.39 and 2.40). Obviously the high-level overexpression of the PFU1CT487 protein fragment leads to accumulation in insoluble aggregates called inclusion bodies (Singh and Panda 2005). About 80 % of the known non-membrane proteins cannot be used for structural analysis due to very low solubility (Trevino et al. 2007). Therefore a variety of strategies to increase solubility of recombinant proteins have been described to date. However, although recommended (Makrides 1996), overexpression of the PFU1CT487 protein at a lower temperature such as 20 °C or changing the growth media by adding less IPTG for induction did not result in higher amounts of purified protein.

It has also been described that changes in the three-dimensional structure of the protein via site-directed mutagenesis might alter the solubility of the protein (Smialowski et al. 2007). As the structure of the C-terminal domain is not yet known, the sequence of the protein fragment was randomly changed by altering the start point of the protein. However, this apparently did not increase the solubility of the PFU1 fragment either (Fig. 2.41, panel A), although a bioinformatic tool calculating the probability of insolubility (<http://www.biotech.ou.edu/>) predicted that the smaller fragments PFU1CT499 and PFU1CT501 possess a much lower probability value of around 50 % compared to the longer fragment PFU1CT487 with around 70 %. This again demonstrates the limits of bioinformatic approaches, which can only be useful to generate hypotheses.

Biochemical tools to easily analyze the solubility of different protein fragments might be more helpful. One of these biochemical assays uses the dihydrofolate reductase gene (DHFR) as a fusion reporter to analyze solubility. The more soluble the target protein fused to DHFR, the higher is the resistance of the *E. coli* cells to the antibiotic trimethoprim (Liu et al. 2006). This would be a good tool to further analyze the solubility of the C-terminal domain of the PFU proteins and might also help to identify specific residues that are responsible for insolubility via site-directed mutagenesis. It has been shown that for example asparagine, glutamine or threonine should be changed to aspartic acid, glutamic acid or serine, as this very often increases protein solubility (Trevino et al. 2007). A first analysis of the soluble fraction of cells expressing the CtoA mutant fragments of the C-terminal domain on a Coomassie stained gel did not reveal an increased solubility (data not shown), suggesting that the conserved cysteine residue is not responsible for the insolubility of this domain. Apart from changing the protein fragment itself, fusion of the target protein to different tags has been reported to increase solubility of recombinant proteins (Davis et al. 2000). When testing smaller tags such as Flag-tag and Strep-tag, the solubility of the C-terminal domain of PFU1 was not obviously improved (Fig. 2.41, panel B). In contrast, when fused to larger tags, such as SUMO or glutathione S-transferase (GST), the amount of recombinant protein purified from *E. coli* was slightly increased (Fig. 2.41, panel C). This is consistent with the fact that fusions to larger protein tags such as the glutathione S-transferase (GST) or the

maltose-binding protein (MBP) have been described to increase the solubility of proteins in *E. coli* (Smith and Johnson 1988; di Guana et al. 1988). However, the amount of soluble protein was still not enough to be used for an NMR analysis.

Therefore a different strategy was applied by solubilizing the protein from the inclusion bodies under strongly denaturing conditions, in this case 8 M urea. The urea concentration was afterwards lowered to 1 M via dialysis to allow refolding of the protein. However, after dialysis the complete protein amount was aggregated, leaving no soluble fraction at all (Fig. 2.42). It has been described by London et al. (2005) that the amount of refolded tryptophanase is the lowest when refolding is performed at intermediate denaturing conditions, such as 2 to 4 M urea. During dialysis the PFU1CT protein fragment was exposed to such intermediate denaturing conditions for a long period of time, which might have impeded folding and rather supported aggregation of the protein. Dialysis might therefore not be the best method to obtain properly refolded soluble protein. Instead, quick dilution of the denatured protein in a buffer containing no urea but specific sulfobetaines, shown to stabilize the protein and therefore increase refolding, might help in obtaining higher amounts of soluble PFU1CT from inclusion bodies (Vuillard et al. 2001). Apart from this, addition of glutamate and arginine to the refolding buffer has also been shown to prevent aggregation and precipitation of the protein (Golovanov et al. 2004).

Although a structural analysis could not be performed with the single C-terminal domain of PFU1, the low protein amounts purified under native conditions could still be applied in co-immunoprecipitation experiments to find out more about the putative interaction between PFU1 and PHO2. Therefore also soluble protein fragments of PHO2 had to be produced in *Escherichia coli*. All attempts to overexpress only the C-terminal domain of PHO2 failed (Fig. 2.38), possibly because this protein fragment might be very short-lived in *E. coli* cells when expressed without other domains of the PHO2 protein.

In contrast to the single C-terminal domain of PHO2, high overexpression could be detected for the larger PHO2 fragments bearing both the UBC domain and the C-terminal part (Fig. 2.38). However, the solubility of the protein was also very low when fused to a single His-tag (Fig. 2.43). This could be explained by the fact that addition of the UBC domain might stabilize the C-terminal domain of PHO2 so that the protein can be overexpressed but it is highly insoluble still.

This insolubility mainly occurs due to the presence of the C-terminal domain because the single UBC domain of PHO2 could be purified under native condition to a higher extent than the UBCCT fragment (Fig. 2.43). Apart from this, also the fusion of the single UBC domain to a GST-tag might contribute to its higher solubility. Still, the elution steps obtained for the UBC domains of both PFU1 and PHO2 revealed that the protein fragments might have been cleaved by proteases during purification, as several additional bands with lower molecular weight appeared on the western blot. Although purification was repeated several times with 1 mM DTT, 1 $\mu\text{g}/\text{ml}$ aprotinin and 1 $\mu\text{g}/\text{ml}$ leupeptin, which usually inhibit proteases, these bands were still visible. This suggested that the proteins are highly unstable and that maybe higher amounts of protease inhibitor are needed during purification to inhibit proteolysis of the UBC fragments. Apart from this, expression and purification of these proteins in a cell-free *in vitro* system, such as wheat-germ, might also

decrease protein degradation via cellular proteases and increase the yield of soluble protein (Endo and Sawasaki 2006). However, the purified fractions of the UBC domains of PFU1 and PHO2 could still be applied in *in vitro* thioester formation assays to analyze the E2 function of the proteins.

For co-immunoprecipitation experiments with PFU1 and PHO2 also a soluble fragment containing the C-terminal domain of PHO2 was needed. Therefore the PHO2UBCCT construct shown to be relatively insoluble when only fused to a His-tag (Fig. 2.43) was further modified. Fusion to the GST-tag was shown to slightly increase the solubility of the C-terminal domain of PFU1. Therefore the protein fragments of PFU1 and PHO2 bearing both UBC and C-terminal domain were also tagged with GST. Apart from that PFU1 was fused to a Strep-tag, whereas a Flag-tag was added to the PHO2 fragment to facilitate the Co-IP experiments. In addition, proline residues were chosen as the start point of the protein fragments, because this amino acid functions as a structural disruptor. Therefore it often marks the borders of a structural domain, which might improve the solubility of the proteins. Whereas the solubility of the PFU1UBCCT fragment was only slightly improved, this combination of different strategies to increase protein solubility finally resulted in a highly soluble recombinant protein fragment of PHO2 (Fig. 2.44), which can be used in future co-immunoprecipitation experiments and thioester assays. It could be even purified to such a high extent that the three-dimensional structure of this protein containing both the UBC and the C-terminal domain can now be analyzed via crystallization.

3.5.2 Co-IP and functionality assays still in the fledgling stages

Insolubility of proteins and aggregation in inclusion bodies have been described to be one of the major bottlenecks in biochemical analysis (Ventura 2005). This turned out to be true also in the case of the PFU proteins. Until the highly soluble PHO2UBCCTlong fragment was identified, biochemical assays such as co-immunoprecipitation experiments and thioester formation had to be performed with the relatively insoluble protein fragments. Therefore only preliminary results of Co-IP and functionality tests can be discussed in this thesis.

In a first Co-IP experiment the PHO2UBCCT fragment bearing a single His-tag was immobilized on Ni-NTA agarose beads after incubation with PFU1CT499Strep. The putatively binding PFU1 fragment was afterwards detected on a western blot with a Strep-Tactin-AP conjugate (Fig. 2.45, panel A). In addition, a negative control lacking the PHO2UBCCT fragment in the reaction was also analyzed on this western blot and revealed that the C-terminal domain of PFU1 can still be detected also in the absence of the PHO2 domains. This suggested that the PFU1CT499Strep is non-specifically binding to the agarose beads, which is a common problem in immunoprecipitation experiments. It could be decreased by using more stringent washing steps for a longer period of time and adding detergents such as Triton-X 100 or Tween-20. Apart from this, PFU1CT499Strep protein might also remain because of improperly removing the washing buffer from the tubes. This problem was avoided by the use of Dynabeads Talon in a second Co-IP attempt (Fig. 2.45, panel B). The magnetic beads can be washed much easier and show according to

the manufacturer's manual less non-specific binding of proteins. The amount of remaining PFU1CT499Strep protein was less but still detectable in the negative control, suggesting that the protein fragment is very sticky and might only detach from the beads after very stringent washing steps. In addition, a third Co-IP attempt testing the interaction of the PFU1CTStrepHis fragment with the soluble PHO2UBCCTlong protein underlined the finding that these proteins seem to be extremely sticky, as again the negative control showed remains of PHO2UBCCT protein (Fig. 2.45, panel C).

In summary, these first Co-IP attempts could not answer the question whether PHO2 and PFU1 are able to interact with each other. However, in all three cases the band detected in the negative control was slightly less intense than the reaction containing both proteins, suggesting that an interaction might take place. Immunoprecipitation experiments with more stringent washing steps might decrease the unspecific background in the negative control. An obvious increase in the band detected for the reaction containing both PFU1 and PHO2 would also solve the problem and might be achieved by the addition of oxidative reagents such as hydrogen peroxide to the test tube.

To further analyze the functionality of the PFU proteins the relatively crude extracts obtained for the UBC domains of PHO2 and PFU1 were tested in a thioester assay. However, these experiments did not reveal any thioester linkage formation with ubiquitin (Fig. 2.46). This could be explained by the fact that the crude protein extracts might have contained many contaminating proteins inhibiting the reaction and that the PFU proteins might have been damaged by proteolytic degradation, as lower molecular weight bands occurred on the western blot after purification (Fig. 2.43). Apart from that, the single UBC domain of the proteins might not be sufficient to perform the thioester reaction with ubiquitin or instead of the human E1 enzyme an *Arabidopsis* E1 is necessary for thioester formation. Another explanation would be that the PHO2 family of ubiquitin conjugating enzymes are not responsible for ubiquitylation of proteins but are forming thioester linkages with ubiquitin-like proteins such as NEDD8/Rub1. This protein modifier possesses 57 % sequence similarity with ubiquitin and has even been shown to be activated by the ubiquitin-activating enzyme and to be transferred to the human ubiquitin-conjugating enzyme E2-25K *in vitro* (Whitby et al. 1998). However, it is relatively unlikely that the PFU proteins are NEDD8/Rub1-conjugating enzymes, as the mammalian homologues E2-230K/UBE2O and BRUCE/Apollon both have been shown to be functional ubiquitin E2s and even bear E3 function (Berleth and Pickart 1996; Bartke et al. 2004).

Kraft et al. (2005) already described the functionality of the majority of the putative ubiquitin E2s in *Arabidopsis thaliana*. However, their analysis of the PHO2 family of ubiquitin conjugating enzymes revealed that PFU1 and PHO2 were completely insoluble when fused to only a His-tag and were therefore not tested in the thioester or ubiquitylation assays. This underlines the findings on the solubility of the proteins obtained in this thesis. In contrast, PFU3 was purified from *Escherichia coli* but only tested for its ability of autoubiquitylation, which was negative. PFU2 was not tested, as a cDNA for this protein was not available in the RIKEN repository and has been cloned for the first time in this thesis. Therefore the analysis performed by Kraft et al. (2005) did not prove the functionality of the PFU proteins at all.

A first step to solve this problem has been made in this thesis by designing the highly soluble PHO2UBCCTlong fragment, which can now be intensively analyzed in *in vitro* ubiquitylation and thioester formation assays under different conditions.

3.6 A first model summarizing the results of this thesis

So far, only for one member of the PHO2 family of ubiquitin conjugating enzymes, PHO2, a function during the phosphate signaling pathway of *Arabidopsis thaliana* could be identified (Bari et al. 2006). This thesis represents a first analysis of the molecular properties of all four family members and reveals a completely new function of the proteins in the regulation of plant programmed cell death in response to abiotic and biotic stresses.

Three members of the family, PHO2, PFU2 and PFU1, have been clearly demonstrated to control the cell death occurring in response to inhibition of the ubiquitin-proteasome system, which induces both fast cell death processes and symptoms typical for senescing plant tissues. The finding that the double mutant *pfu1-1 pho2-10* shows a delayed hypersensitive response suggested that these two proteins might function in the same signaling pathway, which is underlined by the fact that both proteins are able to sense oxidative signals induced by ozone treatment. In contrast, the PFU2 protein is able to sense nitric oxide signals. Both reactive oxygen species (ROS) and reactive nitrogen species (RNS) have been shown to accumulate and regulate programmed cell death events in plants. Figure 3.2 shows a putative mechanism of how the PFU proteins might sense and transmit ROS/RNS signals during programmed cell death induction on the molecular level.

The subcellular localization of the four members could be identified in this thesis. The larger members of the protein family are completely restricted from the nucleus but are located in the cytoplasm and might be associated with the endomembrane system. In contrast, the smaller members PFU1 and PFU3 are located in the nucleus. Apart from this, a diffuse expression in the cytoplasm resembling the localization of the two larger family members has also been detected for PFU1. Several results indicated that PFU1 and PHO2 are able to interact. In addition, yeast experiments suggested that the proteins are also able to form homodimers. However, interaction seems to be highly regulated and might be needed for a proper function of the proteins during PCD induction.

Therefore the model suggests that under normal conditions the PFU proteins are inactive as monomers. A specific domain of the proteins might function as an autoinhibitory domain. It has been for example demonstrated for the HECT-type ubiquitin ligase Smurf2 that the N-terminal domain C2 interacts with the HECT domain and therefore inhibits the activity of the enzyme (Wiesner et al. 2007). This mechanism regulates not only the ubiquitylation of other substrates but also the autoubiquitylation and degradation of the protein itself. The C-terminal domain of the PFU proteins shows the highest probability of interacting with other protein domains or structures. It also possesses a highly conserved cysteine residue, which might be functionally relevant and could be a site for modification via oxidative signals or S-nitrosylation. Therefore, the C-terminal part of the PFU proteins is a good candidate for such an autoinhibitory domain. Regulation of the proteins via

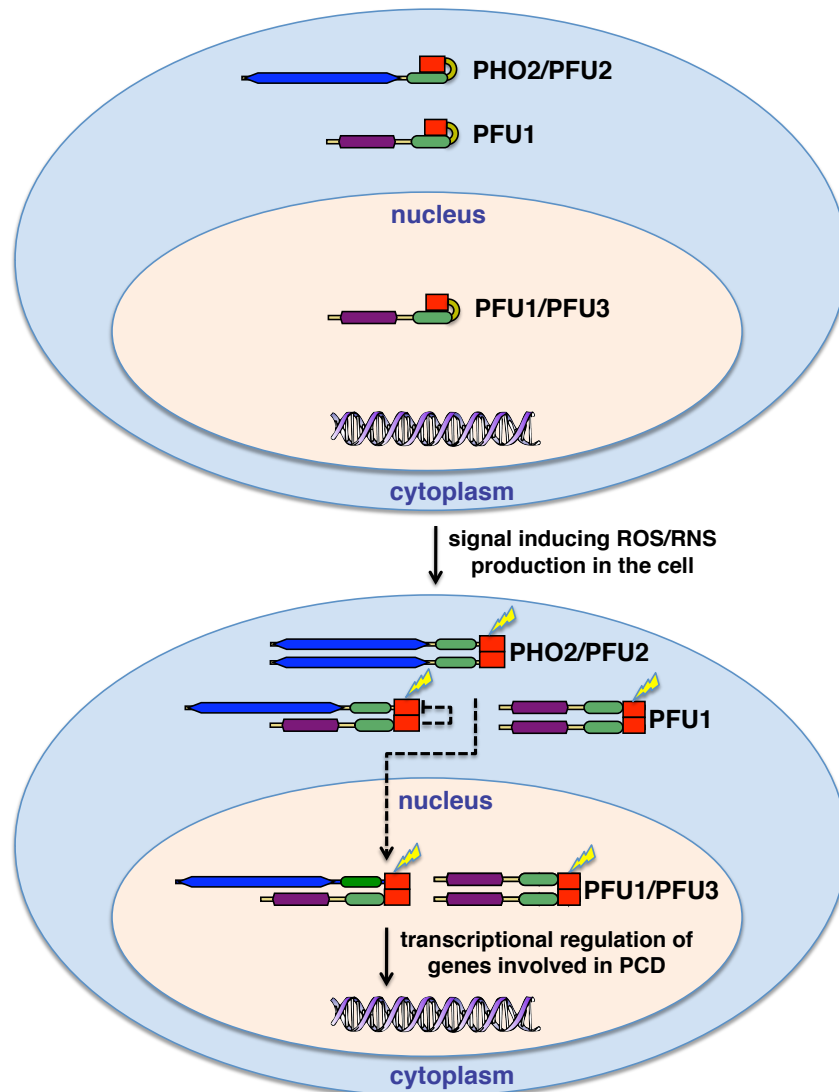


Figure 3.2: A first model of a putative molecular mechanism of the PFU proteins summarizing the results and hypotheses obtained in this thesis. The upper panel demonstrates the putative properties of the PFU proteins before accumulation of ROS/RNS signals in the cell. The proteins might be autoinhibited via the C-terminal domain and are present as monomers. ROS/RNS signals (yellow flash) might modify the conserved cysteine residue of the C-terminal domain (red), which leads to structural modifications and dimerization of the proteins. The dimers can ubiquitylate specific substrates in the cytoplasm and nucleus leading to induction of genes involved in programmed cell death (PCD). Dimerization might also result in translocation of the PFU1/PHO2 heterodimer to the nucleus and to activation of a negative feedback loop, in which PFU1-mediated ubiquitylation leads to degradation of PHO2. green - UBC domain, blue - N-terminal domain of PHO2 and PFU2, purple - N-terminal domain of PFU1 and PFU3

autoinhibition would represent a great mechanism for the plant to always keep an inactive pool of PFU proteins in the cell under normal growth conditions that can be directly activated in response to stress, which is highly important especially during fast cell death processes.

In response to abiotic or biotic stress the ROS/NOS signals in the cell accumulate and might modify the PFU proteins in such a way that they become activated and are able to form homo- and heterodimers. These complexes can then ubiquitylate antiapoptotic proteins in the cytoplasm or in the nucleus and with this target these components for degradation via the proteasome. It is also possible that specific substrates are not degraded but structurally modified via ubiquitylation, which induces the transcription of genes involved in programmed cell death.

According to the co-expression of PFU1 and PHO2 in *N. benthamiana*, the PFU1/PHO2 heterodimer might be able to translocate to the nucleus where it could directly modify transcriptional regulators. However, co-expression of the two proteins in *Arabidopsis* rather suggests that PFU1 activity leads to degradation of the PHO2 protein. This might occur after the proteins have induced downstream signals and could represent a kind of negative feedback loop in the signaling pathway.

The model presented here is highly speculative and can only be considered as a first hypothesis. Many assumptions have not been definitely proven and further analysis on the structure and the molecular mechanism of the PFU proteins is necessary. Especially the N-terminal domain of the proteins has not been addressed at all yet and needs to be involved in further analysis. However, the ideas and results summarized in this thesis represent a new basis, on which future experiments analyzing the function of the PHO2 family of ubiquitin conjugating enzymes in plant programmed cell death can be built on.

Chapter 4

Material and Methods

4.1 Material

4.1.1 Bacterial strains

- *Escherichia coli* XL1-Blue (Stratagene)
genotype: *recA1 endA1 gyrA96 thi-1 hsdR17 supE44 relA1*
lac [F' *proAB lac* ^qZΔM15Tn10(Tet^r)]
- *Escherichia coli* DH5αTM (Invitrogen)
genotype: F⁻ Φ 80*lacZ*ΔM15 Δ(*lacZYA-argF*)U169 *recA1 endA1 hsdR17 (r_k⁻m_k⁺)*
phoA supE44 λ⁻ thi-1 gyrA96 relA1
- *Escherichia coli* BL21 (Stratagene)
genotype: F⁻ *ompT hsdS_B (r_B⁻m_B⁻) gal dcm* (DE3) pLysS (Cam^R)
- *Escherichia coli* RosettaTM (Novagen)
genotype: F⁻ *ompT hsdS_B (r_B⁻m_B⁻) gal dcm* (DE3) pLysSRARE (Cam^R)
- *Agrobacterium tumefaciens* C58C1 pCV2260 (D. Staiger, TU Zürich)

4.1.2 Yeast strain

Saccharomyces cerevisiae, strain PJ96-4α (James et al. 1996)
genotype: *MATα trp1-901 leu2-3,112 ura3-52 his3-200 gal4 gal80LYS2::GAL1-HIS3*
GAL2-ADE2 met::GAL7-lacZ

4.1.3 Plant material

Arabidopsis thaliana:

- wild type, ecotype Columbia (Col-0) (Rédei 1992)

- Col-0 plants expressing the ubK48R transgene (Schlögelhofer et al. 2006)
- T-DNA insertion lines in Col-0 background:
 - *pfu1-1*: insertion in At3g15355 (SALK_005298)
 - *pfu2-1*: insertion in At2g16920 (SALK_040713)
 - *pfu3-1*: insertion in At1g53020 (SAIL_906_C01)
 - *pho2-10*: insertion in At2g33770 (SAIL_846_E05)

Nicotiana benthamiana for transient expression of EGFP/mRFP constructs

4.1.4 Vectors

For standard cloning:

- pBluescript II (Stratagene): This small plasmid is due to the f1 helper phage origin of replication highly replicated in *E. coli*, contains a β -galactosidase gene for a better selection of transformants containing the inserted DNA fragment and confers Ampicillin resistance. It was used to clone the open reading frame of *PFU2*.
- pCR[®]2.1 TOPO[®] vector (Invitrogen): This vector possesses 3' T overhangs for direct ligation of *Taq*-polymerased PCR fragments, containing 3' A overhangs. Apart from this, it also contains an Ampicillin and Kanamycin resistance gene and a β -galactosidase gene for a better selection of transformants. It was used together with the TOPO TA Cloning[®] Kit (Invitrogen) to directly clone the PCR fragments obtained for the *PFU2* leader sequence.

For expression of fusion proteins with EGFP and mRFP in plants:

- pER8 (Zuo et al. 2000): pER8 is a β -estradiol-inducible binary T-DNA cloning vector, conferring Spectinomycin resistance in *Agrobacteria* and Hygromycin resistance in *Arabidopsis*.
- p3: The p3 plasmid combines the backbone of the binary vector pBIB (Becker 1990), containing the constitutive 35 S promoter, with the multiple cloning site of the plasmid pRT103 (Töpfer et al. 1993) and conveys Kanamycin resistance in bacteria and Hygromycin resistance in plants.

For protein overexpression in *E. coli*:

- pET42c (Novagen): pET42c was used for high-level expression of peptides under the control of the T7 promoter. It contains the coding region for a GST-tag, an S-tag and two His-tags and possesses a Kanamycin resistance gene.

- pLysSRARE (Novagen): This plasmid contains a Chloramphenicol resistance gene, the genes encoding the T7 lysozyme and genes for tRNAs with codons rarely used in *E. coli*.

For protein expression in yeast:

- pGBKT7 (Clontech): This vector was applied to express proteins fused to a fragment of the GAL4 DNA binding domain in yeast. It contains both T7 and *ADH1* promoter and carries a Kanamycin resistance gene for selection in *E. coli* and a *TRP1* auxotrophic marker for selection in yeast.
- pGAD424 (Clontech): pGAD424 is a yeast expression vector used to generate fusion proteins with a fragment of the GAL4 activation domain. Proteins are expressed under the control of the *ADH1* promoter in yeast. The vector contains an Ampicillin resistance gene for selection in *E. coli* and a *LEU2* auxotrophic marker gene for selection in yeast.
- pIOX049 (Hirst et al. 2001): This vector was used to amplify the gene fragment of the TUP1 repression domain for further cloning into pGAD424.

4.1.5 Plasmids used in this thesis

The constructs used or constructed in this thesis are summarized in Appendix A.

4.1.6 Chemicals

Chemicals used in this thesis were, if not mentioned differently in the subsequent protocols, purchased from the following companies: Amersham (Munich), Duchefa (Haarlem, Netherlands), Invitrogen (Karlsruhe), Roth (Karlsruhe), Sigma-Aldrich (Steinheim).

4.1.7 Enzymes

Restriction enzymes were purchased from the following companies: Fermentas (St. Leon-Rot), New England Biolabs (Frankfurt) and Roche (Penzberg). The origin of other enzymes is mentioned in the description of the respective method.

4.1.8 Size standards

- GeneRulerTM 1 kb DNA Ladder (Fermentas)
- GeneRulerTM 100 bp DNA Ladder (Fermentas)
- PageRulerTM Prestained Protein Ladder (Fermentas)

4.1.9 Oligonucleotides

Oligos were purchased from Isogen Life Science (De Meern, The Netherlands), Operon (Huntsville, USA) or Microsynth AG (Balgach, Switzerland) and are listed in Appendix B starting with the 5' end.

4.1.10 Antibodies

- anti-GAL4 (DBD) IgG2a antibody (Santa Cruz Biotechnology, Inc.): This antibody derived from mouse was used as a first antibody to detect fusion proteins with the GAL4 DNA binding domain.
- anti-TUP1 IgG antibody (Santa Cruz Biotechnology, Inc.): To visualize fusion proteins with the yeast TUP1 repressor domain or TUP1 alone, this monoclonal antibody was applied as first antibody.
- Ni-NTA alkaline phosphatase conjugate (Quiagen): Recombinant proteins labelled with a His-tag were directly detected with this conjugate without the need of a second antibody.
- Strep-Tactin alkaline phosphatase conjugate (IBA): The Strep-Tactin AP conjugate was used to identify Strep-tagged recombinant proteins.
- anti-ubiquitin antibody: This polyclonal antiserum was produced in rabbits by Dr. A. Bachmair and detects plant ubiquitin.
- anti-rabbit IgG alkaline phosphatase conjugate (SIGMA): This antibody produced in goats was coupled to an alkaline phosphatase and served as a second antibody binding to antibodies derived from rabbits, such as the anti-ubiquitin antibody described above.
- anti-mouse IgG alkaline phosphatase conjugate (SIGMA): This secondary antibody was also produced in goats and coupled with an alkaline phosphatase. It was used to visualize the first antibodies produced in mice, such as the anti-GAL4 and the anti-TUP1 antibody.

4.1.11 Bioinformatic Tools and Databases

- NCBI: National Center for Biotechnology Information, <http://www.ncbi.nlm.nih.gov>
- TAIR: Arabidopsis Information Resource (Swarbreck et al. 2008), <http://www.arabidopsis.org>
- RIKEN: *Arabidopsis* full-length clone Database, <http://www.brc.riken.go.jp/lab/epd/catalog/cdnaclone.html>

- SIGnAL: Salk Institute Genomic Analysis Laboratory, Collection of T- DNA insertion lines for *Arabidopsis*, <http://signal.salk.edu>
- MUSCLE vs 4.0: protein multiple sequence alignment software (Edgar 2004)
- SeaView version 4.1: graphical interface for sequence alignments (Gouy et al. 2010)
- PROSITE database: Database of protein domains, families and functional sites (Hulo et al. 2007), <http://www.expasy.ch/prosite/>
- PredictNLS online: bioinformatic tool to predict nuclear localization signals, <http://cubic.bioc.columbia.edu/cgi/var/nair/resonline.pl>
- NetNES 1.1 Server: for prediction of leucine-rich nuclear export sequences in eukaryotic proteins (la Cour et al. 2004), <http://www.cbs.dtu.dk/services/NetNES>

4.2 Methods

4.2.1 Work with *Escherichia coli*

Cultivation and storage of *Escherichia coli*

E. coli was grown under standard conditions at 37 °C in liquid LB medium or on LB plates to which antibiotics for selectivity were added after autoclaving.

- LB medium (pH 7.0 with NaOH): 10 g tryptone, 5 g yeast extract, 10 g NaCl, 15 g agar (only for plates), dH₂O added to 1 l
- Antibiotics (final concentration): Ampicillin (100 µg/ml), Kanamycin (25 µg/ml), Chloramphenicol (50 µg/ml)

For long-term storage of *E. coli* cells, 650 µl of an overnight culture were mixed with 650 µl of 75 % glycerol and frozen at −80 °C.

Preparation of competent *E. coli* cells

A 5 ml preculture was inoculated with a single colony from plate and grown overnight at 37 °C and 200 rpm. On the following day a 100 ml main culture was inoculated with 2 ml of the preculture and grown at 37 °C and 200 rpm up to an OD₆₀₀ of 0.3–0.4. Then the cells were centrifuged down for 10 min at 4000 rpm and 4 °C. The pellet was resuspended in 10 ml of cold TSS solution and frozen in liquid nitrogen in 200 µl aliquots, which were then stored at −80 °C.

- TSS (pH 6.7): 10 % PEG 4000 and 50 mM MgCl₂ in LB medium
Aliquots of 9.5 ml were stored at −20 °C and 0.5 ml of DMSO was added just before usage.

Transformation of *E. coli*

An aliquot of competent cells was thawed on ice and mixed with 50 – 150 ng of DNA. The samples were incubated for 10 – 20 min on ice before they were heat-shocked for 2 min at 37 °C. Then the cells were imbibed in 750 μ l of LB medium and shaken for 1 hour at 37 °C and 900 rpm. Finally the cells were plated on LB plates with the appropriate antibiotics and grown overnight at 37 °C.

Plasmid preparation from *E. coli*

Plasmids possessing a high replication rate were isolated from *E. coli* either with the kit Nucleospin Plasmid[®] (Macherey-Nagel) or with the PureYieldTM Plasmid Miniprep System (Promega) according to the manufacturers' protocols. Low-copy plasmids were isolated from larger cell cultures with the Plasmid Midi Kit (Qiagen). In both cases the plasmids were eluted in 50 μ l H₂O bidest. and stored at –20 °C.

4.2.2 Work with *Agrobacterium tumefaciens*

Cultivation and storage of *Agrobacterium tumefaciens*

The standard cultivation condition for *A. tumefaciens* was growth at 28 °C in liquid or on solid YEB medium to which the desired antibiotics for selection were added after autoclaving the medium. For storage, glycerol stocks were prepared as already described above for *E. coli*.

- YEB medium (pH 7.2 with NaOH): 5 g beef extract, 1 g yeast extract, 5 g peptone, 5 g sucrose, 15 g agar (only for plates), filled up with dH₂O to 1 l
For a better growth 2 mM MgSO₄ was added after autoclaving.
- Antibiotics (final concentration): Kanamycin (25 μ g/ml), Spectinomycin (50 μ g/ml), Rifampicin (100 μ g/ml)

Preparation of competent *A. tumefaciens* cells

To receive competent Agrobacteria, a preculture of 10 ml YEB medium was inoculated with a single colony and grown overnight at 28 °C and 200 rpm. The next day the cells were diluted 1:25 in fresh medium and the main culture was grown for about 3.5 hours at 28 °C and 200 rpm. Then the cells were harvested by centrifuging for 10 min at 5000 rpm and 4 °C and imbibed in 1 ml cold YEB medium. In the end aliquots of 200 μ l were frozen in liquid nitrogen and stored at –80 °C.

Transformation of *A. tumefaciens*

An aliquot of competent cells was thawed on ice and mixed with 2-5 μ g of plasmid DNA. Then the cells were put into liquid nitrogen for 1 min before they were heat-shocked at

37 °C for 5 min. After addition of 1 ml YEB medium the cells were shaken for 2 hours at 28 °C and 600 rpm and finally plated on selective medium. Positive colonies could be detected after 2 days of incubation at 28 °C.

Plasmid preparation from *A. tumefaciens*

To check whether the Agrobacteria cells contain the correct constructs, plasmids were isolated with the kit Nucleospin Plasmid[®] (Macherey-Nagel). Therefore cells were first grown at 28 °C in 5 ml YEB medium with the respective antibiotics and 2 mM MgSO₄ up to an OD₆₀₀ of 0.8 before proceeding according to the manufacturer's protocol.

4.2.3 Work with *Saccharomyces cerevisiae*

Cultivation and storage of yeast cells

Yeast cells were either grown on full YPD medium or on selective SD medium at 30 °C.

- YPD medium: 1 % bacto-yeast extract, 2 % bacto-peptone, 2 % glucose, 2 % bacto-agar (only for plates), adjust pH to 6.5
- SC medium: 0.67 % bacto-yeast nitrogen base without amino acids, 2 % glucose, 2 % bacto-agar (only for plates), adjust pH to 6.5

Dropout mixes (BD Biosciences) were added in the following amounts:

- –Trp DO supplement: 0.74 g/l
- –Leu DO supplement: 0.69 g/l
- –His DO supplement: 0.77 g/l
- –Leu/–Trp DO supplement: 0.64 g/l

For long-term storage glycerol stocks were prepared mixing 650 µl of an overnight culture with the same amount of 75 % glycerol and storing the stocks at –80 °C.

Yeast transformation

Plasmid DNA was introduced into yeast via heat shock transformation. Therefore a 5 ml preculture was inoculated with a single yeast colony and grown overnight at 30 °C and 200 rpm. The next day 1 ml of the preculture was added to 50 ml of fresh medium and the culture was grown at 30 °C and 200 rpm up to an OD₆₀₀ of 0.7. Then the cells were pelleted by centrifugation for 3 min at 4000 x g and room temperature and washed with 10 ml of ddH₂O. After a second centrifugation step for 3 min at 4000 x g and room temperature the cells were resuspended in 10 ml LiAc solution and then pelleted again for 3 min at 4000 x g. Finally 300 µl of LiAc solution was added to the yeast cells and 50 µl of this cell suspension was mixed with 2–5 µg of plasmid DNA and the same amount of carrier DNA (salmon sperm DNA). To make the cells permeable, 300 µl of PEG solution were carefully

mixed with the samples and the transformation mix was incubated for 20 min at 30 °C and followed by a heat-shock for 20 min at 42 °C. After letting the samples adjust to room temperature, 100 μ l of each were distributed on selective plates and incubated for 2 days at 30 °C.

- LiAc solution: 100 mM lithium acetate, 10 mM Tris (pH 7.5), 1mM EDTA
- PEG solution: 40 % PEG, 100 mM lithium acetate, 10 mM Tris (pH 7.5), 1mM EDTA, solution was filter-sterilized (0.2 μ m pore size) before usage.

Yeast trickle tests

Positive transformants were grown in 5 ml selective SD medium overnight at 28 °C and centrifuged for 4 min at 4000 rpm. The pellet was dissolved in ddH₂O, resulting in an OD₆₀₀ of 2.0. A 1:10 dilution series was performed ending at a dilution level of 10⁻⁴. 5 μ l of each dilution were trickled on the plates and the cells were grown for 2 days at 30 °C.

Protein extracts of yeast cells for Western blotting

A 5 ml culture of the respective yeast strain was grown to an OD₆₀₀ of 1.0 and centrifuged down for 2 min at 4000 rpm. The pellet was resuspended in 0.5 ml of 0.5 M NaOH and incubated for 2 min at room temperature to break the cells. After a second centrifugation step, the pellet was resuspended in 0.5 ml of sterile ddH₂O. This results in a very crude cell extract, which is sufficient to detect the protein of interest on a Western blot. For this, 10 μ l of the sample were denatured in Lämml buffer for 5 min at 99 °C and run on an SDS-PAGE.

4.2.4 Work with *Arabidopsis thaliana*

Cultivation of *Arabidopsis thaliana*

Arabidopsis plants were first grown on MS medium under long day conditions (16 h light/8h dark) at 22 °C during daytime and 18 °C at night under 200 – 400 μ E·m⁻²·s⁻¹ of irradiation energy for about 2 weeks, before they were transferred to soil and grown under the same conditions.

- MS medium (pH 5.7 with KOH): 4.3 g MS salt, 0.5 g MES, 10 g sucrose, 8 g agar (only for plates), filled up with dH₂O to 1 l
Vitamin mix and hygromycin (25 μ g/ml) for selection were added after autoclaving. To avoid growth of *A. tumefaciens* on the plates used for the progeny of freshly transformed plants, Claforan (200 μ g/ml) was included.
- 500 x vitamin mix: 5 g myo-inositol, 1 g thiamine, 50 mg nicotinic acid, 10 mg biotin in a final volume of 100 ml ddH₂O

For analyzing the mutant lines under different conditions, plants were cultivated in liquid medium.

- liquid medium: 1/2 Gamborg's B5 medium (1.53 g/l, Duchefa), 1% Sucrose, adjust pH to 5.7 with KOH, after autoclaving add Gamborg's B5 vitamin mixture (Duchefa)

Sterilization of *Arabidopsis* seeds

A small amount of seeds was shaken in 500 μ l sterilization solution for 15 min at room temperature. Then the seeds were centrifuged down at 14000 rpm for 1 min, the solution was discarded and the seeds were washed three times with 500 μ l dH₂O. Afterwards, they were dried under the sterile hood to either distribute them on soil and plates or to store them at 4 °C. Before putting plates or pots into the culture room, the seeds were stratified for 3 days at 4 °C in the dark.

- Sterilization solution: 15 g of CaCl₂O₂ in 500 ml dH₂O were stirred overnight at room temperature and stored at 4 °C. Shortly before usage, 0.02 % of Triton-X was added to the solution.

Floral dip transformation of *Arabidopsis thaliana*

New transgenes were introduced into *Arabidopsis thaliana* via transformation with *Agrobacterium tumefaciens*, which in nature is a crown gall inducing bacterium. The *Agrobacterium* strain used in this thesis already possesses a helper plasmid containing the *vir* genes responsible for transferring a T-DNA into the plant's nucleus, and is only virulent if a second plasmid with the T-DNA is present in the bacteria. Then these bacterial strains can be used to transform the plants via the following procedure.

Arabidopsis wild type seeds (Col-0) were distributed on soil and grown under short-day conditions (8 hours light/16 hours darkness). After approximately two weeks, nine seedlings were transferred to a separate pot and first shoots were cut to increase the shoot number. A 20 ml preculture of *Agrobacteria* containing the desired T-DNA construct was grown for two days at 28 °C and 2 ml were used to inoculate a 100 ml main culture. The latter was grown overnight at 28 °C and 200 rpm and the next day, the cells were harvested by centrifugation for 15 min at 5000 rpm and room temperature. The pellet was resuspended in 200 ml 5 % sucrose + 0.05 % Silwet L-77 and the plant shoots were dipped for 30 seconds into the bacterial suspension. Then the plants were transferred to the greenhouse and covered with a lid for one day.

Plant crosses

Plants were grown under long-day conditions (16h light/8h darkness). All parts of a flower of the mother plant except for the pistil were completely removed and pollen of the father plant was applied on the pistil. The flower was covered in plastic until a silique formed.

Preparation of *Arabidopsis* samples for microscopic analysis

In this thesis, transgenic *Arabidopsis* plants bearing β -estradiol inducible constructs were used for microscopic analyses. After ten days on MS plates without any supplement, seedlings were transferred to MS plates containing 5 μ M β -estradiol to induce the transgenes. Plants were grown on these plates for three to four more days, before the roots of the seedlings were cut off and analyzed under the confocal microscope.

Microscopic analysis

Expression of the EGFP/mRFP fusion proteins was analyzed under the confocal laser scanning microscope Leica TCS SP2 AOBS with the help of R. Franzen at the CeMic facilities of the Max Planck Institute for Plant Breeding Research in Cologne.

EGFP was excited with the Argon laser at 488 nm and the emitted fluorescence was detected between 505 nm and 535 nm wavelength. The mRFP protein has its excitation maximum at 584 nm and the emitted fluorescence was analyzed between 600 nm and 625 nm. Simultaneous bright-field images were recorded by a transmission detector.

Determination of the P_i content in *Arabidopsis* leaves

The phosphate content of the different mutant lines was compared to wild type in collaboration with Dr. W. R. Scheible at the IPK in Gatersleben. The method used was based on a colorimetric micromethod described by Itaya and Ui (1966). Leaf discs were macerated with a plastic rod in 50 μ l H₂O bidest in a 96-well plate. Then additional water was added up to a volume of 125 μ l and the plate was centrifuged for 4 min at 3000xg. 10 μ l of the supernatant were mixed with 15 μ l H₂O, 100 μ l 1M HCl and 100 μ l of a colour reagent containing one volume of 4.2 % (NH₄)₆Mo₇O₂₄·H₂O in 5 N HCl and three volumes of 0.2 % malachite green dye in water. After 15 min of incubation at room temperature 100 μ l of 1.5 % Tween-20 was added and the samples were incubated for additional 15 min at room temperature. The P_i content was determined by measuring the absorbance at 660 nm wavelength and comparing to a calibration curve.

Induction of the *ubK48R* transgene

To analyze the effect of the *ubK48R* transgene on the different mutant plant lines and wild type, seeds were sown on MS plates containing hygromycin (25 μ g/ml) to select for plants possessing the transgene, and dexamethasone (0.7 μ M in 96 % EtOH) to induce *ubK48R* transgene expression. The growth of the seedlings was monitored after one week.

Ozone treatment of *Arabidopsis* plants

Mutant and wild type plants were treated with ozone in collaboration with Dr. D. Ernst at the Helmholtz Centre in Munich. Approximately four week-old plants were exposed to a

single pulse of O₃ (350 ppb) and the effect of the oxidative stress was monitored after two days.

Nitric oxide treatment of *Arabidopsis* plants

Arabidopsis plants were treated with nitric oxide in liquid cultures and on MS plates. For the treatment in liquid cultures, seeds were grown in 100 ml liquid 1/2 Gamborg's B5 medium containing only the Gamborg's B5 vitamin mix in constantly shaking 200 ml glass flasks. After one week, the plants were treated with different concentrations of nitric oxide by adding 0.1 mM, 0.2 mM or 0.5 mM of sodium nitroferricyanide(III) dihydrate (SIGMA) to the medium every second day.

For nitric oxide treatment on solid medium, seeds were sown on squared plates containing normal MS medium and standing upright in the growth chamber. After ten days on these plates, the seedlings were transferred to squared MS plates containing 0.2 mM sodium nitroferricyanide(III) dihydrate. The number of green seedlings on these plates was counted every day until the experiment was stopped after ten days. At this timepoint, the remaining green plants were transferred back to MS plates without supplement to check for viability under normal growth conditions.

Pathogen treatment of *Arabidopsis* plants

Programmed cell death occurring in response to pathogen treatment was analyzed by performing conductivity measurements in collaboration with Dr. N. Schlaich at the RWTH Aachen. Five week-old *Arabidopsis* plants were infiltrated with the bacterial pathogen *Pseudomonas syringae* pv tomato DC3000 (avrRpt2) at a concentration of 5 x 10⁷ cfu/ml. Per plant line, 24 leaf discs were collected with the lid of a 0.5 ml plastic tube and washed in ddH₂O for 30 min. Afterwards they were transferred to a tube containing 7 ml of ddH₂O and conductivity of the solution was measured 7 h and 21 h after infiltration with the conductivity meter LF 340A fitted with a TetraCon 325 conductivity cell (WTW, Weilheim, Germany).

4.2.5 Work with *Nicotiana benthamiana*

Nicotiana benthamiana seeds were directly put on soil and grown under short-day conditions (8h light/16h darkness).

Transient expression of proteins in *Nicotiana benthamiana*

Agrobacterium tumefaciens strains containing the EGFP/mRFP fusion protein of interest were incubated in AS buffer for 2 h in the dark at 28 °C. Agrobacteria were either taken from a liquid overnight culture or directly scratched from plates. Apart from the strains containing the EGFP/mRFP constructs, a strain obtained from Dr. E. Schmelzer at the CeMic faculty of the MPIPZ expressing the p19 protein of the tomato bushy stunt virus (Voinnet et al. 2003) was also incubated in AS buffer to suppress gene silencing. If only one

fusion protein was expressed together with p19 in the plants, the bacterial suspension in the AS buffer was set to an OD₆₀₀ of 0.5. To coexpress two EGFP/mRFP constructs in *Nicotiana*, the OD₆₀₀ of the suspension was set to 0.33. Finally, the different strains were mixed in an 1:1 ratio. To infiltrate 4 week-old *Nicotiana* plants, small holes were plunged into the leaves with a yellow tip. Leaves were infiltrated with the Agrobacteria cells through these holes using a 1 ml syringe. Two days after the infiltration, a leaf sample was applied to the microscope slide upside down and expression of the EGFP/mRFP fusion proteins was checked under the confocal microscope as described for *Arabidopsis* samples.

- AS buffer: 2 ml MgCl₂ (1M), 2 ml MES (1M, pH 5.68 with KOH), 200 μl Acetosyringone (150 mM in DMSO), ad 200 ml dH₂O

4.2.6 Handling nucleic acids

Quick DNA extraction from *Arabidopsis thaliana*

Plant material of a rosette leaf was put into a microtube and frozen in liquid nitrogen. After adding a small amount of sand and 200 μl of DNA extraction buffer, an electric grinder was used to homogenize the material. The solution was centrifuged for 5 min at 14000 rpm and the supernatant was transferred to a new tube. After adding 200 μl of isopropanol, the samples were incubated for 5 min at room temperature to precipitate the DNA. This was followed by a second centrifugation step for 5 min at 14000 rpm and the resulting pellet was washed with 500 μl of 70 % ethanol. The pellet was dried and resuspended in 70 μl ddH₂O. To increase the purity of the DNA, the samples were boiled twice for 5 min at 65 °C and stirred in between with a pipet tip. Finally the tubes were centrifuged again at 14000 rpm for 2 min and the supernatant with the DNA was transferred to a fresh tube.

- DNA extraction buffer: 200 mM Tris (pH 7.5), 250 mM NaCl, 0.5 % SDS, 25 mM EDTA

High-throughput DNA isolation with the BioSprint 96

Isolation of DNA from a larger number of individual *Arabidopsis* plants was performed making use of the BioSprint 96 DNA Plant Kit (Qiagen). Samples were prepared according to the manual and the robot was set to the program P_100 to achieve highly concentrated DNA eluted in 100 μl ddH₂O.

RNA extraction from *Arabidopsis thaliana*

100 mg of plant material were frozen in liquid nitrogen. The sample was then macerated with a metal pestle in a 2 ml microtube until a homogeneous powder was obtained. For isolation of RNA, the RNeasy Mini Kit (Qiagen) was used according to the manufacturer's manual. 10 % of the resulting RNA solution served as a control for the gel electrophoresis and the rest was stored at -20 °C.

PCR

For the scientific world the polymerase chain reaction might be one of the most important inventions of the last century and can be carried out in many different modifications. If the flanking regions of the DNA fragment of interest are known, billions of copies can be amplified via PCR. The main principle is consists of three different steps.

1. Denaturation at 95 °C: The two strands of the DNA template are separated.
2. Annealing (45 – 60 °C): Chemically synthesized oligonucleotides, complementary to the flanking regions at the 5' and 3' termini of the DNA fragment to be amplified, bind to the DNA strands.
3. DNA synthesis (68 – 72 °C): A thermo-stable DNA polymerase elongates the complementary strands using deoxynucleoside triphosphates (dNTPs) added to the PCR mix before.

These three steps are repeated 25-40 times and the amount of the synthesized copies of the fragment increases exponentially.

Table 4.1: Standard PCR programs to amplify short (up to approx. 1500 bp) and longer DNA fragments

Temp.	Time for short fragments	Time for long fragments	Step
94 °C	4 min	7 min	initial denaturation
94 °C	30 sec	30 sec	denaturation
54 °C	30 sec	30 sec	annealing
72 °C	1 min	8 min	elongation
	repeat 30 times	repeat 35 times	
72 °C	10 min	10 min	final elongation
15 °C	∞	∞	

The annealing temperature differs according to the length and GC content of the oligonucleotides. Also the length of the elongation step was changed according to the applied polymerase and the size of the PCR product to be amplified. Due to this, several different PCR programs were used during this thesis. Analytical PCRs were usually performed with either *GoTaq*[®] (Promega) or *LA Taq*TM (Takara) according to the manufacturer's manual. To amplify DNA fragments used for subsequent cloning, the Platinum[®] *Pfx* DNA Polymerase (Invitrogen) was used.

RT-PCR

Copy DNA or complementary DNA (cDNA) was used to amplify only the coding sequence of the genes to be analyzed and to observe the expression level of transgenes or genes containing a T-DNA insertion. Isolated RNA was transcribed into cDNA by the enzyme reverse transcriptase, originating from retro viruses.

Table 4.2: A standard protocol for cDNA synthesis with the SuperScriptTM II RT

Component	Final concentration	Volume
template RNA	0.1-5 μg	variable
primer mix	1 μM	2 μl
deionized water (nuclease free)		ad 12 μl
5 min, 70 °C, afterwards on ice		
5 x reaction buffer	1 x	4 μl
10 mM dNTP mix	1 mM	2 μl
Protector RNase Inhibitor (40 U/ μl , Roche)	20 U	0.5 μl
6 min, 37 °C		
SuperScript TM II RT (200 U/ μl)	10 U/ μl	1 μl
3 h, 42 °C, then 10 min, 70 °C		in total 20 μl

For standard transcription the SuperScriptTM II Reverse Transcriptase (Invitrogen) was used, whereas the thermostable Transcriptor First Strand Reverse Transcriptase (Roche) was only applied according to the manufacturer's manual when persistent secondary structures in the RNA disturbed the transcription. The reverse oligo also used for the subsequent amplification of the cDNA fragment of interest served as an oligo for this reaction.

Colony-PCR

Colony PCRs were carried out according to the *GoTaq*[®] protocol to analyze putative transformants of either *E. coli* or *Agrobacterium tumefaciens*. The DNA template was added in form of a bacterial colony transferred into the microtube with a toothpick.

Agarose gels

Molecules of different size and charge can be separated in a special gel matrix via electrophoresis. Apart from size and charge of the molecules also the strength of the electric field, the conformation of the molecules and the size of the pores of the gel matrix play an important role in the migration rate of each molecule. Because of the phosphate residues in their backbone, nucleic acids are negatively charged and migrate in an electric field to

the anode. Different agarose concentrations of the gels lead to different resolutions of the nucleic acid molecules. For this thesis, different concentrations of agarose (0.8, 1.0, 1.5 and 2.0 %) were dissolved in 0.5 x TAE buffer, and after adding 3 μ l of ethidium bromide per 100 ml of gel, the solution was poured in horizontal gel trays. The samples to be analyzed were mixed with 1/6 volume of a 6 x loading dye and the electrophoresis was performed at 110 V for large gels and 70 V for smaller gels. Ethidium bromide changes its absorption maximum when intercalating into the aromatic ring structure of the bases of the nucleic acids, and can be detected in UV light (254 nm) as orange bands in the gel. DNA bands identified by this method were compared to a molecular size marker on the same gel.

- 50 x TAE stock: 242 g Tris, 57.1 ml glacial acetic acid, 37.2 g Na₂EDTA·2 H₂O
- 6 x loading buffer: 50 % glycerol, 0.2 M EDTA pH 8.0, 0.003 % bromophenol blue or Orange G

DNA purification from agarose gels

The DNA fragments of interest were cut out from the gel and purified with the help of the kit NucleoSpin[®] Extract II (Macherey-Nagel) or the Wizard[®] SV Gel and PCR Clean-Up System (Promega). The DNA was eluted in 20 μ l ddH₂O. Both kits were also used to directly purify DNA samples without a preceding separation on a gel.

Precipitation of nucleic acids

To further concentrate the nucleic acid or to change buffers, the DNA or RNA was precipitated with 3 volumes of 96 % EtOH and 0.1 volume of 3 M sodium acetate (pH 5.0) overnight at -20 °C. Then the sample was centrifuged for 20 min at 14000 rpm and 4 °C. The resulting pellet was washed twice with 70 % EtOH, dried and resuspended in ddH₂O.

Generation of blunt ends

Blunt ends of a DNA fragment can be either achieved via restriction endonucleases, such as *Sma*I, or via other enzymes, such as the T4 DNA polymerase. For this thesis, the Klenow fragment (Roche) was used. This enzyme contains a 5' – 3' DNA polymerase activity and a 3' – 5' exonuclease activity. It uses deoxynucleoside triphosphates (dNTPs) added to the mix to synthesize the missing end of one strand complementary to the other.

Table 4.3: A standard protocol for the blunting reaction

Component	Final concentration	Volume
PCR product	1 μg	variable
10 x filling buffer	1 x	5 μl
dNTPs	1 mM	2.5 μl
Klenow	2 U	2 μl
ddH ₂ O		ad 50 μl
1 h, 37 °C		

DNA digestion with restriction enzymes

Restriction enzymes cut the DNA template at specific recognition sequences, which usually consist of 4–6 base pairs forming palindromes and differ from enzyme to enzyme resulting in either 5' overlapping cohesive or "sticky" ends, 3' overlapping cohesive ends or blunt ends. A typical reaction mix is shown in the table below (see table 4.4). The reaction was incubated for about one hour for analytical digests or overnight for subsequent ligations at the temperature optimum of the respective enzyme and was stopped by inactivation of the enzyme at 65–80 °C for 20 min.

Table 4.4: A typical reaction mix for digesting DNA

Component	Volume
DNA	e.g. 1 μg
10 x buffer	2 μl
restriction enzyme	0.5 μl
ddH ₂ O	ad 20 μl

Ligation

The enzyme T4 DNA ligase, a gene product of a gene of the *E. coli* bacteriophage T4, is able to ligate a digested PCR fragment into the digested vector by forming a phosphodiester bond between the 3' hydroxyl end of one DNA fragment and the 5' phosphate end of a second linear DNA fragment in an ATP-dependent reaction. All ligation reactions performed during this thesis were incubated overnight at room temperature regardless of blunt or cohesive ends of the DNA fragments. The T4 DNA ligase for classical cloning was obtained from Roche and PROMEGA. Fast cloning of PCR products for subsequent sequencing was

performed with the TOPO TA Cloning[®] Kit (Invitrogen) according to the manufacturer's manual. This kit contains a the pCR[®]2.1 TOPO[®] vector possessing 3'-T overhangs for direct ligation of *Taq*-polymerized PCR products.

Table 4.5: Reaction mix for a standard ligation

Component	Volume
Insert	about 0.5 μg
Vector	about 0.1 μg
10 x Ligase Reaction Buffer (containing ATP)	2 μl
T4 DNA Ligase	1 μl (1 U)
ddH ₂ O	ad 20 μl

Site directed mutagenesis

Amino acid exchanges in the yeast constructs were achieved using the QuikChange[®] II XL Site-Directed Mutagenesis Kit (Stratagene) according to the manufacturer's manual.

Sequencing

Samples to be sequenced were either sent to the Automatic DNA Isolation and Sequencing Service (ADIS) of the Max Planck Institute for Plant Breeding Research in Cologne or to AGOWA genomics (Berlin). DNA and oligos for sequencing were prepared according to the guidelines of the respective sequencing service.

4.2.7 Handling proteins

SDS-PAGE

Proteins can be separated on a polyacrylamide gel according to their molecular weight. As the different electrical charges of the proteins would influence the run in an electrical field, the charged residues were masked by denaturation in an SDS containing Lämmli sample buffer for 5 min at 99 °C. For separation gels with different amounts of acrylamide were used and run in the Mini Protean[®] 3 cell from Biorad at 120 V and room temperature.

- 2 x Lämmli sample buffer (LSB): 50 % glycerol, 20 mM DTT, 2 % SDS, 125 mM Tris-HCl pH 6.8, 0.003 % bromophenolblue
- 5 x Electrophoresis buffer: 7.55 g Tris, 36 g glycine, 0.5 g SDS, dH₂O ad 500 ml

Table 4.6: Ingredients for a 12 % polyacrylamide gel

Ingredient	Stacking gel	Separating gel
30 % acrylamide mix 29:1 (SERVA)	330 μ l	2 ml
1.5 M Tris-HCl	250 μ l (pH 6.8)	1.3 ml (pH 8.8)
10 % SDS	20 μ l	50 μ l
10 % ammoniumpersulfate	20 μ l	50 μ l
TEMED	2 μ l	4 μ l
ddH ₂ O	ad 2 ml	ad 5 ml

Coomassie staining

Proteins can be visualized on a polyacrylamide gel by incubation with Coomassie dye in an acid solution. In this thesis, either a commercially available Coomassie stain (PageBlueTM Protein Staining Solution, Fermentas) or a self-mixed stain as described below was used. In contrast to the commercial stain where gels were treated according to the manufacturer's manual, the gel in the self-made solution was first heated up for 30 sec in a microwave before incubating for another 15 min at room temperature on a shaker. For destaining, the gel was covered with destaining solution lacking the Coomassie. To accelerate the destaining reaction, the gel covered with solution was again incubated for 30 sec in the microwave and then shaken at room temperature until only the stained proteins were visible on the gel.

- Staining/Destaining solution: 10 % acetic acid, 10 % isopropanol, plus 0.1 % Coomassie R-250 only for staining

Western blot

For immunological detection of the proteins, Western blots were performed and the membranes were incubated with different antibodies according to the proteins to be analyzed. First the proteins were separated on an SDS-PAGE. Then they were transferred to a PVDF membrane (Immobilon-P, pore size 0.45 μ m, Millipore) via wet blotting. Therefore, the membrane was first rinsed with 100 % methanol and afterwards incubated for 10 min in transfer buffer. The gel was shaken for 10 min in this buffer as well. Afterwards the blot was put together in a Mini Trans-Blot[®] Electrophoretic Transfer Cell (BioRad) in the following order: black part of the gel holder cassette, sponge, whatman paper, polyacrylamide gel, membrane, whatman paper, sponge, clear part of the cassette. All parts were always fully covered with transfer buffer while putting the blot together, and finally the blotting chamber was completely filled up with buffer. Then the protein transfer was performed for one hour at 50 V and room temperature.

Afterwards the gel was discarded and the membrane was washed for 5 min in 1 x ANT. Then it was blocked with 20 % newborn calf serum in 1 x ANT for either 1 h at room

temperature or overnight at 4 °C. Before addition of the antibody, the membrane was washed two times for 10 min with 1 x ANT/0.05 % Tween[®] 20 to diminish possible background signals. The first antibody was, if not stated otherwise, applied to the membrane in an 1:1000 dilution in 1 x ANT/0.05 % Tween[®] 20 overnight at 4 °C. If the first antibody was coupled to an alkaline phosphatase for detection, the membrane was washed three times with 1 x ANT/0.05 % Tween[®] 20 and directly incubated with the detection mix. To stop the detection, the mix was replaced by dH₂O. If a second antibody fused to an alkaline phosphatase was used, it was diluted in 1 x ANT according to the manufacturer's protocol (usually 1:20000) and applied to the membrane for one hour at room temperature. Then the membrane was washed three more times with 1x ANT/ 0.05 % Tween[®] 20 and the protein of interest was finally visualized using the detection mix described below.

- transfer buffer: 190 mM glycine, 25 mM Tris, 20 % methanol, 0.05 % SDS
- 1 x ANT: 150 mM NaCl, 50 mM Tris-HCl pH 8.0
- detection mix (always freshly prepared): 10 ml of development buffer containing 100 mM Tris-HCl (pH 9.5), 100 mM NaCl and 5 mM MgCl₂ were mixed with 66 μl 5 % NBT (diluted in 70 % DMF) and 33 μl BCIP (diluted in 100 % DMF).

Overexpression of recombinant proteins in *E. coli*

Overexpression constructs were transformed into the *E. coli* overexpression strains Rosetta or BL21 via heat-shock transformation and pre-cultures from the transformants were grown overnight in 5 ml LB with the respective antibiotics at 37 °C and 200 rpm. Functionality of the overexpression was first tested in 20 ml main cultures, whereas for purification of the recombinant proteins 200 ml main cultures of the *E. coli* strains were grown. The main culture was inoculated with 1/100 volume of the pre-culture and grown up to an OD₆₀₀ of 0.8 at 37 °C and 200 rpm. Then, if not mentioned differently, the protein overexpression was induced with 1 mM IPTG at 30 °C and 200 rpm. After three hours the cells were harvested by centrifugation at 4000 rpm and 4 °C and stored at -20 °C.

Purification of recombinant proteins from *E. coli* via His-tag under native conditions

After overexpression, the bacterial cell pellet of a 200 ml culture was thawed on ice and the cells were broken by treating them for 30 min on ice with 1 mg/ml lysozyme in 4 ml lysis buffer containing 50 mM NaH₂PO₄, 300 mM NaCl and 10 mM imidazole (pH 8.0). In addition the cell suspension was sonicated on ice. Then the total lysate (TL) was centrifuged at 14000 rpm for 30 min at 4 °C and the supernatant (SN) containing the soluble fraction of the cells was incubated with 1 ml of 50 % Ni-NTA agarose (Qiagen) for 1 hour at 4 °C. The suspension was added to a column (Poly-Prep[®] Chromatography Columns, BioRad) and the resin was washed three times with 4 ml washing buffer containing 50 mM NaH₂PO₄, 300 mM NaCl and 20 mM imidazole (pH 8.0). Finally the His-tagged protein was eluted

from the agarose beads in three steps by adding 0.5 ml of elution buffer containing 50 mM NaH_2PO_4 , 300 mM NaCl and 250 mM imidazole (pH 8.0) each time. To avoid denaturation of the proteins 0.5 M DTT and the protease inhibitors aprotinin (1 $\mu\text{g}/\text{ml}$) and leupeptin (1 $\mu\text{g}/\text{ml}$) were added to the buffers. An aliquot of each purification step was stored at -20°C to be analyzed on an SDS-PAGE.

Purification of recombinant proteins from *E. coli* via His-tag under denaturing conditions

The purification of His-tagged proteins under denaturing conditions was performed as described for the purification under native conditions. The only difference was the composition of the buffers. All buffers contained 100 mM NaH_2PO_4 , 10 mM Tris-HCl and 8 M urea to denature the proteins, but differed in their pH (lysis buffer: pH 8.0, washing buffer: pH 6.3, elution buffer: pH 4.5).

Purification of recombinant proteins from *E. coli* via Strep-tag

The *E. coli* cells bearing the overexpressed proteins labelled with a Strep-tag were lysed in Buffer W (100 mM Tris-Cl (pH 8.0), 150 mM NaCl, 1 mM EDTA, IBA BioTAGnology) as described for the purification of His-tagged proteins under native conditions. Then the soluble fraction of the cells was incubated with 0.5 ml of Strep-Tactin Sepharose (IBA BioTAGnology) for 1 hour at 4°C . Afterwards, the suspension was added to a column and the resin was washed five times with one column volume Buffer W. The protein was eluted in six steps by always adding half of a column volume of Buffer E (IBA BioTAGnology) containing 100 mM Tris-Cl (pH 8.0), 150 mM NaCl, 1 mM EDTA and 2.5 mM desthiobiotin. During all purification steps, 0.5 M DTT, aprotinin (1 $\mu\text{g}/\text{ml}$) and leupeptin (1 $\mu\text{g}/\text{ml}$) were added to the buffers.

Dialysis

Dialysis was performed overnight with Spectra/Por[®] Float-A-Lyzer G2 (MWCO 3.5-5 kDa, 5 ml max. sample volume) according to the manufacturer's manual, to change the buffer of the protein solution. By this also denaturing agents, such as urea, could be removed to renature the proteins. To assure proper dialysis, the volume of the outer buffer exceeded the sample volume at least 100 times, and the buffer was renewed after three hours of dialysis.

Co-Immunoprecipitation

The possible interaction of two proteins can be proven via Co-immunoprecipitation. Therefore the two proteins of interest were fused to different protein tags and purified as described above. In this thesis, first a His-tagged protein was tested together with a Strep-tagged protein. 50 μl of the first protein were mixed with 50 μl of the second protein and the solution was incubated for 30 min at room temperature. 100 μl of Ni-NTA agarose were added and the solution was incubated for one hour at 4°C . The beads were then centrifuged

down for 30 sec at 14000 rpm, the supernatant was carefully removed, and the beads were washed with 500 μ l of washing buffer (50 mM NaH₂PO₄, 300 mM NaCl, 20 mM imidazole, pH 8.0). This washing step was repeated two more times before the beads were finally incubated in 40 μ l Lämmli buffer for 5 min at 99 °C. Then 15 μ l of the samples were run on an SDS-PAGE and the amount of Strep-tagged protein still present in these samples was documented on a Western blot incubated with a Strep-Tactin alkaline phosphatase conjugate.

In a second attempt with the same proteins, Dynabeads[®] TalonTM (Invitrogen) were used instead of the Ni-NTA agarose. Therefore 50 μ l of Dynabeads[®] TalonTM beads were transferred to a plastic tube, which was placed onto a magnet (DynaMPC). Then the supernatant was removed and the beads were equilibrated with 700 μ l TalonTM Binding and Washing buffer (50 mM NaH₂PO₄, 300 mM NaCl, 0.01% Tween-20, pH8.0). Again the supernatant was removed using a magnet and the beads were resuspended in 100 μ l buffer. Then the proteins, which were incubated together at room temperature for 30 min, were added to the beads and the sample was mixed for 10 min at room temperature. Afterwards the supernatant was removed and the beads were washed four times with 700 μ l TalonTM Binding and Washing buffer. Finally the beads were incubated in 40 μ l Lämmli buffer for 5 min at 99 °C and 15 μ l of the sample were separated on an SDS-PAGE. The amount of remaining Strep-tagged protein was again documented on a Western blot with a Strep-Tactin alkaline phosphatase conjugate.

In a third experiment, a protein with a His- and a Strep-tag was tested together with a protein bearing a His- and a Flag-tag. Both proteins were purified via the His-tag and incubated for 30 min at room temperature. Then 100 μ l of Strep-Tactin Sepharose was added and the samples were incubated for one hour at 4 °C. After centrifugation for 30 sec at 14000 rpm, the supernatant was removed and the beads were washed five times with Buffer W (100 mM Tris-Cl, 150 mM NaCl, 1 mM EDTA, pH8.0). Again, 40 μ l Lämmli buffer were added and the samples were incubated for 5 min at 99 °C. 15 μ l of the samples were run on an SDS-PAGE and the amount of Flag-tagged protein could be directly detected on the Coomassie stained gel.

In all three experiments, a negative control was performed by processing 50 μ l of the second protein without the first protein in the same manner as described for the protein mix.

***In vitro* thioester reaction**

In the second step of the ubiquitylation cascade, ubiquitin is transferred to the E2 and a thioester is formed between the C-terminal glycine of ubiquitin and an internal cysteine residue of the E2. Therefore, ubiquitin is first activated by the ubiquitin activating enzyme making use of ATP. Such thioester reactions were performed *in vitro* by mixing the components described in table 4.7 and incubating the samples for 10 min at 30 °C. The reaction was stopped by addition of 20 μ l non-reducing sample buffer and incubation for 15 min at 30 °C. Afterwards 15 μ l of the sample were separated on a 10 % SDS-PAGE, which was run at 4 °C and not more than 24 mA.

- 10 x reaction buffer: 200 mM Tris (pH 7.6), 500 mM NaCl, 100 mM MgCl₂

- ATP solution: 100 mM ATP, 100 mM Mg(OAc)₂, 20 mM HEPES (pH 7.4)
- non-reducing sample buffer: 50 mM Tris-HCl (pH 6.8), 2 % SDS, 10% glycerol, 4 M urea, 0.003 % bromophenolblue

Table 4.7: Thioester reaction mix

Component	Amount
Ubiquitin (BIOMOL)	1 μ g
UBA1-His (obtained from K. Maderböck)	5 ng
E2	approx. 200 ng
10 x reaction buffer	2 μ l
ATP solution	1 μ l
ddH ₂ O	ad 20 μ l

In vitro ubiquitylation assay

The covalent attachment of ubiquitin to the PHO2 protein fragment was tested by mixing the same components as described for the thioester reaction. The only difference was that in this case a recombinant His-tagged human E1 was obtained from BIOMOL. Then the reaction was incubated for three hours at 25 °C and was finally stopped by addition of 20 μ l Lämmli buffer and incubation for 5 min at 99 °C. 15 μ l of the sample were run on an SDS-PAGE at 120 V and room temperature.

Appendices

Appendix A

Plasmids used or constructed in this thesis

- pBluescript II-PFU2 (**this work**): contains the complete open reading frame of *PFU2* and was produced for further cloning of EGFP/mRFP fusion constructs, cloning described in chapter 2.1.2
- p3-PFU1-EGFP (Dr. A. Bachmair): for transient expression of the PFU1-EGFP fusion protein in *Nicotiana benthamiana* under the control of the constitutive 35S promoter
- p3-PFU2-EGFP (**this work**): for transient expression of the PFU2-EGFP fusion protein in *Nicotiana benthamiana* under the control of the constitutive 35S promoter, cloning described in chapter 2.3.1
- p3-PFU2-mRFP (**this work**): for transient expression of the PFU2-mRFP fusion protein in *Nicotiana benthamiana* under the control of the constitutive 35S promoter, cloning described in chapter 2.3.1
- p3-PFU3-EGFP (Dr. A. Bachmair): for transient expression of the PFU3-EGFP fusion protein in *Nicotiana benthamiana* under the control of the constitutive 35S promoter
- p3-PFU3-mRFP (Dr. A. Bachmair): for transient expression of the PFU3-mRFP fusion protein in *Nicotiana benthamiana* under the control of the constitutive 35S promoter
- p3-PHO2-mRFP (Dr. A. Bachmair): for transient expression of the PHO2-mRFP fusion protein in *Nicotiana benthamiana* under the control of the constitutive 35S promoter
- pER8-PFU1-EGFP (Dr. A. Bachmair): for expression of the PFU1-EGFP fusion protein in stably transformed *Arabidopsis thaliana* plants under the control of a β -estradiol inducible promoter

- pER8-PFU2-EGFP (**this work**): for expression of the PFU2-EGFP fusion protein in stably transformed *Arabidopsis thaliana* plants under the control of a β -estradiol inducible promoter, cloning described in chapter 2.3.1
- pER8-PFU2-mRFP (**this work**): for expression of the PFU2-mRFP fusion protein in stably transformed *Arabidopsis thaliana* plants under the control of a β -estradiol inducible promoter, cloning described in chapter 2.3.1
- pER8-PFU3-EGFP (Dr. A. Bachmair): for expression of the PFU3-EGFP fusion protein in stably transformed *Arabidopsis thaliana* plants under the control of a β -estradiol inducible promoter
- pER8-PFU3-mRFP (Dr. A. Bachmair): for expression of the PFU3-mRFP fusion protein in stably transformed *Arabidopsis thaliana* plants under the control of a β -estradiol inducible promoter
- pER8-PHO2-mRFP (Dr. A. Bachmair): for expression of the PHO2-mRFP fusion protein in stably transformed *Arabidopsis thaliana* plants under the control of a β -estradiol inducible promoter
- pGBKT7-PFU1 (**this work**): for yeast expression of PFU1 fused to the GAL4 DNA-binding domain, cloning described in chapter 2.27
- pGBKT7-PFU1UBCCtoA (**this work**): for yeast expression of a PFU1-GAL4 DBD fusion protein where the conserved cysteine residue in the UBC domain is changed to alanine, cloning described in chapter 2.27
- pGBKT7-PFU1CTCtoA (**this work**): for yeast expression of a PFU1-GAL4 DBD fusion protein where the conserved cysteine residue in the C-terminal domain is changed to alanine, cloning described in chapter 2.27
- pGBKT7-PFU1UBCCCTCtoA (**this work**): for yeast expression of a PFU1-GAL4 DBD fusion protein where the cysteine residues in both the UBC and the C-terminal domain are changed to alanine, cloning described in chapter 2.27
- pGBKT7-PHO2 (**this work**): for expression of PHO2 fused to the GAL4 DNA-binding domain in yeast, cloning described in chapter 2.27
- pGBKT7-PHO2UBCCtoA (**this work**): for yeast expression of a PHO2-GAL4 DBD fusion protein where the conserved cysteine residue in the UBC domain is changed to alanine, cloning described in chapter 2.27
- pGBKT7-PHO2CTCtoA (**this work**): for yeast expression of a PHO2-GAL4 DBD fusion protein where the conserved cysteine residue in the C-terminal domain is changed to alanine, cloning described in chapter 2.27

-
- pGBKT7-PHO2UBCCTCtoA (**this work**): for yeast expression of a PHO2-GAL4 DBD fusion protein where the cysteine residues in both the UBC and the C-terminal domain are changed to alanine, cloning described in chapter 2.27
 - pGAD-TUP1 (**this work**): this vector is a modified form of pGAD424 (Clontech), where the GAL4 activation domain is exchanged by the yeast TUP1 repressor domain, cloning described in chapter 2.4.2
 - pGAD-TUP1-PFU1 (**this work**): for yeast expression of PFU1 fused to the TUP1 repressor domain, cloning described in chapter 2.4.2
 - pGAD-TUP1-PHO2 (**this work**): for yeast expression of PHO2 fused to the TUP1 repressor domain, cloning described in chapter 2.4.2
 - pGBKT7-PFU1CT (**this work**): for yeast expression of the C-terminal domain of PFU1 fused to the GAL4 DNA-binding domain, cloning described in chapter 2.4.3
 - pGBKT7-PHO2CT (**this work**): for yeast expression of the C-terminal domain of PHO2 fused to the GAL4 DNA-binding domain, cloning described in chapter 2.4.3
 - pGAD424-PFU1CT (**this work**): for yeast expression of the C-terminal domain of PFU1 fused to the GAL4 activation domain, cloning described in chapter 2.4.3
 - pET42c-PFU1CT487 (**this work**): for overexpression of the C-terminal domain of PFU1, starting with amino acid 487 and possessing a His-tag at the C-terminus, cloning described in chapter 2.5.1
 - pET42c-PFU1CT489 (**this work**): for overexpression of the C-terminal domain of PFU1, starting with amino acid 489 and possessing a His-tag at the C-terminus, cloning described in chapter 2.5.1
 - pET42c-PFU1CT491 (**this work**): for overexpression of the C-terminal domain of PFU1, starting with amino acid 491 and possessing a His-tag at the C-terminus, cloning described in chapter 2.5.1
 - pET42c-PFU1CT493 (**this work**): for overexpression of the C-terminal domain of PFU1, starting with amino acid 493 and possessing a His-tag at the C-terminus, cloning described in chapter 2.5.1
 - pET42c-PFU1CT495 (**this work**): for overexpression of the C-terminal domain of PFU1, starting with amino acid 495 and possessing a His-tag at the C-terminus, cloning described in chapter 2.5.1
 - pET42c-PFU1CT497 (**this work**): for overexpression of the C-terminal domain of PFU1, starting with amino acid 497 and possessing a His-tag at the C-terminus, cloning described in chapter 2.5.1

- pET42c-PFU1CT499 (**this work**): for overexpression of the C-terminal domain of PFU1, starting with amino acid 499 and possessing a His-tag at the C-terminus, cloning described in chapter 2.5.1
- pET42c-PFU1CT501 (**this work**): for overexpression of the C-terminal domain of PFU1, starting with amino acid 501 and possessing a His-tag at the C-terminus, cloning described in chapter 2.5.1
- pET42c-PFU1CT503 (**this work**): for overexpression of the C-terminal domain of PFU1, starting with amino acid 503 and possessing a His-tag at the C-terminus, cloning described in chapter 2.5.1
- pET42c-PFU1CT499 Flag (**this work**): for overexpression of the C-terminal domain of PFU1, starting with amino acid 499 and possessing a Flag-tag at the C-terminal end, cloning described in chapter 2.5.1
- pET42c-PFU1CT501 Flag (**this work**): for overexpression of the C-terminal domain of PFU1, starting with amino acid 501 and possessing a Flag-tag at the C-terminal end, cloning described in chapter 2.5.1
- pET42c-PFU1CT499 Strep (**this work**): for overexpression of the C-terminal domain of PFU1, starting with amino acid 499 and possessing a Strep-tag at the C-terminal end, cloning described in chapter 2.5.1
- pET42c-PFU1CT501 Strep (**this work**): for overexpression of the C-terminal domain of PFU1, starting with amino acid 501 and possessing a Strep-tag at the C-terminal end, cloning described in chapter 2.5.1
- pET42c-PFU1CT StrepHis (**this work**): for overexpression of the C-terminal domain of PFU1, starting with amino acid 499 and possessing both a Strep- and a His-tag at the C-terminal end, cloning described in chapter 2.5.1
- pSUMOGG (Dr. A. Bachmair): to amplify the open reading frame of the *Arabidopsis SUMO* gene for further cloning of SUMO-PFU fusion constructs
- pET42c-SUMO PFU1CT (**this work**): for overexpression of the C-terminal domain of PFU1, starting with amino acid 487 and possessing SUMO fused to the N-terminus and a His-tag at the C-terminus, cloning described in chapter 2.5.1
- pET42c-GST PFU1CT (**this work**): for overexpression of the C-terminal domain of PFU1, starting with amino acid 487 and possessing a GST-tag at the N-terminus and a His-tag at the C-terminus, cloning described in chapter 2.5.1
- pET42c-PHO2CT (**this work**): for overexpression of the C-terminal domain of PHO2, possessing a His-tag at the C-terminal end, cloning described in chapter 2.5.1

-
- pET42c-SUMO PHO2CT (**this work**): for overexpression of the C-terminal domain of PHO2, fused to the C-terminus of SUMO and possessing a His-tag at the C-terminal end, cloning described in chapter 2.5.1
 - pET42c-GST PHO2CT (**this work**): for overexpression of the C-terminal domain of PHO2, possessing a GST-tag at the N-terminus and a His-tag at the C-terminal end, cloning described in chapter 2.5.1
 - pET42c-PFU1UBC (**this work**): for overexpression of the UBC domain of PFU1 (aa 326-490), fused to a GST-tag, a His-tag and an S-tag at the N-terminus and an additional His-tag at the C-terminus, cloning described in chapter 2.5.1
 - pET42c-PHO2UBC (**this work**): for overexpression of the UBC domain of PHO2 (aa 664-823), fused to a GST-tag, a His-tag and an S-tag at the N-terminus and an additional His-tag at the C-terminus, cloning described in chapter 2.5.1
 - pET42c-PHO2UBC long (**this work**): for expressing a longer fragment of the UBC domain of PHO2 (aa 609-828), fused to a GST-tag, a His-tag and an S-tag at the N-terminus and an additional His-tag at the C-terminus, cloning described in chapter 2.5.1
 - pETUBC27 (Budhiraja et al. 2009): this plasmid is a modified form of pET42c containing the open reading frame of *UBC27* fused to a Flag-tag and was used to replace the *UBC27* fragment by the open reading frame of *PFU1* to obtain a Flag-tagged version of this protein.
 - pET-PFU1Flag (**this work**): for overexpression of the complete PFU1 protein, possessing a Flag- and a His-tag at the C-terminus, cloning described in chapter 2.5.1
 - pET42c-PFU1UBCCT (**this work**): for overexpression of the UBC- and C-terminal domain of PFU1 (aa 326-end), possessing a His-tag at the C-terminus, cloning described in chapter 2.5.1
 - pET42c-PFU1UBCCT short (**this work**): for overexpression of the UBC- and C-terminal domain of PFU1 (aa 326-end), possessing a GST-tag, a His-tag and an S-tag at the N-terminus and an additional His-tag at the C-terminus, cloning described in chapter 2.5.1
 - pET42c-PFU1UBCCT long (**this work**): for overexpression of the UBC- and C-terminal domain of PFU1 (aa 285-end), possessing a GST-tag, a His-tag and an S-tag at the N-terminus and an additional His-tag at the C-terminus, cloning described in chapter 2.5.1
 - pET42c-PHO2UBCCT (**this work**): for overexpression of the UBC and C-terminal domain of PHO2 (aa 664-end), possessing a His-tag at the C-terminus, cloning described in chapter 2.5.1

- pET42c-PHO2UBCCT long (**this work**): for overexpression of the UBC- and C-terminal domain of PHO2 (aa 609-end), possessing a GST-tag, a His-tag and an S-tag at the N-terminus and an additional His-tag at the C-terminus, cloning described in chapter 2.5.1

Appendix B

Oligonucleotides

Oligos used to clone the *PFU2* open reading frame and the EGFP/mRFP fusion proteins

746A-LET2startdn: CCCTCGAGCATATGGAGCATGAGCAAGATGACCCT
747A-LET2Speup: CTTTGAGGAGGATCGTCACTAGTT
805A-LET2Spedn2: CAAAAGTAACTAGTGACGATCCT
807A-LET2Bstup: GTTCTTCTGCCCTTTCGAAGTGGATT
806A-LET2Bstdn: CCACTTCGAAGGGCAGAAGAACCC
808A-LET2Pshup2: TGA CTAGGGTCATCAAGGGAATCTGTT
750A-LET2Pshdn: GCCTCTAGACCAACCCGTCCGATGAAACAGATTCC
751A-LET2endup: GCGGAGCTCCCGGGTTATTGCTGCTGCAGATGCTGGAATT
837A-LET2Kpnup: CGCCGAGCTCGGTACCTTGCTGCTGCAGATGCT
876A-OmXNdetop: TCGAGTACGTAATTTACAATTTAAA
877A-OmXNdebot: TATTTAATTGTAAATTACGTAC

Oligos used to clone the *PFU2* open reading frame and the EGFP/mRFP fusion proteins

746A-LET2startdn: CCCTCGAGCATATGGAGCATGAGCAAGATGACCCT
747A-LET2Speup: CTTTGAGGAGGATCGTCACTAGTT
805A-LET2Spedn2: CAAAAGTAACTAGTGACGATCCT
807A-LET2Bstup: GTTCTTCTGCCCTTTCGAAGTGGATT
806A-LET2Bstdn: CCACTTCGAAGGGCAGAAGAACCC
808A-LET2Pshup2: TGA CTAGGGTCATCAAGGGAATCTGTT
750A-LET2Pshdn: GCCTCTAGACCAACCCGTCCGATGAAACAGATTCC
751A-LET2endup: GCGGAGCTCCCGGGTTATTGCTGCTGCAGATGCTGGAATT
837A-LET2Kpnup: CGCCGAGCTCGGTACCTTGCTGCTGCAGATGCT
876A-OmXNdetop: TCGAGTACGTAATTTACAATTTAAA
877A-OmXNdebot: TATTTAATTGTAAATTACGTAC

Oligos used to determine the length of the *PFU2* leader sequence

535A-LET2dn4: GAGATATAAAGGGATGGGTGATGCCATT
 534A-LET2dn3: CCAGGACAAGCCATTATGTGGGCTGTT
 118A-LET2dn: CACGTTTGGAACACAGGCCACATTT
 966A-LET2dn8: GTAGTTGAACAGAAGAGTGCTATC
 965A-LET2dn7: ACGGCTGAGATTCGGTGAGTGGCC
 964A-LET2dn6: CATTATATATTCGCGTAGAATCTCT
 963A-LET2dn5: CTGTGTTAGCTTGGAGGATGTTGTT
 533A-LET2up3: ATTTGTTGATGTACCAGGGTCATCTT

Oligos used to analyze the *PFU3* gene structure

976A-LET3dn9: GCATAAAGCTAGCTACATCGGTCTT
 975A-LET3up9: GACTGCATCAGGCGAGTCCAAGTCT
 967A-LET3dn5: GGTAAAGGCGGAGTCCAAGACCTT
 968A-LET3up5: CCCTCAGCAGCATAGTGATGATCT

Oligos used to identify homozygous T-DNA insertion lines

SALK LBa1: TGGTTCACGTAGTGGGCCATCG
 GarliCLB1: GCCTTTTCAGAAATGGATAAATAGCCTTGCTTCC
 117A-LET1dn: GATCGCTACTCCTCCTGCCGCTTCTT
 141A-LET1up: CACAAAGGTAGCCACATCTGTCCTAAACT
 198A-LET2up1: CTGATCTCCCTCAAGTGCACCACATT
 533A-LET2up3: ATTTGTTGATGTACCAGGGTCATCTT
 534A-LET2dn3: CCAGGACAAGCCATTATGTGGGCTGTT
 429A-LET3up4: AGCCATTTCTCCCTCGCGCTACCT
 235A-LET3startdn: TGATCGCTTCGGGTTCTAGAACTC
 120A-LET4up: GGTTCCGATTCAGTCGCATCCCACCT
 161A-LET4dn: TATTCAGTTCCATGGCAGGCGTCT

Oligos used to determine the gene expression level in WT and mutant lines

999A-LET2endups: GTTATTGCTGCTGCAGATGCTGGAATT
 527A-LET4Ndn: GCCCTCGAGTCGACATTTACAATTACCATGGAAATGTCCCTTACT
 GACTCT
 525A-LET4Cup: GGCACCACATGTTGGTACCTGATTCTGGTCCAATCTCTTGGAC
 AtUBC9Ndedn: GGAATTCCATATGGCATCGAAACGGATTTTGAAG
 AtUBC9Notup: AATTCGGGGCGGCCGCCCGCCCATGGCATACTTTTGGGT

Oligos used to analyze the expression of the ubK48R transgene

144A-pTAdn: GACCCTTCCTCTATATAAGGAAGTTC

200A-DHFRup: ATCCCATATTTTGGGACAC

Additional oligos used to analyze the expression of the EGFP/mRFP transgenes

471A-GFPup1: GCTCTTGAAGAAGTCGTGCCGCTTC

524A-RFPNseq: GGCCGTTACGGAGCCCTCCAT

526A-LET4Cdn: GGCCTCGAGATTCAGGTGGGATGCGACTGAAT

Oligos used to clone the TUP1 repressor domain into the yeast vector pGAD424

1061-GADH3link2bot: AGCTCCCGGGCGGATATCGATGGTACCTGGCCA

1062-GADH3link2top: AGCTTGGCCAGGTACCATCGATATCCGCCCCGGG

997A-H3TUPdn: GCCGCAAGCTTATTATGACTGCCAGCGTTTCGAATACGCAA

998A-H3TUPup: GCCGCAAGCTTCTAGGTACCCGGGCATATGCGAATTCTGGGC
CACGGAAAC

1075-GADstopexttop: TATGTCCATGGCCTCGAGGTACCTGATTAGTTAGCGTAC

1076-GADstopextbot: GCTAACTAATCAGGTACCTCGAGGCCATGGACA

Oligos used to amplify the C-terminus of *PFU1* for further cloning into pGAD424

1250-LET1CEcodn: CCCGAATTCTCTTTAAAGACTATGGTTTACACC

1269-LET1Cup3: CCCGCCAGATCTTCAACTAGAAGAACTCTGTCTCTCTT

Oligos used to clone different C-terminal fragments of *PFU1* into pET42c

1169-LET1Cdomdn: CCCGCATATGTCTTTAAAGACTATGGTTTACAC

1173-LET1Cup2: GGGCTCGAGACTAGAAGAACTCTGTCTCTCTT

1225-LET1CdomdnKT: CCCGCATATGAAGACTATGGTTTACACCATGAGG

1226-LET1CdomdnMV: CCCGCATATGATGGTTTACACCATGAGGAGACC

1227-LET1CdomdnYT: CCCGCATATGTACACCATGAGGAGACCACC

1228-LET1CdomdnMR: CCCGCATATGAGGAGACCACCCAAGTATTTT

1229-LET1CdomdnRP: CCCGCATATGAGACCACCCAAGTATTTTGAAGACT

1230-LET1CdomdnPK: CCCGCATATGCCCAAGTATTTTGAAGACTTTGCG

1231-LET1CdomdnYF: CCCGCATATGTATTTTGAAGACTTTGCGTATGGACAT

1232-LET1CdomdnED: CCCGCATATGGAAGACTTTGCGTATGGACATTTT

Oligos used to fuse the C-terminus of PFU1 and PHO2 to different protein tags

1235-LET1CFlagup: GGGCTCGAGCTATTTATCATCGTCATCTTTATAATCACTAGAA
GAAACTCTGTCTCT
1234-LET1CStrepup: GGGCTCGAGCTATTTTTTCGAACTGGGGATGGCTCCAACTA
GAAGAACTCTGTCTCT
1242-SUMCT1fusdn: CCGTCTAGAAATAATTTTGTTTAACTTTAAGAAGGAGATATAAA
TATGTCTGCAAACCAGGAGGAA
1243-SUMCT1fusup: CCGCATATGGCCACCAGTCTGATGGAGCAT

Oligos used to amplify the C-terminus of *PHO2* for subsequent cloning into pET42c

1170-LET4Cdomdn: CGGGCATATGTTTCCTCATAACCTGCAAATCCAT
1174-LET4Cup2: GGCTCTCGAGTGATTCTGGTCCAATCTCTTGGAC

Oligos used to amplify the UBCdomains of *PFU1* and *PHO2*

788A-LET1UBCdN: CCGCCATGGCGTCAAAGCAGCATTCAAAGGATT
789A-LET1UBCup: GGGCTCGAGTTAAGTCTTTAAAGACAGTATGAATGT
752A-LET4UBCdN: CCGCCATGGTGAAGAAAGTCCAGCAAGAAT
753A-LET4UBCup: GGGCTCGAGTTATGAGATCATGGATTTGCAGGTTAT
1239-LET4lgUBCdN: CCGCCATGGCTATAGAAGGAAAAGGAATT
1240-LET4lgUBCup: GGGCTCGAGTTACTTACGGAGCATTGAGATC

Additional oligos needed to clone the UBCand the C-terminal domain of *PFU1* and *PHO2* into pET42c

1171-LET1UBCdN2: CCCGCATATGACTTCAAAGCAGCATTCAAAGGATT
1172-LET4UBCdN2: CCCGCATATGGTGGAGGAAGTCCAGCAAGAAT
1279-LET1UBCdN3: CCCGCCATGGCCCCCTCCGGATGATTCCAGAGTT
1249-LET4CFLAG: GGCTCTCGAGCTTGTCATCGTCGTCCTTGTAGTCTGATTCTG
GTCCAATCTCTTG

Appendix C

Abbreviations

All important abbreviations used in this thesis are listed below. Only commonly used SI and IUPAC nomenclature as well as abbreviations for amino acids and organic bases are not explained.

aa	amino acid
ADH1	alcohol dehydrogenase
AIF	apoptosis inducing factor
AMP	adenosine monophosphate
AMPK	adenosine monophosphate kinase
ATE1	arginyl-tRNA:protein arginyl transferase1
ATP	adenosine triphosphate
AtRab5	Ras-related in brain 5 of <i>Arabidopsis thaliana</i>
ASK1	Arabidopsis suppressor of kinetochore protein 1
<i>A. tumefaciens</i>	<i>Agrobacterium tumefaciens</i>
AvrPtoB	avirulence protein (of <i>Pseudomonas syringae</i>) pathovar tomato
Bak	BCL2-antagonist/killer
BARD1	BRCA1 associated RING domain 1
Bax	BCL2-associated X protein
BCL-2	B-cell leukemia/lymphoma 2
bp	base pairs
Bin1	bridging integrator 1
BIR	baculovirus inhibitor of apoptosis repeat
BRCA1	breast cancer 1
BRUCE	BIR repeat containing ubiquitin-conjugating enzyme
bZIP	basic leucine zipper domain
cDNA	copy-DNA
Co-IP	co-Immunoprecipitation
Col-0	Columbia-0

COP9	constitutive photomorphogenic 9
CSN5	COP9 complex homolog subunit 5
C-terminus	carboxy-terminus
DBD	DNA-binding domain
DHFR	dihydrofolate reductase
<i>dls1</i>	<i>delayed leaf senescence1</i>
DNA	deoxyribonucleic acid
DO	dropout
DTT	Dithiothreitol
DTX	deltex
DUB	deubiquitylating enzyme
<i>E. coli</i>	<i>Escherichia coli</i>
EGFP	enhanced green fluorescent protein
EMS	ethyl methylsulfonate
ER	endoplasmatic reticulum
FRET	fluorescence resonance energy transfer
GSNO	S-nitrosoglutathione
GST	glutathione S-transferase
HECT	homology to E6-AP carboxy terminus
HtrA2	mitochondrial high-temperature requirement Serine protease
IAP	inhibitor of apoptosis
<i>IPS1</i>	induced by phosphate starvation1
IPTG	Isopropyl β -D-1-thiogalactopyranoside
JA	jasmonic acid
JAMM	JAB1/MPN/Mov34 metalloenzyme
LB	Lysogeny Broth
LSD1	lysine demethylase 1
Mdm2	mouse double minute 2
miRNA	microRNA
MMS	malignant mesothelioma
MoaD	molybdopterin synthase, small subunit D
mRFP	monomeric red fluorescent protein
mRNA	messenger RNA
MS medium	Murashige and Skoog medium
Nedd8	neural precursor cell expressed, developmentally down-regulated 8
NES	nuclear export signal
Ni-NTA	nickel-nitrilotriacetic acid
NLS	nuclear localization signal
NMR	nuclear magnetic resonance
NO	nitric oxide
N-terminus	amino-terminus
ORE9	oresara 9
ORF	open reading frame

PARP	poly-(ADP-ribose) polymerase
PCD	programmed cell death
PCR	polymerase chain reaction
PFU	PHO2-family ubiquitin conjugating enzyme
PHO2	phosphate 2
PHR1	photolyase 1
Pht	phosphate transporter
P _i	inorganic phosphate
PRT6	proteolysis 6
PSI	phosphate starvation induced
PUB17	plant U-box 17
RDR6	RNA-dependent RNA polymerase 6
RNA	ribonucleic acid
ROS	reactive oxygen species
RNS	reactive nitrogen species
Rpn	proteasome regulatory particle, non-ATPase-like
RT-PCR	reverse transcriptase-polymerase chain reaction
Rub1	related to ubiquitin 1
SA	salicylic acid
SAUL1	senescence-associated E3 ubiquitin ligase 1
SC	synthetic complete
<i>S. cerevisiae</i>	<i>Saccharomyces cerevisiae</i>
SDS-PAGE	sodium dodecyl sulfate polyacrylamide gel electrophoresis
SIZ1	SAP and mIZ-finger domain
Smac	second mitochondria-derived activator of caspase
SPL11	squamosa promoter-binding protein-like 11
SUMO	small ubiquitin-like modifier
T-DNA	transfer DNA
TGN	Trans-Golgi-Network
ThiS	thiamine sulfur carrier protein
t-RNA	transfer-RNA
TRP1	tryptophan biosynthesis 1
TUP1	deoxythymidine monophosphate uptake
Ub	ubiquitin
UBA1	ubiquitin activating enzyme1
UBC	ubiquitin conjugating
UBE2O	ubiquitin-conjugating enzyme E2O
ubK48R	mutant form of ubiquitin with lysine 48 changed to arginine
UBP	ubiquitin-specific protease
UEV	ubiquitin E2-variant
UTR	untranslated region
WT	wild type
YFP	yellow fluorescent protein

Bibliography

- Addepalli, B., Meeks, L. R., Forbes, K. P. and Hunt, A. G. (2004). Novel alternative splicing of mRNAs encoding poly(A) polymerases in *Arabidopsis*. *Biochimica et Biophysica Acta* **1679**, 117–128. 83
- Ahlfors, R., Brosché, M., Kollist, H. and Kangasjärvi, J. (2009). Nitric oxide modulates ozone-induced cell death, hormone biosynthesis and gene expression in *Arabidopsis thaliana*. *Plant Journal* **58**, 1–12. 89
- Al-Hakim, A. K., Zagorska, A., Chapman, L., Deak, M., Peggie, M. and Alessi, D. R. (2008). Control of AMPK-related kinases by USP9X and atypical Lys²⁹/Lys³³-linked polyubiquitin chains. *Biochemical Journal* **411**, 249–260. 6
- Alonso, J. M., Stepanova, A. N., Leisse, T. J., Kim, C. J., Chen, H., Shinn, P., Stevenson, D. K., Zimmerman, J., Barajas, P., Cheuk, R., Gadrinab, C., Heller, C., Jeske, A., Koesema, E., Meyers, C. C., Parker, H., Prednis, L., Ansari, Y., Choy, N., Deen, H., Geralt, M., Hazari, N., Hom, E., Karnes, M., Mulholland, C., Ndubaku, R., Schmidt, I., Guzman, P., Aguilar-Henonin, L., Schmid, M., Weigel, D., Carter, D. E., Marchand, T., Risseuw, E., Brogden, D., Zeko, A., Crosby, W. L., Berry, C. C. and Ecker, J. R. (2003). Genome-wide insertional mutagenesis of *Arabidopsis thaliana*. *Science* **301**, 653–657. 85
- Alves-Júnior, L., Niemeier, S., Hauenschild, A., Rehmsmeier, M. and Merkle, T. (2009). Comprehensive prediction of novel microRNA targets in *Arabidopsis thaliana*. *Nucleic Acids Research* **37**, 4010–4021. 82
- Ameisen, J. C. (2002). On the origin, evolution and nature of programmed cell death: a timeline of four billion years. *Cell Death and Differentiation* **9**, 367–393. 1, 2
- Aung, K., Lin, S. I., Wu, C. C., Huang, Y. T., Su, C. L. and Chiou, T. J. (2006). *pho2*, a phosphate overaccumulator, is caused by a nonsense mutation in a *microRNA399* target gene. *Plant Physiology* **141**, 1000–1011. 85
- Bachmair, A., Novatchkova, M., Potuschak, T. and Eisenhaber, F. (2001). Ubiquitylation in plants: a post-genomic look at a post-translational modification. *Trends in Plant Science* **6**, 463–470. 11, 12, 15, 17, 25, 79

- Bader, M. and Steller, H.** (2009). Regulation of cell death by the ubiquitin–proteasome system. *Current Opinion in Cell Biology* **21**, 878–884. 2
- Bari, R., Pant, B. D., Stitt, M. and Scheible, W.-R.** (2006). PHO2, *MicroRNA399*, and PHR1 define a phosphate-signaling pathway in plants. *Plant Physiology* **141**, 988–999. 15, 16, 20, 23, 35, 83, 84, 86, 108
- Bartke, T., Pohl, C., Pyrowolakis, G. and Jentsch, S.** (2004). Dual role of BRUCE as an antiapoptotic IAP and a chimeric E2/E3 ubiquitin ligase. *Molecular Cell* **14**, 801–811. 19, 20, 36, 80, 107
- Baruffini, E., Serafini, F. and Lodi, T.** (2009). Construction and characterization of centromeric, episomal and GFP-containing vectors for *Saccharomyces cerevisiae* prototrophic strains. *Journal of Biotechnology* **143**, 247–254. 101
- Bassham, D. C. and Raikhel, N. V.** (2000). Plant cells are not just green yeast. *Plant Physiology* **122**, 999–1002. 97
- Beck, K., Eberhardt, W., Frank, S., Huwiler, A., Messmer, U., Muhl, H. and Pfeilschifter, J.** (1999). Inducible NO synthase: role in cellular signalling. *Journal of Experimental Biology* **202**, 645–653. 89
- Becker, D.** (1990). Binary vectors which allow the exchange of plant selectable markers and reporter genes. *Nucleic Acids Research* **18**, 203. 112
- Becker, F., Buschfeld, E., Schell, J. and Bachmair, A.** (1993). Altered response to viral infection by tobacco plants perturbed in ubiquitin system. *Plant Journal* **3**, 875–881. 13, 14
- Belenghi, B., Romero-Puertas, M. C., Vercammen, D., Brackenier, A., Inze, D., Delledonne, M. and Van Breusegem, F.** (2007). Metacaspase activity of *Arabidopsis thaliana* is regulated by S-nitrosylation of a critical cysteine residue. *Journal of Biological Chemistry* **282**, 1352–1358. 89
- Beranger, F., Aresta, S., De Gunzburg, J. and Camonis, J.** (1997). Getting more from the two-hybrid system: N-terminal fusions to LexA are efficient and sensitive baits for two-hybrid studies. *Nucleic Acids Research* **25**, 2035–2036. 102
- Berleth, E. S. and Pickart, C. M.** (1996). Mechanism of ubiquitin conjugating enzyme E2-230K: catalysis involving a thiol relay? *Biochemistry* **35**, 1664–1671. 17, 18, 26, 66, 77, 80, 99, 107
- Bläsing, O. E., Gibon, Y., Gunther, M., Hohne, M., Morcuende, R., Osuna, D., Thimm, O., Usadel, B., Scheible, W. R. and Stitt, M.** (2005). Sugars and circadian regulation make major contributions to the global regulation of diurnal gene expression in *Arabidopsis*. *Plant Cell* **17**, 3257–3281. 86

- Borisjuk, L. and Rolletschek, H.** (2009). The oxygen status of the developing seed. *New Phytologist* **182**, 17–30. 90
- Bouché, N. and Bouchez, D.** (2001). *Arabidopsis* gene knockout: phenotypes wanted. *Current Opinion in Plant Biology* **4**, 111–117. 84
- Budhiraja, R., Hermkes, R., Müller, S., Schmidt, J., Colby, T., Panigrahi, K., Coupland, G. and Bachmair, A.** (2009). Substrates related to chromatin and to RNA-dependent processes are modified by *Arabidopsis* SUMO isoforms that differ in a conserved residue with influence on desumoylation. *Plant Physiology* **149**, 1529–1540. 67, 139
- Callis, J., Carpenter, T., Sun, C. W. and Viestra, R. D.** (1995). Structure and evolution of genes encoding polyubiquitin and ubiquitin-like proteins in *Arabidopsis thaliana* ecotype Columbia. *Genetics* **139**, 921–939. 4, 10
- Capron, A., Ökrész, L. and Genschik, P.** (2003). First glance at the plant APC/C, a highly conserved ubiquitin–protein ligase. *Trends in Plant Science* **8**, 83–89. 12
- Causier, B. and Davies, B.** (2002). Analysing protein-protein interactions with the yeast two-hybrid system. *Plant Molecular Biology* **50**, 855–870. 97, 98
- Chastagner, P., Israel, A. and Brou, C.** (2006). Itch/AIP4 mediated Deltex degradation through the formation of K29-linked polyubiquitin chains. *EMBO Report* **7**, 1147–1153. 6
- Chau, V., Tobias, J. W., Bachmair, A., Marriott, D., Ecker, D. J., Gonda, D. K. and Varshavsky, A.** (1989). A multiubiquitin chain is confined to specific lysine in a targeted short-lived protein. *Science* **243**, 1576–1583. 6
- Chen, Z., Naito, M., Hori, S., Mashima, T., Yamori, T. and Tsuruo, T.** (1999). A human IAP-family gene, *Apollon*, expressed in human brain cancer cells. *Biochemical and Biophysical Research Communications* **264**, 847–854. 19
- Chichkova, N. V., Shaw, J., Galiullina, R. A., Drury, G. E., Tuzhikov, A. I., Kim, S. H., Kalkum, M., Hong, T. B., Gorshkova, E. N., Torrance, L., Vartapetian, A. B. and Taliansky, M.** (2010). Phytaspase, a relocatable cell death promoting plant protease with caspase specificity. *The EMBO Journal* **29**, 1149–1161. 2
- Ciechanover, A., Heller, H., Elias, S., Haas, A. L. and Hershko, A.** (1980). ATP-dependent conjugation of reticulocyte proteins with the polypeptide required for protein degradation. *PNAS* **77**, 1365–1368. 4
- Davis, G. D., Elisee, C., Newham, D. M. and Harrison, R. G.** (2000). New fusion protein systems designed to give soluble expression in *Escherichia coli*. *Biotechnology and Bioengineering* **65**, 382–388. 104

- Delhaize, E. and Randall, P. J.** (1995). Characterization of a phosphate-accumulator mutant of *Arabidopsis thaliana*. *Plant Physiology* **107**, 207–213. 15, 84, 85
- Delledonne, M., Xia, Y., Dixon, R. A. and Lamb, C.** (1998). Nitric oxide functions as a signal in plant disease resistance. *Nature* **394**, 585–588. 89
- Delledonne, M., Zeier, J., Marocco, A. and Lamb, C.** (2001). Signal interactions between nitric oxide and reactive oxygen intermediates in the plant hypersensitive disease resistance response. *PNAS* **98**, 13454–13459. 40
- Deveraux, Q., Ustrell, V., Pickart, C. and Rechsteiner, M.** (1994). A 26 S protease subunit that binds ubiquitin conjugates. *Journal of Biological Chemistry* **269**, 7059–7061. 10
- di Guana, C., Lib, P., Riggsa, P. D. and Inouyeb, H.** (1988). Vectors that facilitate the expression and purification of foreign peptides in *Escherichia coli* by fusion to maltose-binding protein. *Gene* **67**, 21–30. 105
- Dickman, M., Park, Y., Oltersdorf, T., Li, W., Clemente, T. and French, R.** (2001). Abrogation of disease development in plants expressing animal antiapoptotic genes. *PNAS* **98**, 6957–6962. 3
- Doelling, J., Phillips, A., Soyler-Ogretim, G., Wise, J., Chandler, J., Callis, J., Otegui, M. and Vierstra, R.** (2007). The ubiquitin-specific protease subfamily UBP3/UBP4 is essential for pollen development and transmission in *Arabidopsis*. *Plant Physiology* **145**, 801–813. 12
- Dong, W., Nowara, D. and Schweizer, P.** (2006). Protein polyubiquitination plays a role in basal host resistance of barley. *Plant Cell* **18**, 3321–3332. 14
- Edgar, R. C.** (2004). MUSCLE: multiple sequence alignment with high accuracy and high throughput. *Nucleic Acids Research* **32**, 1792–1797. 23, 24, 115
- Eletr, Z. M., Huang, D. T., Duda, D. M., Schulman, B. A. and Kuhlman, B.** (2005). E2 conjugating enzymes must disengage from their E1 enzymes before E3-dependent ubiquitin and ubiquitin-like transfer. *Nature Structural and Molecular Biology* **12**, 933–934. 7
- Elliott, K., Sakamuro, D., Basu, A., Du, W., Wunner, W., Staller, P., Gaubatz, S., Zhang, H., Prochownik, E., Eilers, M. and Prendergast, G. C.** (1999). Bin1 functionally interacts with Myc and inhibits cell proliferation via multiple mechanisms. *Oncogene* **18**, 3564–3573. 102
- Elmayan, T. and Vaucheret, H.** (1996). Expression of single copies of a strongly expressed *35S* transgene can be silenced post-transcriptionally. *Plant Journal* **9**, 787–797. 92, 94

- Eloy, N. B., Coppens, F., Beemster, G. T. S., Hemerly, A. S. and Ferreira, P. C. G. (2006). The *Arabidopsis* anaphase promoting complex (APC). *Cell Cycle* **5**, 1957–1965. 7
- Endo, Y. and Sawasaki, T. (2006). Cell-free expression systems for eukaryotic protein production. *Current Opinion in Biotechnology* **17**, 373–380. 106
- Fang, S., Jensen, J. P., Ludwig, R. L., Vousden, K. H. and Weissman, A. M. (2000). Mdm2 is a RING finger-dependent ubiquitin protein ligase for itself and p53. *Journal of Biological Chemistry* **275**, 8945–8951. 13
- Fashena, S., Serebriiskii, I. and Golemis, E. (2000). The continued evolution of two-hybrid screening approaches in yeast: how to outwit different preys with different baits. *Gene* **250**, 1–14. 98
- Fath, A., Bethke, P., Beligni, V. and Jones, R. (2002). Active oxygen and cell death in cereal aleurone cells. *Journal of Experimental Botany* **53**, 1273–1282. 4
- Fesik, S. W. (2005). Promoting apoptosis as a strategy for cancer drug discovery. *Nature Reviews Cancer* **5**, 876–885. 1
- Fields, S. and Song, O. (1989). A novel genetic system to detect protein-protein interactions. *Nature* **340**, 245–246. 97, 98, 101
- Finley, D. (2009). Recognition and processing of ubiquitin-protein conjugates by the proteasome. *Annual Review of Biochemistry* **78**, 477–513. 10
- Franco-Zorrilla, J. M., Martin, A. C., Leyva, A. and Paz-Ares, J. (2005). Interaction between phosphate-starvation, sugar, and cytokinin signaling in *Arabidopsis* and the roles of cytokinin receptors CRE1/AHK4 and AHK3. *Plant Physiology* **138**, 847–857. 17
- Franco-Zorrilla, J. M., Valli, A., Todesco, M., Mateos, I., Puga, M. I., Rubio-Somoza, I., Leyva, A., Weigel, D., García, J. A. and Paz-Ares, J. (2007). Target mimicry provides a new mechanism for regulation of microRNA activity. *Nature Genetics* **39**, 1033–1037. 17
- Fujii, H., Chiou, T. J., Lin, S. I., Aung, K. and Zhu, J. K. (2005). A miRNA involved in phosphate-starvation response in *Arabidopsis*. *Current Biology* **15**, 2038–2043. 15, 82
- Gallie, D. R., Sleat, D. E., Watts, J. W., Turner, P. C. and Wilson, T. M. (1987). The 5'-leader sequence of tobacco mosaic virus RNA enhances the expression of foreign gene transcripts *in vitro* and *in vivo*. *Nucleic Acids Research* **15**, 3257–3273. 44
- Gao, H., Brandizzi, F., Benning, C. and Larkin, R. M. (2008). A membrane-tethered transcription factor defines a branch of the heat stress response in *Arabidopsis thaliana*. *PNAS* **105**, 16398–16403. 96

- Garzón, M.** (2008). Links between the ubiquitin-proteasome system and cell death pathways in *Arabidopsis thaliana*. *PhD thesis* . 88
- Garzón, M., Eifler, K., Faust, A., Scheel, H., Hofmann, K., Koncz, C., Yephremov, A. and Bachmair, A.** (2007). *PRT6/At5g02310* encodes an *Arabidopsis* ubiquitin ligase of the N-end rule pathway with arginine specificity and is not the *CER3* locus. *FEBS letters* **581**, 3189–3196. 12
- Gechev, T. S., Van Breusegem, F., Stone, J. M., Denev, I. and Laloi, C.** (2006). Reactive oxygen species as signals that modulate plant stress responses and programmed cell death. *Bioessays* **28**, 1091–1101. 4
- Geldner, N., Déneraud-Tendon, V., Hyman, D. L., Mayer, U., Stierhof, Y. D. and Chory, J.** (2009). Rapid, combinatorial analysis of membrane compartments in intact plants with a multicolor marker set. *Plant Journal* **59**, 169–178. 93
- Golovanov, A. P., Hautbergue, G. M., Wilson, S. A. and Lian, L. Y.** (2004). A simple method for improving protein solubility and long-term stability. *Journal of the American Chemical Society* **126**, 8933–8939. 105
- Goritschnig, S., Zhang, Y. and Li, X.** (2007). The ubiquitin pathway is required for innate immunity in *Arabidopsis*. *Plant Journal* **49**, 540–551. 11
- Gouy, M., Guindon, S. and Gascuel, O.** (2010). SeaView version 4: a multiplatform graphical user interface for sequence alignment and phylogenetic tree building. *Molecular Biology and Evolution* **27**, 221–224. 24, 115
- Greenberg, J. T.** (1996). Programmed cell death: A way of life for plants. *PNAS* **93**, 12094–12097. 1
- Groll, M., Bajorek, M., Kohler, A., Moroder, L., Rubin, D. M., Huber, R., Glickman, M. H. and Finley, D.** (2000). A gated channel into the proteasome core particle. *Nature Structural Biology* **7**, 1062–1067. 9
- Grün, S., Lindermayr, C., Sell, S. and Durner, J.** (2006). Nitric oxide and gene regulation in plants. *Journal of Experimental Botany* **57**, 507–516. 39
- Gupta, K. J., Stoimenova, M. and Kaiser, W. M.** (2005). In higher plants, only root mitochondria, but not leaf mitochondria reduce nitrite to NO, *in vitro* and *in situ*. *Journal of Experimental Botany* **56**, 2601–2609. 89
- Gusmaroli, G., Feng, S. and Deng, X. W.** (2004). The *Arabidopsis* CSN5A and CSN5B subunits are present in distinct COP9 signalosome complexes, and mutations in their JAMM domains exhibit differential dominant negative effects on development. *Plant Cell* **16**, 2984–3001. 86

- Haas, A. L., Warms, J. V., Hershko, A. and Rose, I. A. (1982). Ubiquitin-activating enzyme. Mechanism and the role in protein-ubiquitin conjugation. *Journal of Biological Chemistry* **257**, 2543–2548. 7
- Halliday, K. J., Hudson, M., Ni, M., Qin, M. and Quail, P. H. (1999). *poc1*: an *Arabidopsis* mutant perturbed in phytochrome signaling because of a T DNA insertion in the promoter of *PIF3*, a gene encoding a phytochrome-interacting bHLH protein. *PNAS* **96**, 5832–5837. 84
- Hao, Y., Sekine, K., Kawabata, A., Nakamura, H., Ishioka, T., Ohata, H., Katayama, R., Hashimoto, C., Zhang, X., Noda, T., Tsuruo, T. and Naito, M. (2004). Apollon ubiquitinates SMAC and caspase-9, and has an essential cytoprotection function. *Nature Cell Biology* **6**, 849–857. 19
- Hatfield, P. M., Gosink, M. M., Carpenter, T. B. and Vierstra, R. D. (1997). The ubiquitin-activating enzyme (E1) gene family in *Arabidopsis thaliana*. *Plant Journal* **11**, 213–226. 11
- Hauser, H.-P., Bardroff, M., Pyrowolakis, G. and Jentsch, S. (1998). A giant ubiquitin-conjugating enzyme related to IAP apoptosis inhibitors. *The Journal of Cell Biology* **141**, 1415–1422. 19, 92
- Hershko, A., Ciechanover, A. and Rose, I. A. (1981). Identification of the active amino acid residue of the polypeptide of ATP-dependent protein breakdown. *Journal of Biological Chemistry* **256**, 1525–1528. 4
- Hicke, L. (2001). Protein regulation by monoubiquitin. *Nature Reviews* **2**, 195–201. 6
- Hirst, M., Ho, C., Sabourin, L., Rudnicki, M., Penn, L. and Sadowski, I. (2001). A two-hybrid system for transactivator bait proteins. *PNAS* **98**, 8726–8731. 57, 58, 99, 102, 113
- Hochstrasser, M. (2006). Lingering mysteries of ubiquitin-chain assembly. *Cell* **124**, 27–34. 7
- Hoeller, D., Hecker, C. M., Wagner, S., Rogov, V., Dötsch, V. and Dikic, I. (2007). E3-independent monoubiquitination of ubiquitin-binding proteins. *Molecular Cell* **26**, 891–898. 8, 99
- Hofmann, R. M. and Pickart, C. (1999). Noncanonical *MMS2*-Encoded Ubiquitin-Conjugating Enzyme Functions in Assembly of Novel Polyubiquitin Chains for DNA Repair. *Cell* **96**, 645–653. 7
- Huang, L., Zhang, W. and Roth, S. (1997). Amino termini of histones H3 and H4 are required for $\alpha 1$ - $\alpha 2$ repression in yeast. *Molecular and Cellular Biology* **17**, 6555–6562. 99

- Hulo, N., Bairoch, A., Bulliard, V., Cerutti, L., Cuče, B. A., de Castro, E., Lachaize, C., Langendijk-Genevaux, P. S. and Sigrist, C. J. A. (2007). The 20 years of PROSITE. *Nucleic Acids Research* **36**, Database issue D245–D249. 25, 115
- Husnjak, K., Elsasser, S., Zhang, N., Chen, X., Randles, L., Shi, Y., Hofmann, K., Walters, K. J., Finley, D. and Dikic, I. (2008). Proteasome subunit Rpn13 is a novel ubiquitin receptor. *Nature* **453**, 481–488. 10
- Huyen, Y., Zgheib, O., DiTullio Jr., R. A., Gorgoulis, V. G., Zacharatos, P., Petty, T. J., Sheston, E. A., Mellert, H. S., Stavridi, E. S. and Halazonetis, T. D. (2004). Methylated lysine 79 of histone H3 targets 53BP1 to DNA double-strand breaks. *Nature* **432**, 406–411. 80
- Hwang, N. R., Yim, S. H., Kim, Y. M., Jeong, J., Song, E. J., Lee, Y., Lee, J. H., Choi, S. and Lee, K. J. (2009). Oxidative modifications of glyceraldehyde-3-phosphate dehydrogenase play a key role in its multiple cellular functions. *Biochemical Journal* **423**, 253–264. 102
- Itaya, K. and Ui, M. (1966). A new micromethod for the colorimetric determination of inorganic phosphate. *Clinica Chimica acta; International Journal of Clinical Chemistry* **14**, 361–366. 35, 120
- Jach, G., Pesch, M., Richter, K., Frings, S. and Uhrig, J. F. (2006). An improved mRFP1 adds red to bimolecular fluorescence complementation. *Nature Methods* **3**, 597–600. 43, 91
- James, P., Halladay, J. and Craig, E. A. (1996). Genomic libraries and a host strain designed for highly efficient two-hybrid selection in yeast. *Genetics* **144**, 1425–1436. 111
- Janjusevic, R., Abramovitch, R. B., Martin, G. B. and Stebbins, C. (2006). A bacterial inhibitor of host programmed cell death defenses is an E3 ubiquitin ligase. *Science* **311**, 222–225. 14
- Jesenberger, V. and Jentsch, S. (2002). Deadly encounter: ubiquitin meets apoptosis. *Nature Reviews Molecular Cell Biology* **3**, 112–121. 13
- Jin, J., Li, X., Gygi, S. P. and Harper, J. W. (2007). Dual E1 activation systems for ubiquitin differentially regulate E2 enzyme charging. *Nature* **447**, 1135–1138. 11
- Jin, L., Williamson, A., Banerjee, S., Philipp, I. and Rape, M. (2008). Mechanism of ubiquitin-chain formation by the human anaphase-promoting complex. *Cell* **133**, 653–665. 6
- Kaminaka, H., Näke, C., Epple, P., Dittgen, J., Schütze, K., Chaban, C., Holt III, B. F., Merkle, T., Schäfer, E., Harter, K. and Dangl, J. L. (2006). bZIP10-LSD1 antagonism modulates basal defense and cell death in *Arabidopsis* following infection. *EMBO Journal* **25**, 4400–4411. 96

- Kangasjärvi, J., Jaspers, P. and Kollist, H.** (2005). Signalling and cell death in ozone-exposed plants. *Plant Cell and Environment* **28**, 1021–1036. 87
- Kim, M., Ahn, J. W., Jin, U. H., Choi, D., Paek, K. H. and Pai, H. S.** (2003). Activation of the programmed cell death pathway by inhibition of proteasome function in plants. *Journal of Biological Chemistry* **278**, 19406–19415. 13
- Kirkpatrick, D. S., Hathaway, N. A., Hanna, J., Elsasser, S., Rush, J., Finley, D., King, R. W. and Gygi, S. P.** (2006). Quantitative analysis of *in vitro* ubiquitinated cyclin B1 reveals complex chain topology. *Nature Cell Biology* **8**, 700–710. 6
- Klemperer, N. S., Berleth, E. S. and Pickart, C. M.** (1989). A novel, arsenite-sensitive E2 of the ubiquitin pathway: purification and properties. *Biochemistry* **28**, 6035–6041. 17, 18
- Konrat, R.** (2009). The protein meta-structure: a novel concept for chemical and molecular biology. *Cellular and Molecular Life Sciences* **66**, 3625–3639. 61, 102
- Kraft, E., Stone, S. L., Ma, L., Su, N., Gao, Y., Lau, O.-S., Deng, X.-W. and Callis, J.** (2005). Genome analysis and functional characterization of the E2 and RING-type E3 ligase ubiquitination enzymes of *Arabidopsis*. *Plant Physiology* **139**, 1597–1611. 11, 15, 17, 79, 98, 99, 103, 107
- Krysko, D., Vanden Berghe, T., D’Herde, K. and Vandenabeele, P.** (2008). Apoptosis and necrosis: detection, discrimination and phagocytosis. *Methods* **44**, 205–221. 1
- Kuchin, S. and Carlson, M.** (1998). Functional relationships of Srb10-Srb11 kinase, carboxy-terminal domain kinase CTDK-I, and transcriptional corepressor Ssn6-Tup1. *Molecular and Cellular Biology* **18**, 1163–1171. 99
- Kuras, L., Rouillon, A., Lee, T., Barbey, R., Tyers, M. and Thomas, D.** (2002). Dual regulation of the met4 transcription factor by ubiquitin-dependent degradation and inhibition of promoter recruitment. *Molecular Cell* **10**, 69–80. 6
- la Cour, T., Kiemer, L., Mølgaard, A., Gupta, R., Skriver, K. and Brunak, S.** (2004). Analysis and prediction of leucine-rich nuclear export signals. *Protein Engineering, Design and Selection* **17**, 527–536. 27, 115
- Lake, M. W., Wuebbens, M. M., Rajagopalan, K. V. and Schindelin, H.** (2001). Mechanism of ubiquitin activation revealed by the structure of a bacterial MoeB-MoaD complex. *Nature* **414**, 325–329. 4
- Lam, E. and Del Pozo, O.** (2000). Caspase-like protease involvement in the control of plant cell death. *Plant Molecular Biology* **44**, 417–428. 2

- Lam, E., Kato, N. and Lawton, M.** (2001). Programmed cell death, mitochondria and the plant hypersensitive response. *Nature* **411**, 848–853. 1
- Lan, P., Li, W. and Fischer, R.** (2006). *Arabidopsis thaliana* wildtype, *pho1*, and *pho2* mutant plants show different responses to exogenous cytokinins. *Plant Physiology and Biochemistry* **44**, 343–350. 17
- Lee, U., Wie, C., Fernandez, B. O., Feelisch, M. and Vierling, E.** (2008). Modulation of nitrosative stress by S-nitrosoglutathione reductase is critical for thermotolerance and plant growth in *Arabidopsis*. *Plant Cell* **20**, 786–802. 89
- Leitner, M., Vandelle, E., Gaupels, F., Bellin, D. and Delledonne, M.** (2009). NO signals in the haze: Nitric oxide signalling in plant defence. *Current Opinion in Plant Biology* **12**, 451–458. 89
- Leshem, Y. Y.** (1996). Nitric oxide in biological systems. *Plant Growth Regulation* **18**, 155–159. 39
- Lim, P. O., Kim, H. J. and Nam, H. G.** (2007). Leaf senescence **58**, 115–136. 86, 87
- Lin, S. I., Chiang, S. F., Lin, W. Y., Chen, J. W., Tseng, C. Y., Wu, P. C. and Chiou, T. J.** (2008). Regulatory network of *microRNA399* and PHO2 by systemic signaling. *Plant Physiology* **147**, 732–746. 17
- Liu, J. W., Boucher, Y., Stokes, H. W. and Ollis, D. L.** (2006). Improving protein solubility: the use of the *Escherichia coli* dihydrofolate reductase gene as a fusion reporter. *Protein Expression and Purification* **47**, 258–263. 104
- Liu, L., Hausladen, A., Zeng, M., Que, L., Heitman, J. and Stamler, J. S.** (2001). A metabolic enzyme for S-nitrosothiol conserved from bacteria to humans. *Nature* **410**, 490–494. 89
- London, J., Skrzynia, C. and Goldberg, M. E.** (2005). Renaturation of *Escherichia coli* tryptophanase after exposure to 8 M urea. *European Journal of Biochemistry* **47**, 409–415. 105
- Lorenzo, H., Susin, S., Penninger, J. and Kroemer, G.** (1999). Apoptosis inducing factor (AIF): a phylogenetically old, caspase-independent effector of cell death. *Cell death and differentiation* **6**, 516–524. 2
- Lotz, K., Pyrowolakis, G. and Jentsch, S.** (2004). BRUCE, a giant E2/E3 ubiquitin ligase and inhibitor of apoptosis protein of the trans-Golgi network, is required for normal placenta development and mouse survival. *Molecular and Cellular Biology* **24**, 9339–9350. 20
- Lowenstein, C. J. and Snyder, S. H.** (1992). Nitric oxide, a novel biologic messenger. *Cell* **70**, 705–707. 39

- Makrides, S. C.** (1996). Strategies for achieving high-level expression of genes in *Escherichia coli*. *Microbiology and Molecular Biology Reviews* **60**, 512–538. 104
- Matsukura, S., Mizoi, J., Yoshida, T., Todaka, D., Ito, Y., Maruyama, K., Shinozaki, K. and Yamaguchi-Shinozaki, K.** (2010). Comprehensive analysis of rice DREB2-type genes that encode transcription factors involved in the expression of abiotic stress-responsive genes. *Molecular Genetics and Genomics* **283**, 185–196. 83
- Michelle, C., Vourc'h, P., Mignon, L. and Andres, C. R.** (2009). What was the set of ubiquitin and ubiquitin-like conjugating enzymes in the eukaryote common ancestor? *Journal of Molecular Evolution* **68**, 616–628. 7, 11, 17, 79
- Millar, A. H., Carrie, C., Pogson, B. and Whelan, J.** (2009). Exploring the function-location nexus: using multiple lines of evidence in defining the subcellular localisation of the plant proteins. *Plant Cell* **21**, 1625–1631. 93, 95
- Miller, J. D., Arteca, R. N. and Pell, E. J.** (1999). Senescence-associated gene expression during ozone-induced leaf senescence in *Arabidopsis*. *Plant Physiology* **120**, 1015–1023. 39
- Mishina, T. E., Lamb, C. and Zeier, J.** (2007). Expression of a nitric oxide degrading enzyme induces a senescence programme in *Arabidopsis*. *Plant, Cell and Environment* **30**, 39–52. 89
- Mittler, R. and Rizhsky, L.** (2000). Transgene-induced lesion mimic. *Plant Molecular Biology* **44**, 335–344. 86
- Miura, K., Rus, A., Sharkhuu, A., Yokoi, S., Karthikeyan, A. S., Raghothama, K. G., Baek, D., Koo, Y. D., Jin, J. B., Bressan, R. A., Yun, D.-J. and Hasegawa, P. M.** (2005). The *Arabidopsis* SUMO E3 ligase SIZ1 controls phosphate deficiency responses. *PNAS* **102**, 7760–7765. 16
- Mizoguchi, T. and Coupland, G.** (2000). ZEITLUPE and FKF1: novel connections between flowering time and circadian clock control. *Trends in Plant Science* **5**, 409–411. 86
- Moore, I. and Murphy, A.** (2009). Validating the location of fluorescent protein fusions in the endomembrane system. *Plant Cell* **21**, 1632–1636. 93, 95
- Mueller, T. D., Kamionka, M. and Feigon, J.** (2004). Specificity of the interaction between ubiquitin-associated domains and ubiquitin. *Journal of Biological Chemistry* **279**, 11926–11936. 5
- Mukhopadhyay, D. and Riezman, H.** (2007). Proteasome-independent functions of ubiquitin in endocytosis and signaling. *Science* **315**, 201–205. 6

- Mur, L. A., Kenton, P., Lloyd, A. J., Ougham, H. and Prats, E.** (2008). The hypersensitive response; the centenary is upon us but how much do we know? *Journal of Experimental Botany* **59**, 501–520. 3, 42, 88, 91
- Murakami, Y., Matsufuji, S., Kameji, T., Hayashi, S., Igarashi, K., Tamura, T., Tanaka, K. and Ichihara, A.** (1992). Ornithine decarboxylase is degraded by the 26S proteasome without ubiquitination. *Nature* **360**, 597–599. 10
- Nicol, F., His, I., Jauneau, A., Vernhettes, S., Canut, H. and Höfte, H.** (1998). A plasma membrane-bound putative endo-1, 4-beta-D-glucanase is required for normal wall assembly and cell elongation in *Arabidopsis*. *The EMBO Journal* **17**, 5563–5576. 84
- Nicotera, P., Leist, M. and Ferrando-May, E.** (1999). Apoptosis and necrosis: different execution of the same death. *Biochemical Society Symposium* **66**, 69–73. 1
- Odell, J. T., Nagy, F. and Chua, N. H.** (1985). Identification of DNA sequences required for activity of the cauliflower mosaic virus 35S promoter. *Nature* **313**, 810–812. 92
- Olsen, B. R., Reginato, A. M. and Wang, W.** (2000). Bone development. *Annual Review of Cell and Developmental Biology* **16**, 191–220. 1
- Orzáez, D., de Jong, A. and Woltering, E.** (2001). A tomato homologue of the human protein PIRIN is induced during programmed cell death. *Plant Molecular Biology* **46**, 459–468. 2
- Overmyer, K., Brosché, M. and Kangasjärvi, J.** (2003). Reactive oxygen species and hormonal control of cell death. *Trends in Plant Science* **8**, 335–342. 88
- Overmyer, K., Brosche, M., Pellinen, R., Kuittinen, T., Tuominen, H., Ahlfors, R., Keinanen, M., Saarma, M., Scheel, D. and Kangasjarvi, J.** (2005). Ozone-induced programmed cell death in the *Arabidopsis radical-induced cell death1* mutant. *Plant Physiology* **137**, 1092–1104. 88
- Pickart, C. M. and Fushman, D.** (2004). Polyubiquitin chains: polymeric protein signals. *Current Opinion in Chemical Biology* **8**, 610–616. 5
- Pickart, C. M., Kasperek, E. M., Beal, R. and Kim, A.** (1994). Substrate properties of site-specific mutant ubiquitin (G76A) reveal unexpected mechanistic features of ubiquitin-activating enzyme (E1). *Journal of Biological Chemistry* **269**, 7115–7123. 7
- Pike, S. M., Zhang, X. C. and Gassmann, W.** (2005). Electrophysiological characterization of the *Arabidopsis avrRpt2*-specific hypersensitive response in the absence of other bacterial signals. *Plant Physiology* **138**, 1009–1017. 91

- Pohl, C. and Jentsch, S.** (2008). Final stages of cytokinesis and midbody ring formation are controlled by BRUCE. *Cell* **132**, 832–845. 19, 20, 25, 80
- Qiu, X. B. and Goldberg, A. L.** (2005). The membrane-associated inhibitor of apoptosis protein, BRUCE/Apollon, antagonizes both the precursor and mature forms of Smac and caspase-9. *Journal of Biological Chemistry* **280**, 174–182. 19, 20
- Quaghebeur, M. and Rengel, Z.** (2004). Arsenic uptake, translocation and speciation in *pho1* and *pho2* mutants of *Arabidopsis thaliana*. *Physiologia Plantarum* **120**, 280–286. 17
- Raab, S., Drechsel, G., Zarepour, M., Hartung, W., Koshiba, T., Bittner, F. and Hoth, S.** (2009). Identification of a novel E3 ubiquitin ligase that is required for suppression of premature senescence in *Arabidopsis*. *Plant Journal* **59**, 39–51. 14, 87
- Rao, M. V., Koch, J. R. and Davis, K. R.** (2000). Ozone: a tool for probing programmed cell death in plants. *Plant Molecular Biology* **44**, 345–358. 87, 88, 90
- Rao, M. V., Lee, H. and Davis, K. R.** (2002). Ozone-induced ethylene production is dependent on salicylic acid, and both salicylic acid and ethylene act in concert to regulate ozone-induced cell death. *Plant Journal* **32**, 447–456. 88
- Ravid, T. and Hochstrasser, M.** (2008). Diversity of degradation signals in the ubiquitin-proteasome system. *Nature Reviews* **9**, 679–689. 8
- Rédei, G. P.** (1992). Methods in *Arabidopsis* Research, chapter A: heuristic glance at the past of *Arabidopsis genetics*. Koncz C., Chua N. H. and Schell J. (eds.). *World Scientific, Singapore*, 1–15. 111
- Riedl, S. J. and Shi, Y.** (2004). Molecular mechanisms of caspase regulation during apoptosis. *Nature Reviews Molecular Cell Biology* **5**, 897–907. 2
- Romero-Puertas, M. C., Laxa, M., Matte, A., Zaninotto, F., Finkemeier, I., Jones, A. M. E., Perazzolli, M., Vandelle, E., Dietz, K. J. and Delledonne, M.** (2007). S-nitrosylation of peroxiredoxin II E promotes peroxynitrite-mediated tyrosine nitration. *Plant Cell* **19**, 4120–4130. 89
- Rusterucci, C., Espunya, M. C., Diaz, M., Chabannes, M. and Martinez, M. C.** (2007). S-nitrosoglutathione reductase affords protection against pathogens in *Arabidopsis*, both locally and systemically. *Plant Physiology* **143**, 1282–1292. 89
- Sanchez, P., de Torres Zabala, M. and Grant, M.** (2000). AtBI-1, a plant homologue of Bax inhibitor-1, suppresses Bax-induced cell death in yeast and is rapidly upregulated during wounding and pathogen challenge. *Plant Journal* **21**, 393–399. 2

- Saracco, S. A., Hansson, M., Scalf, M., Walker, J. M., Smith, L. M. and Viestra, R. D. (2009). Tandem affinity purification and mass spectrometric analysis of the ubiquitylated proteins in *Arabidopsis*. *Plant Journal* **59**, 344–358. 5, 6
- Saul, H., Elharrar, E., Gaash, R., Eliaz, D., Valenci, M., Akua, T., Avramov, M., Frankel, N., Berezin, I., Gottlieb, D., Elazar, M., David-Assael, O., Tcherkas, V., Mizrachi, K. and Shaul, O. (2009). The upstream open-reading frame of the *Arabidopsis* AtMHX gene has a strong impact on transcript accumulation through the nonsense-mediated mRNA decay pathway. *Plant Journal* **60**, 1031–1042. 82
- Schlegel, R. and Williamson, P. (2001). Phosphatidylserine, a death knell. *Cell death and differentiation* **8**, 551–563. 2
- Schlögelhofer, P., Garzón, M., Kerzendorfer, C., Nizhynska, V. and Bachmair, A. (2006). Expression of the ubiquitin variant ubR48 decreases proteolytic activity in *Arabidopsis* and induces cell death. *Planta* **223**, 684–697. 13, 21, 37, 85, 112
- Schrader, E. K., Harstad, K. G. and Matouschek, A. (2009). Targeting proteins for degradation. *Nature Chemical Biology* **5**, 815–822. 9
- Schulman, B. A. and Harper, J. W. (2009). Ubiquitin-like protein activation by E1 enzymes: the apex for downstream signalling pathways. *Nature Reviews* **10**, 319–331. 7
- Schwartz, L. M., Myer, A., Kosz, L., Engelstein, M. and Maier, C. (1990). Activation of polyubiquitin gene expression during developmentally programmed cell death. *Neuron* **5**, 411–419. 13
- Schwechheimer, C. and Villalobos, L. I. A. C. (2004). Cullin-containing E3 ubiquitin ligases in plant development. *Current Opinion in Plant Biology* **7**, 677–686. 12
- Sekine, K., Hao, Y., Suzuki, Y., Takahashi, R., Tsuruo, T. and Naito, M. (2005). HtrA2 cleaves Apollon and induces cell death by IAP-binding motif in Apollon-deficient cells. *Biochemical and Biophysical Research Communications* **330**, 279–285. 19
- Singh, S. M. and Panda, A. K. (2005). Solubilization and refolding of bacterial inclusion body proteins. *Journal of Bioscience and Bioengineering* **99**, 303–310. 104
- Smalle, J. and Vierstra, R. D. (2004). The ubiquitin 26S proteasome proteolytic pathway. *Annual Review of Plant Biology* **55**, 555–590. 12
- Smialowski, P., Martin-Galiano, A. J., Mikolajka, A., Girschick, T., Holak, T. A. and Frishman, D. (2007). Protein solubility: sequence based prediction and experimental verification. *Bioinformatics* **23**, 2536–2542. 104
- Smith, D. B. and Johnson, K. S. (1988). Single-step purification of polypeptides expressed in *Escherichia coli* as fusions with glutathione S-transferase. *Gene* **67**, 31–40. 105

- Söding, J., Remmert, M. and Biegert, A.** (2006). HHrep: *de novo* repeat detection and the origin of TIM barrels. *Nucleic Acids Research* **34**, Server issue W137–W142. 80
- Spence, J., Gali, R. R., Dittmar, G., Sherman, F., Karin, M. and Finley, D.** (2000). Cell cycle-regulated modification of the ribosome by a variant multiubiquitin chain. *Cell* **102**, 67–76. 6
- Spence, J., Sadis, S., Haas, A. L. and Finley, D.** (1995). A ubiquitin mutant with specific defects in DNA repair and multiubiquitination. *Molecular Cell Biology* **15**, 1265–1273. 6
- Srinivasula, S. M. and Ashwell, J. D.** (2008). IAPs: What's in a Name? *Molecular Cell* **30**, 123–135. 13, 19
- Stevenson, K. J., Hale, G. and Perham, R. N.** (1978). Inhibition of pyruvate dehydrogenase multienzyme complex from *Escherichia coli* with mono- and bifunctional arsenoxides. *Biochemistry* **17**, 2189–2192. 18
- Stone, S. L. and Callis, J.** (2007). Ubiquitin ligases mediate growth and development by promoting protein death. *Current Opinion in Plant Biology* **10**, 624–632. 12
- Swarbreck, D., Wilks, C., Lamesch, P., Berardini, T. Z., Garcia-Hernandez, M., Foerster, H., Li, D., Meyer, T., Muller, R., Ploetz, L., Radenbaugh, A., Singh, S., Swing, V., Tissier, C., Zhang, P. and Huala, E.** (2008). The *Arabidopsis* Information Resource (TAIR): gene structure and function annotation. *Nucleic Acids Research* **36**, D1009–D1014. 114
- Thastrup, O., Tullin, S., Poulsen, L. K. and Björn, S.** (1995). Fluorescent proteins. *United states patent, Application number 08/819,612* . 91
- Thut, C. J., Goodrich, J. A. and Tijan, R.** (1997). Repression of p53-mediated transcription by MDM2: a dual mechanism. *Genes and Development* **11**, 1974–1986. 7
- Töpfer, R., Maas, C., Hörnicke-Grandpierre, C., Schell, J. and Steinbiss, H. H.** (1993). Expression vectors for high-level gene expression in dicotyledonous and monocotyledonous plants. *Methods in Enzymology* **217**, 67–78. 112
- Traven, A., Jelicic, B. and Sopta, M.** (2006). Yeast Gal4: a transcriptional paradigm revisited. *EMBO Reports* **7**, 496–499. 98
- Trevino, S. R., Scholtz, J. M. and Pace, C. N.** (2007). Amino acid contribution to protein solubility: Asp, Glu, and Ser contribute more favorably than the other hydrophilic amino acids in RNase Sa. *Journal of Molecular Biology* **366**, 449–460. 104
- Turner, S., Gallois, P. and Brown, D.** (2007). Tracheary element differentiation. *Annual Review of Plant Biology* **58**, 407–433. 4

- Van Criekinge, W. and Beyaert, R.** (1999). Yeast two-hybrid: State of the art. *Biological Procedures Online* **2**, 1–38. 97, 102
- Vaucheret, H.** (2005). MicroRNA-dependent trans-acting siRNA production. *Science's STKE* **2005**, 43–45. 96
- Ventura, S.** (2005). Sequence determinants of protein aggregation: tools to increase protein solubility. *Microbial Cell Factories* **4**, 11–18. 106
- Vernooy, S. Y., Chow, V., Su, J., Verbrugghe, K., Yang, J., Cole, S., Olson, M. R. and Hay, B. A.** (2002). *Drosophila* Bruce can potently suppress Rpr- and Grim-dependent but not Hid-dependent cell death. *Current Biology* **12**, 1164–1168. 19
- Vernoud, V., Horton, A. C., Yang, Z. and Nielsen, E.** (2003). Analysis of the small GTPase gene superfamily of *Arabidopsis*. *Plant Physiology* **131**, 1191–1208. 94
- Vierstra, R. D.** (1996). Proteolysis in plants: mechanisms and functions. *Plant Molecular Biology* **32**, 275–302. 9
- Vierstra, R. D.** (2009). The ubiquitin-26S proteasome system at the nexus of plant biology. *Nature Reviews* **10**, 385–397. 10, 12
- Voges, D., Zwickl, P. and Baumeister, W.** (1999). The 26S proteasome: a molecular machine designed for controlled proteolysis. *Annual Review of Biochemistry* **68**, 1015–1068. 10
- Voinnet, O., Rivas, S., Mestre, P. and Baulcombe, D.** (2003). An enhanced transient expression system in plants based on suppression of gene silencing by the p19 protein of tomato bushy stunt virus. *Plant Journal* **33**, 949–956. 92, 121
- Vuillard, L., Rabilloud, T. and Goldberg, M. E.** (2001). Interactions of non-detergent sulfobetaines with early folding intermediates facilitate *in vitro* protein renaturation. *European Journal of Biochemistry* **256**, 128–135. 105
- Wang, C., Xi, J., Begley, T. P. and Nicholson, L. K.** (2001). Solution structure of ThiS and implications for the evolutionary roots of ubiquitin. *Nature Structural Biology* **8**, 47–51. 5
- Watanabe, N. and Lam, E.** (2005). Two *Arabidopsis* metacaspases AtMCP1b and AtMCP2b are arginine/lysine-specific cysteine proteases and activate apoptosis-like cell death in yeast. *Journal of Biological Chemistry* **280**, 14691–14699. 2
- Wefes, I., Mastrandrea, L. D., Haldeman, M., Koury, S. T., Tamburlin, J., Pickart, C. M. and Finley, D.** (1995). Induction of ubiquitin-conjugating enzymes during terminal erythroid differentiation. *PNAS* **92**, 4982–4986. 17

- Weissmann, A. (1891). Essays upon heredity and kindred biological problems. *Oxford University Press, London* . 1
- Wendehenne, D., Pugin, A., Klessig, D. F. and Durner, J. (2001). Nitric oxide: comparative synthesis and signaling in animal and plant cells. *Trends in Plant Science* **6**, 177–183. 89
- Whalen, M. C., Innes, R., Bent, A. F. and Staskawicz, B. J. (1991). Identification of *Pseudomonas syringae* pathogens of *Arabidopsis* and a bacterial locus determining avirulence on both *Arabidopsis* and soybean. *Plant Cell* **3**, 49–59. 42, 91
- Whitby, F. G., Xia, G., Pickart, C. M. and Hill, C. P. (1998). Crystal structure of the human ubiquitin-like protein NEDD8 and interactions with ubiquitin pathway enzymes. *Journal of Biological Chemistry* **273**, 34983–34991. 107
- Wiesner, S., Ogunjimi, A. A., Wang, H. R., Rotin, D., Sicheri, F., Wrana, J. L. and Forman-Kay, J. D. (2007). Autoinhibition of the HECT-type ubiquitin ligase Smurf2 through its C2 domain. *Cell* **130**, 651–662. 108
- Williams, F. E., Varanasi, U. and Trumbly, R. J. (1991). The CYC8 and TUPI proteins involved in glucose repression in *Saccharomyces cerevisiae* are associated in a protein complex. *Molecular and Cellular Biology* **11**, 3307–3316. 61, 100
- Winterbourn, C. C. (2008). Reconciling the chemistry and biology of reactive oxygen species. *Nature Chemical Biology* **4**, 278–286. 88
- Woo, H. R., Chung, K. M., Park, J. H., Oh, S. A., Ahn, T., Hong, S. H., Jang, S. K. and Nam, H. G. (2001). ORE9, an F-box protein that regulates leaf senescence in *Arabidopsis*. *Plant Cell* **13**, 1779–1790. 13
- Wu-Baer, F., Lagrazon, K., Yuan, W. and Baer, R. (2003). The BRCA1/BARD1 heterodimer assembles polyubiquitin chains through an unconventional linkage involving lysine residue K6 of ubiquitin. *Journal of Biological Chemistry* **278**, 34743–34746. 6
- Xirodimas, D., Saville, M. K., Edling, C., Lane, D. P. and Lain, S. (2001). Different effects of p14ARF on the levels of ubiquitinated p53 and Mdm2 *in vivo*. *Oncogene* **20**, 4972–4983. 103
- Xu, P., Duong, D. M., Seyfried, N. T., Cheng, D., Xie, Y., Robert, J., Rush, J., Hochstrasser, M., Finley, D. and Peng, J. (2009). Quantitative proteomics reveals the function of unconventional ubiquitin chains in proteasomal degradation. *Cell* **137**, 133–147. 5, 6
- Yang, C. W., Gonzalez-Lamothe, R., Ewan, R. A., Rowland, O., Yoshioka, H., Shenton, M., Ye, H., O'Donnell, E., Jones, J. D. G. and Sadanandom, A. (2006). The E3 ubiquitin ligase activity of *Arabidopsis* PLANT U-BOX17 and its

- functional tobacco homolog ACRE276 are required for cell death and defense. *Plant Cell* **18**, 1084–1098. 14
- Yang, P., Fu, H., Walker, J., Papa, C., Smalle, J., Ju, Y. and Vierstra, R.** (2004). Purification of the *Arabidopsis* 26 S Proteasome: biochemical and molecular analyses revealed the presence of multiple isoforms. *Journal of Biological Chemistry* **279**, 6401–6413. 9
- Yin, X. J., Volk, S., Ljung, K., Mehlmer, N., Dolezal, K., Ditengou, F., Hanano, S., Davis, S. J., Schmelzer, E., Sandberg, G., Teige, M., Palme, K., Pickart, C. and Bachmair, A.** (2007). Ubiquitin lysine 63 chain forming ligases regulate apical dominance in *Arabidopsis*. *Plant Cell* **19**, 1898–1911. 6
- Yoshida, S., Ito, M., Callis, J., Nishida, I. and Watanabe, A.** (2002). A delayed leaf senescence mutant is defective in arginyl-tRNA: protein arginyltransferase, a component of the N-end rule pathway in *Arabidopsis*. *Plant Journal* **32**, 129–137. 14
- Youle, R. and Strasser, A.** (2008). The BCL-2 protein family: opposing activities that mediate cell death. *Nature Reviews Molecular Cell Biology* **9**, 47–59. 2
- Zeng, L. R., Qu, S., Bordeos, A., Yang, C., Baraoidan, M., Yan, H., Xie, Q., Nahm, B. H., Leung, H. and Wang, G. L.** (2004). *Spotted leaf11*, a negative regulator of plant cell death and defense, encodes a U-box/armadillo repeat protein endowed with E3 ubiquitin ligase activity. *Plant Cell* **16**, 2795–2808. 14
- Zeng, L. R., Vega-Sánchez, M. E., Zhu, T. and Wang, G. L.** (2006). Ubiquitination-mediated protein degradation and modification: an emerging theme in plant-microbe interactions. *Cell Research* **16**, 413–426. 14
- Zimmermann, P., Hirsch-Hoffmann, M., Henning, L. and Gruissem, W.** (2004). GENEVESTIGATOR. *Arabidopsis* microarray database and analysis toolbox. *Plant Physiology* **136**, 2621–2632. 11
- Zuo, J., Niu, Q. W. and Chua, N. H.** (2000). Technical advance: An estrogen receptor-based transactivator XVE mediates highly inducible gene expression in transgenic plants. *Plant Journal* **24**, 265–273. 112

Acknowledgements

The last words of my thesis are dedicated to all the great people who accompanied and supported me during these four years of my PhD.

Mein allergrößtes Dankeschön gilt natürlich zunächst meinem lieben Chef **Andreas Bachmair**. Sein Spaß an der Wissenschaft und seine Neugier an jedem noch so kleinen Experiment waren immer ansteckend und so hat er es geschafft, dass es nie an Motivation und Ideen fehlte. Immer frei nach dem Motto: „Quand tu veux construire un bateau, ne commence pas par rassembler du bois, couper des planches et distribuer du travail, mais reveille au sein des hommes le desir de la mer grande et large.“ (Antoine de Saint-Exupéry)
Lieber Andreas, vielen lieben Dank, dass durch dich meine Faszination für Biologie und mein Spaß an der Wissenschaft immer wach gehalten wurden.

Außerdem möchte ich **Prof. Dr. George Coupland**, **Prof. Dr. Jürgen Dohmen**, **Dr. Bernd Reiss** und **Prof. Dr. Ute Höcker** herzlich dafür danken, dass sie sich bereiterklärt haben, Teil meines Prüfungskomitees zu sein und mir dadurch die Möglichkeit bieten, trotz des Umzugs ins schöne Wien immer noch in Köln promovieren zu können.

Special thanks go to **Dr. Nikolaus Schlaich** at the RWTH Aachen for the help with the pathogen treatment, to **Dr. Dieter Ernst** at the Helmholtz Centre in Munich, who performed the ozone treatment, and to **Dr. Wolf-Rüdiger Scheible** at the MPIMP in Potsdam for determination of the phosphate contents. Many thanks also to **Katharina Maderböck** and **Dr. Andrea Pichler** at the MFPL, who supported me during the thioester experiments and supplied me with the necessary enzymes. Apart from that I want to thank **Dr. Maria Novatchkova** at the IMP in Vienna for the bioinformatic analysis of the PFU proteins and **Dr. Robert Konrat** at the Structural and Computational Biology Department (MFPL, Vienna) for the meta-structure analysis.

A big thank you to all the "Bachmairs" that accompanied me during my time in Cologne and Vienna, especially **Andrea, Rebecca, Prabha, Konstantin and Kerstin**. It was always a great feeling to know that there are people in the lab you can always chat and laugh with and that always helped when there was need. I especially want to thank Kerstin for the great help with the genotyping of the mutant lines.

Vielen lieben Dank auch an meine liebsten Freunde im schönen Rheinland, besonders an **Marcus und Nico**, die mich mit ihrer Herzlichkeit immer auf andere Gedanken bringen konnten und die nie zugelassen haben, dass ich mich wegen der 1000 km Entfernung alleine fühlen muss. Muchas Gracias también para la gran ayuda en problemas informáticos!

Auch meiner liebsten „Ex-Doktorandin“ **Katrin**, die trotz ihres „richtigen“ Jobs wiederum keine Mühen gescheut hat, meine geistigen Ergüsse zu korrigieren, vielen vielen Dank.

Ein riesiges Dankschön geht an **meine Eltern, meinen Bruder Tim und an Oma und Opa**, die mir die Grundregeln der Botanik schon früh beigebracht haben: „Auch der stärkste Baum geht ein, wenn er keine Wurzeln hat“. Danke, dass ihr immer als ein Fundament aus Ruhe und Gelassenheit für mich da seid.

Zuletzt möchte ich **Martin** von Herzen danken. Du hast mir mal wieder gezeigt, dass du immer an mich glaubst und in allen Höhen und Tiefen zu mir stehst. Nostro futuro può arrivare!!! :-)

Erklärung

Ich versichere, dass ich die von mir vorgelegte Dissertation selbständig angefertigt, die benutzten Quellen und Hilfsmittel vollständig angegeben und die Stellen der Arbeit – einschließlich Tabellen, Karten und Abbildungen –, die anderen Werken im Wortlaut oder dem Sinn nach entnommen sind, in jedem Einzelfall als Entlehnung kenntlich gemacht habe; dass diese Dissertation noch keiner anderen Fakultät oder Universität zur Prüfung vorgelegen hat; dass sie – abgesehen von unten angegebenen Teilpublikationen – noch nicht veröffentlicht worden ist sowie, dass ich eine solche Veröffentlichung vor Abschluss des Promotionsverfahrens nicht vornehmen werde. Die Bestimmungen der Promotionsordnung sind mir bekannt. Die von mir vorgelegte Dissertation ist von Prof. Dr. Andreas Bachmair und von Prof. Dr. George Coupland (Max-Planck-Institut für Pflanzenzüchtungsforschung) betreut worden.

Köln, den 08.04.2010

Karolin Eifler

Curriculum Vitae

Persönliche Daten

Name: **Karolin Eifler**
Geburtsdatum: 26. Mai 1981
Geburtsort: Meisenheim
Familienstand: ledig
Adresse: Am Hypperich 27
54538 Bausendorf

Ausbildung

07.06.2010 **Doktor** der Biologie an der Universität Köln (Note 1.3)
Okt. 2008 – Juni 2010 **Weiterführung der Doktorarbeit** in der Gruppe von Dr. A. Bachmair in den Max F. Perutz Laboratories, Universität **Wien**
Apr. 2006 – Okt. 2008 **Doktorarbeit** am Max-Planck-Institut für Pflanzenzüchtungsforschung (MPIPZ, **Köln**) in der Arbeitsgruppe von Dr. A. Bachmair mit dem Thema „The PHO2 family of ubiquitin conjugating enzymes in *Arabidopsis thaliana* and its contribution to plant programmed cell death“
23.01.2006 **Diplom** in Biologie an der Rheinischen Friedrich-Wilhelms-Universität Bonn (Note 1.0)
Jan. 2005 – Jan. 2006 **Diplomarbeit** in der Arbeitsgruppe von Prof. Dr. Volker Knoop: „Molecular and functional analyses of *Arabidopsis thaliana* cation transport: *in planta* studies and heterologous expression of membrane transport proteins in yeast“
Okt. 2000 – Jan. 2006 **Studium** der Biologie an der Rheinischen Friedrich-Wilhelms-Universität **Bonn**
Juni 2000 – Sept. 2000 **Auslandsaufenthalt** in **Monterey** (Kalifornien) als Volunteer im Point Lobos State Park
Mai 2000 **Abitur** am Cusanus Gymnasium **Wittlich** (Note 1.7)
Sept. 1999 Schülerakademie: Kurs Ökosystemanalyse
1991 – 2000 Besuch des Cusanus Gymnasiums Wittlich
1987 – 1991 Besuch der Grundschule Alftal

Publikationen

- Gebert, M., Meschenmoser, K., Svidová, S., Weghuber, J., Schweyen, R., **Eifler, K.**, Lenz, H., Weyand, K., Knoop, V.: A root-expressed magnesium transporter of the MRS2/MGT gene family in *Arabidopsis thaliana* allows for growth in low-Mg²⁺ environments, *Plant Cell* (2009) 12, 4018-4030
- Garzón, M., **Eifler, K.**, Faust, A., Scheel, H., Hofmann, K., Koncz, C., Yephremov, A., Bachmair, A.: *PRT6/At5g02310* encodes an *Arabidopsis* ubiquitin ligase of the N-end rule pathway with arginine specificity and is not the *CER3* locus, *FEBS Letters* (2006) 581, 3189-3196
- Knoop, V., Groth-Malonek, M., Gebert, M., **Eifler, K.**, Weyand, K.: Transport of magnesium and other divalent cations: evolution of the 2-TM-GxN proteins in the MIT superfamily, *Molecular Genetics and Genomics* (2005) 274, 205-216

Ausgewählte Präsentationen

- **Eifler, K.**, Scheible, W.-R., Schlaich, N., Novatchkova, M., Ernst, D., Garzón, M., Luxa, K., and Bachmair, A.: A family of ubiquitin conjugating enzymes involved in plant cell death regulation senses oxidative signals, Inproteolys: Barcelona Proteasome Meeting 2009 (Spanien), **Biochemical Journal Young Investigator Award Winner**
- **Eifler, K.**, Garzón, M., Luxa, K. and Bachmair, A.: The LETs - a protein family of putative ubiquitin conjugating enzymes in *Arabidopsis thaliana*, PhD Conference 2007 am Max-Planck-Institut für Pflanzenzüchtungsforschung Köln, **Posterpreis**
- **Eifler, K.**, Garzón, M., Faust, A., Scheel, H., Hofmann, K., Koncz, C., Yephremov, A., Bachmair, A.: An *Arabidopsis* ubiquitin ligase of the N-end rule pathway with arginine specificity, EMBO conference on ubiquitin and ubiquitin-like modifiers in cellular regulation 2007, Riva del Garda (Italien)